Author:
Lawler, Catherine

Title:
Molecular basis of Streptococcus gordonii biofilm formation and eDNA release

Molecular basis of *Streptococcus gordonii* biofilm formation and eDNA release

Catherine Rosalind Erika Lawler

A dissertation submitted to the University of Bristol in accordance with the requirements for award of the degree of PhD in Oral and Dental Science in the Faculty of Health Sciences in the School of Oral and Dental Sciences in September 2018.

55608 words

Abstract

Streptococcus gordonii is a primary coloniser of the clean tooth surface. It forms part of the dental plaque biofilm, and can influence the way in which this polymicrobial community develops through its interactions with host molecules and other microbes. These interactions and the capacity for *S. gordonii* to form biofilms are facilitated, in large part, by LPxTG family surface proteins. However, not all such proteins have been fully characterised. In this project, six LPxTG proteins were investigated for their role in *S. gordonii* adhesion and biofilm formation. This included development of a novel imaging and analysis technique to enable quantification of extracellular DNA (eDNA) strands within biofilms, an important component of biofilm matrix. PalA was found to bind cellular fibronectin, with potential implications for mucosal tissue interactions and the pathogenesis of infective endocarditis. SedA and SndA were both implicated in eDNA stranding during biofilm development. Further studies into the mechanistic basis of eDNA release and assembly implied that SedA and SndA mediated their effects through binding eDNA strands on the surface of *S. gordonii*. Furthermore, induction of eDNA by competence stimulating peptide (CSP) in *S. gordonii* biofilms was implied to occur via the Hpp system, in a pathway involving autolysins AtlS and LytF. Taken together, these data provide further insights into the molecular basis of *S. gordonii* colonisation, and could provide research avenues for future therapeutic development.

Dedication

For Sandwich

Thank you for being my Friend.

Acknowledgements

First, I would like to thank my supervisors Angela Nobbs and Mark Jepson for the enormous effort they have put in. Their guidance, patience and dedication has been truly outstanding. They are inspirational researchers I will always look up to.

I would next like to thank Jane Brittan and Lindsay Dutton for the technical assistance they gave me. Thank you for bearing with me and helping me laugh along the way.

Special thanks to Dominic Alibhai, without whose specialised knowledge I would not have been able to develop the techniques used in my thesis.

Thank you to all the staff and students I have overlapped with, especially Grace, Debbie and Cat in Oral and Dental Science and Tania, Jen and Lorna in Biochemistry. You have kept me going with your laughter.

Thank you to my friends for supporting me and the sacrifices I've made to complete my PhD. Special thanks to the Bristol Leftovers.

To Jess, thank you for helping me keep everything in perspective, helping me let off some steam at the weekends and sticking with me these last 23 years.

To my family, thank you for always believing in me. To my Mum and Dad, I can't express my gratitude for the opportunities you have given me in life which have led me to where I am today. Thank you for every card, every text, every word of support which have kept me going. To my brother, thanks for keeping me sane with cat videos and making sure I get one good meal a week!

To Chris, for waking me up and feeding me toast when I haven't eaten. Thank you for walking this path with me, supporting me tirelessly and making me a better person. I love you.

Declaration

I declare that the work in this dissertation was carried out in accordance with the requirements of the University's Regulations and Code of Practice for Research Degree Programmes and that it has not been submitted for any other academic award. Except where indicated by specific reference in the text, the work is the candidate's own work. Work done in collaboration with, or with the assistance of, others, is indicated as such. Any views expressed in the dissertation are those of the author.

SIGNED: ..... DATE:.....

Table of Contents

List of Figures

List of Tables

List of Abbreviations

aa - amino acid
Ab - antibody
ATP - adenosine triphosphate
bp - base pair
CF - cystic fibrosis
CSP - competence stimulating peptide
dH_2O - deionised H_2O
DNA - Deoxyribonucleic acid
dsDNA - double stranded DNA
ECM - extracellular matrix
eDNA - extracellular DNA
EPS - extracellular polymeric substance
FISH - fluorescent in situ hybridization
FITC – fluorescein isothiocyanate
FRET - Förster resonance energy transfer
gDNA - genomic DNA
GOI - gene of interest
gt- goat
IE - infective endocarditis
Ig - immunoglobulins
MIC - minimum inhibitory concentration
ms - mouse
MSCRAMM - microbial surface component recognising adhesive matrix molecules
NET - neutrophil extracellular trap
PCR - polymerase chain reaction
RNA - ribonucleic acid
sCSP - scrambled CSP
SDS-PAGE - sodium dodecyl sulphate polyacrylamide gel electrophoresis
TCRS - two component regulatory system
VGS - viridans group streptococci
WT – wild type

Chapter 1 - Introduction

1.1 Biofilms

Biofilms are sessile multispecies communities of microorganisms which display some characteristics found in multicellular organisms, e.g. division of labour (Claessen *et al.*, 2014), despite being composed of only unicellular organisms. Biofilms grow in a co-operative manner on a wide variety of surfaces and are found ubiquitously in nature. They are characterised as being recalcitrant to antibiotic treatment (Goodman et al., 2011; Wu et al., 2016).

Biofilms are often found at solid to liquid interfaces, and were first observed as a slime layer in water purification systems. They impact a wide variety of fields, for example, agriculture, food production and health care. Biofilms are involved in chronic and acute bacterial and fungal infectious diseases, such as cystic fibrosis (Høiby *et al*., 2017) and vaginal thrush (Nobile & Johnson, 2015). Furthermore, biofilms are particularly pertinent to medical devices such as catheters and implants, the use of which is increasing globally (López *et al.*, 2010). Some diseases, such as periodontal disease, can be caused by multispecies biofilms (Park *et al*., 2014). The presence of different species can alter the ability the pathogenesis of the biofilm. For instance, *in vitro*, addition of another bacterial species (*Anaeroglobus geminatus*) to a ten species biofilm (designed to mimic the periodontal environment) shifted the biofilm towards virulence (Bao *et al*., 2017). Additionally, changes in proportions of different microbes in an ecological niche can cause transition from carriage to diseased state (Langdon *et al.*, 2016). Taken together with the need to reduce antibiotic usage to combat bacterial antimicrobial resistance, a new frontier has opened in drug development which specifically targets biofilms, rather than targeting individual bacteria (Ribeiro *et al.*, 2016).

Biofilm formation begins with microbial attachment to a surface. This is reversable and occurs within seconds. Bacteria can then form stronger connections to the substratum and divide (Nobbs *et al*., 2007). Bacteria excrete an extracellular polymeric substance (EPS) which encases the biofilm. Mature biofilms are ordered in distinct microcolonies with water channels to maintain hydration throughout the biofilm and remove waste products from the bacteria (Flemming & Wingender, 2010). These structures have been observed in biofilms formed *in vitro* with a variety of bacteria, including Gram-positive *Streptococcus pneumoniae* (Yadav *et al*., 2012*)* and Gram-negative *Pseudomonas aeruginosa* (Davies *et al*., 1998), as well as in multispecies biofilms, such as those grown from subgingival plaque (Hope & Wilson, 2006). Bacteria can disperse from the biofilm and may reattach at another place on the substratum or grow planktonically (Kaplan, 2010). Together, these events form a biofilm life cycle (Figure 1.1).

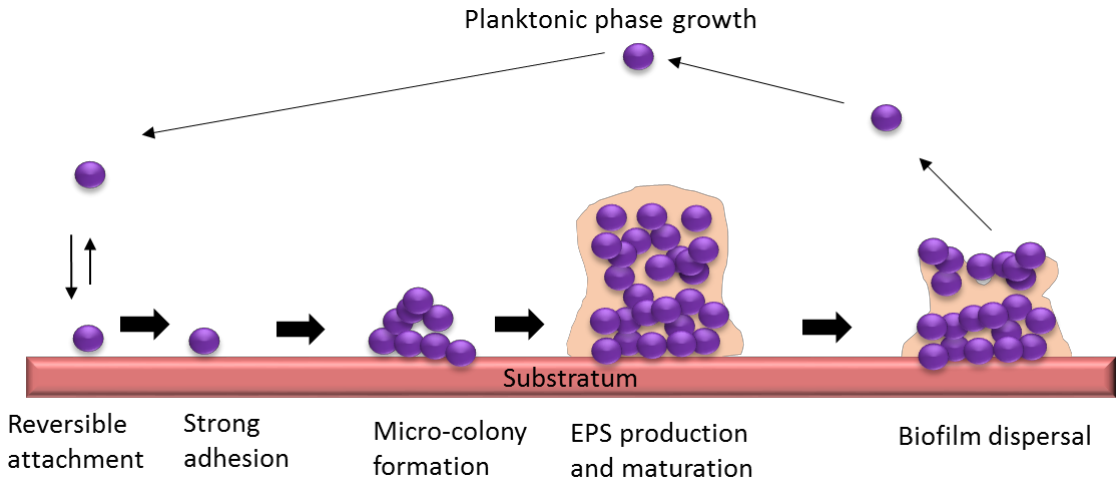

Figure 1.1 - Biofilm life cycle
Adapted from Toyofuku et al., 2016

Microorganisms grow in a biofilm state for a number of potential reasons: increased resistance to environmental stressors (O'Toole & Stewart, 2005), tolerance to otherwise toxic surroundings (Lapaglia & Hartzell, 1997), or persistence on a surface which experiences high shear forces (Donlan &

Costerton, 2002). Additionally, increased resistance to extremes of pH, temperature or radiation (Vorkapic *et al.*, 2016). Bacteria, such as Gram-negative *Pseudomonas aeruginosa,* typically require much higher concentrations of antibiotics to reach the minimum inhibitory concentration (MIC) when grown in biofilms compared to their planktonic counterparts (Goodman *et al.*, 2011; Wu *et al.*, 2016).

Established biofilms have architectures which support their ecological functions, such as persistence. Ensuring nutrients can penetrate and waste can leave the biofilm ensures survival of all cell. In *Bacillus subtilis*, this is facilitated by channels, which are full of liquid and responsible for the movement of waste and nutrients (Wilking *et al.*, 2013). Biofilm phase *B. subtilis* not only share nutrients, but also co-ordinate growth through the biofilm by signalling, pausing expansion of the biofilm at the periphery in times of scarcity and increasing nutrient availability to bacteria in the centre of the biofilm (Liu *et al.*, 2015). Cells in biofilms have recently been found to fit into two groups: those proliferating at the edge and those in stationary phase within the biofilm (Carvalho et al., 2017). In this way, the biofilm is differentiated phenotypically, with exterior cells protecting the interior cells physically, in addition to preventing the starvation of the interior cells within the biofilm. In biofilms formed with oxygen-dependent bacteria, such as *P. aeruginosa*, the diffusion of oxygen through these channels is limiting, and this defines which cells can and cannot rapidly divide, creating the two groups of cells (Williamson *et al.*, 2012). These differences have the potential be important when treating biofilm-related infections clinically, as faster dividing group of cells are more susceptible to antibiotic treatment, whereas slow growing persister cells are recalcitrant to antibiotic treatment (Carvalho *et al*., 2017).

Diversity is present in many facets of biofilm formation. Whilst many biofilms are found at solid liquid interfaces, they can also be present at solid-air and liquid-air interfaces. Some bacteria, such as *Acinetobacter baumannii*, are capable of forming biofilms at more than one type of interface, for instance solid-liquid and air-liquid (Marti *et al*., 2011). Increased microbial diversity allows bacteria to sustain biofilms with more ecological functions, such as productivity

and stress tolerance (Peter *et al.,* 2011). Whilst diversity of the consortium allows for multi-functionality, maintaining multiple functions in a biofilm also relies on nutrient availability (Peter *et al*., 2011). In this way, nutrient availability feeds back into the diverse properties of biofilms. Diversity is also apparent in the biofilm excreted polymeric substance (EPS), a matrix which supports biofilm formation. Heterology in the EPS can arise from variations in microbial constituents and environmental conditions, for example, changes in nutrient availability (Ras *et al.,* 2011). The presence of EPS is a factor in biofilms recalcitrance to antibiotics (Lebeaux *et al*., 2014), therefore diversity in the EPS may alter biofilm responsiveness to antibiotics. Biofilms are complex, dense, often multispecies communities with additional diversity introduced by environment. This diversity makes studying biofilms *in vitro,* by replicating the consortia and conditions, in a way which meaningfully replicates biofilms *in vivo* difficult. Mimicking growth conditions is important however, as microbes within biofilms typically display different phenotypic and metabolic activities compared to their planktonic phase counterparts (Hung & Henderson, 2009).

Communication between organisms in biofilms is essential for differentiation, such as between fast dividing and persister cells. Much of this communication is likely via diffusion through the biofilm, however, in *Bacillus subtilis* biofilms, long range communications using ionic signalling are made via aqueous channels (Prindle *et al.*, 2015). Quorum sensing (QS) allows bacteria to regulate gene expression in response to changes in density of cells within a biofilm (Miller & Bassler, 2001). QS can occur between bacteria of the same species, and is hypothesised to occur between bacteria of different species via a shared QS mechanism. For instance, auto-inducer 2 signalling is found in both Gram-positive and Gram-negative bacteria has this system has been suggested as a “universal language” used for inter-species communication (Li & Tian, 2012). Interspecies communication would be important in the frequently multi-cellular communities which form biofilms. Quorum sensing bacteria release autoinducers, the local concentration of which increases in the presence of more quorum sensing bacteria. In Gram positive organisms, autoinducers are oligopeptides. Typically, at a threshold concentration of extracellular

autoinducer, a phosphorylation event on a surface associated sensor kinase results in the activation of a response regulator by phosphorylation, which in turn alters gene expression (Miller & Bassler, 2001). This can affect processes such as biofilm formation and competence. Competence induction in streptococci is an example of a QS system, whereby competence stimulating protein (CSP) induces a phosphorylation of surface protein complex ComDE, resulting in the activation of *comX*, which turns on competence related genes. This system is discussed more in Section 5.1.

1.1.1 EPS

Biofilms are embedded in an EPS matrix, which usually consists of bacterial proteins, lipids, polysaccharides and nucleic acids (Mccrate *et al.*, 2013), but can also incorporate host components and environmental particles. The EPS makes up around 90% of the biofilm biomass (Flemming & Wingender, 2010) and facilitates some of architecture seen in biofilms. For example, a putative carbohydrate component of *Pseudomonas aeruginosa* EPS, psl, allows for the development of biofilm structure, (Ma *et al*., 2006), and EPS in *Staphylococcus aureus* biofilms allows for formation of architecture such as towers and channels (Im *et al.*, 2015). Whilst much of the biofilm architecture is facilitated by EPS, in multispecies biofilms, the microbes themselves may function to give structure to biofilms – for instance, in oral biofilms *Corynebacterium* filaments appear to provide a structural scaffold which extends through the biofilm, away from the substratum (Ferrer & Mira, 2016).

EPS can modulate pH within a microenvironment (Xiao *et al.*, 2012), maintain the biofilm in a hydrated state under dry conditions, prevent shedding under shear forces, and forms a protective layer around the bacteria to shield them from host defences and antimicrobials, thus facilitating persistence.

The constituents of the biofilm EPS vary based on the bacterium or bacteria which form the community, but a major component is often protein. Proteins in the EPS may be secreted via bacterial secretion systems (discussed in 1.3.2.1). Until recently, it was thought only Gram-negative bacteria would form

membrane vesicles, but it has been found that Gram-positive bacteria, including streptococcal species (Resch *et al.*, 2016), can also form vesicles. Proteins on these vesicles can be incorporated into the EPS. Cell debris also contributes to the proteinaceous component of the EPS (Toyofuku *et al.*, 2012).

Lipids typically make up a small proportion of the biofilm EPS. In activated sludge (used in waste-water treatment) multispecies biofilms formed from fungi and Gram-positive and -negative bacteria, lipids were found to constitute around 2% of the EPS (Conrad *et al.*, 2003). Lipid-bound fatty acids can be produced by Gram-positive and Gram-negative bacteria and enable adaptation of the microorganisms to the thermic environment (Conrad *et al.*, 2003). Altering the EPS lipid composition is used by bacteria as an adaptive response to changes in substratum and medium (Shen *et al.*, 2015).

In one multispecies biofilm comprised of fungi and Gram-positive and -negative bacteria (used in waste-water treatment), carbohydrates were found to constitute around 10% of the EPS (Conrad *et al.*, 2003). Some simple polysaccharide (carbohydrate) molecules such as mannose appear in biofilms formed by many different species (Limoli *et al.*, 2015) and are likely to act as a nutrient store. Polysaccharide composition alters the chemical and physical properties of the biofilms, for example, changes in charge and hydrophobicity. Some polysaccharide molecules, such as PIA in *Staphylococcus aureus* (Majerczyk *et al*., 2007) can contribute to the persistence of an organism, which in turn may increase pathogenesis. This is the case for *P. aeruginosa,* where Pel and alginate are protective, shielding the biofilm from the innate immune response and increasing the amount of antibiotic necessary to disrupt biofilm formation. (Colvin *et al.,* 2011; Hodges & Gordon, 1991).

Targeting the EPS specifically is a relatively new field of therapeutic development, where the use of an EPS disrupter works alongside an antibiotic to allow for lower dosage of antibiotic to be used (Rajendran *et al.*, 2013). Ensuring full removal of biofilms, including persister cells, may help prevent the occurrence of multi-drug resistant microorganisms.

1.1.2 eDNA

Extracellular DNA (eDNA) is a recently identified component of the biofilm EPS. In *Aspergillus fumigatus* biofilms, it accounts for around 1-2% of biofilm biomass (Rajendran *et al.*, 2013). eDNA is proposed to contribute to a number of the properties associated with biofilms, but many aspects regarding the source and mechanisms for release of eDNA remain to be fully defined.

1.1.2.1 Origins of eDNA

The predominant source of DNA for eDNA in biofilms is hypothesised to be bacterial chromosomal DNA: this has been shown in *P. aeruginosa*, where chromosomal markers and random amplification has been used to show eDNA is of chromosomal origin (Muto *et al.*, 1986; Steinberger *et al.*, 2005; Allesen-Holm *et al*., 2006). Despite the predominance of bacterial-derived eDNA, it should be noted that fungal chromosomal DNA can contribute to biofilm eDNA, as shown for *Aspergillus fumigatus* (Shopova *et al.*, 2013), and host DNA has been found to contribute to eDNA networks in disease-related biofilms, such as cystic fibrosis (Goodman *et al.*, 2011; Wilton *et al.,* 2015). It is possible that neutrophil extracellular traps (NETs), made up of DNA, may also be degraded and remodelled into the EPS (Vorkapic *et al.*, 2016; Lethem *et al*., 1990).

1.1.2.2 Potential DNA release mechanisms

The precise mechanisms which control the release of eDNA from bacteria are currently little understood, but there is evidence for both active and lysis-dependent DNA release. Active DNA release may occur via ATP-driven excretion from viable cells, e.g. by a type IV secretion system or via the conjugative apparatus. The former has been shown for early stage *Enterococcus faecalis* biofilms (Barnes *et al.*, 2012). By contrast, in *P. aeruginosa* biofilms, eDNA predominantly appears to be released by a sub-set of dead cells (Wang *et al.*, 2015).

There are a number of ways in which bacterial cell lysis can be induced. Environmental extremes such as salt concentration, temperature and pH may result in bacterial autolysis (Ramírez-Nuñez *et al.*, 2011), therefore releasing DNA. Explosive cell lysis, induced by stressors such as genotoxic or antimicrobial compounds, can occur in *P. aeruginosa* biofilms (Turnbull *et al.*, 2016). Unlike traditional cell lysis, explosive cell lysis results in membrane fragmentation and the formation of membrane vesicles, which have been found to contain eDNA (Turnbull *et al.*, 2016). Generation of membrane vehicles has also been associated with eDNA in a lysis-independent release mechanism. Membrane vesicles containing eDNA have been found for *P. aeruginosa* (Renelli *et al.*, 2004). In *Streptococcus mutans*, the presence of eDNA in membrane vesicles has also been shown and relies on the presence of housekeeping transpeptidase SrtA (Liao *et al.*, 2014), implicating bacterial surface proteins in this potential mechanism of eDNA release.

Lysis in bacterial cells can also be triggered by lysogenic bacteriophages. For example, prophages are encoded on the chromosome of *Streptococcus pneumoniae*, and spontaneous induction, or induction by genotoxic stressors (Turnbull *et al.*, 2016), of these prophages results in fractional lysis of the bacterial population (Carrolo *et al.*, 2010). Such a lysis event could allow genomic DNA to exit bacterial cells for incorporation into an eDNA network.

Inter-bacterial communication can trigger lysis events in a controlled manner. A controlled lysis event may be fratricidal or suicidal (Montanaro *et al.*, 2011). A fratricidal event would involve signals from other bacteria inducing a cell to die, whereas a suicidal event would be cell death triggered as a response to its own signals. As Gram-positive bacteria grow in a biofilm, quorum sensing is used in some species to monitor and respond to the environment - such systems have been observed in *Bacillus subtilis*, *Streptococcus pneumoniae* and *Staphylococcus aureus* (Kleerebezem *et al.*, 1997). In QS, peptide pheromones are recognised by two-component regulatory systems. The effect of quorum sensing is alteration of gene expression, for example to modulate competence, antimicrobial peptide production or virulence (Miller & Bassler, 2001; Kleerebezem *et al.*, 1997). Quorum sensing and pheromone signalling have both

been implicated in eDNA release (Montanaro *et al.*, 2011). For example, in *Staphylococcus aureus*, quorum sensing system TraP regulates peptidoglycan synthesis, which appears to alter cell lysis and therefore eDNA release, promoting biofilm formation (Brackman *et al.*, 2016). In *P. aeruginosa*, quinolone quorum sensing known as the *Pseudomonas* quinolone signal, is a predominant quorum sensing system in this bacterium (Fernandez-Pinar *et al*., 2011). This system has been implicated in alteration of many behaviours in biofilm formation, including eDNA release (Thomann *et al,* 2016).

Controlled cell lysis is often regulated by autolysins; proteins which digest the peptidoglycan of the bacterial cell wall, leading to cell rupture. These peptidoglycan hydrolases were first recognised to have a role in cell wall remodelling, possibly during cell division (Shockman *et al.*, 1996). Further work in *Streptococcus gordonii* found they were also involved in the cell stress response (Liu & Burne, 2011). Likewise, in *S. mutans*, calcium ion concentration was shown to signal via VicK, a sensor kinase important for stress tolerance, resulting in autolysin activation, cell lysis and eDNA release (Jung *et al.*, 2017). Hydrogen peroxide has also been implicated as a signal molecule in eDNA release via autolysins. In *S. gordonii*, this signal has been associated with two autolysins, AtlS and LytF (Montanaro *et al.*, 2011; Xu & Kreth, 2013). In *E. faecalis*, quorum sensing and autolysis are linked in a fratricidal mechanism and under tight control. The quorum sensing system induces release of autolysin AtlA. Cells can be protected by SprE, which sequesters AtlA and prevents the lytic response, but a sub-population of cells are not protected and so are lysed (Thomas *et al.*, 2009).

Another potential lysis-dependent mechanism for eDNA release is via cyclic di-AMP signalling. Cyclic di-AMP is a well-recognised second messenger which modulates bacterial fitness, virulence and biofilm formation (Peng *et al.*, 2016). Cyclic di-AMP has been implicated in eDNA release in *Staphylococcus. aureus*, where downstream signalling via GdpP and XdrA was shown to alter gene expression, changing the properties of the cell surface (Defrancesco *et al.*, 2017). Altered cell surface homeostasis is proposed to destabilise the cell membrane, resulting in cell rupture and DNA release.

1.1.2.3 Potential roles of eDNA

DNA is used to store genetic information. eDNA can therefore be used to facilitate the acquisition of a mutation within a biofilm population (Steenackers *et al.*, 2016) by naturally-occurring transformation, a type of horizontal gene transfer (Li *et al.*, 2016). Furthermore, horizontal gene transfer rates are usually higher in biofilm phase, as opposed to planktonic phase culture (Madsen *et al*., 2012).

DNA is a very stable molecule, (with half-life of years, as opposed to minutes for RNA (Morten *et al.*, 2012; Chen *et al*., 2008)) which is required for long term information storage. This stability may be exploited to give mechanical strength to the biofilm matrix. For example, *P. aeruginosa* biofilms lacking eDNA are impaired in biofilm development (Petrova *et al*, 2011). eDNA has been implicated in relaxation of the biofilm following the application of mechanical stress in a variety of bacterial genera, including *Staphylococcus* and *Streptococcus* (Peterson *et al.*, 2013 (A)). DNA may also act as a structural scaffold. This is seen in *P. aeruginosa* biofilms, where eDNA allows for self-organisation of bacteria at the leading edge of the biofilm (Gloag *et al*., 2013). The organisation guides biofilm growth and maintains the nutrient and water flow through a series of furrows (Gloag *et al.*, 2013).

eDNA can promote development of biofilms by influencing adhesion events (Tang *et al.*, 2013). In *Listeria monocytogenes*, it is necessary for initial adhesion and early biofilm formation (Harmsen *et al.*, 2010). eDNA appears to promote bacterial attachment to both hydrophilic and hydrophobic surfaces in several Gram-positive bacteria, such as *Staphylococcus epidermidis*, *Staphylococcus aureus* and *Streptococcus mutants* (Das *et al.*, 2010). Furthermore, eDNA can facilitate non-specific, longer-range interactions between the substratum and bacteria – this has demonstrated by Das *et al.*, 2011 in *Streptococcus mutans*, *Pseudomonas aeruginosa* and *Staphylococcus epidermidis*. In *S. mutans* and *Staphylococcus epidermidis*, presence of eDNA causes bacterial cells to adhere to both surface types more quickly and in greater numbers (Das *et al.*, 2010). Adhesion to hydrophilic surfaces appears to occur

partially via acid base interactions facilitated by eDNA (Das *et al.*, 2010). These forces are thought not only to mediate bacterial: surface interactions, but also interbacterial interactions, increasing the cohesive strength of the biofilm. Similar to acid base interactions, eDNA can mediate adhesion by charge. eDNA in *Staphylococcus epidermidis* cultures resulted in bacteria with a highly negatively charged surface, potentially facilitating stronger adhesion to positively charged surfaces (Okshevsky & Meyer, 2015). Acidification, also modulated by eDNA, can trigger biofilm formation in some *Streptococcus* strains (D'urzo *et al.*, 2014). eDNA can also facilitate aggregation of bacterial cells (Jung *et al.*, 2017), an important step in biofilm initiation. Such effects are thought to be facilitated by the hydrophobicity provided by eDNA (Das *et al.*, 2010).

In addition to a structural role as a large and stable molecule, eDNA can serve a protective role chemically to biofilms. In *P. aeruginosa*, biofilms lacking eDNA are more susceptible to disruption by SDS (Allesen-Holm *et al.*, 2006). eDNA can also be protective by reducing the efficacy of anti-microbial agents against biofilms (Rajendran *et al.*, 2013). In *P. aeruginosa* biofilms, eDNA sequesters metal ions to trigger a transcriptional event which alters the lipoprotein composition at the cell surface, making the bacterium more resistant to antimicrobials (Okshevsky & Meyer, 2015). Bacteria also use eDNA production as a defence following sub-lethal antibiotic treatment of biofilms (Song *et al.*, 2016). In *P. aeruginosa*, eDNA acidifies the biofilm and causes downstream signalling via a two-component regulatory system which increases resistance to aminoglycosides (Wilton *et al.*, 2016) – a class of antibiotics. This results in changes to surface chemistry to prevent drug uptake by the bacteria, and turns on the type VI secretion system (Wilton *et al.*, 2016), which has been linked to virulence and increases drug resistance (Wang *et al.*, 2018). eDNA not only reduces the efficacy of therapeutic antimicrobials, but also human antimicrobial peptides, for instance , in *Haemophilus influenzae*, anionic eDNA binds to and sequesters the cationic human antimicrobial peptide β-defensin (Jones *et al.*, 2013), thus impairing the bacterial membrane permeabilization and inhibition of bacterial synthesis pathways typically caused by β-defensin (Sass *et al.*, 2008).

Sugars and phosphate which comprise the backbone of DNA may additionally act as a nutrient store (Rajendran *et al.*, 2013). Some bacterial strains, such as *Vibrio cholerae*, induce uptake of nucleosides when they are free-growing in low nutrient environments (Schild *et al.*, 2007; Vorkapic *et al.*, 2016). However, little work has been conducted to date on the potential for bacteria to use eDNA as a nutrient source when grown in biofilms.

1.1.2.4 Effects of eDNA removal and therapeutics

In vivo, eDNA can be digested by bacterial DNases, which may allow for bacterial release from the biofilm. For example, DNA degradation has been shown to be important in *Staphylococcus aureus* and *S. mutans* biofilm dispersal (Liu *et al.*, 2017). Nuc1, a nuclease from *Staphylococcus aureus* can disrupt the biofilm forming capability of many different bacteria, such as *Pseudomonas aeruginosa*, *Actinobacillus pleuropneumoniae*, and *Haemophilus parasuis* (Tang *et al*., 2013). NucB, an endonuclease from *Bacillus licheniformis*, can disperse biofilms and has the potential to be used a therapeutic agent (Basle *et al.*, 2018). Whilst DNase treatment is effective on many biofilm forming bacterial species, an exception of *Fusobacterium nucleatum* and *Porphyromonas gingivalis* biofilm has been identified *in vitro* (Ali Mohammed *et al.*, 2013). Anti-biofilm therapeutic strategies are therefore being developed based on the addition of exogenous DNase.

The use of DNase to treat disease is already seen in the clinic for cystic fibrosis (CF), a disease which manifests in reduced clearance of DNA-containing sputum from the lungs. The morbidity and mortality of the disease is compounded by the formation of biofilms by bacterial pathogens in the lungs, which can cause pneumonia. Treatment of cystic fibrosis patients with human DNase I (Pulmozyme®) reduces rates of infection and inflammation, and results in improved lung function (Cramer & Bosso, 1996; Konstan & Ratjen, 2012). Much of the DNA in CF sputum is human (Lethem *et al.*, 1990), however, some is bacterial (Feigelman *et al.*, 2017). Pulmozyme® cleaves DNA resulting in less viscous sputum which is more easily cleared (Brandt *et al.*, 1995). Pulmozyme®

can also be used to treat other lung conditions where disease from bacterial infection is a risk factor, such as collapsed lung (pulmonary atelectasis) (Thornby *et al.*, 2014).

For several species, DNase treatment can make other traditional antimicrobials more effective against biofilms by increasing the penetration of antibiotics into the biofilm (Tetz *et al.*, 2009). DNase and antibacterial co-therapy can be effective in both topical and systemic infections (Okshevsky & Meyer, 2015; Czaikoski *et al.*, 2016). This work highlights the broad and important impact that targeting eDNA within biofilms may have on diseases caused by both Gram-positive and Gram-negative organisms.

1.2 The oral cavity

1.2.1 Components of the oral cavity

The oral cavity consists of hard and soft surfaces. Soft surfaces are the cheeks (buccal mucosa) and lips, tongue, gums (gingivae), salivary glands and the hard and soft palate (Figure 1.2). The gums partially encase the hard tissue i.e. teeth. The hard palate divides the oral and nasal cavity, and the soft palate is made of muscles and used for swallowing and breathing. The salivary glands produce saliva. The oral cavity has, on average, a surface area of 214.7 cm^2, of which approximately 20% is teeth and 80% is epithelium (Collins & Dawes, 1987).

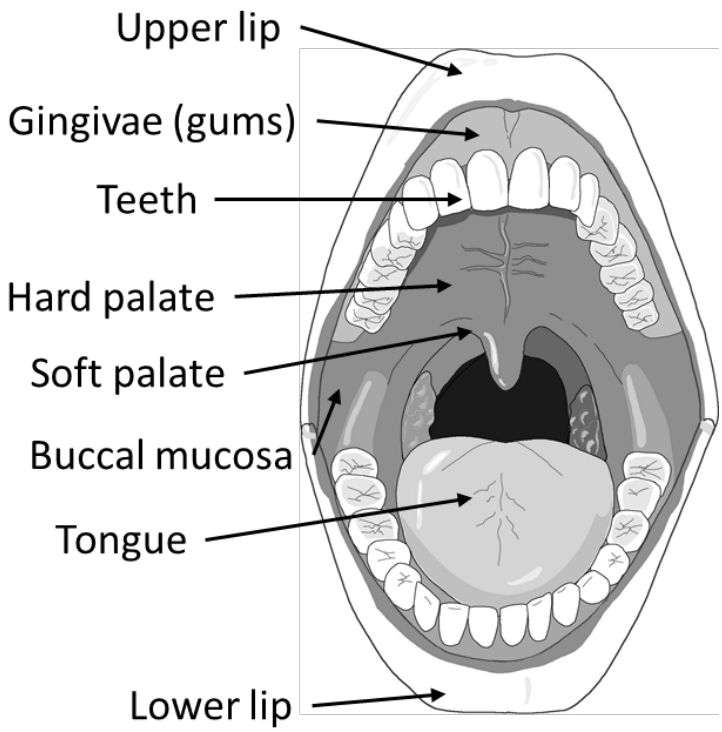

Figure 1.2 - Anatomy of the human mouth
(Unlabelled diagram sourced from anatomyid.com, 2017)

Teeth are hard structures in the mouth. They are coated in a layer of highly mineralised enamel, which surrounds dentin (Goldberg *et al.*, 2012). Dentin consists of collagen-containing proteins which form tubules (Goldberg *et al.*, 2012). Enamel and dentin form a protective layer over the dental pulp, through which blood is supplied from the root of the tooth to the crown (Yu & Abbott, 2012). Following eruption, the teeth are rapidly coated in the acquired salivary pellicle (Hannig, 2002). Salivary pellicle is glycoprotein layer which serves to partially protect the teeth from acid damage, but also acts as a substratum for bacterial adhesion (Huang *et al*., 2011).

1.2.2 Saliva

Saliva is a complex solution which serves multiple roles. The primary role is lubrication of the oral surfaces and initiation of starch digestion (Iorgulescu, 2009). Typical salivary flow in healthy mouths (at swallowing) is approximately

300-400 µl/minute (Iorgulescu, 2009). Saliva bathes the oral surfaces and this flow allows loosely attached microorganisms to be washed away and swallowed (Tiwari *et al*., 2011). Saliva also facilitates the formation of the acquired salivary pellicle on teeth.

Saliva contains ions such as phosphate and carbonate which aid buffering to maintain a consistent pH within the mouth (Iorgulescu, 2009. Calcium ions within saliva help prevent enamel demineralisation (Hegde & Sajnani, 2017). Saliva is usually around pH 6-7 but can be as low as pH 5 in low flow and pH 8 in high flow (Baliga *et al*., 2013). If the pH falls below 5.5, this can trigger enamel demineralisation (Struzycka, 2014).

Many components of saliva are antimicrobial, such as mucins. Salivary mucins MG1 and MG5 form part of the salivary pellicle and can prevent bacterial attachment directly to the tooth surface and shields the teeth from dietary acid (Frenkel & Ribbeck, 2015). MG2 has been shown to induce aggregation in *S. mutans*, which may lead to increased clearance by swallowing (Heo *et al.*, 2013). Saliva also contains immunoglobulins (Igs). IgA predominates, but IgG and IgM are also present (Grönblad, 1971). These Igs are produced in response to bacterial colonisation and form part of the innate immune system (Marcotte & Lavoie, 1998). Saliva also contains several antimicrobial peptides, proteins and enzymes (Humphrey & Williamson, 2001). One such enzyme is lysozyme, which cleaves peptidoglycan of the bacterial cell wall, causing cells to rupture (Humphrey & Williamson, 2001). Saliva also contains glycoproteins – a major component of saliva is gp-340 (salivary agglutinin) (Gunput *et al*., 2016). When in solution, gp-340 can mediate agglutination, an antibacterial mechanism which induces bacterial clumping and subsequent removal by salivary flow or clearance by neutrophils, for instance as demonstrated in Itzek *et al.*, 2017 with *Streptococcus gordonii*. By contrast, gp-340 can also serve as a target for microbial attachment, as seen in the case of *S. gordonii* surface proteins SspA/B which bind to gp-340 (Ito *et al.*, 2017). Additionally, salivary components can be incorporated into oral biofilms and used as a nutrient source, for instance in *Streptococcus mitis* and *Streptococcus mutans* biofilms (Kindblom *et al*., 2012).

1.2.3 Oral microbes and the human host

Bacteria from the oral cavity were the first bacteria to be described: in 1683 Antonie van Leeuwenhoek viewed bacteria from his own mouth using a single lens microscope. Since then, it has been shown that the mouth can be colonised by over 800 different species of bacteria (Sands *et al.*, 2016). These form multispecies biofilms (Dewhirst *et al.*, 2010), with an individual healthy mouth being colonised by between 100 and 200 species at a time (Kolenbrander *et al.*, 2010). Healthy mouths have a more diverse oral microbiome than unhealthy mouths, but antibiotic treatment can reduce microbiome diversity (Cabral *et al.*, 2017). Dental plaque is a common multispecies biofilm which forms mainly at the gingival margins of the tooth (Rüdiger *et al*., 2002) and can be removed by mechanical force e.g. tooth brushing (Terézhalmy *et al*., 2008).

The oral microbiota experiences changes in pH, salivary glucose and temperature due eating and drinking (Pachori *et al.,* 2017; Moore *et al.,* 1990; Puttaswamy *et al.,* 2017) and shear stress due to continuously flowing saliva (Fernández *et al*., 2017). Microbes also experience different oxygen levels (oxygen tension) depending on their location within the oral cavity, which appears to influence the microbiological composition at a given site (Loesche *et al.,* 1983). The oral cavity presents a wide variety of niches for bacterial colonisation, and switching to growth in biofilm phase may facilitate persistence of these microorganisms in this changeable environment (Balaban *et al*., 2004).

Oral microbes may be beneficial to the human host. These include mediating anti-inflammatory properties and preventing colonisation by pathogens (colonisation resistance) (Kilian *et al*., 2016). Oral dysbiosis however, can lead to not only oral diseases, but has also been hypothesised to affect a range of conditions from cardiovascular disease to pregnancy outcomes (Kilian *et al.*, 2016). It has also has been implicated in increased inflammatory diseases, such as rheumatoid arthritis (Lee & Kim, 2017).

Overgrowth of dental plaque can lead to gingivitis i.e. inflammation of the gingivae. The host produces a disproportionate response to these biofilms, which leads to aberrant inflammation (Cekici *et al.*, 2000). Continued inflammation can lead to periodontitis, where connective tissue and bone destruction occurs which can lead to tooth loss (Kilian *et al.*, 2016). Periodontitis is the most common chronic disease which affects humans, and is thought to affect around 14% of the global population (Rocco *et al.*, 2016).

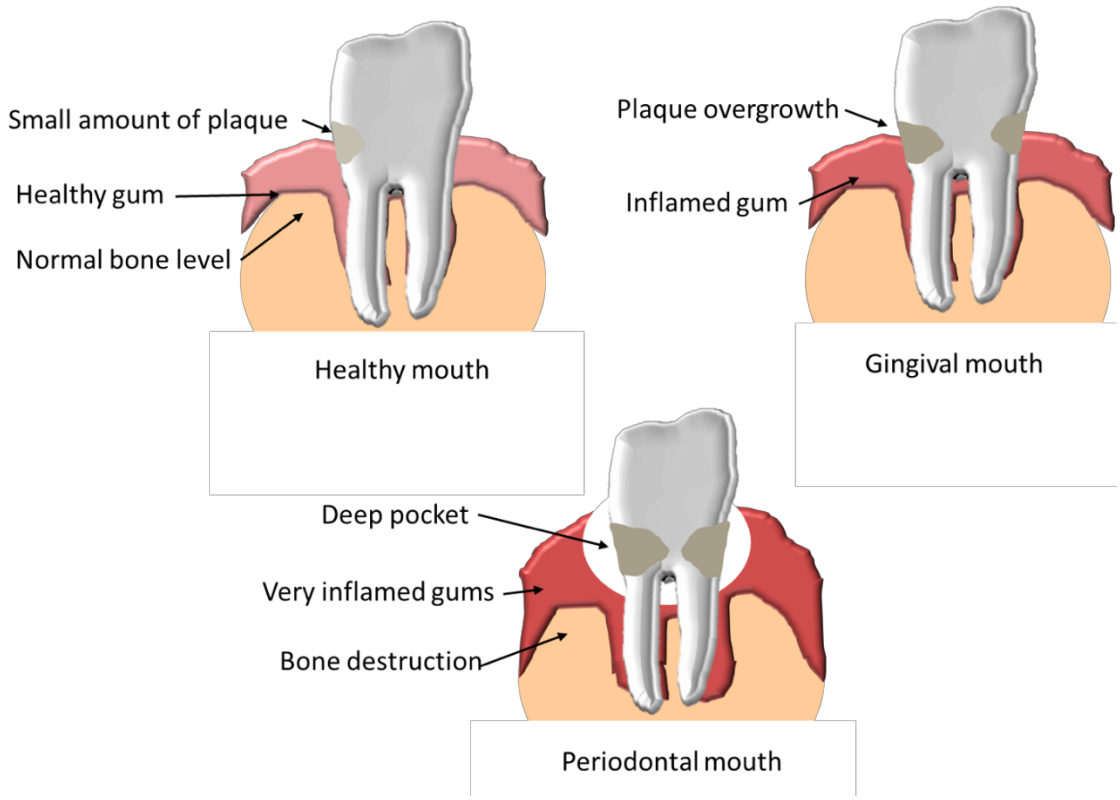

Figure 1.3 – Development of periodontal disease. Excess plaque causes gum inflammation, shifting the mouth from a healthy to gingival state. Continued inflammation at the gum line leads to bone destruction and potentially tooth loss in a periodontal mouth.

1.2.4 Oral microbes and plaque accretion

1.2.4.1 Salivary pellicle interactions

Plaque accretion relies heavily on interactions between oral bacteria and the salivary pellicle and on interbacterial interactions. *Actinomyces*, *Streptococcus*, *Haemophilus*, *Veillonella* and *Neisseria* species are all early colonisers in the oral environment (Huang *et al*., 2011). Different microbes colonise different areas of the human oral cavity. *Streptococcus* bacteria, which dominate the oral cavity (Aas *et al.*, 2005), are found almost ubiquitously, but species belonging to the genus *Haemophilus* are more prevalent at the buccal mucosa and *Actinomyces* at the sub-gingival level (Huttenhower *et al.*, 2012). Primary colonisers have capacity to adhere to a range of host substrata, including salivary pellicle. This can be via specific or non-specific interactions.

Non-specific interactions include those mediated by Van der Waals forces, electrostatic interactions and acid-base interactions (Heo *et al.*, 2013). These are non-covalent interactions, the total of which form the extended DVLO theory, whereby thermodynamic interactions with a surface can be predicted (Bostrom *et al.*, 2006). This theory relies on the system moving to the state of most free energy (lowest energetic state). A subset of acid-base interactions are hydrophobic interactions. In an environment which contains an aqueous phase, such as the saliva of the oral cavity, hydrophobic interactions are especially important. Thus the initial attachment of bacterial cells in saliva to the acquired salivary pellicle on the tooth surface is mediated predominantly by hydrophobic and electrostatic interactions at long range (Van Oss *et al.*, 1995).

Shorter range interactions then come into play and these are usually specific - these may involve proteins on the bacterial cell surface with specific binding capacities i.e. adhesins which recognise unique ligands (Nobbs *et al.,* 2007). Many direct specific interspecies and host interactions have been characterised for key members of the plaque oral microbiota, including *S. gordonii* - these

interactions can be mediated by several different families of surface proteins and are covered in section 1.3.2.

1.2.4.2 Coaggregation

Bacterial clumping (aggregation) is an important step of biofilm initiation and development. Bacteria may auto-aggregate, but another critical mechanism which facilitates aggregation is co-aggregation with a different species. For instance, *S. gordonii* can co-aggregate with *Actinomyces oris* (Back *et al*., 2015). Co-aggregation promotes persistence of bacterial colonisation (Khemaleelakul *et al.*, 2006). *Fusobacterium nucleatum* is an organism which co-aggregates with many different oral bacterial genera, including *Streptococcus*. In the oral cavity, *F. nucleatum* serves as a bridging organism between early and late colonising organisms (Merritt *et al.*, 2009). *F. nucleatum* cannot interact well with the salivary pellicle directly, so relies on the presence of primary colonisers, such as *S. gordonii*, to adhere to the tooth surface. It binds *S. gordonii* using two surface adhesins, RadD and CmpA (Lima *et al.*, 2017) (Figure 1.8H). As a bridging organism, *F. nucleatum* also binds to late colonising species, such as *P. gingivalis* (Park *et al.*, 2016), which is a major causative agent of periodontal disease. Secondary colonisers are more commonly Gram-negative bacterial species, which bind to primary colonisers to facilitate their incorporation into the oral biofilm. They are incorporated later into the biofilm and are more commonly associated with disease. They are usually not able to bind to the salivary pellicle directly (Rosan & Lamont, 2000), and their adhesion relies more heavily on specific interactions. One such Gram-negative bacterium, *P. gingivalis* is a major periodontal pathogen (How *et al*., 2016). The incorporation of this bacterium into the biofilm is upregulated by the presence of the primary coloniser *S. gordonii* (Cook *et al*., 1998).

1.2.4.3 Metabolic and chemical interactions

Whilst physical interactions between oral microbes are critical for dental plaque formation, is it important to note that chemical interactions also influence the development of these multispecies communities. These relationships may be symbiotic or competitive. One example is the interaction which *S. gordonii* makes with *Veillonella atypica*, another primary coloniser of the clean tooth surface. Using small diffusible molecules which have not yet been identified, *V. atypica* upregulates carbohydrate fermentation in *S. gordonii* to produce lactic acid, which *V. atypica* then utilises (Egland *et al.*, 2004). In turn, the removal of lactic acid by *V. atypica* raises the local pH, preventing the pH stress and toxicity to *S. gordonii* which would otherwise result from acid accumulation (Johnson *et al.*, 2009). This partnership is driven by a metabolic dependency of *V. atypica* on *S. gordonii*, but is beneficial for both.

Actinomyces naeslundii gains an advantage in colonisation by being able to interact with *S. gordonii* physically and colonise hard oral surfaces, but this relationship is also symbiotic due to chemical interactions. *A. naeslundii* induces *S. gordonii* to produce arginine, facilitating survival in arginine-depleted environments (Jakubovics *et al.*, 2008 (A)). In kind, production of arginine serves to protect *A. naeslundii* from oxidative stress caused by the hydrogen peroxide produced by *S. gordonii* (Jakubovics *et al.*, 2008 (B)). Another relationship may be based on alteration of the oxygen environment by one organism to benefit another. Bacteria like *F. nucleatum* and *S. gordonii* are facultatively anaerobic and reduce the oxygen in the local environment, which allows for growth on anaerobic organisms such as *P. gingivalis* in this oxygen depleted environment which would not otherwise be possible (Bradshaw & Marsh, 1998).

As mentioned, these interspecies interactions are not always symbiotic, as exemplified by the production of bacteriocins. Bacteriocins are a group of proteinaceous toxins which are produced by one bacteria and negatively affect another. Through the generation of bacteriocins, *S. mutans* is able to out-compete several oral streptococci including *S. gordonii* (Tanzer *et al.*, 2012). However, *S. gordonii* presence in a biofilm can influence *S. mutans* to reduce

bacteriocin production via quorum sensing, and thus allowing *S. gordonii* to persist within its environmental niche (Wang & Kuramitsu, 2005).

Taken together, these physical and chemical interactions make up a highly complex network of inter-species and inter-kingdom relationships within the biofilms in the oral cavity.

1.3 *Streptococcus* bacteria

Streptococcal species, from the Greek "streptos" meaning chain and "coccus" meaning sphere, are Gram-positive, facultatively anaerobic bacteria. Streptococcal species are largely found as part of the resident (commensal) microbiota of their hosts, but can serve as opportunistic pathogens or true pathogens. For example, *S. pneumoniae* is the main causative agent of community-acquired pneumonia (File, 2014). The World Health Organisation estimates around 1.5 million deaths occur per year in children under 5 due to pneumonia (Krzysciak *et al.*, 2013).

The genus *Streptococcus* can be divided into seven taxonomic groups based on 16S rRNA sequence (Figure 1.4). These are pyogenic, anginosus, mitis, sanguinis, salivarius, bovis and mutans. Commonly occurring oral streptococci belong to all of these groups, except for pyogenic and bovis. Another frequently used classification for these bacteria is the viridans group streptococci (VGS). The species within this group are either α- or non-haemolytic. Many of the oral streptococci can be classified as VGS.

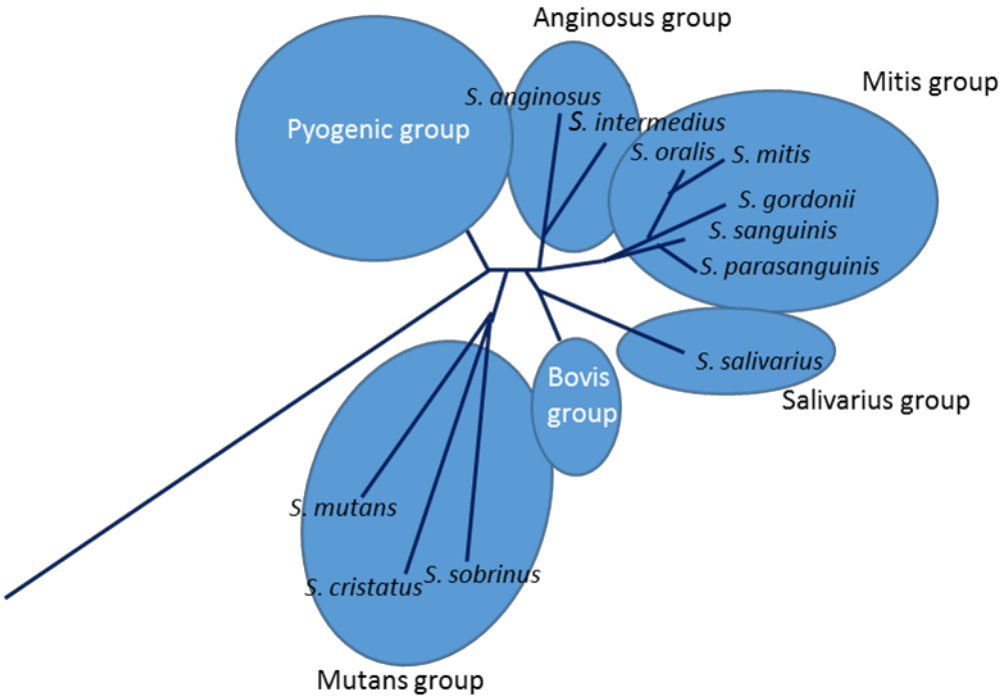

Figure 1.4 - Taxonomic classification of oral streptococci based on 16S rRNA sequence, using the neighbour joining method, where increased distance between species indicates increased heterology in sequence. Based on Kawamura et al., 1995.

.

Carriage of some oral streptococci, such as *Streptococcus sanguinis* and *S. gordonii*, has been associated with oral health, while that of other oral streptococci, such as *Streptococcus mutans* and *Streptococcus sobrinus*, has been associated with disease (Kreth *et al.*, 2008). *S. mutans* is a major causative agent of dental caries (tooth decay). The presence of fermentable carbohydrates, especially sucrose, in the oral cavity increases *S. mutans* growth. Metabolism of sucrose by *S. mutans* results in acid production, which decreases the local pH. Below pH 5.5, demineralisation occurs, which weakens the enamel and can result in cavitation (Forssten *et al.*, 2010). Untreated dental caries in permanent teeth is the most prevalent health condition globally, affecting 35% of the population (Frencken *et al.*, 2017). Carriage of *S. mutans* in saliva and sub-gingival plaque has also been associated with chronic periodontitis (Dani *et al.*, 2016), which affects around 10% of the global population (Frencken *et al.*, 2017).

1.3.1 *Streptococcus gordonii*

S. gordonii is part of the mitis group of *Streptococcus*, which are usually commensals. Like other members of the genus *Streptococcus*, *S. gordonii* appears as either chains or diplococci (Figure 1.5).

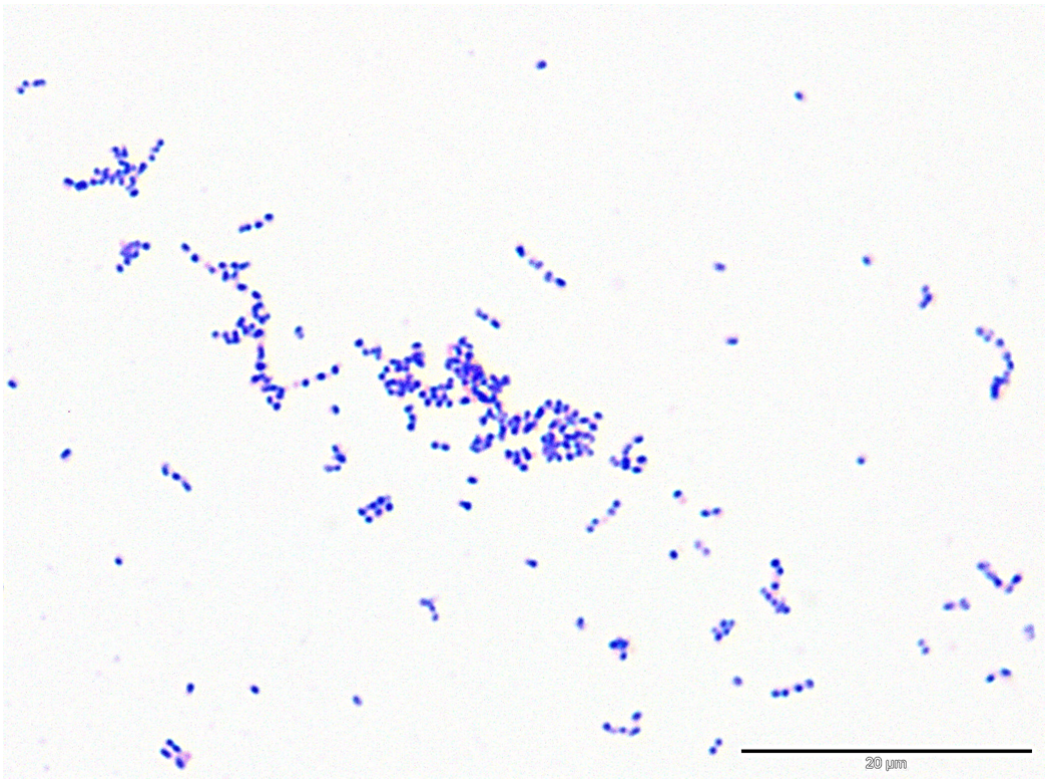

Figure 1.5 – Light micrograph of Gram-stained S. gordonii *DL1 showing diplococci and chain forms. Scale bar = 20 µm*

S. gordonii is a primary coloniser of the clean human tooth surface (Kreth *et al.*, 2009), and can modulate the other microorganisms within the plaque biofilm. The resulting pro- or dys-biotic microbiota (Langdon *et al.*, 2016) can predispose the mouth to oral health or disease. *S. gordonii* carriage and presence in oral biofilms has been associated with oral health and the lack of cariogenic species (Nobbs *et al*., 2009).

S. gordonii can also contribute to disease as an opportunistic pathogen, and is associated with infective endocarditis (IE) (Vogkou *et al*., 2016). IE is a disease of the myocardium, in which inflammation of the heart endothelium is

triggered by infection (Holland *et al*., 2017). *Staphylococcus aureus* is the most common causative agent of IE, followed by oral streptococcal species from the viridans group (Vogkou *et al*., 2016). These bacteria can enter the blood stream from the mouth either during dental work or normal abrasion, which can occur during eating or toothbrushing (Lockhart *et al*., 2009). Once in the blood stream, bacteria can travel to the heart valves. If damaged, for example due to a congenital defect or the result of heart surgery, the disturbed blood flow means that bacteria have the opportunity to attach to the damaged heart valves (Holland *et al*., 2017). Bacteria attached to the endothelium can then activate platelets and cause unwanted thrombus (clot) formation (Fitzgerald *et al*., 2006). If left untreated, IE is considered fatal (Horstkotte *et al*., 2004). The morbidity is caused by damage to the heart valves which results in regurgitation of blood back though the valves, meaning blood is no longer circulating properly, leading to death (Keynan & Rubinstein, 2013). Even with treatment, which includes antibiotics and possibly surgery on the damaged tissue to remove the thrombus (Wallace *et al.*, 2002), the mortality rate of IE remains around 20% (Alkhawam *et al*., 2016).

1.3.2 Streptococcal surface proteins

One of the main reasons for the success of oral streptococci such as *S. gordonii* as colonisers is their capacity to interact with multiple substrata. This is mediated, in large part, by an array of surface-expressed proteins, some of the major groups of which are detailed below.

1.3.2.1 Protein secretion

Gram-positive bacteria, such as streptococci, have a thick (20-80 nm) layer of peptidoglycan on their cell wall (Schneewind & Missiakas, 2014). When proteins are displayed externally, they are therefore often anchored onto the cell surface via this peptidoglycan layer. However, to access this layer, proteins must

first translocate across the cell membrane. This is usually initiated by a N-terminal signal sequence on the protein (Navarre & Schneewind, 1994), often YSIRK in *S. gordonii* (Bae & Schneewind, 2003). These signal sequences can control where a protein is targeted to, and thus where on the bacterial cell it is displayed (Dedent *et al.*, 2008).

There are three main secretion systems to move bacterial proteins across the cytoplasmic membrane: Sec, SecA2 and Tat. The Sec pathway and SecA2 usually transport unfolded proteins, whereas the Tat (twin arginine transport) pathway transports folded proteins. The Tat-pathway features TatB and TatC, which bind to folded proteins on the cytoplasmic side of the membrane and target the protein to the transmembrane transporter, TatA (Natale *et al.*, 2008). *S. gordonii* uses Sec for most proteins (secreted, membrane-bound and membrane-embedded), but SecA2, the accessory secretion system, is used for some specific proteins such as GspB, a heavy glycosylated LPxTG family protein (Bensing & Sullam, 2002). The proteins transported through the SecA2 pathway are more commonly associated with stress response or virulence. The SecA2 pathway works similarly to the Sec pathway, but features a different protein which plays a role homologous to SecA, SecA2, which has altered binding to the SecYEG translocon (Green & Mecsas, 2016).

To initiate the canonical Sec system, SecB or another cytosolic chaperone, bound to the unfolded target pre-protein, binds to SecA on the cytoplasmic side of the membrane and guides the target to the translocase complex SecYEG. SecA is a homo-dimeric protein which is an ATPase and provides the power required for transmembrane locomotion of the protein (Vrontou & Economou, 2004). In addition to ATP, proton motive force has been shown to speed up protein translocation, although is not essential (Duong & Wickner, 1997). SecA can also be bound by ribosomes, meaning that proteins are more likely to be excreted as soon as they are translated. SecYEG is a protein conducting channel which is formed of three proteins. Associated with this are three proteins, SecDF and YajC, which assist with targeting of the pre-protein on the cytoplasmic side to the translocase and regulating the action of SecA (Duong & Wickner, 1997). SecDF is powered by proton motive force and facilitates the ATP-independent

translocation of proteins through SecYEG (Tsukazaki *et al.*, 2011). YajC is a transmembrane protein which is complexed with SecDF (Fang & Wei, 2011). The exact function of YajC is still known, but loss of this protein reduces the amount of association of SecA to SecYEG, reducing protein translocation (Kato *et al.*, 2003). SecY spans the membrane 10 times, SecE three times and SecG twice. Together, they form a hetero-tetrameric channel (Veenendaal *et al.*, 2004). Following translocation of the nascent pre-protein through the SecYEG translocon, the leader peptide is cleaved to allow for the release of the mature peptide from the cell membrane (Bae & Schneewind, 2003) (Figure 1.6).

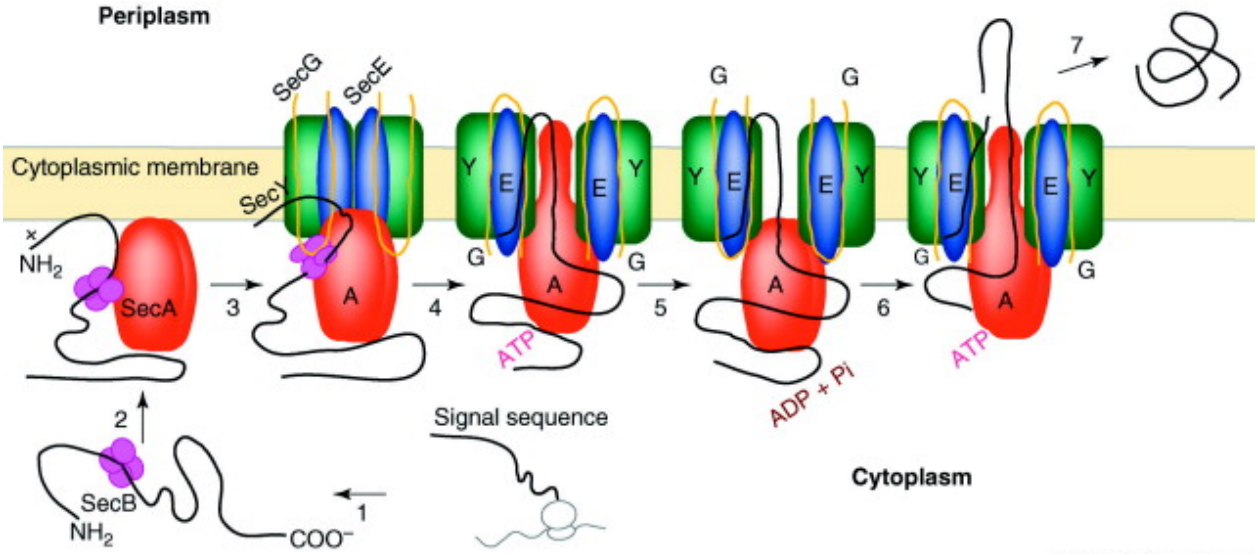

Figure 1.6 - Sec secretion system

1) *Cytoplasmic SecB or other cytosolic chaperone binds signal sequence (e.g. YSIRK) on pre-protein*
2) *SecB or other cytosolic chaperone binds to and transfers pre-protein to membrane associated SecA*
3) *SecA binds to transmembrane hetero-tetramer SecYEG*
4) *Pre-protein is fed into protein conducting channel*
5) *Hydrolysis of ATP by SecA allows for protein translocation*
6) *The signal peptide is cleaved*
7) *The protein is released or further bound on the periplasmic side of the membrane*

Diagram from Mori & Ito, 2001

1.3.2.2 Protein anchoring

One of the major groups of cell surface proteins associated with streptococcal colonisation and pathogenesis is the LPxTG family. These proteins

are so-called as they attach to peptidoglycan using an LPxTG motif, where X can be any amino acid (Navarre & Schneewind, 1994). The cysteine residue in the active site of membrane-associated housekeeping sortase A transpeptidase cleaves the amine bond before the threonine (T) residue of the LPxTG motif. This forms an acyl-enzyme intermediate which is resolved by nucleophilic attack of amino groups, typically provided by the lipid II precursor of peptidoglycan, to form a lipid-linked protein intermediate. The final stage is incorporation of the lipid II precursor, via the trans-glycosylation and transpeptidation reactions of cell wall synthesis, into the peptidoglycan of the cell wall. This results in the mature protein being covalently anchored into the cell wall and displayed on the cell surface (Hendrickx *et al.*, 2011) (Figure 1.7).

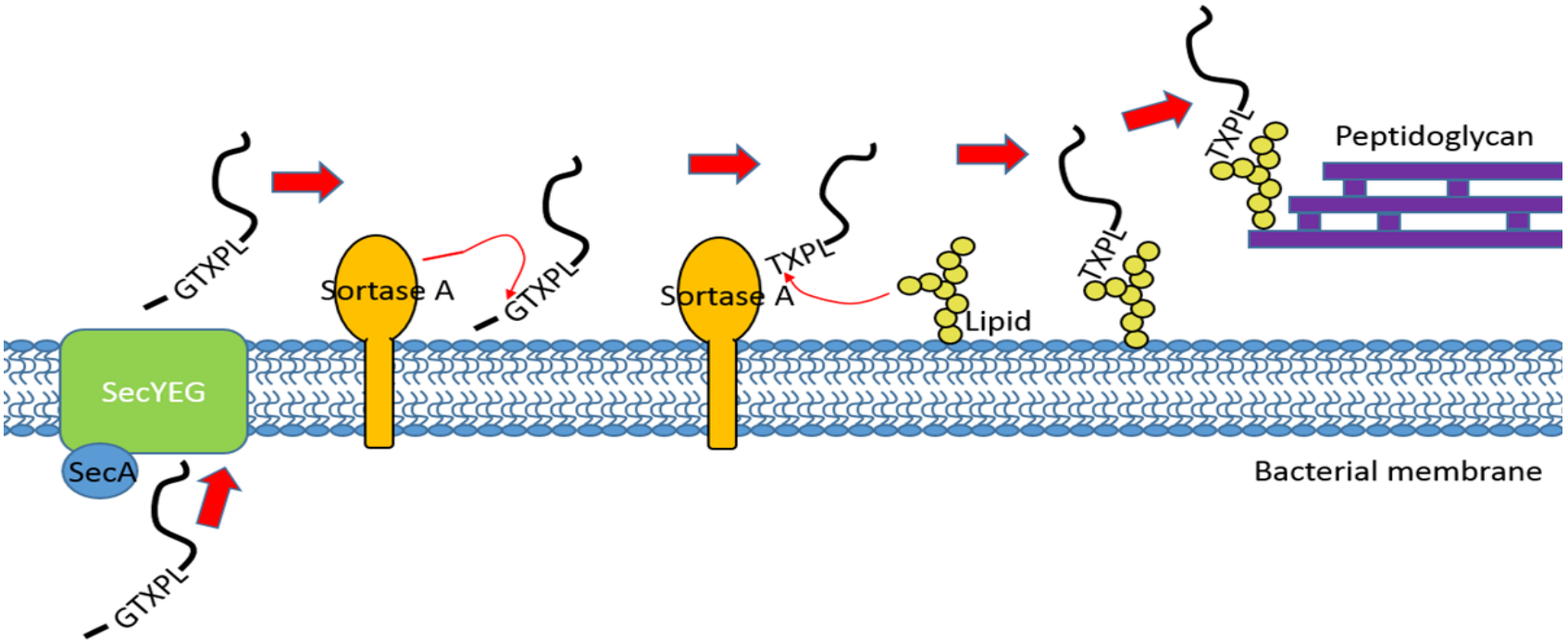

Figure 1.7 - ***Processing LPxTG proteins for display on Gram-positive bacterial cell walls*** *(Adapted from Hendrickx et al, 2011)*
An unfolded LPxTG motif-containing protein is transported across the bacterial membrane via the canonical Sec secretion system. It reacts with sortase A to form an acyl-enzyme intermediate. Nucleophilic attack from lipid A occurs, forming a lipid-linked intermediate. The lipid is then incorporated into peptidoglycan. The mature protein can then be displayed on the exterior of the Gram-positive bacterial cell

1.3.2.3 MSCRAMMs

MSCRAMMs (microbial surface component recognising adhesive matrix molecules) are bacterial proteins which bind to human targets to facilitate initial attachment to a host substratum. Their targets are often components of the human extracellular matrix (ECM). They are characterised as having two adjacent immunoglobulin-like folds in the N-terminal region (Foster et al., 2014).

Collagen is a major component of the human extracellular matrix and basement membrane. Several collagen binding MSCRAMMs have been identified, such as Cnm in *Streptococcus mutans*. This protein has been implicated systemic disease, for instance, infective endocarditis, where it facilitates the adherence of this bacteria to the cardiac endothelium (Nobbs *et al*, 2017). Collagen is also a major component of dentin. Collagen binding proteins, for example CbdA on *S. gordonii*, can bind to collagen found in dentin tubules, thus potentially facilitating bacterial persistence on the tooth surface (Moses *et al.*, 2013) (Figure 1.8.A).

Fibronectin is part of the host ECM and can be bound by CshA of *S. gordonii* (Back *et al*., 2017). This may enable *S. gordonii* to attach to epithelial cells in the oral cavity (Figure 1.8B), as well as to damaged cardiac endothelium during IE. Like many MSCRAMMS, CshA is multifunctional and has additionally been implicated in the binding of proteins on the surface of other bacterial species. For example, CshA has been implicated in mediating the interactions between *S. gordonii* and *S. oralis* (Mcnab *et al.*, 1996) (Figure1.8.C) and *S. mutans* (Figure 1.8D). However, the targets for CshA in these interactions are not known. CshA is a fimbrial surface protein. As such, it adopts a long, thin filamentous conformation, and has been shown to extend around 60 nm from the bacterial cell surface (McNab *et al.*, 1999). As for all fimbriae, this length means that CshA is able to make long distance interactions with its cognate receptors.

1.3.2.4 SRRPs

Serine-rich repeat proteins (SRRPs) are made of repeating domains which form around 80% of the protein and are serine-rich (Ramboarina *et al.*, 2010). Different strains of *S. gordonii* carry one of two SRRPs, Hsa and GspB, both of which can bind to sialic acid-containing moieties. Consequently, these proteins can target a number of components within the salivary pellicle, including salivary mucin (MG2) and gp-340 (Takamatsu *et al.*, 2006) (Figure 1.8A). Hsa is important in adhesion to salivary pellicle on teeth (Haworth *et al*., 2017) (Figure 1.8A). SRRPs facilitate colonisation of oral surfaces by the bacterium but can also contribute to IE. For instance, GspB is the predominant platelet binding protein on *S. gordonii* and is crucial to the pathogenesis of IE (Bensing *et al*., 2014), and Hsa of *S. gordonii* can activate platelets (Haworth *et al*., 2017).

1.3.2.5 Antigen I/II family proteins

Antigen I/II (Ag I/II) family proteins are expressed by virtually all streptococci indigenous to the oral cavity, including *Streptococcus gordonii*, *Streptococcus intermedius* and *Streptococcus mutans* (Jakubovics *et al*., 2005) and can adhere to a range of substrata, including salivary pellicle. *S. gordonii* expresses two Ag I/II family proteins, SspA and SspB - these proteins can bind to gp340, a component of saliva which is found in the acquired salivary pellicle (Ito *et al*., 2017) (Figure 1.8A). This facilitates *S. gordonii* adherence to a saliva coated surface (Ito *et al*., 2017). SspA/B can also interaction with epithelial cells (Nobbs *et al*., 2007 B) (Figure 1.8B), reducing cytokine production, which may subvert the innate immune system (Andrian *et al*., 2012): this has the potential to facilitate bacterial persistence. SspA/B have also been implicated in IE by triggering platelet aggregation (Kerrigan *et al.*, 2007).

Ag I/II proteins are implicated in the inter-microbial interactions required for the formation of cohesive oral biofilms (Silverman *et al.*, 2010;). For example, *C. albicans* is a pleomorphic fungus which is a major human opportunistic pathogen and colonises the oral cavity, in addition to the skin, gastrointestinal and

genitourinary tracts (Southern, *et al*., 2008). *C. albicans* is often co-localised with *S. gordonii* in dental plaque (Montelongo-Jauregui *et al.*, 2016), and it has been shown that binding of *S. gordonii* SspB to *C. albicans* surface protein Als3 is largely responsible for this physical interkingdom interaction (Silverman *et al.*, 2010) (Figure 1.8E). Whilst *C. albicans* can bind to salivary pellicle independently, interactions with *S. gordonii* can enhance biofilm formation (Jack *et al.*, 2015). In addition, *S. gordonii* can disrupt *C. albicans* farnesol signalling to stimulate candidal filamentation, a process that could potentially promote *C. albicans* carriage and pathogenicity (Bamford *et al.*, 2009). *A. oris* is another primary coloniser of the clean tooth surface and can also co-aggregate with *S. gordonii*. Again, this interaction is mediated by SspB, which binds to polysaccharide on the surface of *A. oris* (Back *et al.*, 2015) (Figure 1.8F). SspB also binds to Mfa1 on the surface of *P. gingivalis*, a major periodontal pathogen, thus facilitating its incorporation into an *S. gordonii* biofilm (Figure 1.8G) (Lamont *et al*., 2002).

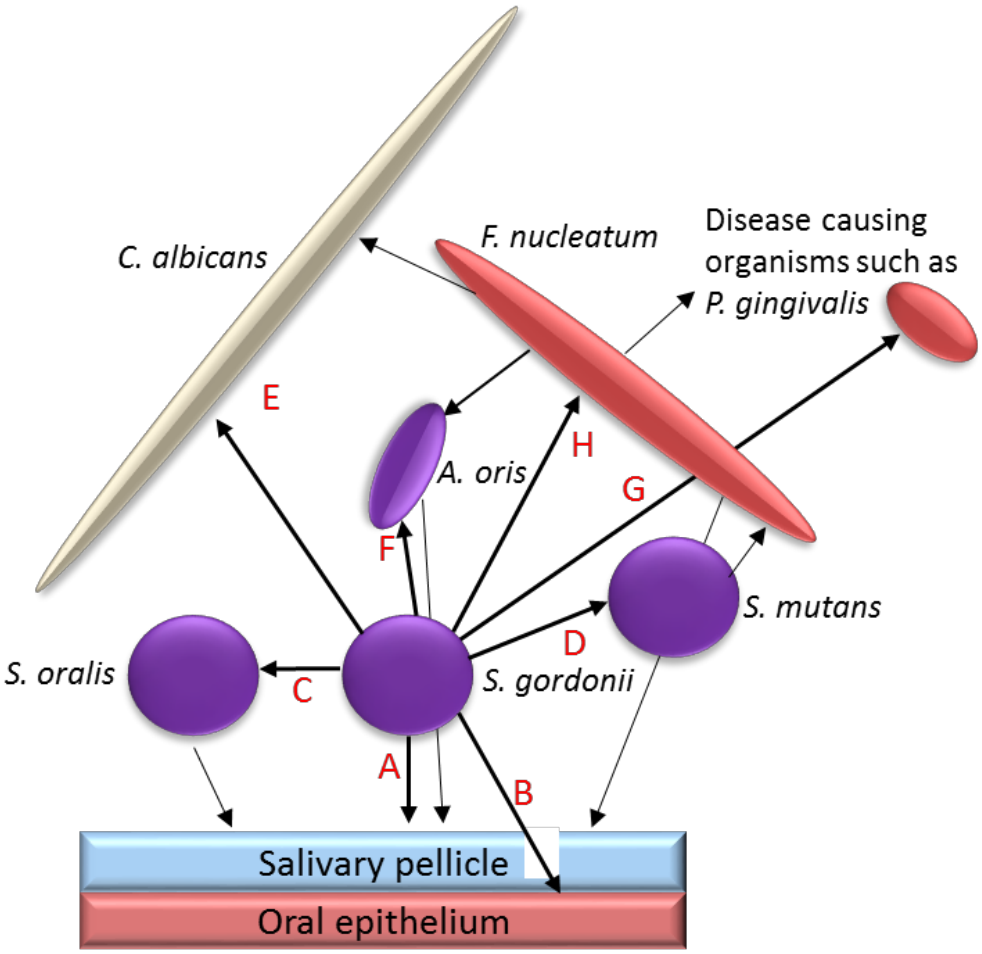

Figure 1.8 – S. gordonii direct interactions in the oral cavity
S. gordonii adhesin and target
A) Hsa and GspB - salivary agglutinin (gp-340) and salivary mucin MG2 in salivary pellicle, Cnm – collagen on dentine tubules
B) CshA - fibronectin on human epithelium, SspB – epithelial cells
C) CshA - S. oralis (receptor unknown)
D) CshA - S. mutans (receptor unknown)
E) SspB - Als3 on C. albicans
F) SspB – Polysaccharide on A. oris
G) SspB - Mfa1 P. gingivalis
H) Unknown S. gordonii receptor(s) - CmpA and RadD on F. nucleatum

1.4 Aims and objectives

S. gordonii is a primary coloniser of the clean tooth surface and can modulate development of the oral plaque biofilm towards health or disease. The interactions that *S. gordonii* makes as a primary coloniser and as part of the

plaque biofilm are mediated, in large part, by surface proteins. However, not all of these surface proteins have been fully characterised with regards to *S. gordonii* colonisation and pathogenesis. Furthermore, very little is understood about how bacterial surface proteins may be associated with the presence of eDNA within biofilm EPS, despite the potential for eDNA to serve as a target in the development of novel therapeutic agents. The aim of this research was therefore to advance understanding of the role of LPxTG family proteins in *S. gordonii* colonisation and pathogenesis, with particular focus on their involvement in biofilm development and the presence of eDNA.

The specific objectives of this project were to:

1) Investigate the production of eDNA in *S. gordonii* biofilms and the influence of environmental conditions
2) Explore the role of poorly characterised LPxTG proteins in *S. gordonii* biofilm formation, colonisation and pathogenesis
3) Determine the mechanistic basis for eDNA release and assembly in *S. gordonii* biofilms.

Chapter 2 Materials and Methods

2.1 Bacterial culture

Bacterial strains used in these studies are listed in Table 2.1. Streptococcal strains were routinely grown in BHY broth (3.7% w/v Brain Heart Infusion (BD), 0.5% w/v Yeast Extract (BD)) at 37 °C in an oxygen-reduced environment (candle jar). Staphylococcal strains were grown in TSB (3% Tryptone Soya Broth (OXOID)) at 37 °C and shaken at 220 rpm. *Escherichia coli* was grown in Luria Bertani broth (Thermo) at 37 °C with agitation (200 rpm). *Actinomyces oris* was grown in TYG (0.5% Tryptone (OXOID), 0.5% Yeast Extract (BD), 0.4% K_2HPO_4 (Sigma), 0.5% glucose (Fisher)) at 37 °C in an oxygen-reduced environment (candle jar). The appropriate media were additionally supplemented with 1.2% agar (OXOID) for solid media (plates).

Table 2.1 - List of bacterial strains used in this study

Microorganism	Strain	Relevant characteristics	Source / reference	UoB Reference #
Streptococcus gordonii	DL1 Challis			
		Wild type	Pakula & Walczak, 1963	1507
		Δ*atlS::aad9*	This study	2952
		Δ*cbdB::aad9*	This study	2868
		Δ*comC::aad9*	Jack *et al*., 2015	2660
		Δ*comC::aad9* Δ*hppA::ermAM*	This study	2954
		Δ*comCDE::aad9*	Jack *et al.*, 2015	2347
		Δ*cshA::aad9*	Back *et al*, 2017	2011
		∆*hppA::ermAm*	This study	2953
		Δ*hppA::ermAM* Δ*comCDE::aad9*	This study	2958
		Δ*lytF::aad9*	This study	2957
		Δ*padA::aad9*	This study	2864
		Δ*padB::aad9*	This study	2833
		Δ*palA::aad9*	This study	2826
		Δ*sedA::aad9*	This study	2869
		Δ*sedA::aad9* p*SedA*	This study	2945
		Δ*sndA::aad9*	This study	2827
		Δ*sndA::aad9* pDL276-*sndA*	This study	2886
		Δ*sedA::aad9 ΔsndA::ermAM*	This study	2936
		Δ*sedA::aad9 ΔsndA::ermAM* pDL276-*sedA*	This study	2937
		Δ*sedA::aad9 ΔsndA::ermAM* pDL276-*sndA*	This study	2938
		Δ*srtA::ermAM*	Nobbs *et al*., 2007	2576
Staphylococcus aureus	Col	Wild type	Dyke *et al*., 1966	1834
Escherichia coli	DH5α	Plasmid-free *recA* cloning host	Invitrogen	776
	EC1000	Cloning host that provides RepA in trans	Leenhouts *et al*., 1996	1962
Actinomyces oris	T14V	Wild type	Cisar *et al*., 1988	2163

Table 2.2 - List of plasmids used in this study

Plasmid	Relevant characteristics	Source / reference
pDL276	*E. coli*-streptococcal integration shuttle vector; Kan^R	Tao *et al*., 1992
pDL276-*sedA*	pDL276 carrying *sedA* CDS	This study
pDL276-*sndA*	pDL276 carrying *sndA* CDS	This study
pORI280	Source of *ermAM* cassette; Erm^R	Leenhouts *et al*., 1996
pFW5	Source of *aad9* cassette; $Spec^R$	Podbielski *et al*., 1996

2.2 Gram staining

Bacterial suspensions were dried onto glass microscope slides then stained with 0.25% w/v crystal violet for 1 min. Slides were washed with dH_2O then stained with iodine for 1 min. Acetone was used to de-stain cells. A counter-stain was performed with 0.25% w/v safranin for 1 min.

2.3 Bacterial attachment and biofilm formation in C medium or salivary media

Saliva-coated cover slips were produced by incubating 1 ml saliva with sterile 19 mm glass cover slips (VWR) for 16 h at 4 °C. Overnight cultures of bacteria were harvested by centrifugation at 5,000 *g* for 7 min, washed and resuspended to OD_{600} = 0.1 in C medium or salivary medium (1% saliva, 0.4% glucose). 1 ml of bacterial suspension was incubated on saliva-coated cover slips in 12-well plates (Greiner) for 1 h (adhesion) or 24 h (biofilm formation) at 37 °C. The cover slips were washed in C medium or salivary medium, stained with 0.5% crystal violet for 1 min, and excess stain removed by further washing. Biofilm biomass was then quantified following stain release by 5 min incubation with 0.25 ml 10% acetic acid (Fisher) and measurement of A_{595}. Some biofilms were then imaged using confocal microscopy.

2.4 Soluble DNA quantification from biofilms

Biofilms were grown as described previously (Loo *et al.*, 2000). The biofilms were washed once in phosphate buffered saline (PBS, Thermo) then scraped into 0.5 ml TE buffer (10 mM Tris, 1 mM EDTA; Sigma) and centrifuged at 13,000 *g*, 3 min, 4 °C. The concentration of DNA within the supernatant was determined by using a NanoDrop (Thermo), based on A_{260}. Alternatively, the supernatant was transferred to a fresh tube, mixed with 0.3 ml phenol: chloroform: isoamyl alcohol (25:24:1; Fisher) and vortexed for 30 s. The mixture was centrifuged as above. The aqueous phase was removed and 80 µl 3 M sodium acetate (Fisher; pH 5.8) and 0.5 ml propan-2-ol (Fisher) was added to this. This was incubated at -20 °C for 1 h to precipitate DNA, then centrifuged at 13,000 *g*, 3 min, 4 °C. The pellet was washed in 70% -20 °C ethanol (Fisher) and allowed to air dry, before it was dissolved in dH_2O. DNA concentration was measured as above.

2.5 Bioinformatics

The genomic sequence of *S. gordonii* CH1 Challis had been completed by the Institute for Genomic Research (Vickerman *et al.*, 2007), which allowed for the identification of LPxTG family proteins in *S. gordonii* via NCBI search and BLAST. BLAST was also used to find homologous proteins whilst conserved domain finder (from NCBI) was used to identify conserved domains based on the predicted protein sequence. BPROM (from Softberry) was used to find predicted bacterial promoter sites and ARNOLD (from Institut de Génétique et Microbiologie) was used to find predicted bacterial terminators.

https://www.ncbi.nlm.nih.gov/genome/proteins/
http://linux1.softberry.com/
http://molbiol-tools.ca/Promoters.htm

2.6 PCR (Polymerase chain reaction)

PrimestarMAX (Clontech) at a total volume of 25 µl was used for high fidelity amplification of DNA. GoTaq polymerase (Promega) was used for screening, with a 25 µl final volume. Amplified products were purified with QIAquick PCR Purification Kit (QIAgen) or QIAquick Gel Extraction Kit (QIAgen) and eluted in 30-50 µl sterile PCR dH_2O (DNAse and RNAse free water (VWR)).

2.7 gDNA extraction from *S. gordonii*

Overnight cultures of *S. gordonii* were sub-cultured into fresh BHY and grown at 37 °C until OD_{600} = 0.4. Glycine (3% w/v; Thermo) was added and cells were incubated for a further 1 h. Cells were harvested at 5,000 *g* for 10 min at 4 °C. The pellet was suspended in TE buffer (pH 8; Sigma). Cells were pelleted and resuspended in Tris-Glucose (50 mM Tris-HCl (Sigma), 25% w/v glucose (Fisher)). Cells were incubated with 1% w/v lysozyme (Sigma) in dH_20 and 10,000 U/ml mutanolysin (Sigma) at 37 °C for 1 h. DEPC (10 µl; Thermo) and 1 M EDTA (5 µl; Sigma) were added to 0.025 M TE buffer and incubated on ice for 5 min. Cells were lysed in 0.25% SDS (Thermo) in TE buffer (pH 8), with incubation at 65 °C for 1 h. 5 ml TES (50 mM Tris-HCl (Sigma), 5 mM EDTA (Sigma), 0.15 M NaCl (AnalaR)) and 25 ml chloroform: isoamyl alcohol ((24:1); Fisher) were added and the mixture was agitated for 10 min, then centrifuged at 8,000 *g* for 20 min at 4 °C. -20 °C EtOH (Fisher) was used to precipitate DNA, which was then spooled out and dissolved into 5 ml TES. RNase was added to produce a solution with 10 µg/ml RNase (Sigma) and this was incubated at 37 °C for 1 h. Proteinase K was added to produce a solution of 10 µg/ml proteinase K (Sigma) – this was incubated at 37 °C for 1 h. 25 ml Chloroform: isoamyl alcohol was added and the mixture was agitated for 10 min. The mixture was centrifuged at 8,000 *g* for 20 min at 4 °C. The aqueous phase was removed and -20 °C ethanol was used to precipitate DNA for 1 h. DNA was harvested at 8,000 *g* for 20 min at 4 °C, then

washed in -20 °C 70% EtOH and centrifuged again. The pellet was air-dried and resuspended in dH_2O. The concentration was then determined using a NanoDrop (Thermo), based around absorbance at A_{260}.

2.8 Mutagenesis strategy

S. gordonii knockout mutants were generated through allelic replacement, where the gene of interest (GOI) was exchanged with an antibiotic resistance cassette (Figure 2.1). Primers (Eurofins) were designed to amplify approximately 500 bp regions up- and down-stream of the GOI (Table 2.3). These primers were used in a PCR reaction using *S. gordonii* genomic DNA as template. Primers were designed so that amplicons were generated with an 18 bp overlap with the relevant antibiotic resistance cassette e.g. *aad9*. The antibiotic resistance cassette was amplified by PCR from the appropriate plasmid. The upstream and downstream GOI and antibiotic resistance cassette amplicons were ligated by stitch PCR. The resultant amplicon was used to transform competent *S. gordonii*. The 500 bp flanking regions of the GOI allows for homologous recombination with the chromosomal DNA. Mutants could then be identified using positive selection on the relevant antibiotic-containing agar and confirmed using sequencing.

To transform *E. coli* with plasmids, cells were made competent (Hanahan *et al*., 1983) and transformed with up to 5 µg of DNA.

To transform wild-type *S. gordonii,* 50 µl overnight broth culture was sub-cultured into 5 ml BHY supplemented with 1% foetal calf serum (Sigma) and 0.1% glucose (Fisher) and grown for 3 h at 37 °C. The sub-culturing was then repeated as above with the +/- 10 ng/ml CSP (Sigma), and the suspension grown for a further 1 h. At this point 1 µg DNA was added, and the cells were grown for a further 4 h and plated out onto relevant antibiotic selective plates. Potential transformant colonies were screened using Gene Release (Eurogentec) and PCR,

then confirmed by DNA sequencing. Bacteria which has been transformed using a plasmid were screened by performing a mini-prep using QIAprep Spin Miniprep Kit (QIAgen), then sequenced.

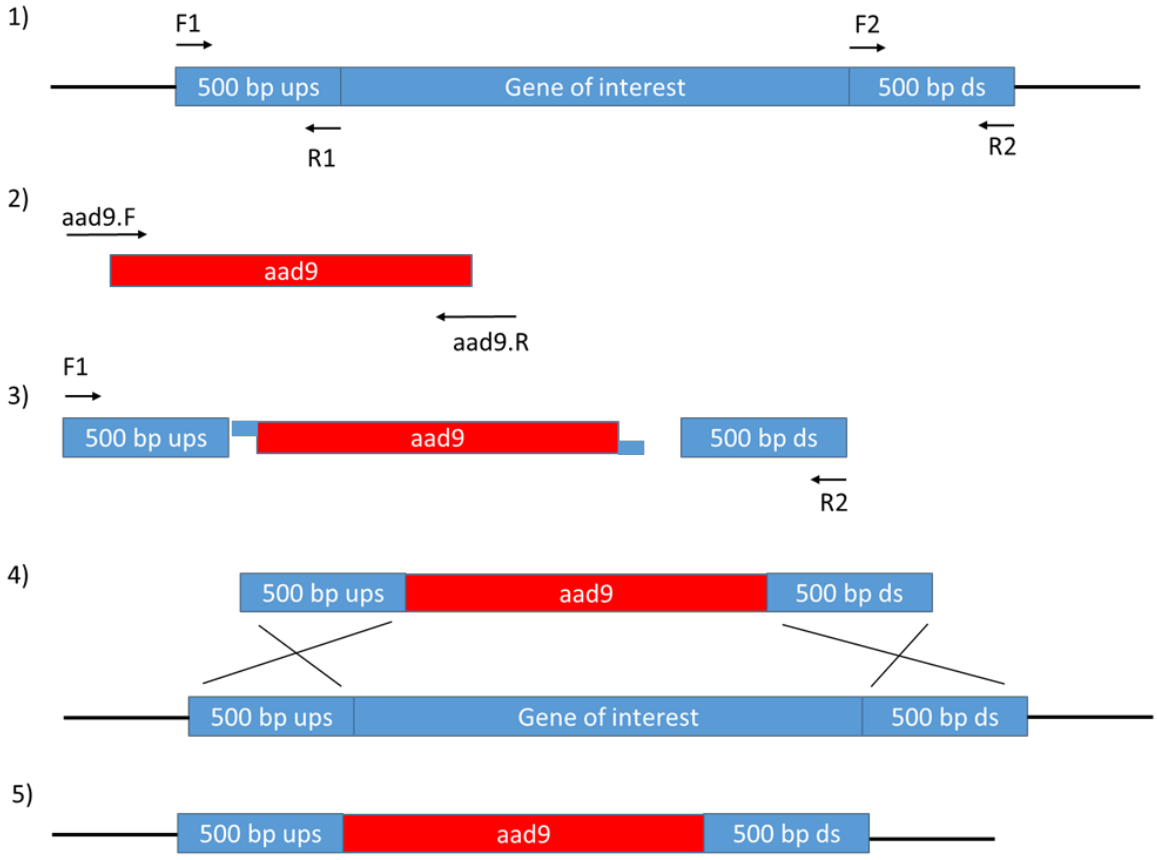

*Figure 2.1 - **Mutagenesis strategy**.*
1) Amplification of 500 bp regions up- and down-stream of gene of interest from genomic DNA.
2) Amplification of aad9 from appropriate plasmid with overlapping regions.
3) Ligation of upstream and downstream GOI regions with aad9 with overlapping regions by stitch PCR.
4) Transformation of S. gordonii and homologous recombination.
5) Resultant genomic DNA in generated mutants.

Table 2.3 – Primers used in this study

Target gene	Primers	Primer sequence (5' -3')
cshA	cshA.F1	CATGCCATGGAATCCACACCTGCGTAAG
	cshA.R1	ACTCTCGGGAGCTCCCACCTTGTGGATCCAAG
	cshA.F2	AGGTGGGAGCTCCCGAGAGTGACAGAAATTCC
	cshA.R2	TGCTCTAGACACAGGCAATCTTCAGCC
palA	PalA.F1	GCGATTATCCAGTATTCAGTAC
	PalA.R1	TCATAGGATCCTCCTTATATTTT
	PalA.F2	AGATTCAAATCATTTAAAAATTAGT
	PalA.R2	CACTCTCTCAGGATTACTGGC
	PalA.aad9.F	AAGGAGGATCCTATGAATACATACGAACAAATTAATA
	PalA.aad9.R	AAATGATTTGAATCTTATAATTTTTTTAATGTCTTATTTAA
sndA	SndA.F1	TTTTATCAGAAATTGATTG
	SndA.R1	AAAGTTCTCCTTTTCCTA
	SndA.F2	CCTAGAGTAAGCTCTAAACA
	SndA.R2	TGTCAAAGCTACCAGTAC
	SndA.aad9.F	AGGAGAACTTTATGAATACATACGAACAAATTAATA
	SndA.aad9.R	AGCTTACTCTAGGTTTATAATTTTTTTAATGTCTTATTTAA
	SndA.comp.F	GGTACCCGGGGATCCTTACTCTAGGTTAGATGA
	SndA.comp.R	ACCGAGCTCGAATTCAAAATACTATTTTGCAGT
SGO_0707	SGO_0707.F1	CGTAATGTTAAATCTGGTTTG
	SGO_0707.R1	TCATCCGACTTCTCCTTT
	SGO_0707.F2	AATTTTCAGCTGAATAAGGAA
	SGO_0707.R2	GCATTAACCAATGTTACCCTTC
	SGO_0707.aad9.F	GGAGAAGTCGGATGAATACATACGAACAAATTAATA
	SGO_0707.aad9.R	ATTCAGCTGAAAATTTTATAATTTTTTTAATCTGTTATTTAA
padB	PadB.F1	GATTCCGAATAAGGCTACTG
	PadB.R1	CATAATGATTTTCCTTTAATCTT
	PadB.F2	AGAATTAGGTTGAAAAAATAGAAG
	PadB.R2	CATCTAAAATGAGTATTTTGCC
	PadB.aad9.F	AGGAAAATCATTATGAATACATACGAACAAATTAATA
	PadB.aad9.R	TTTCAACCTAATTCTTTATAATTTTTTTAATCTGTTATTTAA
cdbB	CbdB.F1	GATTTCAGATGAGACGGC
	CbdB.R1	CATGCAATCTTCCTTTCTC
	CbdB.F2	AACAAGAAACAAGTGTCAATG
	CbdB.R2	GTTTCCTGTGTTGAAAGAG
	CbdB.aad9.F	AAGGAAGATTGCATGAATACATACGAACAAATTAA
	CbdB.aad9.R	CACTTGTTTCTTGTTTTATAATTTTTTTAATCTGTTATTTAAA
padA	PadA.F1	CATTGCTGGTCCTAACAG
	PadA.R1	CATGCTATTTTAAAGCCTATATA
	PadA.F2	TGTAAGATAGTCCAGGAGAGC
	PadA.R2	GCCGTGTGAAAAAGTCTG

	PadA.aad9.F	CTTTAAAATAGCATGAATACATACGAACAAATTAA
	PadA.aad9.R	CTGGACTATCTTACATTATAATTTTTTCAACCTGTTATTTAAA
sedA	SedA.F1	GTATGAGATCGATGATGATGAG
	SedA.R1	CATAAAAACTCTCCTTTGTGT
	SedA.F2	ATTTTTTGAAGAAGCTATAGATATAG
	SedA.R2	AACGTCCCTTGCTATTAAC
	SedA.aad9.F	AGGAGAGTTTTTATGAATACATACGAACAAATTAA
	SedA.aad9.R	GCTTCTTCAAAAAATTTATAATTTTTTTAATCTGTTATTTAAA
	SedA.comp.F	ACGCGTCGACGTATCAGATGGTTTCTAAATTAACC
	SedA.compR	GCGGGATCCCCAAAAACGATTTTAGTTCC
atlS	AtlS.F1	GAAGTTTGAAGGGCTTGC
	AtlS.R1	GTAACTCCCTCTTTAACACG
	AtlS.F2	ACAAAAGGTTGAAGAAAGTTG
	AtlS.R2	CCCAGAGATTTGATTGGT
	AtlS.aad9.F	AGAGGGAGTTACATGAACAAAAATATAAAAATATTCTC
	AtlS.aad9.R	TCAACCTTTTGTTTATTTCCTCCCGTTAAATA
lytF	LytF.F1	CAGCTTGGTTAAAATCATCTAC
	LytF.R1	ACATCTCCTTTACGTTATTTTTTTG
	LytF.F2	CCCTATCATTTAGCACCTC
	LytF.R2	GGTAGGACAAGAATTGACC
	LytF.aad9.F	ACGTAAAGGAGATGTATGAACAAAAATATAAAATATTCTC
	LytF.aad9.R	TGC TAAATGATAGGGTTATTTCCTCCCGTTAAATA

Underlined sections indicate overlapping sequences

2.9 Growth curves

Overnight cultures of bacteria were harvested by centrifugation at 5,000 *g* for 7 min, and washed once with 5 ml PBS. The cells were suspended in 1 ml PBS and adjusted to OD_{600} 1. A 1 in 10 dilution of this suspension was made into BHY, C medium (0.25% proteose peptone #2 (BD), 0.75% yeast extract, 10 mM K_2HPO_4 (GPR), 0.4 mM $MgSO_4.7H_2O$ (AnalaR), 17 mM NaCl (Fisher), 0.2% glucose, pH 7.5) or YPTG (0.67% YNB (Fisher), 0.4% glucose, 0.1% tryptone, adjusted to pH 7 with KH_2PO_4), and incubated at 37 °C in a candle jar. Growth (OD_{600}) was measured every 1 h until stationary phase was reached.

2.10 Saliva preparation

Saliva was collected, processed, stored, used and disposed of in accordance with the Human Tissue Act (2004). The saliva bank has ethical approval from Health Research Authority (08/H0606/87). Informed consent was given by saliva donors prior to the anonymisation, pooling and treatment of saliva with 2.5 mM dithiothreitol (Sigma). Following this, mucins were removed from the saliva by centrifugation at 12,000 *g* for 10 min, before being diluted 1 in 10 into dH_20 and sterilised using a 0.5 µm filter.

2.11 Biofilm formation in YPTG

Glass-bottomed plates (Greiner) (for use in eDNA stranding assays) or 19 mm sterile glass cover slips (for measuring biomass) were coated in 10% saliva by incubation overnight at 4 °C. Overnight broth cultures were harvested at 8,000 *g* for 7 min, washed in YPT (0.67% YNB, 0.1% tryptone, 20 mM Na_2HPO_4, adjusted to pH 7 with KH_2PO_4), then resuspended in YPTG to OD_{600} 0.25. The coverslips were washed with YPT, then 1 ml of bacterial suspension was added, and the plates were incubated for 5 h at 37 °C, 50 rpm in a humid environment. Some biofilms were treated as described in Table 2.4.

Table 2.4 - Biofilm treatments

Biofilm treatments	Source	Amount	units	Duration
DNase I (bovine pancreas)	Sigma	1	µg/ml	5 h
		10	µg/ml	5 h
		25	µg/ml	5 h
		50	µg/ml	5 h
		100	µg/ml	5 h
		50	µg/ml	Final 1 h
		100	µg/ml	Final 1 h
RNase A (bovine pancreas)	Sigma	1	µg/ml	5 h
		10	µg/ml	5 h
		50	µg/ml	5 h
Proteinase K	Sigma	1	µg/ml	5 h
		10	µg/ml	5 h
		50	µg/ml	5 h
		50	µg/ml	Final 1 h
Dextranase	Sigma	1	µg/ml	5 h
		10	µg/ml	5 h
		50	µg/ml	5 h
Glucose	Fisher	0.2	%	5 h
		0.4	%	5 h
		0.8	%	5 h
		1.6	%	5 h
Sucrose	Fisher	0.2	%	5 h
		0.4	%	5 h
		0.8	%	5 h
		1.6	%	5 h
pH (via HCl/NaOH)	Sigma	5	pH units	5 h
		6	pH units	5 h
		7	pH units	5 h
		8	pH units	5 h
Superoxide dismutase	Sigma	10	µg/ml	5 h
Catalase	Sigma	1	µg/ml	5 h
		5	µg/ml	5 h
		10	µg/ml	5 h
		50	µg/ml	5 h
CSP (DVRSNKIRLWWENIFFNKK)	GenicBio	1	µg/ml	5 h
		2	µg/ml	5 h
		5	µg/ml	5 h
		10	µg/ml	5 h
		50	µg/ml	5 h
sCSP (DKRFKWWILKVFNSNEINR)	GenicBio	10	µg/ml	5 h
H_2O_2	Fisher	120	mM	5 h

The bacterial suspension was removed from the well and the coverslips were washed twice with YPT.

For biomass assays, biofilms were stained with 0.5% crystal violet for 1 min, and excess stain removed by further washing. Biofilm biomass was then quantified following stain release by 5 min incubation with 0.25 ml 10% acetic acid (Fisher) and measurement of A_{595}.

For eDNA stranding assays, biofilms were fixed overnight with 0.5 ml 4% paraformaldehyde (Sigma) at 4 °C, washed with 0.5 ml PBS, and blocked with 25 µl 2% w/v BSA (Bovine Serum Albumin (Sigma)) for 45 min at room temperature. Biofilms were washed with PBS, then incubated with 25 µL mouse anti-double stranded DNA primary mAb (Thermo) (1:1000 dilution into PBS) for 45 min. Biofilms were washed with PBS, then incubated with 25 µL goat anti-mouse secondary Ab conjugated to Alexa594 (Thermo) (1:1000 dilution into PBS) in the dark for 45 min. The biofilms were then washed with 0.5 ml PBS and incubated with 25 µL TO-PRO3 (Thermo; general DNA stain) (1:1000 dilution into PBS) in the dark for 15 min. Biofilms were then washed with 0.5 ml PBS and stored in 0.5 ml PBS at 4 °C for a maximum of 3 days before visualisation using widefield or confocal microscopy.

For widefield microscopy, an N Plan x20/0.40 lens was used on a widefield Leica DMi6000 microscope. A mark and find macro written by Dr Dominic Alibhai was used to image 8 positions in a tile scan in the centre of each well, to cover 1.5 x 2 mm, which was captured with a Leica DFC365FX camera. Tile scans required a 10% image overlap for assembly. At each position an autofocus- routine with a range of 80 and 150 µm was used to identify focus positions with optimal contrast. A Z-stack of 12 µm, in 25 x 0.5 µm steps was then taken per field of view.

To analyse the micrographs, the proprietary Leica format (.lif) files were loaded into MATLAB where a code developed by Dr Dominic Alibhai was used. This code finds the level of best focus within Z, and then uses ridge-finding to identify regions of intensity which correlate to eDNA stranding (Section 7.1). Regions where potential strands are too small or too circular are excluded, as they are likely to be colloidal particles. Images were outputted where stranding was overdrawn and labelled for cross-referencing to Excel, where the length of the strand was recorded. In this way, it was possible to find not only the length of the strand, but also the frequency of stranding events, both of which contribute to total levels of eDNA stranding.

For confocal microscopy, a Leica SPE confocal laser scanning microscope was used to image eDNA-stained biofilms. The objective chosen was ACS APO x63/1.30 oil. The pinhole was set at 1 Airy unit to optimise resolution. A Z-stack of around 10 µm was used to capture the biofilm, with Z-step sizes of 0.25 µm. A zoom of 2.5 x was used. Images were 1392x1040 pixels.

Volocity (Improvisation) was used to analyse the volume of different components and Z height objects in biofilms.

2.12 Hydrophobicity assay

Overnight broth culture suspensions were harvested at 8,000 *g* for 7 minutes washed once with PBS, then suspended in PBS to OD_{600} 0.5 in glass test tubes. Hexadecane (500 µl; Sigma) was added and tubes vortexed for 30 s. Tubes were incubated at room temperature for 30 min. The OD_{600} of the aqueous phase was measured, and hexadecane association was calculated as 100 - ((OD_{600} final / OD_{600} initial) x 100).

2.13 Autoaggregation assay

Overnight broth cultures were harvested at 8,000 *g* for 7 min, washed in PBS, then suspended in aggregation buffer (1 mM Tris (Sigma), 0.1 mM $CaCl_2$ (Fisher), 0.1 mM $MgCl_2$ (Fisher), 0.15 mM NaCl (AnalaR), 3.1 mM NaN_3 (Fisher)) to OD_{600} 0.5 in plastic tubes. Suspensions were left for 1, 6 or 24 h, after which 1 ml of suspension sampled close to the meniscus was transferred to a cuvette and the OD_{600} was measured. Percentage aggregation was measured as 100- ((OD_{600} final/OD_{600} initial) x 100).

2.14 Co-aggregation with *A. oris*

Overnight broth cultures were harvested at 8,000 *g* for 7 min, washed in co-aggregation buffer (1 mM Tris, 150 mM NaCl, 0.1 mM $CaCl_2$, 0.1 mM $MgCl_2$, 0.02 % NaN_3) and resuspended to OD_{600} 1. Equal volumes (2 x 5 ml) of *A. oris* and *S. gordonii* strains were mixed and vortexed for 10 s. This mixture was then incubated at room temperature for 5 min and centrifuged at 600 *g* for 1 min. Co-aggregates were visually scored using a scale of 0-4 developed by Cisar (Cisar *et al.*, 1979). The scale is as follows: 0 = Evenly turbid suspension of bacteria; 1 = Finely dispersed clumps in a turbid background; 2 = Definite clumps bacteria are easily seen but do not settle immediately and remain in a turbid background; 3 = Clumps settle immediately with a slight turbid background and 4 = Clumps settle immediately and supernatant completely clear.

2.15 Collagen binding assay

Overnight broth cultures were harvested at 8,000 *g* for 7 min, washed once with TBSC (10 mM Tris-HCl pH 7.5, 150 mM NaCl, 5 mM $CaCl_2$), then resuspended in TBSC to OD_{600} 1. Type 1 collagen-coated 96-well plates (Fisher) were blocked for

1 h with 0.2% BSA in TBSC. The plate was washed twice with TBSC, before bacterial suspensions (200 µl) were added to each well and incubated at room temperature for 2 h at 50 rpm. Plates were then washed twice with TBSC, after which 100 µl 0.1% Triton X-100 (Sigma) in TBSC was added and the well contents agitated. These suspensions were serially diluted, plated onto agar plates, and incubated overnight at 37 °C in a candle jar. Viable counts (CFU/ml) were then calculated.

2.16 Fibronectin binding assay

Human fibronectin (Sigma) was diluted into coating buffer (20 mM Na_2CO_3 (Fisher), 20 mM $NaHCO_3$ (Fisher), pH 9.3) and incubated at 1 µg/well (50 µl final volume) in a 96-well plate (Immulon) for 16 h at 4 °C. The wells were washed with TBSC, blocked with TBSC containing 3% BSA and 0.05% Tween-20 (Fisher) for 1 h at 37 °C, then washed with TBSC. Overnight broth cultures were harvested (5,000 *g*, 4 °C, 5 min) and adjusted to OD_{600} 0.1. Cell suspensions (100 µl) were added to the wells and incubated for 2 h at 37 °C. The wells were then washed twice with 200 µl TBS and fixed with 100 µl 9% formaldehyde (Sigma) at 25 °C for 30 min. The wells were washed twice with 200 µl TBS, then stained with 100 µl 0.5% crystal violet at 25 °C for 2 min. Crystal violet was released with 100 µl 7% acetic acid (Fisher) and A_{595} measured.

2.17 Extracellular nuclease activity

Overnight broth cultures were harvested (5000 g, 10 min, 25 °C) and suspended to OD_{600} 1 in PBS. Sterile filter paper disks (0.5 cm diameter) were placed onto DNA-containing agar plates (Thermo) and inoculated with 2 µl bacterial suspension. These were incubated overnight at 37 °C in a candle jar. The plate was flooded with 1 M HCl (Sigma) to precipitate the DNA, and the diameter of the circle of clearance produced was measured.

2.18 DNA: bacteria binding assay

For planktonic assays, overnight broth cultures were harvested at 8,000 *g* for 7 min, washed once in PBS, then resuspended in PBS to OD_{600} = 1. 1 µg/ml lambda phage DNA (Invitrogen) was added to some suspensions. Mixtures were vortexed and incubated at room temperature for 30 minutes. Bacterial cells (and any bound DNA) were pelleted at 13,000 *g* for 3 minutes. 0.5 ml of supernatant was transferred to black glass-bottomed 24 well plates (Greiner). The remaining cells were resuspended in 0.5 ml PBS and transferred to the plate.

For biomass assays, biofilms were grown as described for eDNA stranding assays. 1 µg/ml lambda phage DNA (Invitrogen) was added to some biofilms. The supernatant was removed and transferred to a black glass-bottomed 24 well plates. 0.5 ml YPTG was added to the biofilm.

0.5 ml of Quant-it PicoGreen (prepared according to kit instructions (Invitrogen)) were mixed with the sample or biofilm, incubated at room temperature for 3 minutes, then measured in a fluorescent plate reader using excitation 485 nm, emission 520 nm. RFU were converted to DNA concentration using a calibration curve.

2.19 ATP determination assay

Biofilms were prepared as for eDNA stranding assays. Biofilm supernatant (10 µl) was removed and mixed with 90 µl of Standard Reaction Solution, prepared following instructions in the ATP Determination Kit (Invitrogen). An ATP standard curve from 1 nM to 1 µM was performed alongside each assay. Luminescence was measured on a plate reader, and the standard curve generated was used to convert luminescence units into extracellular ATP concentration.

2.20 Zymogram assay

Cell pellets were prepared for addition into SDS-PAGE separating gels as follows: overnight *S. gordonii* broth culture was diluted 1:100 into fresh BHY and incubated at 37 °C until OD_{600} = 0.2. Cells were harvested at 8,000 *g* for 7 minutes, washed twice in Tris-HCl buffer, and suspended in 1 ml dH_2O. Cells were heat killed at 95 °C for 10 minutes prior to addition into 10% acrylamide SDS-PAGE separating gels (1.5 M Tris-HCl (pH 8.8), 10% SDS), rendering the gel opaque. 4% acrylamide SDS-PAGE stacking gel (0.5 M Tris-HCl (pH 6.8), 4% SDS) was used.

To test enzymatic activity, overnight broth cultures of bacteria were harvested at 8,000 *g* for 7 min, washed once in PBS, then resuspended in YPTG to OD_{600} = 0.25. Cultures were incubated at 37 °C for 5 h. Cells were harvested at 8,000 *g* for 7 min, the supernatant removed, and the pellet resuspended in 1 ml dH_2O. Samples were heat killed at 95 °C for 10 minutes, prior to loading onto the prepared cell pellet-containing SDS-PAGE gels.

Gels were run for 2 h at 120 V. Gels were then washed twice in dH_2O and once in refolding buffer (20 mM Tris HCl, 50 mM NaCl, 20 mM $MgCl_2$ (Fisher), 0.5% Triton-100 (Sigma), pH 7.4), before incubation for at least 48 h in refolding buffer. Gels were stained with methylene blue (0.1% methylene blue (Sigma), 0.01% KOH (Fisher)) for 30 min to allow for visualisation of zones of clearance.

2.21 Statistics

Data were analysed using GraphPad Prism 7.0. All data are presented as the mean ± standard deviation of at least three independent experiments. Comparisons between multiple groups were performed with an ANOVA followed by Tukey's multiple comparison test, whereas comparisons with only two groups

were performed using a two-tailed Student's T-test. An alpha value of 0.05 was chosen, therefore *P* values of less than 0.05 were considered statistically significant. Regression analysis was also used where points are plotted and values compared a regression line. R squared values show the difference between the points and the regression line. A high R squared value indicates higher validity of the regression line. The R squared value and number of points minus one (degrees of freedom) can then be used to calculate a P value.

Chapter 3 Presence of eDNA in *S. gordonii* biofilms

3.1 Introduction

The extracellular polymeric substance (EPS) is a vital component of biofilms which facilitates bacterial growth in biofilm phase. The EPS forms a slime layer which coats the biofilm and can promote its persistence within a given ecological niche, as well as protecting bacteria from host immune defences or antimicrobial treatment. EPS production is most prevalent during early biofilm formation (sub 24 hours) (Zhang *et al.*, 2011) and in some species can account for 90% of biofilm biomass (Kavita *et al.*, 2013). EPS can be composed of proteins, polysaccharides, eDNA and lipids. To date, with the exception of perhaps *S. mutans*, there has been limited investigation into the EPS components of oral streptococcal biofilms and the relative contributions they make to biofilm formation. This is particularly pertinent for eDNA.

eDNA has recently been recognised as a component of biofilms formed by many different microorganisms (Whitchurch *et al.*, 2002). eDNA has been shown to be present in the biofilms formed by both Gram-positive and Gram-negative bacteria (Tetz *et al.*, 2009), and across a wide range of bacterial genera, including *Bordetella*, *Enterococcus*, *Aggregatibacter*, *Streptococcus*, *Staphylococcus*, *Neisseria*, *Vibrio*, *Campylobacter*, *Klebsiella* and *Haemophilus* (Okshevsky & Meyer, 2015). eDNA is thought to make up only a small proportion of biofilm biomass. Nonetheless, disruption of eDNA often causes loss of biofilm biomass of approximately 50% (Okshevsky & Meyer, 2015), implying an important role for eDNA in biofilm development. This effect extends to oral biofilms, where eDNA has been shown to contribute to dental biofilm stability (Schlafer *et al.*, 2017).

To date, analysis of eDNA in biofilms has largely been achieved using two main strategies: i) quantification by measuring soluble DNA concentration, and ii)

qualitatively assessing eDNA using microscopy. Using the latter approach, eDNA has been shown to appear as networks of constellation-like stranding patterns (Jack *et al.*, 2015; Barnes *et al.*, 2012). eDNA structures in *Enterococcus faecalis* biofilms which have been grown for less than 4 hours have been observed. These were observed to be mesh-like, called “sweaters” or fibre-like, called “yarns”. While the bundled appearance of DNA in “sweaters” was consistent with what could be produced passively by bulk cell lysis, the long “yarns” were not (Barnes *et al*., 2012) (Figure 3.1).

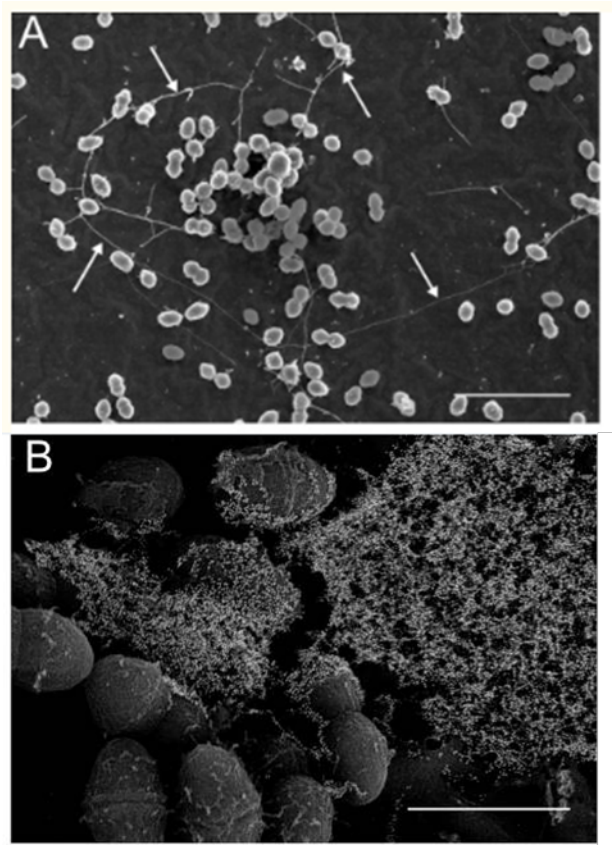

Figure 3.1 – Micrographs from Barnes et al., 2012 showing contrasting “yarn” (A) and sweater (B) eDNA structures in Entrococcus faecalis. Scale bar A = 5 µm, scale bar B = 1 µm.

However, no method has yet been devised to allow these stranding patterns to be quantified. This has hampered determination of the parameters that may influence these precise eDNA stranding events during biofilm development.

Oral biofilms and their EPS can be influenced by a variety of potential parameters: which and how many microbial species make up the biofilm,

nutrient availability, saliva flow rate, pellicle constituents, biofilm age, temperature and pH (Nobbs *et al.*, 2009). For example, sugar availability can greatly fluctuate based on the frequency and type of food consumed. The pH of the oral cavity also varies in oral health and disease. The average pH of saliva is pH 6.7, but can range from pH 5 during dental caries to pH 8 in cases of gingivitis, when measured around plaque (Baliga *et al.*, 2013). Again, little is currently understood regarding how such parameters might specifically influence eDNA production and assembly.

The initial objectives of this study were therefore to develop a methodology to quantitatively assess eDNA stranding in biofilms, and to use this methodology to determine how eDNA stranding might be influenced by different EPS components and environmental conditions. Oral bacterium *S. gordonii* was selected as the model for these studies, due to its well-characterised capacity to form biofilms on salivary pellicle, and to interact with a wide range of host molecules and other oral microbes.

3.2 Quantification of eDNA in *S. gordonii* biofilms

While eDNA had been reported as a component of *S. gordonii* biofilms (Jack *et al.,* 2015), a detailed analysis of its production had not been performed. The first objective of this project was therefore to analyse eDNA production in *S. gordonii* biofilms over time. A biofilm protocol which had previously been shown to result in eDNA production for *S. gordonii* dual-species biofilms with fungus *C. albicans* was tested in the first instance (Jack *et al.*, 2015). This involved growth on saliva-coated glass coverslips at 37 ^{o}C with gentle shaking (50 rpm) in YPTG for 5 h. Two approaches were used to quantify soluble eDNA found in *S. gordonii* biofilms, with ('precipitation') or without ('collection only') inclusion of a phenol: chloroform: isoamyl alcohol step to allow separation of the aqueous and organic phases. The aqueous phase containing dissolved DNA is removed, and DNA is then precipitated in ethanol. The quantity of eDNA in these biofilms was found to be approximately 1.6 μg/biofilm using either method (Figure 3.2). While both

DNA quantification methods gave comparable results, the decision was taken to use the 'precipitation' approach for future work, as this had potential to be the more sensitive method, as a reduced volume of dH_2O can be used to resuspend DNA (unlike in collection only, where DNA is not precipitated and resuspended), resulting in a readable concentration of DNA from a biofilm with low DNA.

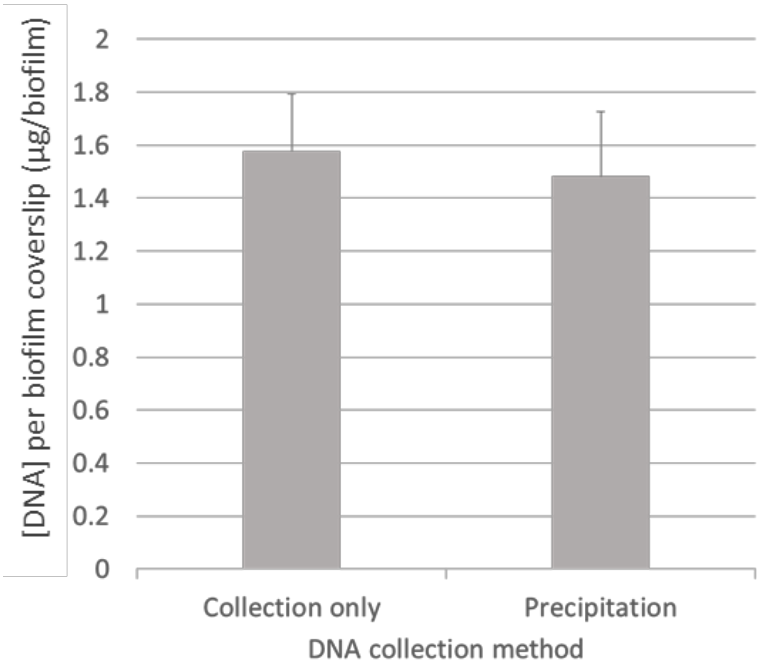

Figure 3.2 – ***Quantification of soluble eDNA in S. gordonii biofilms using two different methods.*** *WT S. gordonii biofilms were grown at 37 °C in YPTG on saliva-coated glass cover slips for 5 h. Biofilms were washed with PBS, collected into TE buffer and biomass removed by centrifugation. Levels of soluble eDNA in the supernatants were quantified directly (collection only) or following phenol: chloroform: isoamyl alcohol precipitation (precipitation) by measurement on nanodrop spectrophotometer (Thermo). Data are presented as mean DNA concentration ± SD; n=3. Experiments were performed in triplicate. A Student's two-tailed heteroscedastic T-test was used with α=0.05. No significant difference was found.*

Having verified eDNA production in *S. gordonii* biofilms after 5 h under these conditions, the next step was to determine more regarding the dynamics of eDNA production during biofilm growth, hypothesising that eDNA levels would change over time. Biofilm biomass and eDNA concentration were measured hourly over 7 h. Biofilm biomass showed a time-dependent increase over the 7 h time course (Figure 3.3A), and this was confirmed by regression analysis ($P<0.0005$; Figure 3.4).

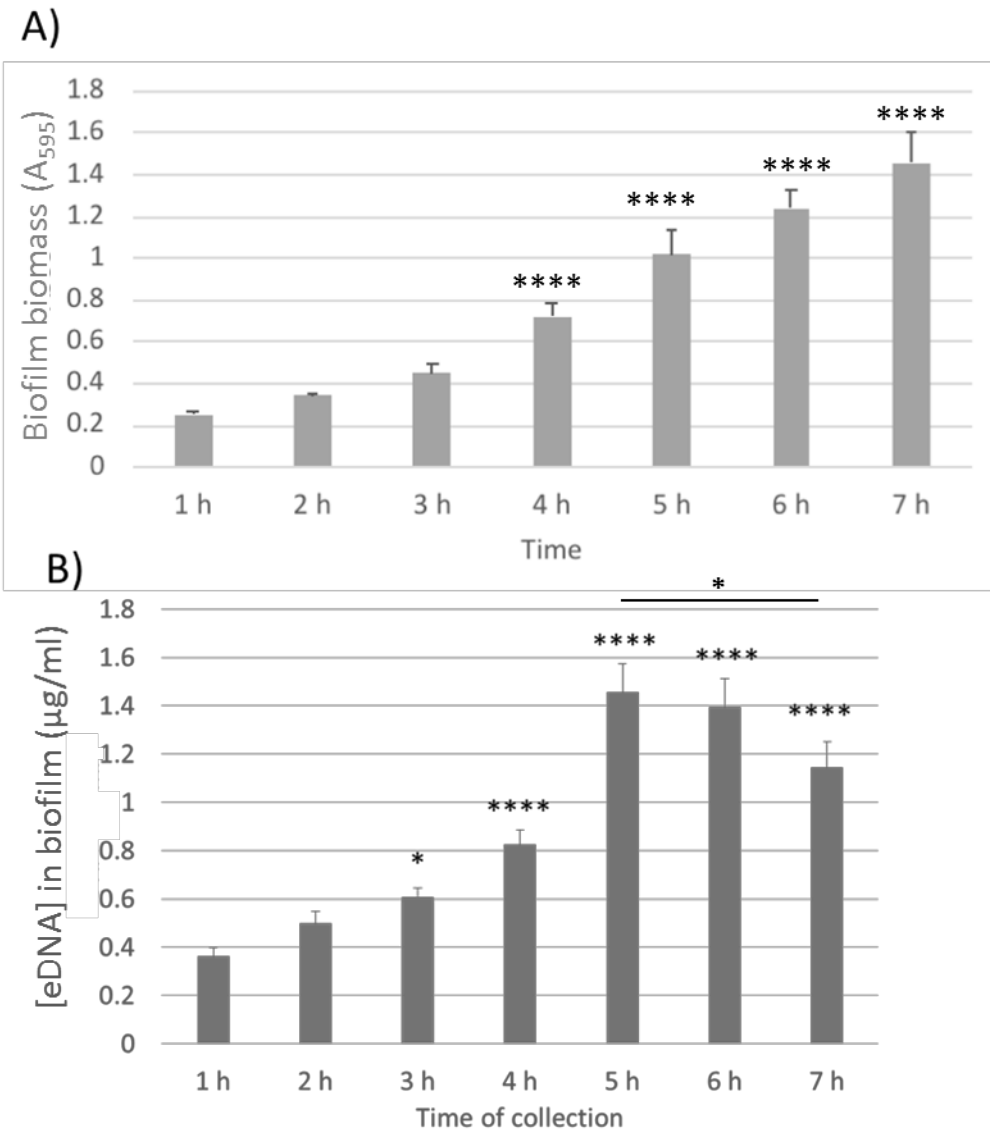

Figure 3.3 – ***Biomass increases over 7 h, but soluble eDNA peaks at 5 h during biofilm formation.*** *WT S. gordonii biofilms were grown at 37 °C in YPTG on saliva-coated glass-bottomed wells for between 1 and 7 h. A) Biofilms were stained with 0.25% crystal violet; the stain was released with acetic acid and the absorbance measured at A_{595}. B) Biofilms were washed with PBS, collected into TE buffer and biomass removed by centrifugation. Levels of soluble eDNA in supernatants were precipitated with phenol: chloroform: isoamyl alcohol before measurement at A_{260}. Experiments were performed in triplicate. Data are presented as mean absorbance/DNA concentration ± SD; n=3. A one-way unpaired ANOVA was used with α=0.05. * P < 0.05. **** P< 0.0001, compared to 1 h.*

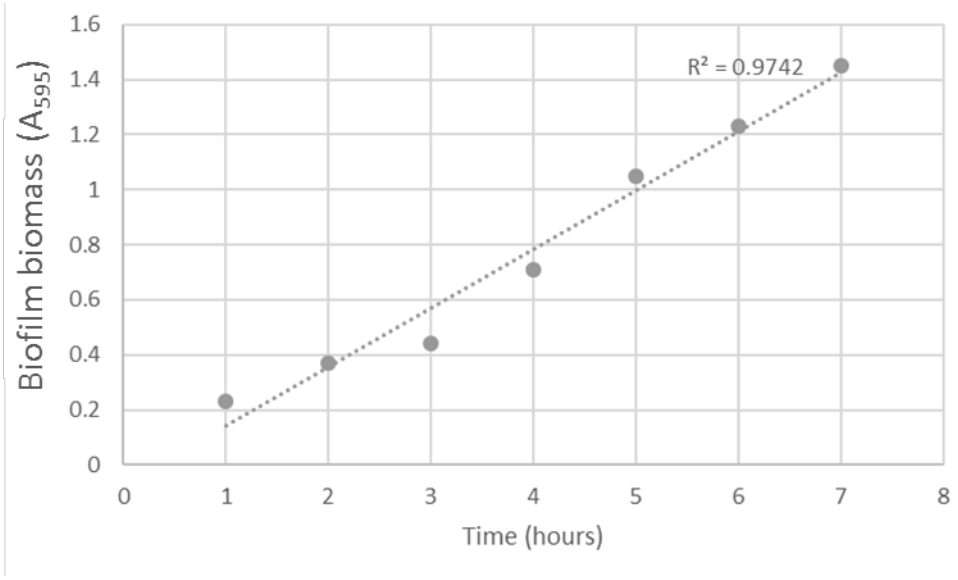

Figure 3.4 - ***Regression analysis of biofilm biomass formation vs time.***

Soluble eDNA concentration in the biofilm increased significantly every hour until it peaked at 5 h (Figure 3.3B). This was a 4-fold increase compared to 1 h. DNA concentrations within the biofilm subsequently reduced for the remaining time (2 further hours). This suggested that eDNA was most abundant and therefore potentially most important during initial biofilm accretion, up to 5 h. For this reason, 5 h was chosen as the time point for future eDNA investigations. The calculated eDNA abundance correlated with that shown previously for *S. pneumoniae*, for which eDNA was found to be important (and most abundant) during early biofilm accretion (Moscoso *et al.*, 2006).

3.3 Effect of DNase treatment on *S. gordonii* biofilms

The highly stable structure of DNA is hypothesised to be exploited in biofilms, meaning that eDNA may have a role in providing overall biofilm stability. To assess this potential role in *S. gordonii* biofilms, the effect of DNase treatment on biofilm biomass was investigated. A range of DNase concentrations were used (1 to 100 µg/ml) which had been shown previously to be effective on streptococcal biofilms, causing, for example, a dose-dependent reduction of up to 40% in biomass for *S. pyogenes* over this concentration range (Tetz *et al.*,

2009). Heat-inactivated DNase was used as the control, to ensure that it was the activity of the enzyme, and not the addition of protein, responsible for any effects seen. Biofilms were enzymatically treated during or post formation, to investigate if there were differences in any effects of DNase relative to biofilm development versus dispersal post formation. DNase treatment at 1 µg/ml did not significantly alter biofilm formation compared to the heat-inactivated control (Figure 3.5). At concentrations of DNase at 10 µg/ml or higher, biomass was significantly reduced. The greatest reduction of biomass was seen with 100 µg/ml DNase, causing a 32% reduction compared to biofilms which were treated with heat-inactivated DNase. By contrast, when 50-100 µg/ml DNase were added to preformed 4-h biofilms, no significant reduction in biomass was seen. Taken together, these data suggested that eDNA may be important in the initial accretion of the biofilm, but that loss of eDNA once the biofilm is already established did not cause biofilm disruption.

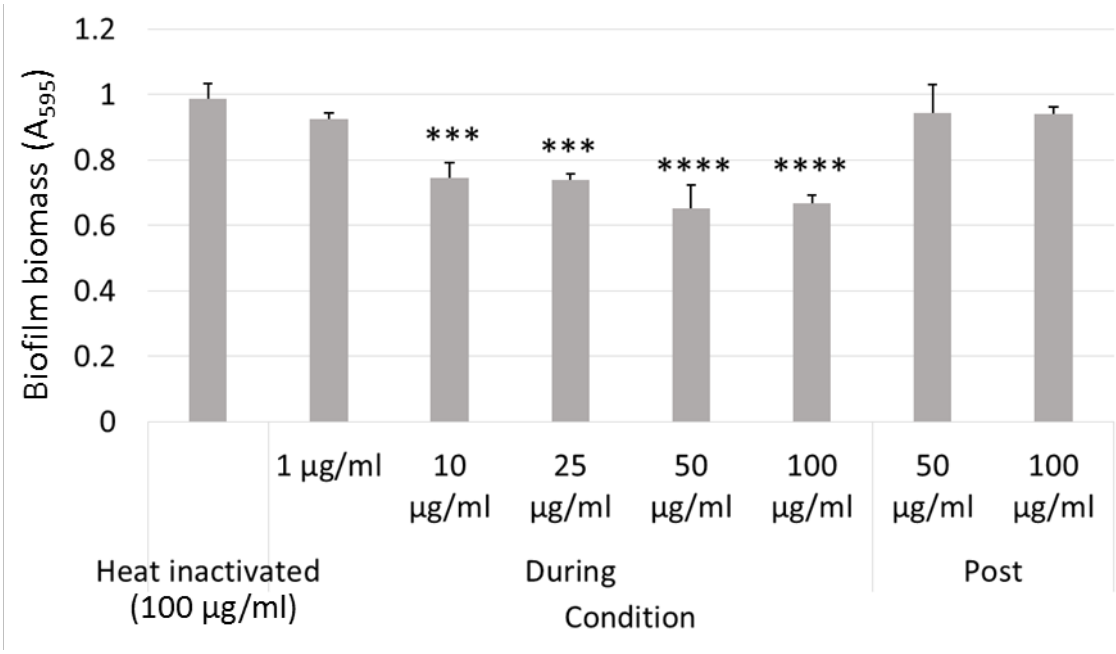

Figure 3.5 - ***DNase treatment disrupts biofilm development.*** *S. gordonii biofilms were grown in YPTG at 37 °C for 5 h on saliva-coated glass-bottomed wells with a range of DNase concentrations (during). Alternatively, DNase was added after 4 h and the biofilm incubated for a further 1 h (post treatment). Biofilms were stained with 0.25% crystal violet, the stain released with acetic acid, and the absorbance measured at A_{595}. Data are presented as absorbance ± SD; n=3. A one-way unpaired ANOVA was used with α=0.05. *** P < 0.0005, **** P< 0.0001, compared to heat-inactivated DNase.*

Regression analysis revealed that increasing DNase concentration when used during biofilm formation correlated significantly with decreasing biofilm biomass ($P<0.0001$; Figure 3.6). This added further support to the hypothesis that eDNA may facilitate early biofilm development.

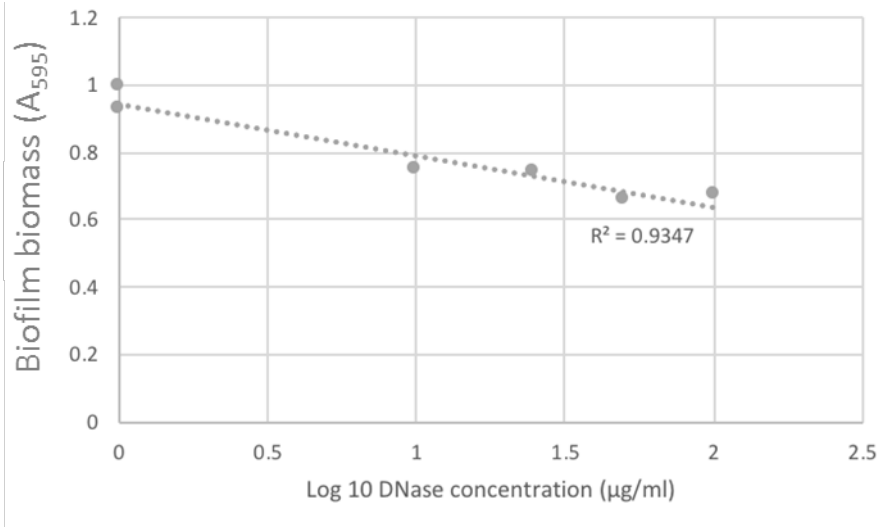

Figure 3.6 – ***Regression analysis of DNase concentrations vs biofilm biomass.***

3.4 Visualisation and quantification of eDNA stranding in biofilms

A limitation of the soluble DNA quantification approach used above is that it does not distinguish between eDNA released as a result of total cell lysis and the seemingly more organised phenomenon of eDNA stranding, as reported for *E. faecalis* biofilms (Barnes *et al.*, 2012). Since eDNA stranding is predicted to contribute to biofilm development, particularly in the early stages, studies next sought to determine whether, under these conditions, eDNA strands were formed during *S. gordonii* biofilm development. Based on the approach of Barnes *et al*., 2012, eDNA strands were visualised using antibody labelling, which allowed for the signal amplification required to detect this phenomenon. Alongside, bacterial chromosomal DNA was stained with TO-PRO3 to localise bacterial cells within the biofilm. Using this staining and imaging technique,

eDNA strands could be visualised, which appeared as straight lines between points and somewhat resembled schematics of star constellations (Figure 3.7). This images of eDNA stranding consistent with others in the literature e.g. eDNA in *Enterococcus* biofilms (Barnes *et al.,* 2012) (Figure 3.7B).

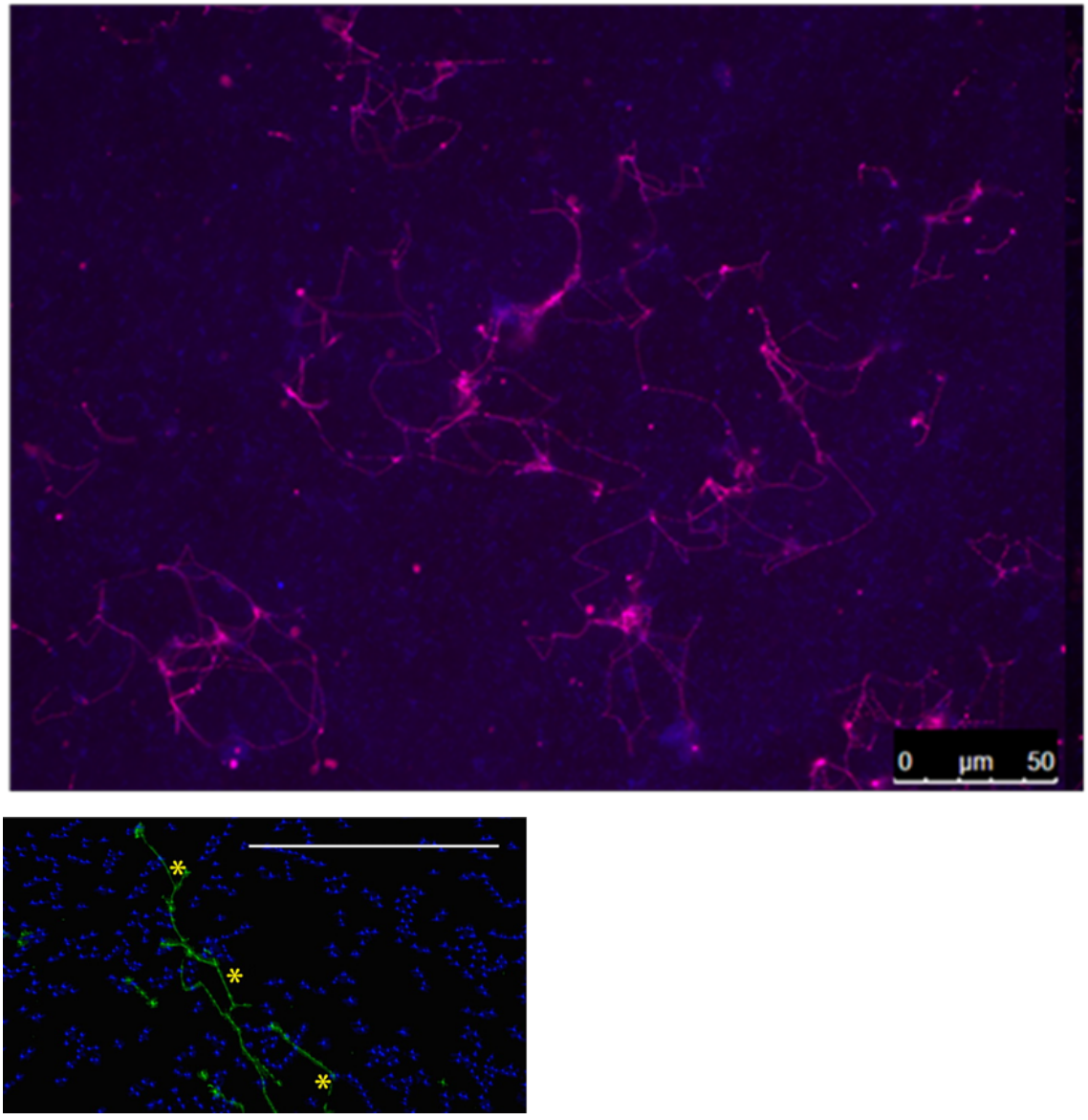

Figure 3.7 - ***Widefield micrograph image of eDNA stranding in a S. gordonii biofilm.***
A) *S. gordonii biofilms were grown in YPTG at 37 °C, 50 rpm for 5 h on saliva-coated cover slips. Bacterial cells were stained with TO-PRO3 (blue), while eDNA strands were labelled with an anti-ds DNA antibody (pink) and visualised on a widefield Leica DMi6000 microscope. Scale bar = 50 µm. B) Immunofluorescent micrograph from Barnes et al., 2012, showing eDNA stranding in E. faecalis biofilms. Scale bar = 25 µm.*

To investigate this phenomenon further, the next challenge was to devise a means to quantify these eDNA stranding events. At the time of this project,

while methods to stain extracellular double-stranded DNA existed, no approach to measure these eDNA strands that did not involve manual selection and measurement of strands using an imaging program had been reported. This was particularly problematic in the context of eDNA stranding due to the highly heterogeneous nature of these events. This would mean a large amount of time would need to be spent to manually analyse the eDNA strands from the vast number of images required. The requirement for quantitative analysis and fast processing of many images resulted in the conclusion that computational processing power would be required to analyse eDNA stranding data. Using macros written by Dr Dominic Alibhai (Section 7.1), a computer code was developed specifically for detection of eDNA strands. The development of this unique eDNA measurement programme had two phases: i) optimisation of image acquisition and ii) optimisation of image analysis.

3.4.1 Optimisation of image acquisition

First, a widefield microscope was chosen for image acquisition as it delivered the resolution necessary to resolve strands, whilst imaging quickly enough to allow for a high number of images to be acquired in a reasonable time. It was established that a Z stack would have to be taken on every field of view, as eDNA strands were found not to lie flat within Z. A Z-stack size of 12 μm was chosen, which was slightly greater than the height of the biofilm. This was around 8 μm under these conditions, consistent with what has been found previously for *S. gordonii* monospecies biofilms (Jack *et al.*, 2015). Z-step sizes of 0.5 μm were found to be optimal because they were sufficient to have eDNA stranding in focus, whilst low enough that the size of the data gathered was not too large as to be unmanageable. This resulted in 25 Z-steps per field of view. Initially, images were taken using a x 40 magnification lens, where 64 images were required to cover a 3 mm^2 area. However, the time taken to complete this imaging (16 h) was considered unfeasible for the longer-term project, so a lower magnification (NA 0.78) x20 magnification lens was sourced. This allowed the same area to be covered in only 8 fields of view, whilst still having fine enough

resolution to resolve eDNA strands. This reduced image acquisition time to approximately 5 h per plate.

At this stage manual selection of the Z-step was still required, as individual cover slips on which biofilms had been grown were being used. To overcome this, biofilms were instead grown on glass-bottomed plates, which could be imaged directly. This meant 24 biofilms could be imaged without user input, based on lack of variation in position of biofilms in X, Y in plates compared to mounted cover slips. Using plates also greatly reduced the variability in Z compared to using individual cover slips and allowed for the use of Best Focus and Adaptive Focus on the microscope system to identify the in-focus region around which a fine Z-step would then be performed. The Z depth over which the Best Focus and Adaptive Focus varied from plate to plate were set manually, but was typically around 100 μm. This range was covered coarsely in steps of around 8 μm, to allow for accurate identification of the eDNA strands, after which the fine Z-stack would be taken. This vastly reduced the time required to image each biofilm plate to approximately 3 h, compared to if this bi-phasic Z-step approach had not been used.

Plates with 24 wells were selected as these provided sufficient surface area for biofilm formation that allowed the capture of thousands of eDNA stranding events per well, whilst allowing up to 8 conditions to be investigated at once (minimum of 3 biological replicates per assay). The exposure and gain were set manually on each plate depending on the specific levels of antibody labelling, which did vary slightly across independent experiments.

3.4.2 Optimisation of image analysis

Following image acquisition, images went through several steps before data was outputted for analysis. First, Z-stacked images were projected to Best Focus images, which is designed to take the brightest (and hopefully therefore the most in focus) pixel in Z from every X, Y position. This initial step meant that all the stranding events captured should appear to be in focus, ready for further analysis.

A macro was developed in MATLAB by Dr Dominic Alibhai, which initially used a FIJI binary threshold programme. Pixels above a certain brightness were included and those which were not were excluded; for example, above and below 0.6. This allowed stranding to be picked out from the background. However, after further imaging, it was found that what would be detected manually differed from that identified by the program across fields of view, as the background varied in intensity. Therefore, the code was re-written to instead use ridge finding. This enabled, for example, an intensity of 2 to be picked up against a background of "1"s, but an intensity of 6 could also be picked up against a background of "5"s, within the same image.

Some regions of intensity were then excluded based on criteria designed to pick out the signal from the noise. One criterion excluded regions that were less than 0.5 μm, as these were considered likely to be DNA in chromatin from lysed cells and not the eDNA strands this methodology aimed to identify. Objects which were too circular were also excluded, as these regions were again likely to either represent DNA from lysed cells or diffraction of light around sub-resolution particles. The remaining regions of intensity identified by ridge finding were then linked to other regions if they were less than 0.5 μm apart.

The full code for MATLAB and macros required for FIJI can be found in the appendices (Section 7.1). Stranding information was then outputted into Excel and overdrawn onto the micrographs and saved. This allowed for comparison between what the programme identified as eDNA stranding on the overdrawn images, and what would be identified as eDNA stranding manually on the inputted images, to ensure the program was detecting eDNA stranding as intended (Figure 3.8).

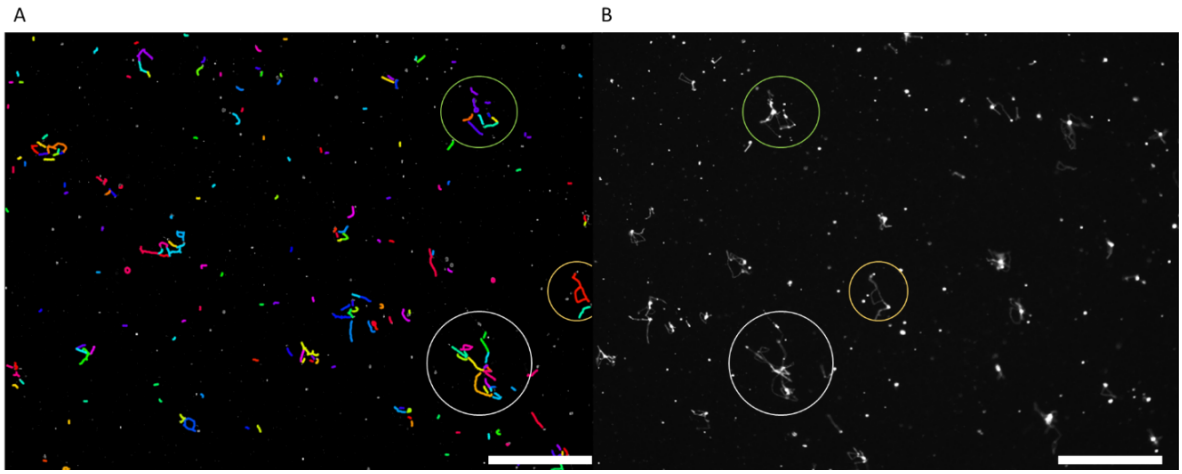

Figure 3.8 - Analysis of eDNA stranding in S. gordonii biofilms. *S. gordonii biofilms were grown in YPTG at 37 °C, 50 rpm for 5 h on saliva-coated cover slips. Biofilms were fixed in 2% PFA then labelled with an anti-dsDNA antibody and visualised using widefield microscopy. A) Output of ridge finding analysis in MATLAB with detected eDNA stranding overdrawn. B) Original widefield micrograph. Coloured circles label eDNA stranding and the detected counterparts. Scale bars = 100 µm.*

After development of the program, a complete data set from a 24 well plate was collected. However, these data took approximately 3 days to be processed. Performing such experiments in a minimum of triplicate meant that it would take up to 9 days of computing time to analyse only 6 conditions. For this reason, binning was introduced, which is a process whereby pixels are grouped and the data on the brightest pixel in this group is retained. 2 x 2 binning was used, and this reduced the size of the data set 4-fold, meaning that running the image analysis programme for a 24-well data set now took 4 times less - approximately 16 h. The computer analysis of 6 conditions would therefore take approximately 3 days.

Since the programme labelled and saved the length of each individual stranding event, it was possible to measure the average length of eDNA stranding, the average frequency of stranding events per area, and the total amount of eDNA stranding within an area. As total stranding per area reflects changes in both frequency and length of stranding events, this was chosen as the default metric.

3.5 Factors affecting eDNA stranding

3.5.1 DNase

The newly developed eDNA stranding quantification methodology offered the potential to quickly and quantitatively gather and analyse meaningful data on eDNA stranding in biofilms. To ensure the programme was working reliably, further validation was required. DNase I treatment was chosen for initial validation of the eDNA standing analysis, as DNase-treated biofilms would be expected to have lower levels of total eDNA stranding relative to an untreated control. The same DNase concentration used to determine the effects of DNase treatment on biofilm biomass (section 3.3) were used to investigate DNase stranding. This meant changes in eDNA stranding due to altered biomass could be accounted for.

Wild type *S. gordonii* biofilms produced an average of 1780 µm/mm^2 total eDNA stranding. When DNase was applied during biofilm formation, total levels of eDNA stranding were significantly reduced relative to untreated control in what appeared to be a dose-dependent manner (Figure 3.8). DNase treatment at 1 µg/ml during biofilm formation caused a reduction of 36% of total eDNA stranding compared to no treatment. Higher concentrations of DNase resulted in biofilms with less eDNA stranding. The highest DNase concentrations of 100 µg/ml resulted in biofilms with a 70% reduction in eDNA stranding. Regression analysis confirmed a significant relationship between increasing DNase concentration during biofilm development and reducing eDNA stranding ($P<0.005$; Figure 3.10). When 50 µg/ml or 100 µg/ml DNase was applied to biofilms following 4 h development, biofilms exhibited reductions in levels of eDNA stranding of 40% or 51% respectively (Figure 3.9).

A

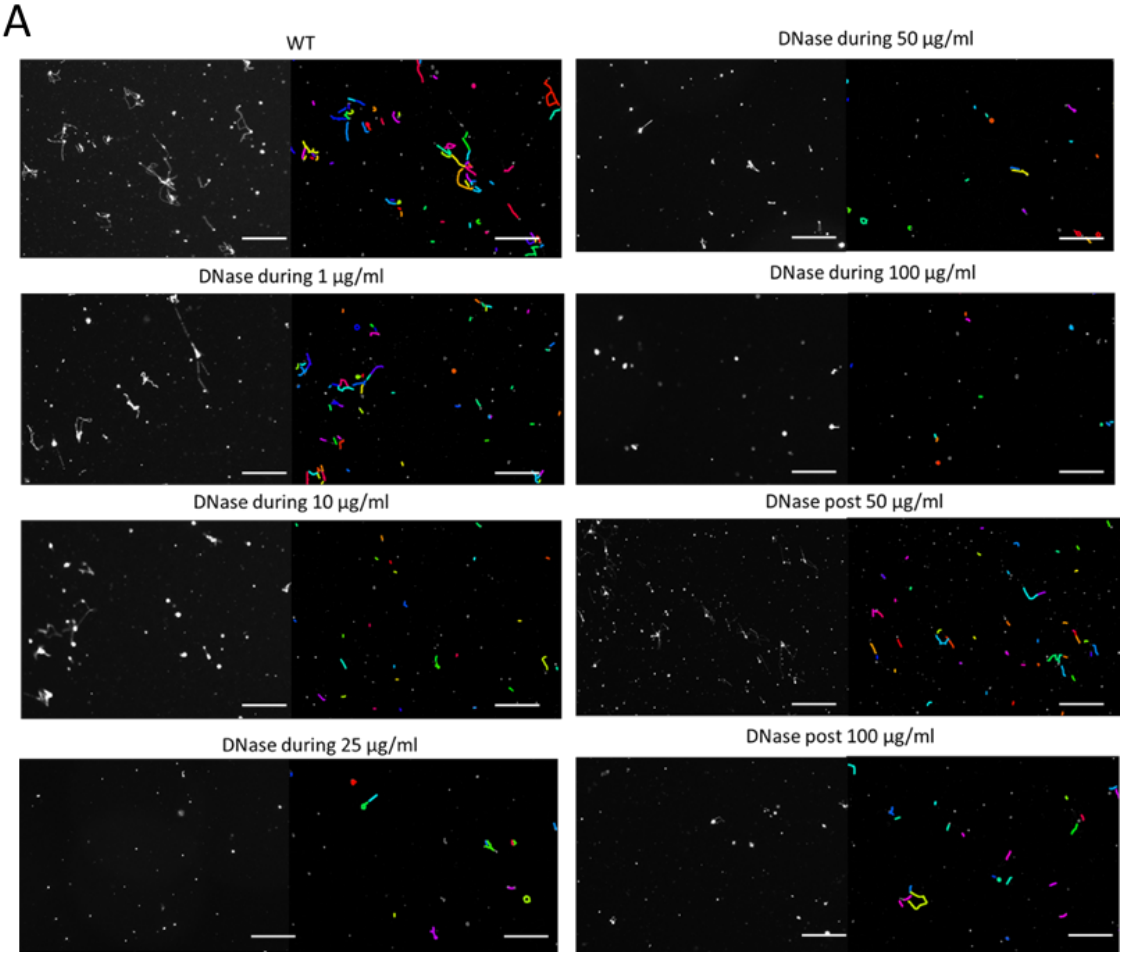
WT
DNase during 50 µg/ml
DNase during 1 µg/ml
DNase during 100 µg/ml
DNase during 10 µg/ml
DNase post 50 µg/ml
DNase during 25 µg/ml
DNase post 100 µg/ml

B

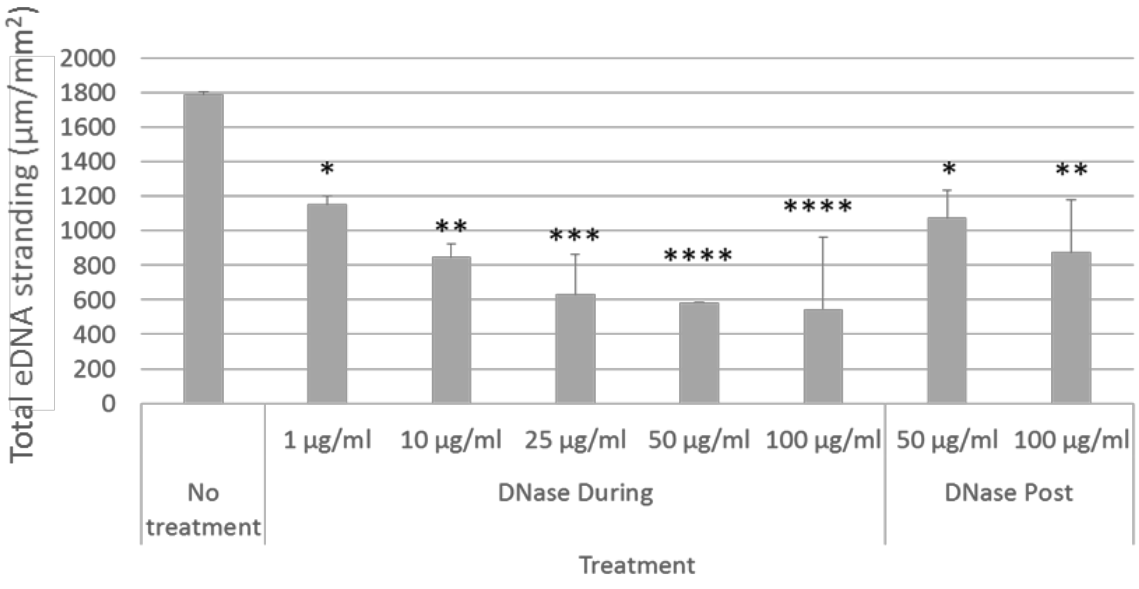
Total eDNA stranding (µm/mm²)
2000
1800
1600
1400
1200
1000
800
600
400
200
0
*
**
***
****
****
*
**
No treatment
1 µg/ml
10 µg/ml
25 µg/ml
50 µg/ml
100 µg/ml
50 µg/ml
100 µg/ml
DNase During
DNase Post
Treatment

Figure 3.9 – DNase treatment reduces eDNA stranding in S. gordonii biofilms. *S. gordonii biofilms were grown in YPTG at 37 ˚C for 5 h on saliva-coated glass-bottomed wells with a range of DNase concentrations (during). Alternatively, DNase was added after 4 h and the biofilm incubated for a further 1 h (post treatment). Biofilms were stained with TO-PRO3, labelled with an anti-ds DNA antibody, followed by an anti-Ig antibody conjugated to a fluorophore and visualised using widefield microscopy. A) Gallery of images pre- (left) and post-ridge finding analysis in MATLAB (right). Scale bars = 100 µm. B) Quantification of total eDNA stranding. Data are presented as mean total stranding per mm² ± SD; n=3. A one-way unpaired ANOVA was used with α=0.05. * = P<0.05, ** = P<0.005 *** = P < 0.0005. **** = P< 0.0001, compared to no treatment control.*

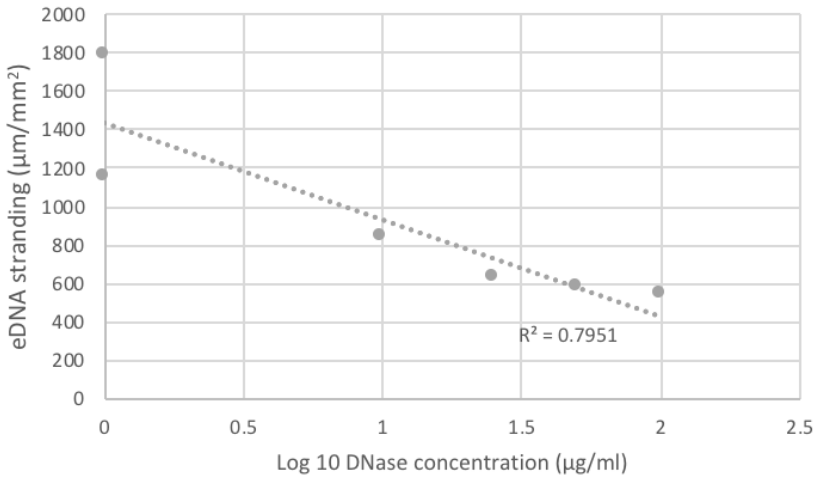

Figure 3.10 - ***Regression analysis of DNase concentration vs eDNA stranding.***

eDNA removal by DNase treatment also directly correlated with reduction in biofilm biomass during early stage formation (0-5 h) (P<0.05; Figure 3.11), whereas DNase treatment of more mature (4 h) biofilms reduced eDNA stranding but had no significant disruption of overall biomass levels. This indicates that eDNA may facilitate bacterial-substratum attachment or stabilise initial co-aggregation events, both of which are crucial steps of early biofilm formation.

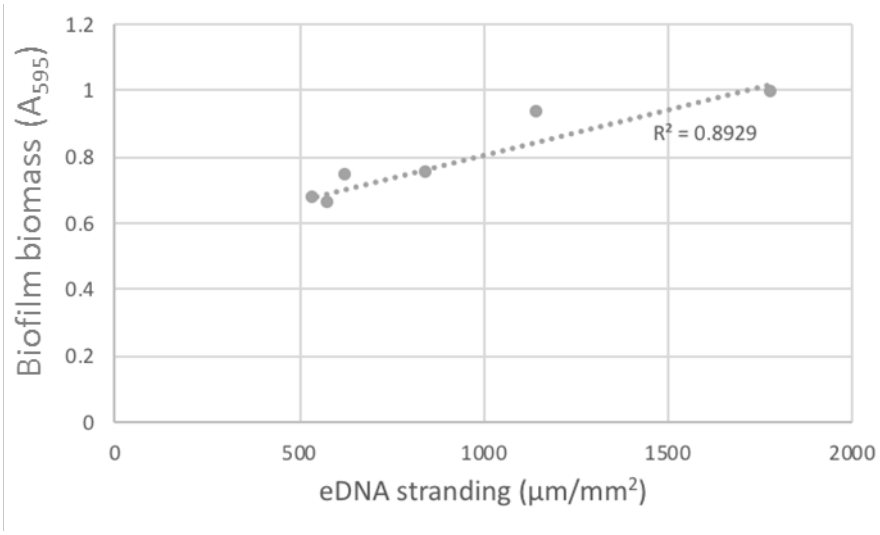

Figure 3.11 - ***Regression analysis of eDNA stranding vs. biomass during continuous DNase treatment.***

Together, these data showed that both eDNA stranding and biomass decreased with DNase treatment, which was consistent with what had been shown for DNase treatment and biomass previously (Hall-Stoodley *et al.*, 2008). As this outcome correlated with the prediction that DNase treatment would degrade eDNA strands, resulting in lower total eDNA stranding, the eDNA stranding quantification approach had been validated. Furthermore, this indicated that eDNA stranding may be important in biofilm accretion.

3.5.2 RNase

The strands of nucleic acid visible in biofilms are widely assumed to be DNA, but this is rarely verified. The effects of RNase treatment on *S. gordonii* biofilm formation and eDNA stranding were therefore investigated. RNase was used in the same concentration range as DNase treatment, to allow for comparison if any effect caused by RNase treatment were observed. The DNase and RNase used had similar specific activities: 1 U/µg and 1.5 U/µg respectively (A unit of activity was defined as the ability to degrade 1 µg of the appropriate nucleic acid to oligonucleotides in 10 minutes at 37 °C). RNase treatment was shown to have no effect on biofilm biomass (Figure 3.12) or eDNA stranding (Figure 3.13). While RNA would not be directly visualised with this analysis approach, the fact that

RNase treatment had no significant effects on either *S. gordonii* biofilm biomass or total eDNA stranding confirmed that the observed stranding structures did not contain RNA and suggests that RNA was not a significant component of the overall biofilm.

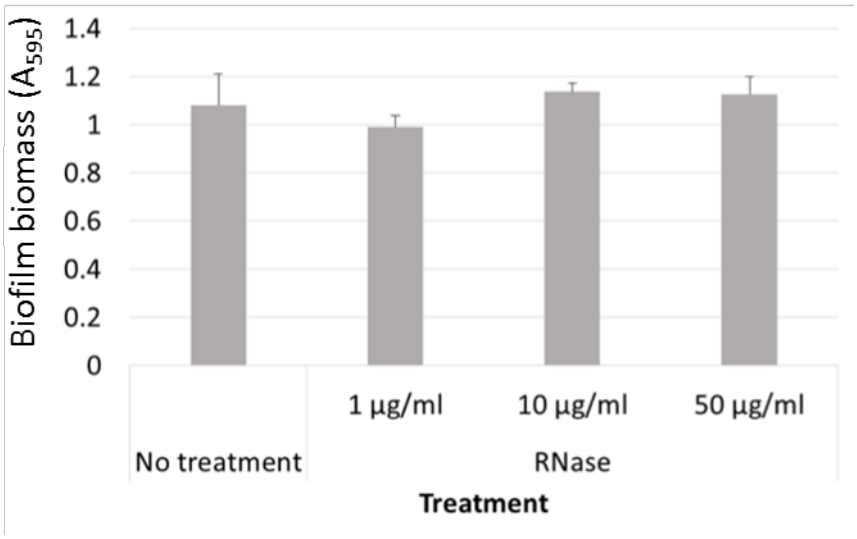

Figure 3.12 - ***RNase treatment does not affect biofilm biomass.*** *WT S. gordonii biofilms were grown at 37 °C in YPTG on saliva-coated glass cover slips for 5 h with no treatment, 1, 10 or 50 µg/ml RNase. Biofilms were washed with PBS then stained with crystal violet. This stain was released with acetic acid and A_{595} measured. Data are presented as absorbance ± SD; n=3. A one-way unpaired ANOVA was used with α=0.05. No significant difference was found compared to no treatment.*

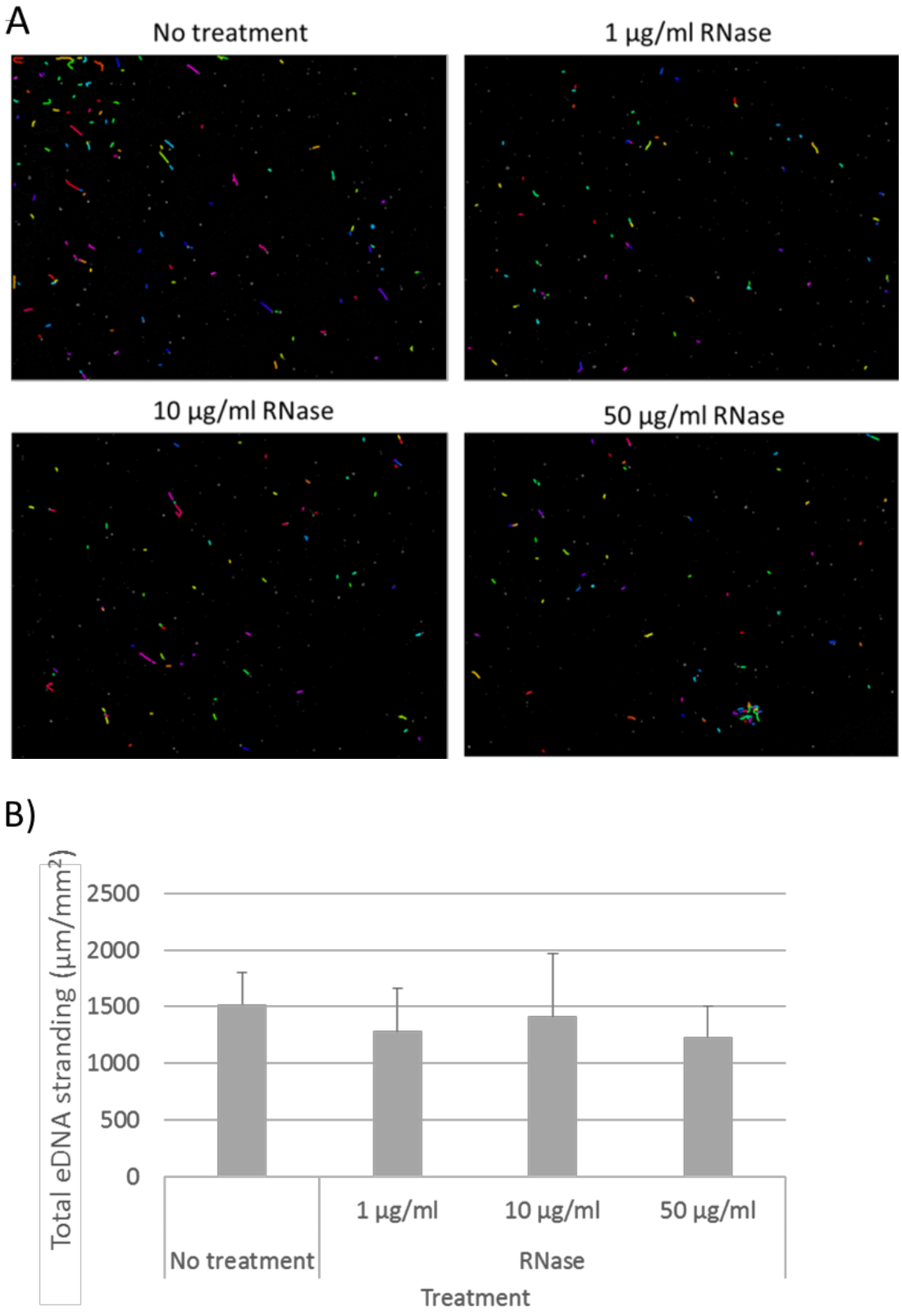

*Figure 3.13 – **RNase treatment does not affect eDNA stranding in biofilms.** WT S. gordonii biofilms were grown at 37 °C in YPTG on saliva-coated glass cover slips for 5 h with no treatment, 1, 10 or 50 µg/ml RNase. A) Biofilms were labelled an anti-ds DNA antibody, followed by an anti-Ig antibody conjugated to a fluorophore and TO-PRO3. Widefield microscopy was used to capture an area of each biofilm. B) Ridge*

finding code on MATLAB was used to quantify eDNA stranding. Data are presented as mean total stranding per mm² ± SD; n=3. A one-way unpaired ANOVA was used to compare to no treatment with α=0.05. No significant difference was found.

3.5.3 Protease

Proteins are known to be major components of biofilm EPS, so their potential role in biofilm accretion and eDNA stranding was investigated. The proteinase K concentrations chosen were the same as used in the DNase assays (section 3.5.1). The specific activity of proteinase K used was identical to that of the DNase used (1 U/µg). *S. gordonii* biofilms were exposed to a range of proteinase K concentrations, both during biofilm formation and following 4 h biofilm development.

Biofilms which were treated with 10 µg/ml or greater proteinase K during biofilm formation had significantly less biomass than untreated biofilms. The greatest reduction occurred at 50 µg/ml proteinase K, where absorbance was significantly reduced by 74% (Figure 3.14). Proteinase K treatment disrupting biofilm accretion is consistent with previous studies which have shown that protease treatment can disrupt streptococcal biofilm formation (Wang *et al.*, 2011). By contrast, when 4 h biofilms were exposed to an equivalent concentration of proteinase K there were no significant effects on biomass.

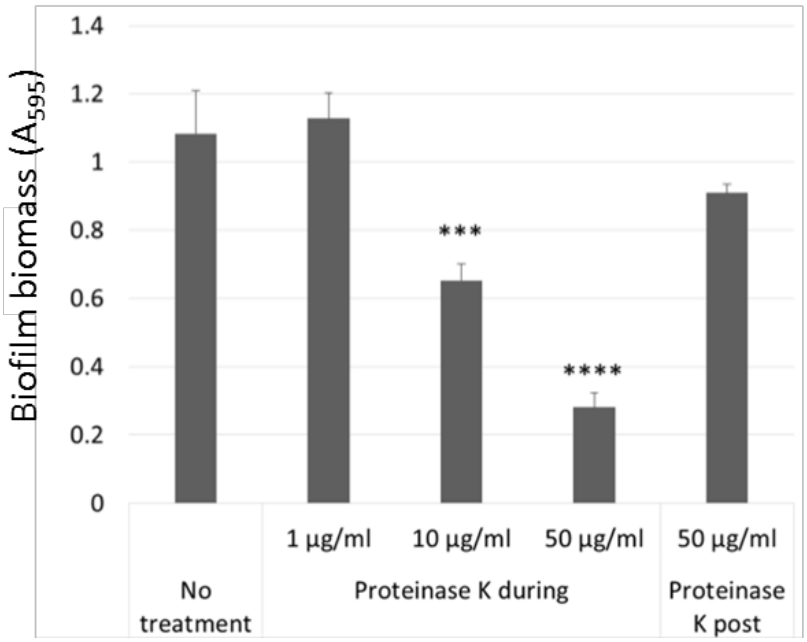

*Figure 3.14 - **Proteinase K treatment reduces biofilm biomass.** WT S. gordonii biofilms were grown at 37 °C in YPTG on saliva-coated glass cover slips for 5 h with no treatment, 1, 10 or 50 µg/ml proteinase K, or proteinase K was added at 4 h. Biofilms were washed with PBS then stained with crystal violet. This stain was released with acetic acid and A_{595} measured. Data are presented as absorbance ± SD; n=3. A one-way unpaired ANOVA was used with α=0.05. *** P<0.0005, **** P<0.0001, compared to no treatment.*

The effect of proteinase K treatment on eDNA stranding was also investigated. Biofilms treated with 50 µg/ml proteinase K produced 98% less stranding than untreated biofilms (Figure 3.15). Treating biofilms with proteinase K post formation however did not cause a significant change in eDNA stranding. The large reduction in both biomass and eDNA stranding in the presence of proteinase K indicated the important and extensive role which proteins play during biofilm development.

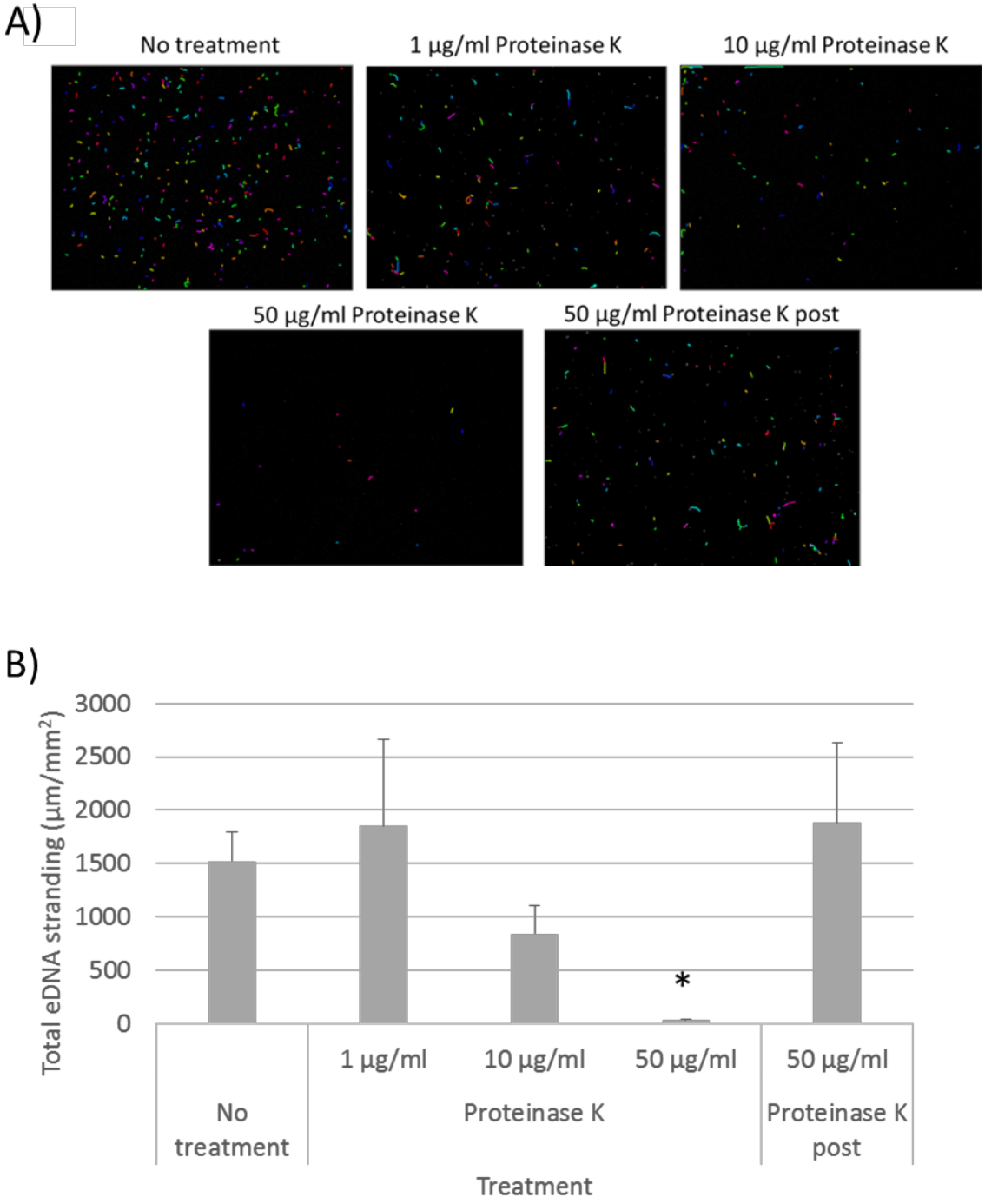

Figure 3.15 – ***Proteinase K treatment reduces eDNA stranding during biofilm formation.*** *WT S. gordonii biofilms were grown at 37 °C in YPTG on saliva-coated glass cover slips for 5 h with no treatment, 1, 10 or 50 µg/ml proteinase K, or proteinase K was added at 4 h. A) Biofilms were labelled with an anti-dsDNA antibody, then an anti-Ig antibody conjugated a fluorophore, and TO-PRO3. Widefield microscopy was used to capture an area of each biofilm. B) Ridge finding code on MATLAB was used to quantify eDNA stranding. Data are presented as mean total stranding per mm² ± SD; n=3. A one-way unpaired ANOVA was used with α=0.05. * = P < 0.05 compared to no treatment.*

Regression analysis showed proteinase K treatment significantly predicted reduced eDNA stranding, even when adjusted for altered biomass ($P<0.0005$; Figure 3.16).

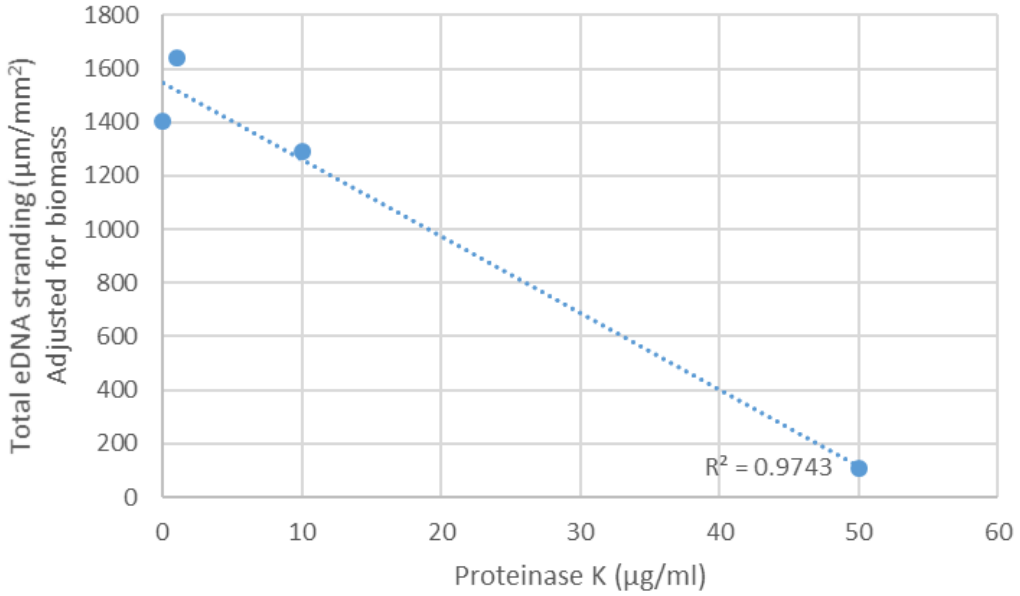

Figure 3.16 - ***Regression analysis of proteinase K treatment vs. eDNA stranding following adjustment for biomass***

3.5.4 Dextranase

Glucans were known to be important for biofilm accretion by oral streptococci, but it was unknown if they had any association with eDNA stranding. Dextranase is an enzyme which breaks down dextran, a complex glucan that is a common component of bacterial EPS (Koo *et al.*, 2010). To investigate the role dextran may play in *S. gordonii* biofilm formation and eDNA stranding, biofilms were treated with a range of dextranase concentrations (Figure 3.17). The specific activity of dextranase used was 1 U/µg, so the concentrations chosen for dextranase treatments were matched to those of DNase and proteinase K used in the prior experiments, to allow for comparison

of any effects. Treatment with 10 µg/ml of dextranase or higher produced biofilms with significantly less biomass than their untreated counterparts, confirming that dextran is a component of *S. gordonii* biofilms and in line with previous studies (Ricker *et al.*, 2014).

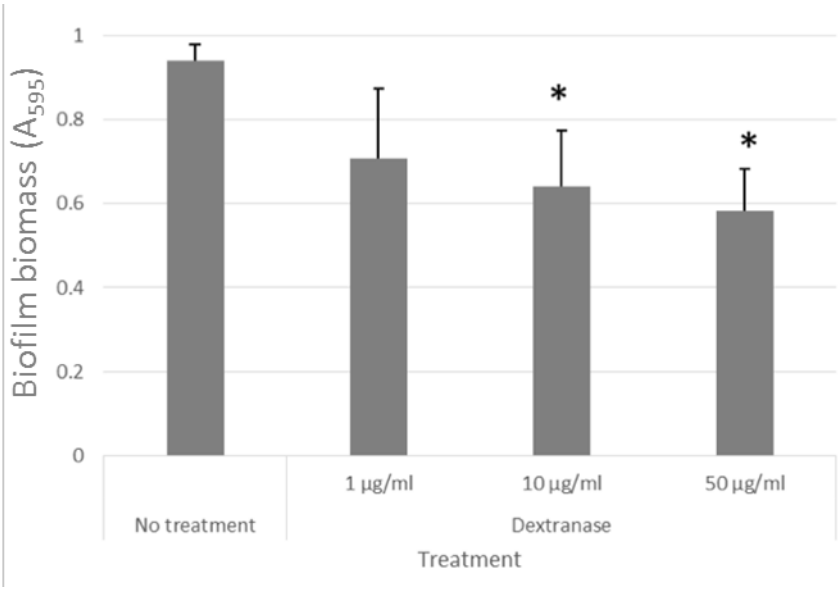

*Figure 3.17 – **Dextranase treatment reduces biofilm biomass**. WT S. gordonii biofilms were grown at 37 °C in YPTG on saliva-coated glass cover slips for 5 h with no treatment, 1, 10 or 50 µg/ml dextranase. Biofilms were washed with PBS then stained with crystal violet. This stain was released with acetic acid and A_{595} measured. Data are presented as mean absorbance ± SD; n=3. A one-way unpaired ANOVA was used with α=0.05. * P<0.05 compared to no treatment.*

Next, the potential role of dextran in eDNA stranding was investigated. Dextranase treatment did not significantly affect eDNA stranding (Figure 3.18). No change was observed with any concentration of dextranase tested, indicating that dextran-containing polysaccharides were unlikely to be part of the observed strands or required for eDNA strand assembly.

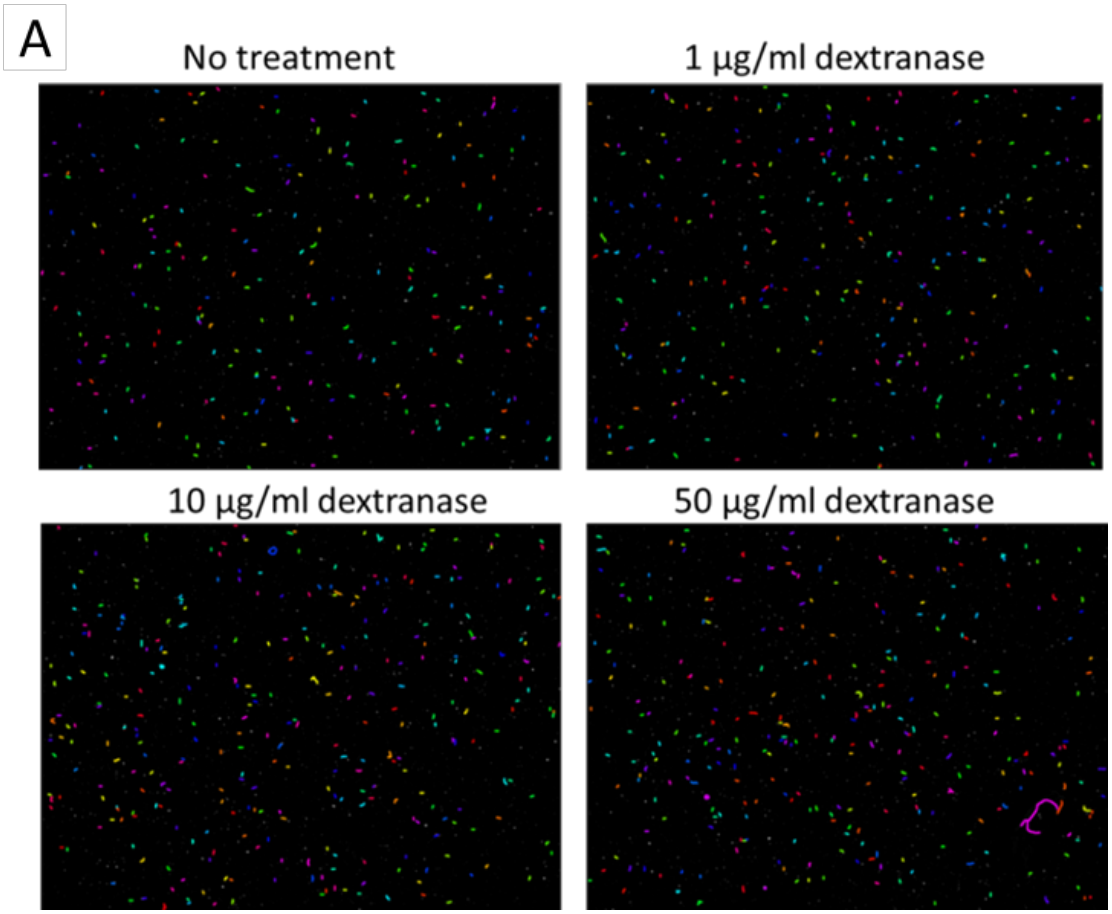

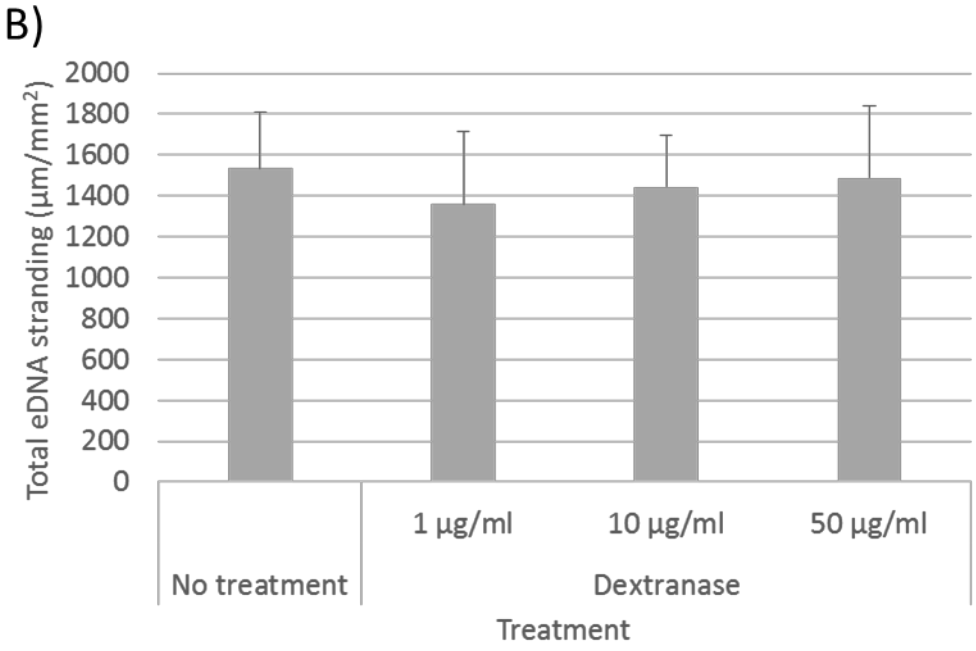

Figure 3.18 – ***Dextranase treatment does not affect eDNA stranding.*** *WT S. gordonii biofilms were grown at 37 °C in YPTG on saliva-coated glass cover slips for 5 h with no treatment, 1, 10 or 50 µg/ml dextranase. A)*

Biofilms were labelled with an anti-dsDNA antibody, then an anti-Ig antibody conjugated to a fluorophore, and TO-PRO3. Widefield microscopy was used to capture an area of each biofilm. B) Ridge finding code on MATLAB was used to quantify eDNA stranding. Data are presented as mean total stranding per mm^2 ± SD; n=3. Experiments were performed in triplicate. A one-way unpaired ANOVA was used to compare to no treatment with α=0.05. No significant differences were found.

3.5.5 Sucrose vs. glucose

The studies presented so far in this Chapter utilised enzymatic treatments that targeted specific components of the biofilm. However, environmental conditions and nutrient supply are also well-established parameters that can influence biofilm development. Additionally, the potential role for eDNA strands to act as nutrient stores added to our interest in how sugar availability may affect this phenomenon. To this end, the effects of carbohydrate source on *S. gordonii* biofilm formation and eDNA stranding were investigated. Specifically, the effects of sucrose versus glucose were examined, since these sugars have been shown to modulate the biofilm EPS profile in streptococcal species, such as *S. mutans* (Decker *et al.*, 2014). In *S. gordonii*, the sugar source had been found to modulate the polysaccharides found within biofilms (Ricker *et al.*, 2014).

The effect on biofilm formation of using different sugars and at different concentrations was investigated. An 8-fold range of concentrations based on the routine glucose concentration used in the biofilm model (0.4% w/v) and the sucrose/glucose concentrations (1% w/v) shown to modulate *S. gordonii* biofilm EPS (Ricker *et al.*, 2014) were tested. The range of concentrations of sugar used to supplement media were shown to support biofilm formation. Biomass was not significantly different between different sugar types or between different concentrations (Figure 3.19).

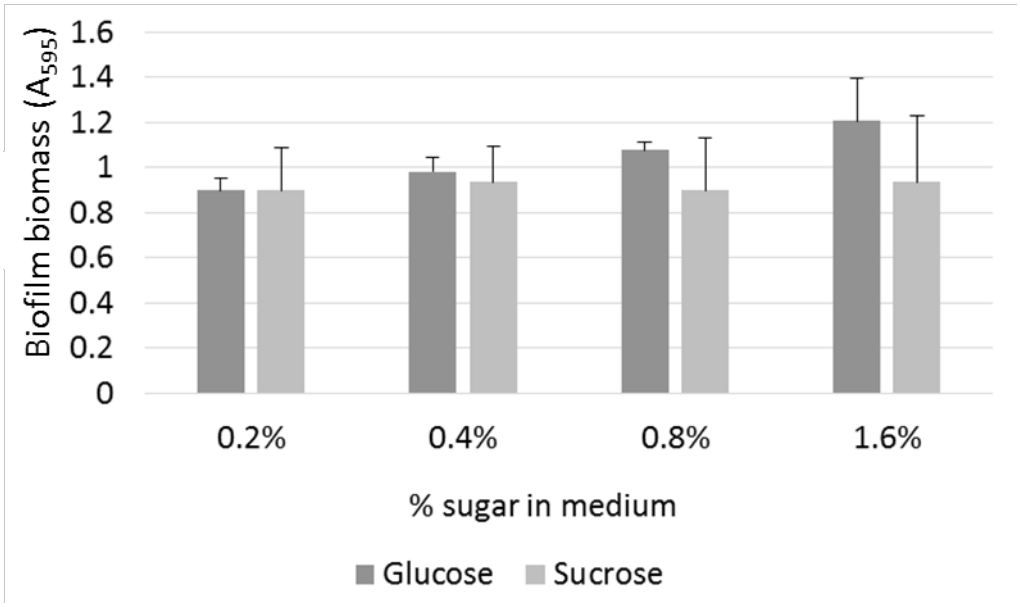

Figure 3.19 - ***S. gordonii biofilms are comparable in media supplemented with 0.2-1.6% glucose or sucrose****. WT S. gordonii biofilms were grown at 37 °C in YPT on saliva-coated glass cover slips for 5 h with 0.2, 0.4, 0.8 or 1.6% sucrose or glucose. Biofilms were washed with PBS then stained with crystal violet. This stain was released with acetic acid and A_{595} measured. Data are presented as mean absorbance ± SD; n=3. A one-way unpaired ANOVA was used with α=0.05. No significant differences were found.*

Next, the effect of sugar type and concentration on eDNA stranding was investigated. At 0.2% sugar supplementation, stranding in sucrose was significantly higher than in glucose (Figure 3.20). Low glucose, but not low sucrose, was limiting to eDNA stranding. Taken together, these data showed that although eDNA stranding increased with increasing glucose, biofilm biomass did not. This suggested that eDNA stranding might be related to specific carbohydrate source and availability.

A

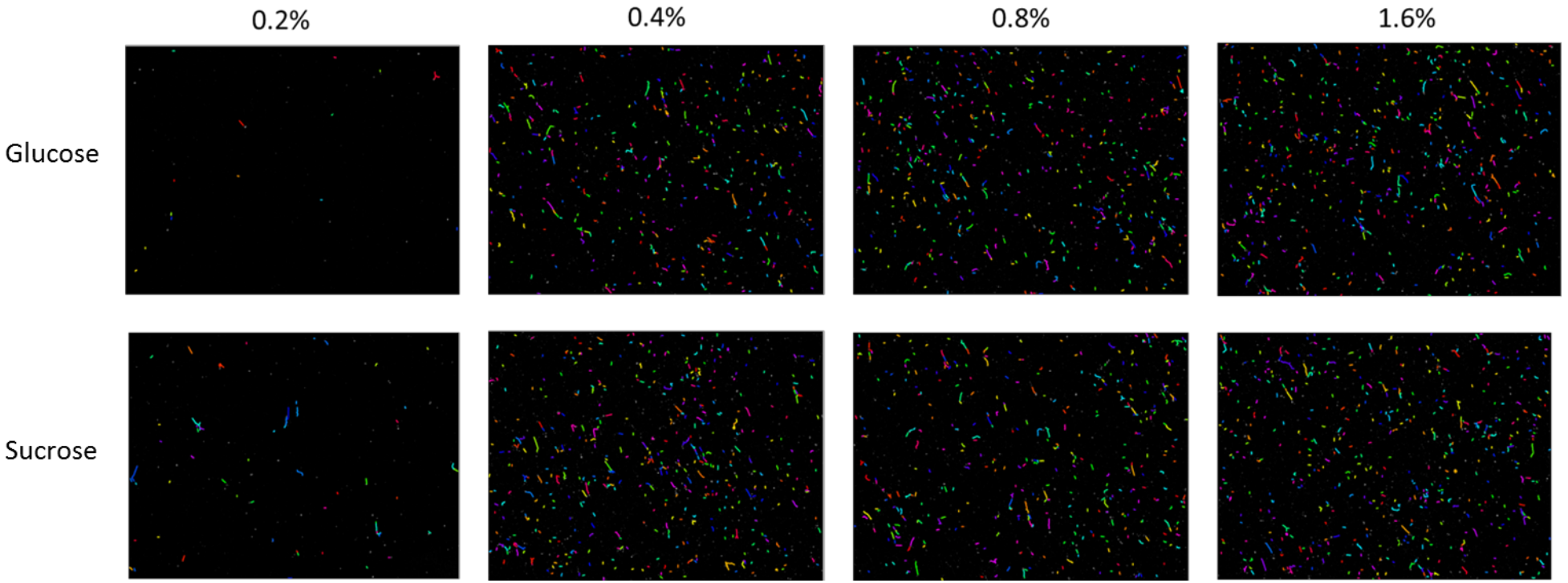

B

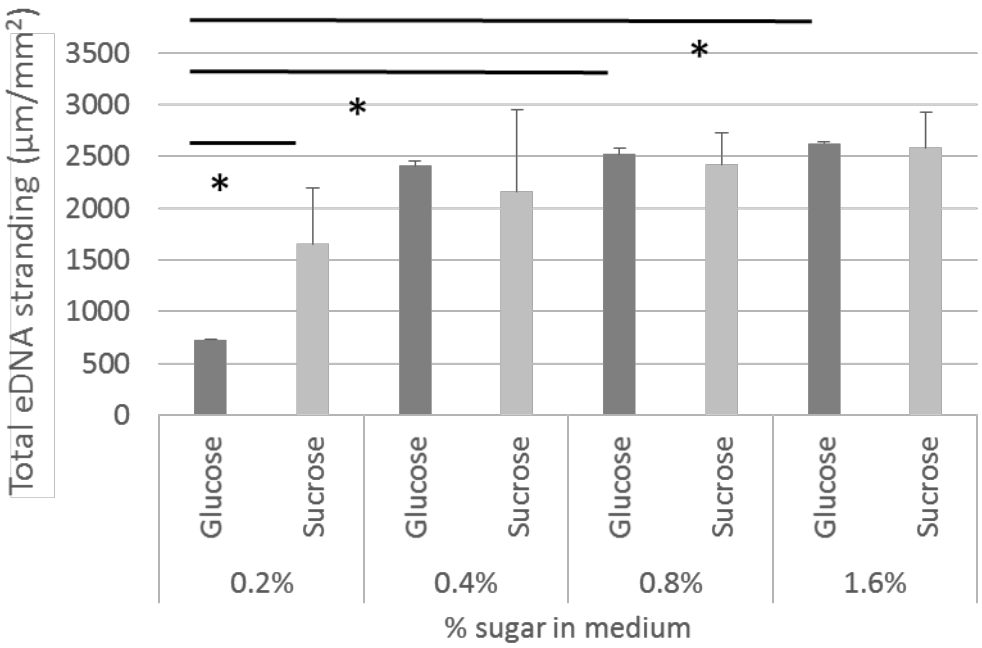

Figure 3.20 - ***The effects of glucose vs. sucrose supplementation on eDNA stranding in S. gordonii biofilms.*** *WT S. gordonii biofilms were grown at 37 °C in YPT on saliva-coated glass cover slips for 5 h with 0.2, 0.4, 0.8 or 1.6 % glucose or sucrose supplementation. A) Biofilms were labelled with an anti-dsDNA antibody, then an anti-Ig antibody conjugated to a fluorophore, and TO-PRO3. Widefield microscopy was used to capture an area of each biofilm. B) Ridge finding code on MATLAB was used to quantify eDNA stranding. Data are presented as mean total stranding per mm² ± SD; n=3. Experiments were performed in triplicate. A one-way unpaired ANOVA was used with α=0.05. P<0.05 = * compared to 0.2% sugar supplementation.*

3.5.6 pH

The pH of the oral cavity varies in oral health and disease, and influences biofilm constituents (Nobbs *et al.*, 2009). Since the average pH in the oral cavity is pH 6.7, but can range from pH 5 to pH 8, this range was selected to investigate the effects of pH on *S. gordonii* biofilm formation and eDNA stranding. The pH of the medium in which *S. gordonii* biofilms were grown was found not to significantly influence the resultant biomass of the biofilms between pH 5 and pH 8 (Figure 3.21).

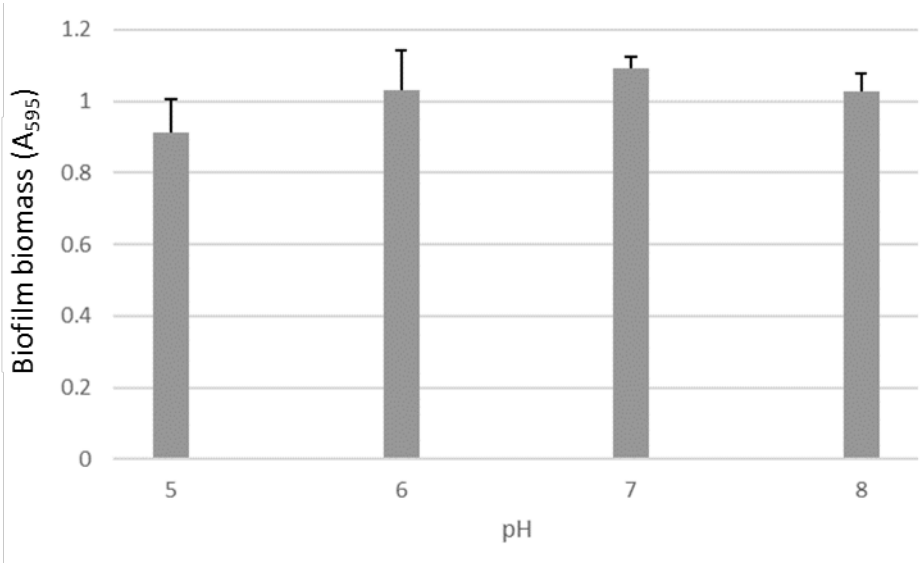

*Figure 3.21 – **pH does not affect S. gordonii biofilm biomass**. WT S. gordonii biofilms were grown at 37 °C in YPTG at pH 5, 6, 7, or 8 on saliva-coated glass cover slips for 5 h. Biofilms were washed with PBS then stained with crystal violet. This stain was released with acetic acid and A_{595} measured. Data are presented as mean absorbance ± SD; n=3. A one-way unpaired ANOVA was used with α=0.05. No significant differences were found.*

eDNA stranding under different pH conditions was then investigated (Figure 3.22). Highest eDNA stranding occurred in biofilms grown at pH 6, however this was not significantly different from those grown at pH 7 (the pH used in previous experiments). Biofilms grown at pH 5 or 8 produced around half the eDNA of those grown at pH 7. These findings indicated that a pH of 6 or 7 was optimal for eDNA stranding, and pH 7 was maintained in subsequent investigations.

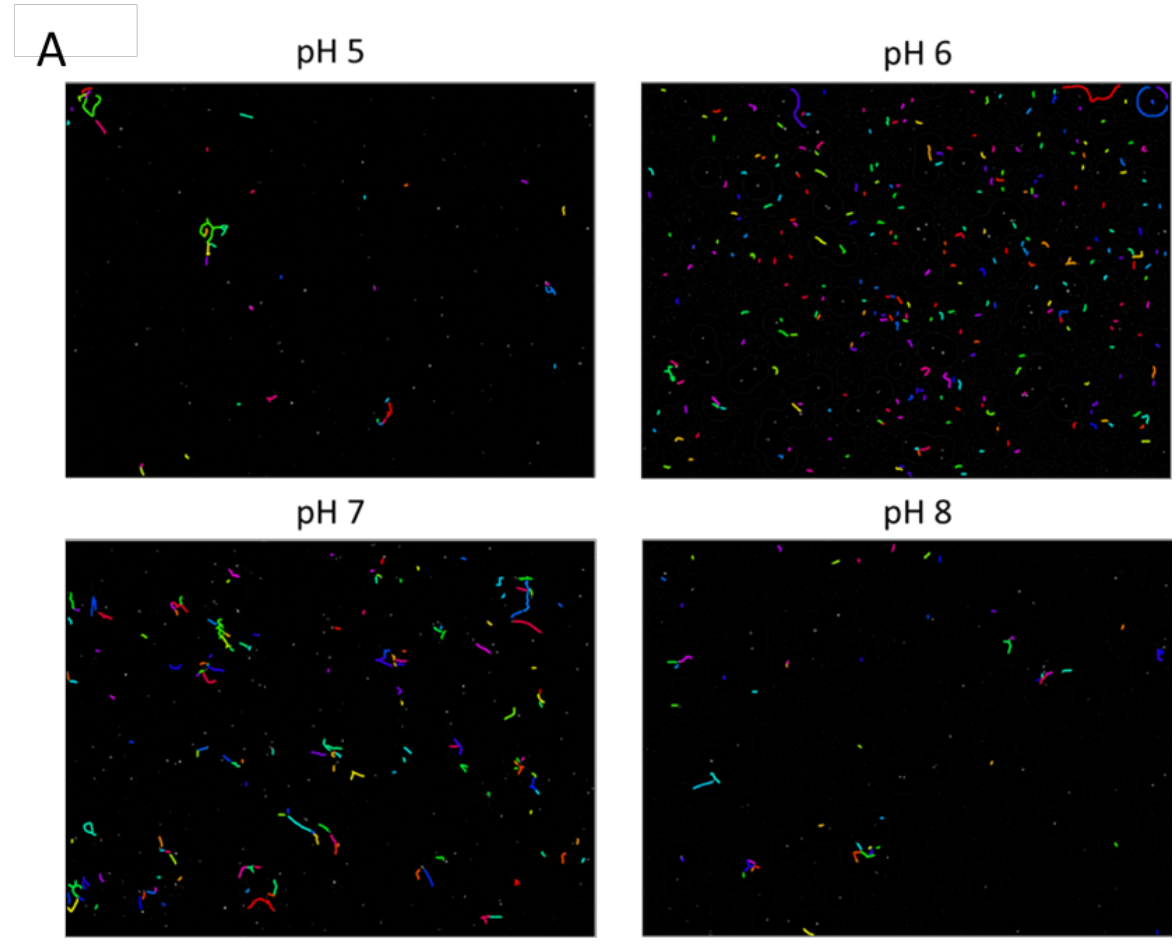

B

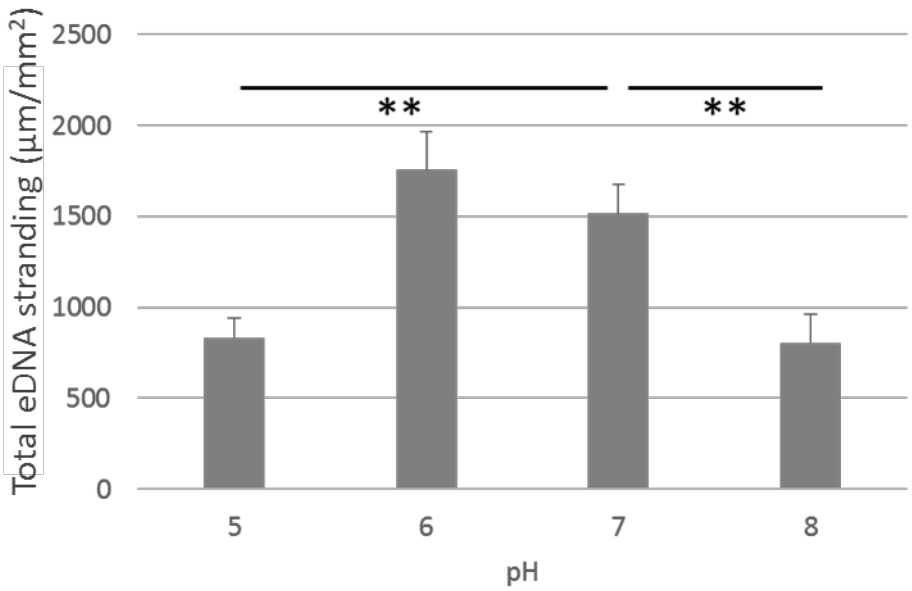

*Figure 3.22 - **eDNA stranding is highest in biofilms grown at pH 6-7.** WT S. gordonii biofilms were grown at 37 °C in YPTG at pH 5, 6 or 7 on saliva-coated glass cover slips for 5 h. A) Biofilms were labelled with an anti-dsDNA antibody, then an anti-Ig antibody conjugated to a fluorophore, and TO-PRO3. Widefield microscopy was used to capture an area of each biofilm. B) Ridge finding code on MATLAB was used to quantify eDNA*

*stranding. Data are presented as mean total stranding per mm² ± SD; n=3. Experiments were performed in triplicate. A one-way unpaired ANOVA was used with α=0.05. ** = P<0.005.*

3.6 Discussion

3.6.1 eDNA in *S. gordonii* biofilms and its quantification

eDNA was first recognised as a component of *P. aeruginosa* biofilm EPS in 2002 (Whitchurch *et al.*, 2002) and since then, the widespread presence of these eDNA structures across bacterial biofilms has been recognised and their functionality investigated. This work found *S. gordonii* monospecies biofilms produced approximately 1.4 µg/ml eDNA, consistent with a previous study using similar conditions (Jack *et al.*, 2015).

EPS generation and thus eDNA production has been found to be most prevalent during early biofilm formation (less than 24 h) for a number of bacteria, including *Pseudomonas*, *Microbacterium*, *Serratia* and *Enterococcus* species (Zhang *et al.*, 2011; Tang *et al.*, 2013; Barnes *et al.*, 2012). A similar trend was demonstrated for *S. gordonii* monospecies biofilms here, with eDNA concentration peaking at 5 h and then declining. This suggests that the role eDNA is serving within the biofilm may be most important during the initial stages of biofilm formation and that after this phase, other mechanisms and interactions predominate.

After 5 h of biofilm development, biomass and eDNA concentration were no longer significantly related - biomass continued to increase beyond 5 h, whereas eDNA stranding did not. This is in contrast to *S. mutans*, where eDNA concentration is proportional to the amount of bacteria in the biofilm up to 52 hours (Kim *et al.*, 2018). The lack of correlation in biomass and eDNA in *S. gordonii* biofilms post 5 hours suggests that the concentration of eDNA in the biofilm was not purely due to the number of cells that had accumulated, which may in turn imply that eDNA stranding was not simply occurring via a passive

process. Furthermore, when visualising eDNA, constellation-like networks were observed. Any organisation poses an energic burden to a system. This supports the hypothesis that eDNA production in *S. gordonii* biofilms may be an active process, and that the organisation relates to the beneficial role of eDNA in biofilm development, possibly facilitating accretion.

In this work, a unique mass image acquisition and semi-automated analysis strategy was developed, which built on the eDNA labelling methodology developed by (Barnes *et al.*, 2012). This novel strategy combines the quantitative capability offered by other approaches with the benefits of being able to focus specifically on the eDNA stranding networks that are associated with biofilms. This has enabled the presence of eDNA within *S. gordonii* biofilms to be analysed from an entirely new perspective and, moreover, the technology has potential to be applied across the field of biofilm research.

3.6.2 Role of other components within biofilms

Proteinase K treatment has been shown to disrupt biofilm formation in Group A *Streptococcus* by 90% (Doern *et al.*, 2009). Similarly, this study showed that proteinase K treatment of *S. gordonii* biofilms reduced biomass by 74%, which reinforces the importance of proteins in biofilm accretion by these streptococci. The effect of proteinase K on eDNA stranding had not previously been investigated, but this work found that eDNA stranding was highly susceptible to protease treatment. Of note, proteinase K treatment appeared to cause greater disruption in eDNA stranding than biomass, suggesting that there may be a proteinaceous component involved in eDNA stranding. Possible roles for a proteinaceous component(s) involved in eDNA stranding include remodelling DNA strands, binding DNA or complexing with DNA in strands, for example, as seen in the case of instance, Huβ, a DNABII protein of *P. gingivalis* (Tjokro et al., 2014). This invites further research into the potential interactions between proteins and eDNA strands within these biofilms.

Dextranase treatment reinforced previous studies that have shown the importance of dextran in oral streptococcal biofilm EPS (Koo *et al.*, 2010), but there was no evidence that this sugar was associated with eDNA stranding.

Although eDNA has been hypothesised to facilitate biomass accretion based on the results from Section 3.5.1, eDNA stranding no longer significantly predicted biofilm biomass (or visa versa) when data from the different enzymatic treatments were combined. The possibility that eDNA stranding is not proportional to biofilm biomass suggests eDNA may not be a result of uncontrolled cell lysis, therefore will the subject of further investigation. Alternatively, the lack of relationship could suggest eDNA stranding is not necessary for biofilm accretion – other potential roles of eDNA in biofilms will be explored.

3.6.3 Media effects on biofilm formation and eDNA stranding

As an oral microbe, *S. gordonii* experiences diverse environmental conditions influenced, in large part, by the eating and drinking behaviour of the host (Hans *et al.*, 2016). The effects of sugar and pH on eDNA stranding in biofilms was therefore explored. eDNA stranding was found to be sensitive to the type of sugar available, which correlates with evidence of EPS modulation in *S. mutans* biofilms according to sugar source (Decker *et al.*, 2014). Moreover, eDNA stranding in *S. gordonii* biofilms was reduced in low glucose concentrations, which may indicate that eDNA stranding is down-regulated during low nutrient and thus low energy conditions. This would correlate with the hypothesis that eDNA stranding is controlled by an active mechanism.

Unlike the response to sugar, no significant effects were seen for *S. gordonii* biofilm biomass over a pH range of 5-8. By contrast, while eDNA stranding also occurred across the pH range, levels were highest at pH 6 and 7. This may indicate that eDNA stranding within dental plaque biofilms could be expected to be highest under conditions of oral health (Baliga *et al.*, 2013). As with all these studies, however, it is important to recognise that this work has been performed using a monospecies biofilm. The role of eDNA stranding in the multispecies oral

biofilms found *in vivo* and the effects of environmental parameters are areas for future investigation.

3.6.4 Summary

This work has developed a novel eDNA quantification methodology which has been applied to investigate eDNA stranding in *S. gordonii* biofilms. Protease treatment, sugar source and concentration, and pH have all been shown to affect eDNA stranding levels. Furthermore, the data presented support a potential role for eDNA stranding in the initial stages of *S. gordonii* biofilm accretion, and indicate that this process may not be a passive phenomenon.

Chapter 4 Role of LPxTG family proteins in *S. gordonii* colonisation and biofilm development

In Chapter 3, investigation into factors which contribute to both *S. gordonii* biofilm formation and eDNA stranding highlighted proteins as a potential area for further research. Using confocal microscopy, seemingly precise eDNA patterns were observed, which implied that surface molecules of *S. gordonii* may additionally have a role as anchor points for eDNA.

Bacterial surface proteins can contribute to colonisation and pathogenesis by influencing the range of interactions which bacteria make with host surfaces (e.g. Van der Waals, electrostatic or direct ligand-receptor interactions) and other microbes (e.g. coadhesion). Many of these interactions had already been identified for *S. gordonii*, of which those involving LPxTG-family proteins were the best characterised (Table 4.1). For example, adhesins Hsa and homologous protein GspB both bind to salivary mucins and salivary agglutinin (gp340) (Takamatsu *et al.*, 2006). Likewise, Ag I/II family proteins SspA and SspB can target gp340 (Ito et al., 2017), while amylase-binding protein AbpA can bind amylase (Chaudhuri *et al*., 2017), another common constituent of the salivary pellicle. PadA has additionally been shown to bind the salivary pellicle (Haworth *et al.*, 2017), although its specific receptor(s) has yet to be identified. These proteins can all contribute to colonisation of the tooth surface by *S. gordonii.*

Other *S. gordonii* LPxTG-family proteins facilitate interactions with ECM proteins. CbdA has been shown to interact with type I collagen (Moses *et al.*, 2013), and facilitate persistence on collagen-containing surfaces (Moses *et al.*, 2013). Hsa binds fibronectin, a component of the human ECM (Haworth *et al.*, 2017), and this is also targeted by adhesins PadA and CshA (Back *et al.*, 2017; Haworth *et al.*, 2017). Such interactions may facilitate colonisation of the soft tissues (mucosae) of the oral cavity.

Additionally, LPxTG-family proteins can mediate coadhesion of *S. gordonii* with other members of the oral microbiota. SspB interacts with polysaccharide

on the surface of *A. oris* (Back *et al.*, 2015), while CshA and CshB have been shown to facilitate interactions with other oral bacteria, including *S. oralis* (Mcnab *et al.*, 1996).

Given the data from Chapter 3 and the critical role that the LPxTG-family proteins listed in Table 4.1 make to the colonisation capabilities of *S. gordonii*, it was hypothesised that additional LPxTG-family proteins may also contribute to *S. gordonii* colonisation and biofilm formation, including potential association with eDNA stranding. This was explored in the studies presented in this chapter, using a panel of *S. gordonii* adhesin knockout mutants generated for this study.

Table 4.1 - ***S. gordonii LPxTG-family adhesins characterised to date***

Adhesin	**Binds**	**Known/predicted function**	**References**
AbpA	Amylase	Colonisation of oral surfaces	Chaudhuri *et al*., 2017
CbdA	Type I collagen	Colonisation of soft tissues	Moses *et al.,* 2013
CshA	Fibronectin	Colonisation of soft tissues	Back *et al.,* 2017
	Other bacteria	Multispecies biofilm formation	Mcnab *et al.,* 1996
CshB	Other bacteria	Multispecies biofilm formation	Mcnab *et al.,* 1996
GspB	Salivary mucin & agglutinin	Colonisation of oral surfaces	Takamatsu *et al.,* 2006
	Platelets	Platelet activation	Bensing *et al.*, 2014
Hsa	Salivary mucin & agglutinin	Colonisation of oral surfaces	Takamatsu *et al.,*2006
	Platelets	Platelet activation and aggregation	Kerrigan *et al*., 2017
	Fibronectin	Colonisation of soft tissues	Haworth *et al.,* 2017
PadA	Salivary pellicle	Colonisation of oral surfaces	Haworth *et al.,* 2017
	Fibronectin	Colonisation of soft tissues	Haworth *et al.,* 2017
	Vitronectin	Colonisation of soft tissues	Haworth *et al.,* 2017
SspA/B	Epithelial cells	Colonisation of soft tissues	Andrian *et al*., 2012
	gp340	Colonsation of oral surfaces	Ito *et al*., 2017
	Platelets	Platelet aggregation	Kerrigan *et al*., 2007
	Other bacteria	Multispecies biofilm formation	Back *et al.,* 2015

4.1 Identifying LPxTG proteins

The requirement of an LPxTG motif for cell surface display meant that bioinformatics could be used to verify all *S. gordonii* proteins within this family. For the first step, PBLASTP was used to search for all LPxTG combinations within the *S. gordonii* genome, were X can be any amino acid. Following this, BPROM and Arnold were used to identify bacterial terminators and promoters respectively. This way sequences with a C-terminal LPxTG motif could be identified. These sequences were then searched for homology to protein domains with known functionality, using BLASTP, and compared for similarity to other annotated proteins.

Bioinformatics identified 27 LPxTG-containing proteins encoded on the *S. gordonii* genome, of which 8 had been previously reported (Table 4.2). These proteins were also mapped onto the *S. gordonii* genome (Figure 4.1). From this list, proteins were selected with predicted or known functionality which centred around two key themes: interactions with host molecules or eDNA. These were both considered important for *S. gordonii* colonisation and biofilm formation. Additionally, proteins were prioritised that had either not been studied before or not studied extensively in the context of *S. gordonii* biofilm formation. This led to six LPxTG proteins being chosen for further investigation.

Table 4.2 - ***Identification of all LPxTG proteins in S. gordonii***

Start	Stop	Length bp	Length aa	Locus Tag	Protein name	Known/Predicted Function	Published?	Chosen?
111740	114952	3212	1071	SGO_RS00535	Collagen binding domain D - CbdD	collagen binding		
219788	224515	4727	1576	SGO_RS01030	Streptococcal Surface Protein A - SspA	colonisation of hard/soft oral surfaces,		
						platelet aggregation, co-aggregation		
224934	229433	4499	1500	SGO_RS01035	Streptococcal surface protein B- SspB	colonisation of hard/soft oral surfaces,		
						platelet aggregation, co-aggregation		
338351	342835	4484	1495	SGO_RS01555	Serine Protease - SepA	serine protease		
342920	347404	4484	1495	SGO_RS01560	Serine Protease - SepB	serine protease		
424014	427271	3257	1086	SGO_RS01935	zinc carboxypeptidase	zinc carboxypeptidase		
441373	444945	3572	1191	SGO_RS02020	Beta-N-acetylhexosaminidase	beta-N-acetylhexosaminidase		
446803	452745	5942	1981	SGO_RS02035	zinc metalloproteinase B (peptidase M26)	zinc metalloproteinase		
475283	477943	2660	887	SGO_RS02135	Surface exclusion domain A - SedA	surface exclusion protein		
746855	751804	4949	1650	SGO_RS03480	cell surface protein	Mc 5b adhesin		
896889	904412	7523	2508	SGO_RS04190	Cell surface hydrophobicity A - CshA	coadhesion and fibronectin binding		
896889	904412	7523	2508	SGO_RS04375	Collagen binding domain C - CbdC	collagen-binding		
1011957	1012238	281	94	SGO_RS04730	streptococcal haemagglutinin - Hsa	platelet activation and aggregation, colonisation of oral surfaces		
1194141	1201019	6878	2293	SGO_RS05650	Cell surface hydrophobicity B - CshB	multispecies biofilm formation		
1232116	1234203	2087	696	SGO_RS05815	PavB-like protein A - PalA	fibronectin binding		
1293067	1295253	2186	729	SGO_RS06125	metallophosphatase	metallophosphatase		
1464176	1467349	3173	1058	SGO_RS06940	LPXTG cell wall surface protein			
1485718	1486950	1232	411	SGO_RS07040	rod shape-determining protein			
1535957	1543009	7052	2351	SGO_RS07290	beta-galactosidase	beta-galactosidase		
1543282	1548594	5312	1771	SGO_RS07295	Collagen binding domain B - CbdB	collagen binding		
1627202	1627888	686	229	SGO_RS07705	O-methyltransferase	O-methyltransferase		
1711886	1713970	2084	695	SGO_RS08085	Collagen binding domain A - CbdA	type I collagen binding; colonisation of soft tissues		
1714343	1716682	2339	780	SGO_RS08090	Streptococcal nuclease domain A - SndA	endonuclease		
1796391	1797956	1565	522	SGO_RS08465	glutamine ABC transporter substrate-binding protein	glutamine ABC transporter substrate-binding protein		
2056098	2057972	1874	625	SGO_RS09805	Platelet adhesin domain B - PadB			
2060617	2068989	8372	2791	SGO_RS09810	Platelet adhesin domain A - PadA	platelet activation, colonisation of oral surfaces		
2167409	2167996	587	196	SGO_RS10300	Amylase-binding protein - AbpA	amylase binding; colonisation of oral surfaces		

L-R: Start position on genome (bp), stop position on genome (bp), length of gene in bp, length of protein in amino acid (aa) residues, locus tag, protein name from publication or database (green highlight is proteins which have been named as part of this project), known/predicted functionality, published (green if yes at time of bioinformatics search), chosen (green if selected for investigation in this study).

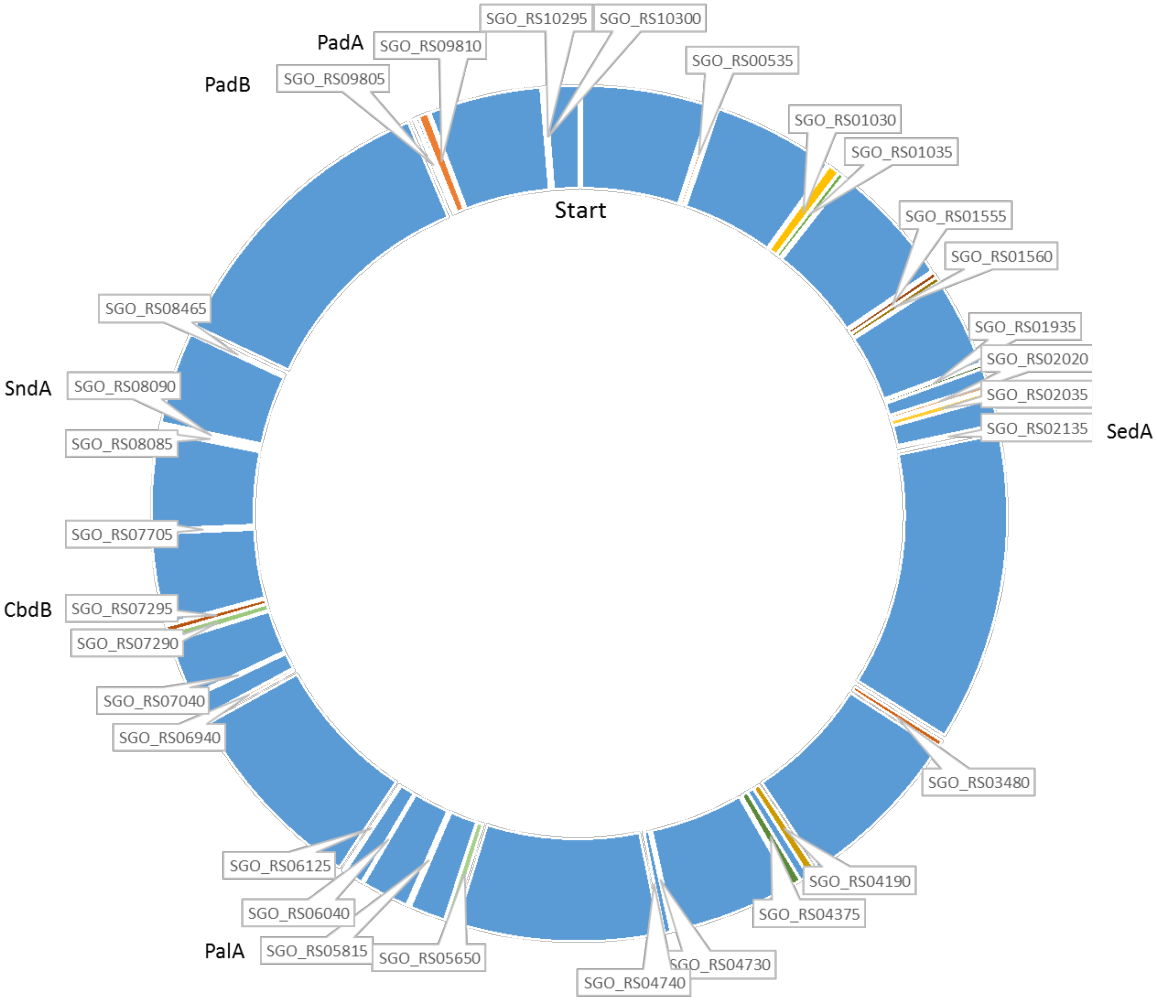

Figure 4.1 – ***Location of all LPxTG proteins within the S. gordonii genome.*** *All LPxTG proteins marked with locus tag. Proteins of interest selected for this project additionally marked with names.*

4.1.1 CbdB

A region encoding a putative 1770 aa LPxTG containing protein was identified. Homology searches revealed it contained domains which may interact with collagen. A collagen-binding *S. gordonii* protein had been previously described and was designated CbdA (Moses *et al.*, 2013), therefore this protein was designated CbdB (Collagen binding domain B) (Figure 4.2).

The gene encoding CbdB, SGO_RS07295, is within a single gene operon and predicted to carry 11 repeating CnaB domains. These domains, when associated with CnaA domains, can be polymerised and incorporated into pilin (Kang *et al.*, 2009). These domains are between 100-120 Å in length and 30-40 Å in width. They have been shown to have a conserved core structure, but variable outer regions, which may allow these domains to interact with a wide variety of substrates. Longer pilin structures can form pili, which may be involved in processes like motility or bacterial conjugation, whilst smaller pilin structures form fimbriae which are used in cell adhesion (Telford *et al.*, 2006). CbdB was found to share 92% homology to a putative collagen-binding protein in *S. mitis*, but the CnaB domains which CbdB contains are also found in *S. mutans*, in a protein designated Cnm. This is a collagen- and laminin-binding protein which has been shown to be a major virulence factor (Avilés-Reyes *et al.*, 2014).

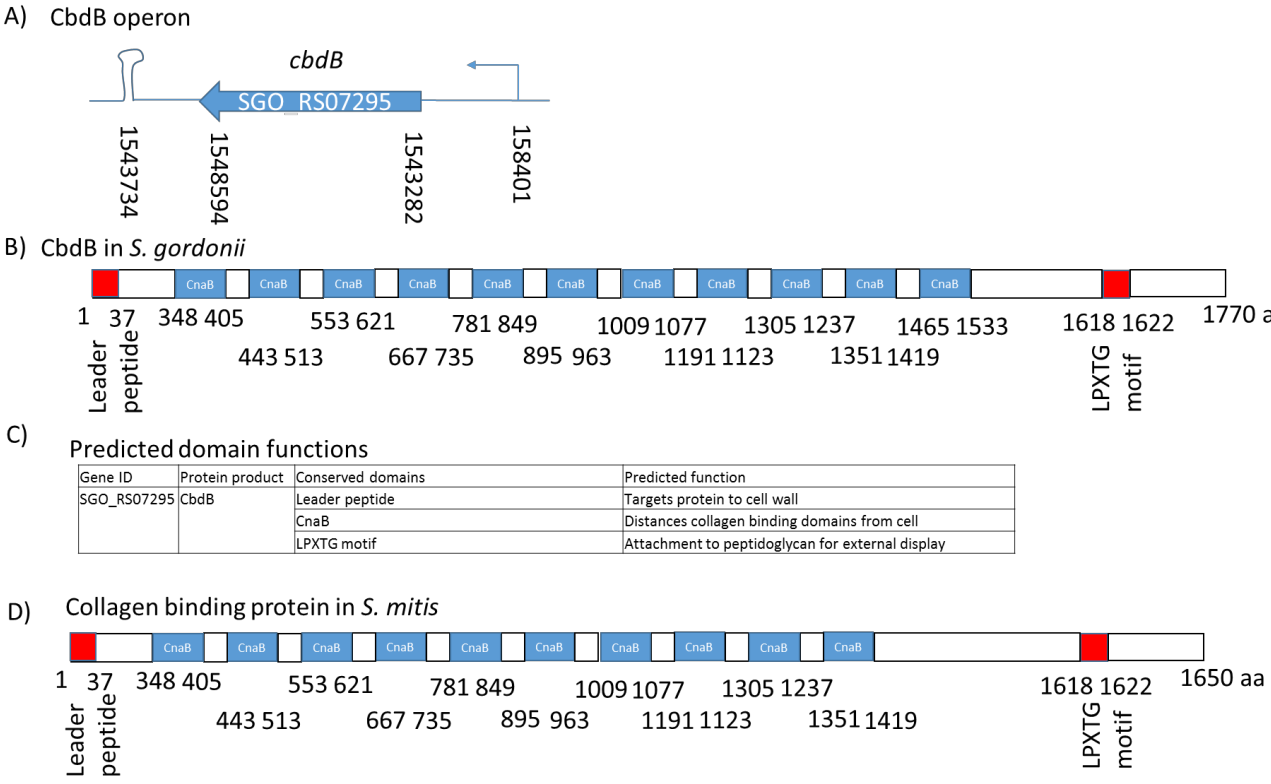

C) Predicted domain functions

Gene ID	Protein product	Conserved domains	Predicted function
SGO_RS07295	CbdB	Leader peptide	Targets protein to cell wall
		CnaB	Distances collagen binding domains from cell
		LPXTG motif	Attachment to peptidoglycan for external display

*Figure 4.2 - **Bioinformatics analysis of cbdB.***
A) Operon containing cbdB. Arrows are identified genes with gene ID. Above is the name of the gene. Values below genes are positions in base pairs within the genome. Predicted promoter and terminator indicated.
B) Conserved domains within CbdB protein. Values below protein are amino acid residue numbers.
C) Predicted functions of CbdB protein domains.
D) Streptococcal protein of closest homology to CdbB – collagen binding protein (WP_045635133.1) in S. mitis; exhibits 100% coverage and 92% identity.

4.1.2 PadA

PadA (Platelet activation domain A) is a protein of 3646 amino acids and has been shown to bind to and activate platelets (Petersen *et al.*, 2010), which is likely to facilitate thrombus formation during the pathogenesis of IE (Keane *et al.*, 2013). However, a potential role for PadA in *S. gordonii* biofilm formation and colonisation had not been extensively investigated. The gene which encodes PadA, SGO_RS09810, is found in a three-gene operon (Figure 4.3). Upstream of PadA is a protein designated PadC, which is a thioredoxin. Thioredoxins in bacteria are involved in the oxidative stress response and regulating redox-dependent gene expression (Zeller & Klug, 2006). Downstream of *padA* is a gene

which has been designated *padB* – it encodes an LPxTG motif containing protein which has not yet been the subject of investigation (see section 4.1.3).

PadA contains a von Willebrand factor domain. von Willebrand factor is required for blood coagulation in wound healing (Sadler, 1998) and thus this domain is implicated in facilitating initiation of thrombus formation in IE (Ileri *et al.*, 2003). PadA also contains 17 RgbB domains: fimbrial isopeptide domains. Isopeptide bonds have been shown to stabilise the structure of long fibrillar proteins, such as pili, giving strength and stability to these structures on Gram-positive organisms (Kang *et al.*, 2007). As fimbrial proteins are often involved in adhesion, the presence of these stabilising isopeptide bonds may indicate that PadA facilitates strong adhesive interactions. This supports the proposed functions of PadA in facilitating adhesion to host ECM molecules, fibronectin and vitronectin, and biofilm formation on salivary pellicle (Haworth *et al.*, 2017). The protein which shares most homology (62% identity) with PadA is a protein in *S. mitis* which has not yet been investigated. The highest homology shared with a protein which has been investigated is FmtB (59% identity) of *S. oralis*, a cell-wall associated protein which has been associated with methicillin resistance (Komatsuzawa *et al.*, 2000).

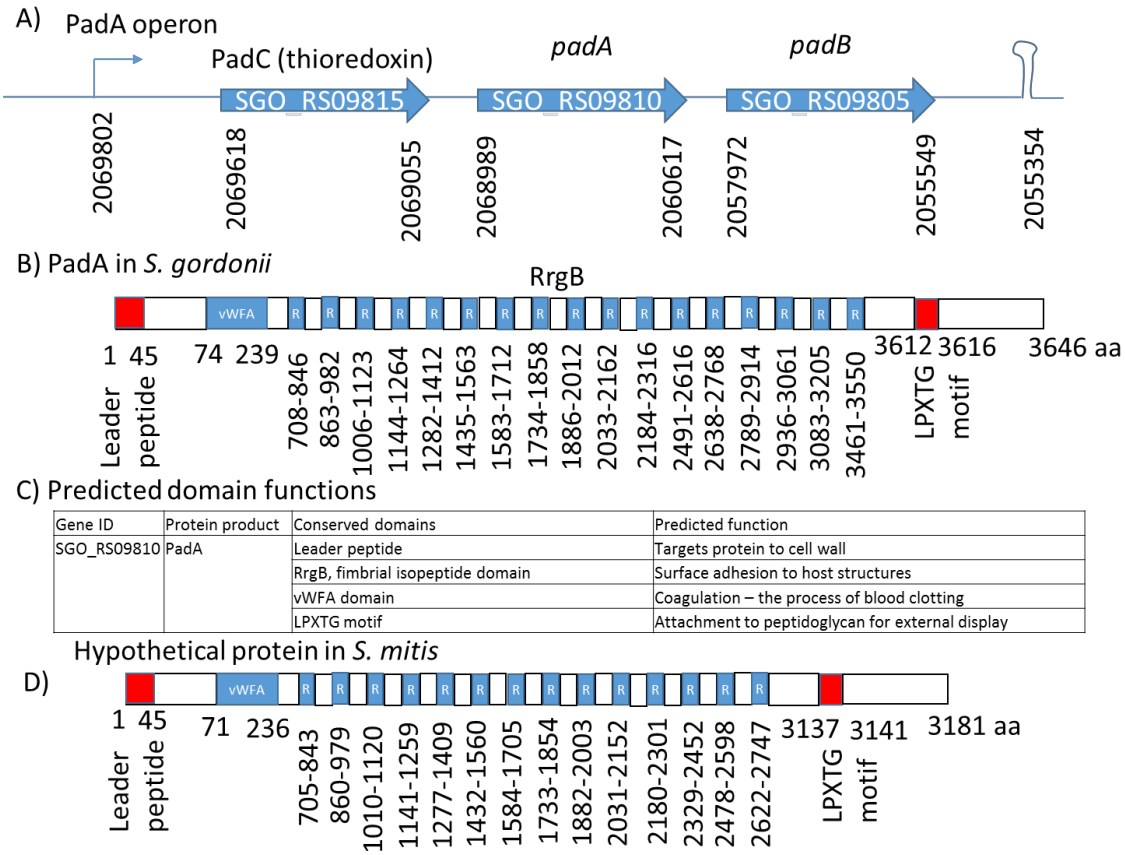

Gene ID	Protein product	Conserved domains	Predicted function
SGO_RS09810	PadA	Leader peptide	Targets protein to cell wall
		RrgB, fimbrial isopeptide domain	Surface adhesion to host structures
		vWFA domain	Coagulation – the process of blood clotting
		LPXTG motif	Attachment to peptidoglycan for external display

*Figure 4.3 - **Bioinformatics analysis of padA.***
A) Operon containing padA. Arrows are identified genes with gene ID. Above is the name of the gene. Values below genes are positions in base pairs within the genome. Predicted promoter and terminator indicated.
B) Conserved domains within PadA protein.
C) Predicted functions of PadA protein domains.
D) Streptococcal protein of closest homology to PadA - hypothetical protein (WP_001204254.1) in S. mitis; exhibits 97% coverage and 62% identity.

4.1.3 PadB

PadB is comprised of 807 amino acids and the gene which encodes this, SGO_RS09805, is found downstream of *padA* in the same three-gene operon (Figure 4.4). The location of *padA* and *padB* in the same operon implies that their respective proteins may function together in *S. gordonii*.

PadB contains 7 G5 motifs. G5 domains bind *N*-acetylglucosamine and facilitate biofilm formation in *Staphylococcus aureus* (Bateman *et al.*, 2005). G5 domains are also often found in proteins with enzymatic activity, some of which have been shown to be involved in bacterial cell wall metabolism (Bateman *et*

al., 2005). Since eDNA in bacterial biofilms are largely thought to comprise bacterial genomic DNA, processes involving enzymatic activity on the bacterial cell wall may enable this DNA to be released. G5 domains are also found in a protein homologous to PadB, which is an IgA-specific zinc metalloproteinase in *S. oralis* (50% identity). Ig-specific proteases can contribute to immune evasion, allowing for colonisation of mucosal surfaces (Bateman *et al.*, 2005).

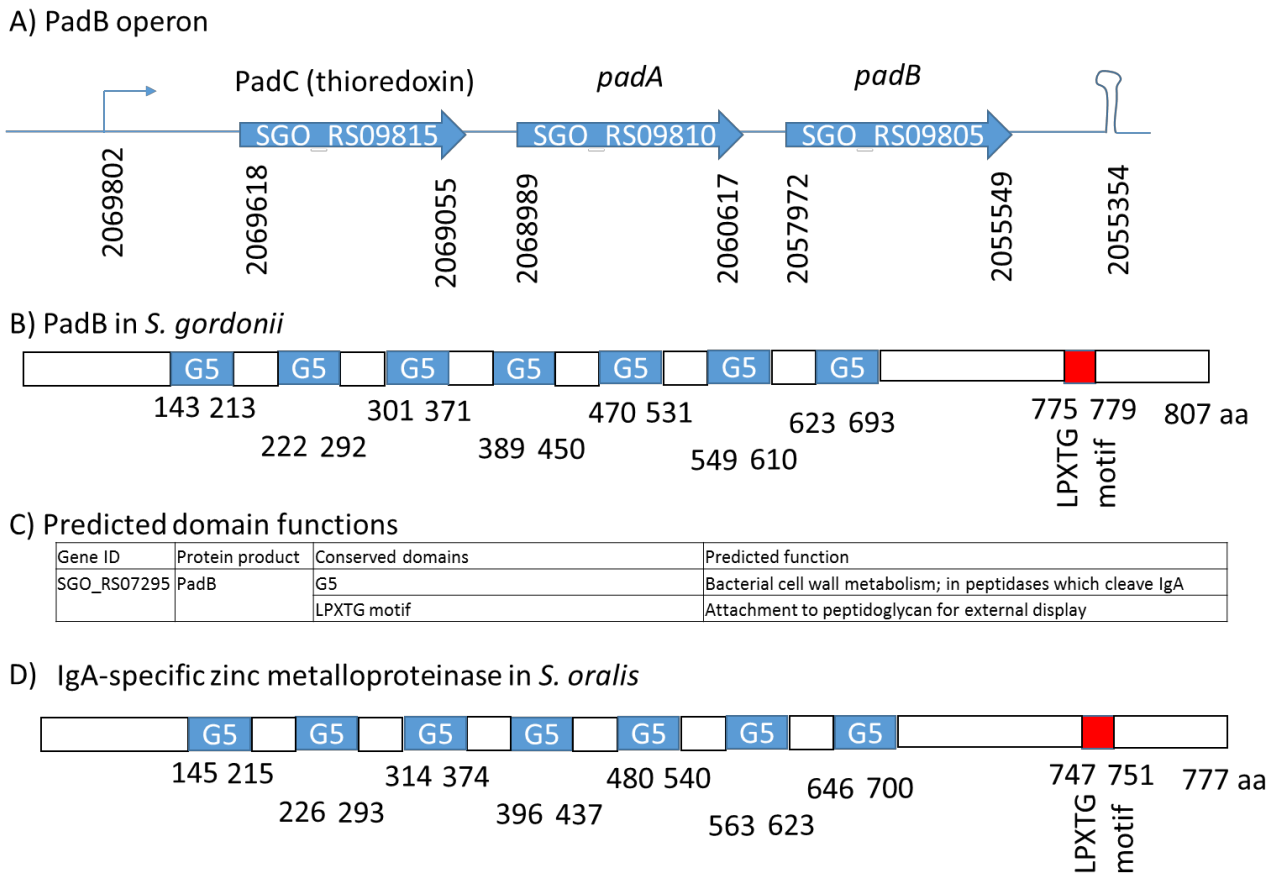

Figure 4.4 - ***Bioinformatics analysis of padB.***
A) Operon containing padB. Arrows are identified genes with gene ID. Above is the name of the gene. Values below genes are position in base pairs within the genome. Predicted promoter and terminator indicated.
B) Conserved domains within PadB protein.
C) Predicted functions of protein PadB protein domains.
D) Streptococcal protein of closest homology to PadB - IgA-specific zinc metalloproteinase (KJQ75184.1) in S. oralis, exhibits 99% coverage and 50% identity.

4.1.4 PalA

A 696-amino acid protein sequence was found that shared homology to PavB (Pneumococcal adherence and virulence factor B) in *S. pneumoniae* (Jensch et al., 2010). This protein was therefore designated PalA (PavB-like protein A) (Figure 4.5). Other proteins had higher homology to PalA than PavB (e.g. WP_005592244.1 in *S. cristatus*), but these had not been characterised. The gene encoding PalA, SGO_RS05815, is found in a three-gene operon. Immediately downstream of PalA is a transcriptional regulator (SGO_RS05810 (formerly SGO_1181)) and downstream of this is a sensor histidine kinase (SGO_RS05805 (formerly SGO_1180)). Together these comprise a two-component signalling system, which, via lipoteichoic acid, can sense and propagate the signal from LPxTG proteins SspA and SspB. This occurs upon SspA/B recognition of human mucin protein MUC5B and allows *S. gordonii* to adapt to changing environments using a phosphorylation cascade to alter LPxTG-protein encoding gene expression (M. Herzberg, Univ. Minnesota; personal communication).

PalA contains three SSURE (Streptococcal Surface Repeats) domains, which are also found in PavB. SSURE domains interact with human fibronectin and plasminogen in *S. pneumoniae*. Proteins containing these domains facilitate *S. pneumoniae* colonisation (Jensch *et al.*, 2010).

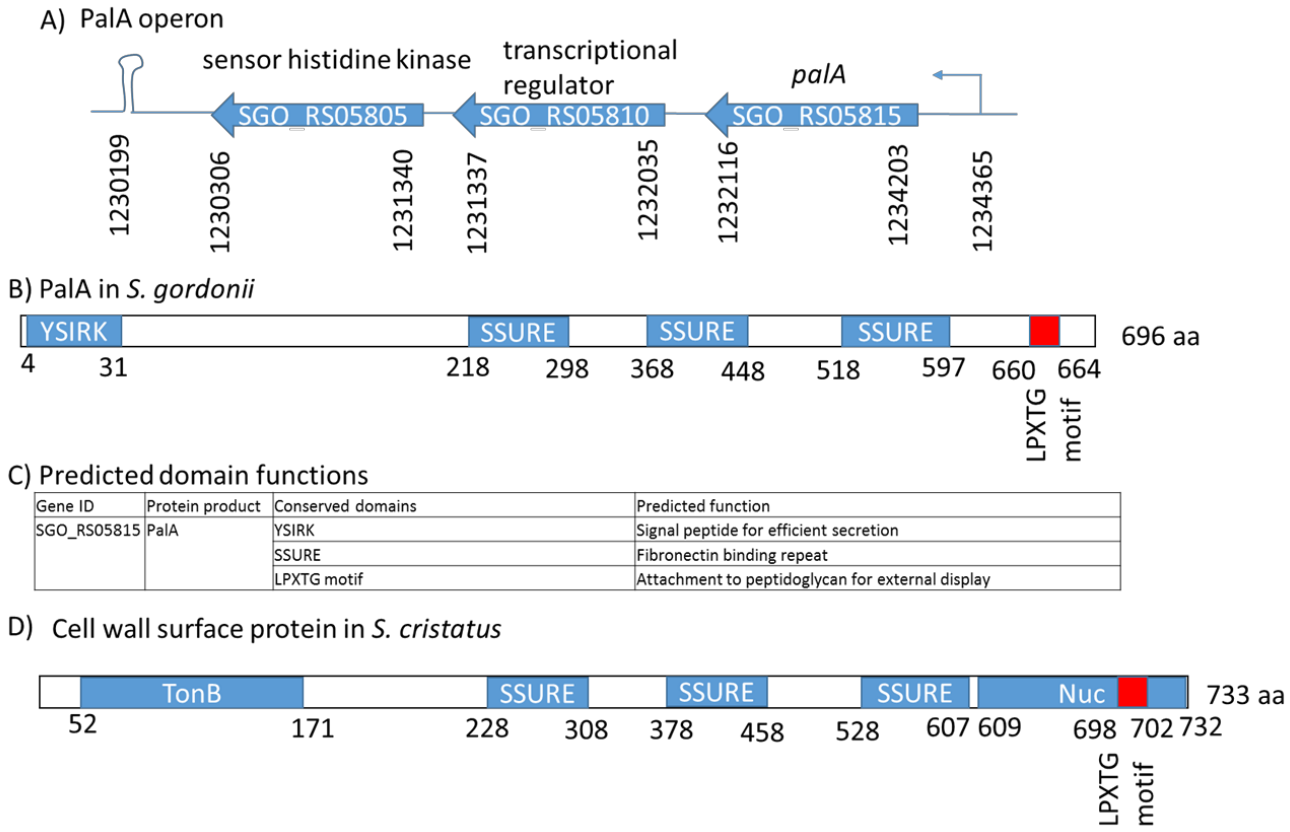

Gene ID	Protein product	Conserved domains	Predicted function
SGO_RS05815	PalA	YSIRK	Signal peptide for efficient secretion
		SSURE	Fibronectin binding repeat
		LPXTG motif	Attachment to peptidoglycan for external display

Figure 4.5 - ***Bioinformatics analysis of palA.***
A) Operon containing palA. Arrows are identified genes with gene ID. Above is the name of the gene. Values below genes are position in base pairs within the genome. Predicted promoter and terminator indicated.
B) Conserved domains within PalA protein.
C) Predicted functions of PalA protein domains.
D) Streptococcal protein of closest homology to PalA – Cell wall surface protein (WP_005592244.1) in S. cristatus, exhibits 100% coverage and 79% identity.

4.1.5 SedA

A putative protein of 886 amino acids was found to carry a predicted surface exclusion domain and so was designated SedA (Surface Exclusion Domain A) (Figure 4.6). The gene encoding SedA, SGO_RS02135, is located within a three-gene operon. Downstream of *sedA* is the gene which encodes CodY, a transcriptional repressor. This is a GTP-sensing repressor which, in *Bacillus subtilis,* is involved in the change from exponential to stationary phase bacterial growth (Levdikov *et al.*, 2017). Downstream of *codY* is an isochorismatase, which

converts chorismite to pyruvate as part of the biosynthetic pathway (Hubrich *et al.*, 2015).

SedA contains a PgrA surface exclusion domain. Surface exclusion domains are involved in competence and transformation, where they have been shown in *Escherichia coli* to inhibit the potentially energetically wasteful process of uptake of plasmids which the bacterial cell already possesses (Achtman *et al.*, 1977). Although the precise mechanism(s) of surface exclusion is not known, the inference is that such domains have capacity to interact with DNA.

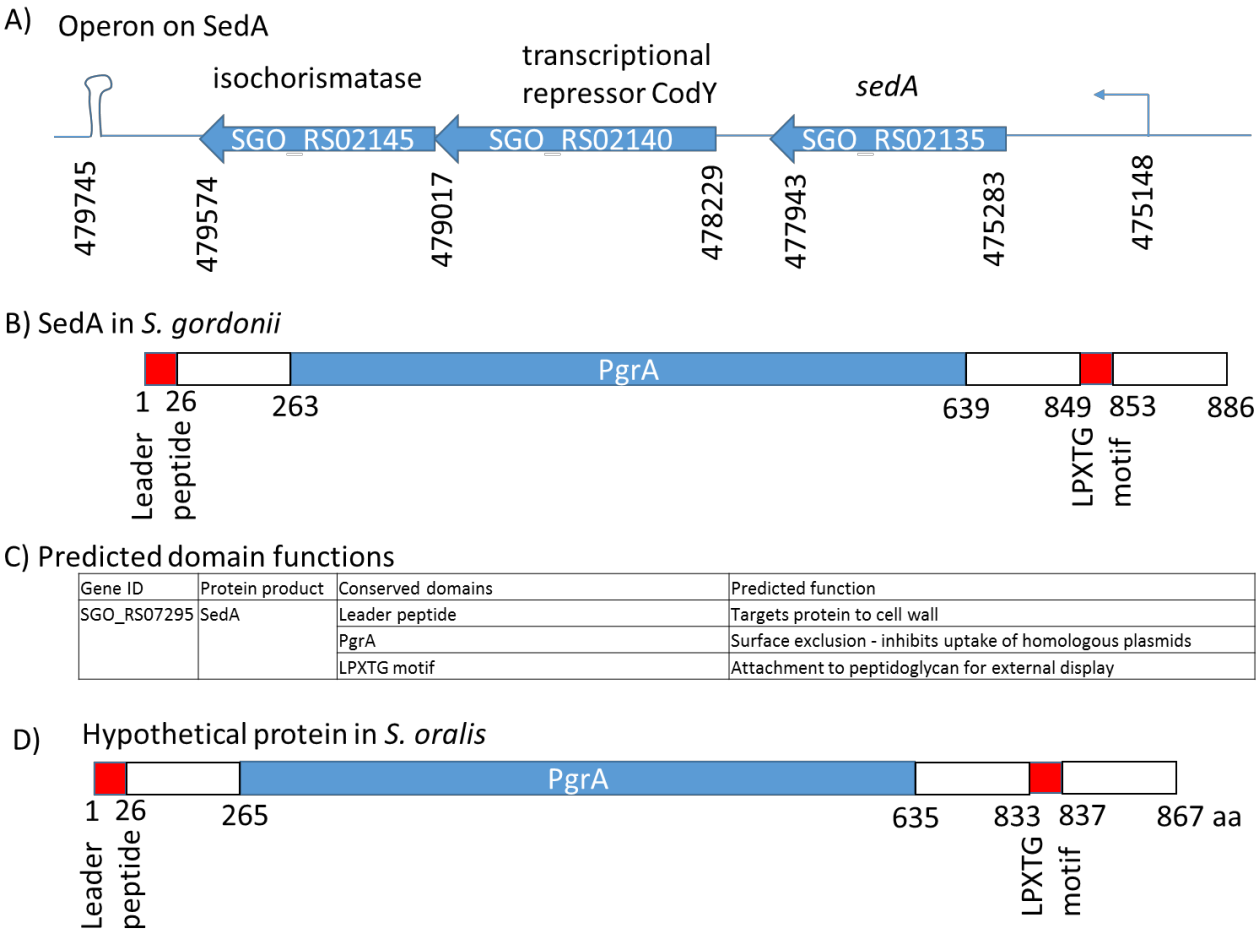

Gene ID	Protein product	Conserved domains	Predicted function
SGO_RS07295	SedA	Leader peptide	Targets protein to cell wall
		PgrA	Surface exclusion - inhibits uptake of homologous plasmids
		LPXTG motif	Attachment to peptidoglycan for external display

*Figure 4.6 - **Bioinformatics analysis of sedA.***
A) Operon containing sedA. Arrows are identified genes with gene ID. Above is the name of the gene. Values below genes are position in base pairs within the genome. Predicted promoter and terminator indicated.
B) Conserved domains within SedA protein.
C) Predicted functions of protein SedA protein domains.
D) Streptococcal protein of closest homology to SedA - hypothetical protein (WP_061853123.1) in S. oralis, exhibits 99% coverage and 52% identity.

4.1.6 SndA

A 779-amino acid putative protein was identified which shared 76% homology to SWAN (streptococcal wall-anchored nuclease) in *S. sanguinis*. This protein was therefore designated SndA (Streptococcal nuclease domain A) (Figure 4.7). The gene which encodes SndA, SGO_RS08090, is found within a four-gene operon.

Downstream of *sndA* in this operon is a gene encoding another LPxTG protein, CbdA. CbdA facilitates binding to collagen in *S. gordonii* (Moses *et al.*, 2013) but does not contain domains which indicate it may serve additional functions. Upstream of *sndA* is a gene encoding an α-amylase, which hydrolyses complex polysaccharides, such as starch and glycogen, to the simple carbohydrates: glucose and maltose. α-amylases are secreted by bacteria (Mehta & Satyanarayana, 2016) to digest the surrounding nutrients into a form which can be taken up and utilised. Upstream of α-amylase is a gene encoding a phosphotransferase system transporter subunit. These systems are responsible for the selective transport of glucose across the bacterial membrane (Mccoy *et al.*, 2015). In this way, the PTS transporter unit and α-amylase may be working concomitantly to provide glucose to the bacteria.

SndA contains an OB-fold, which is predicted to bind nucleic acid (Murzin, 1993), and a MnuA nuclease-like domain, which has the potential to function as a DNase or an RNase and cleave phosphodiester bonds (Jarvill-Taylor *et al.*, 1999). Thus, it was considered that this protein may have capacity to associate with eDNA.

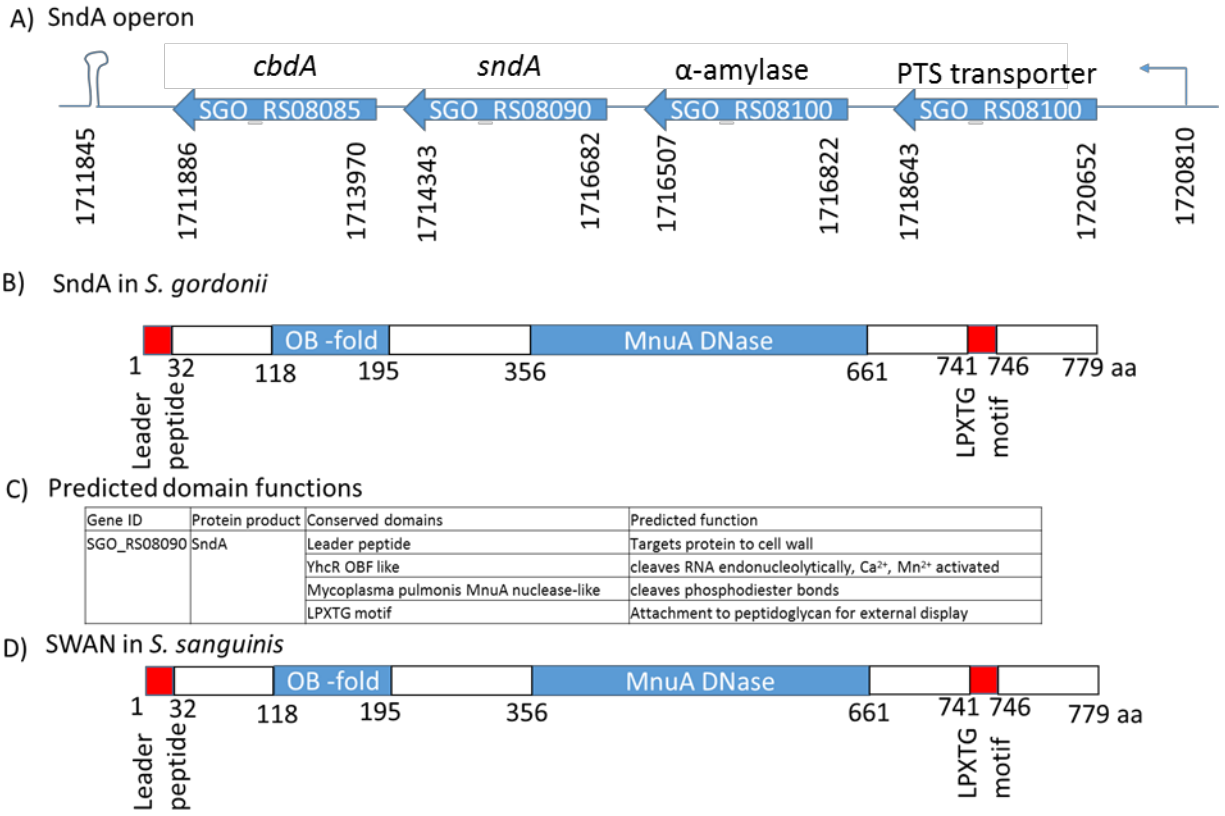

Figure 4.7 - ***Bioinformatics analysis of sndA.***
A) Operon containing sndA. Arrows are identified genes with gene ID. Above is the name of the gene. Values below genes are position in base pairs within the genome. Predicted promoter and terminator indicated
B) Conserved domains within SndA protein.
C) Predicted functions of protein SndA protein domains.
D) Streptococcal protein of closest homology to SndA - SWAN (WP_045773093.1) in S. sanguinis, exhibits 100% coverage and 76% identity to SndA. Conserved domains are indicated.

4.2 Generation of *S. gordonii* mutants

Knockout mutants were generated be allelic exchange in *S. gordonii* for each of the six selected genes: Δ*cbdB*, Δ*padA*, Δ*padB*, Δ*palA*, Δ*sedA* and Δ*sndA*. In each case, the gene of interest was replaced by the *aad9* antibiotic resistance cassette, encoding spectinomycin resistance, the expression of which was placed under the control of the native promoter. In the first instance, the growth profiles of these mutants were checked relative to wild-type *S. gordonii*, as any growth defects could affect subsequent studies relating to biofilm formation. Growth was tested in BHY, a rich medium, and YPTG, the more minimal medium

used in biofilm assays in Chapter 3. All strains were found to grow similarly to WT as planktonic cultures in BHY and YPTG (Figure 4.8), and this was confirmed using regression analysis (not shown).

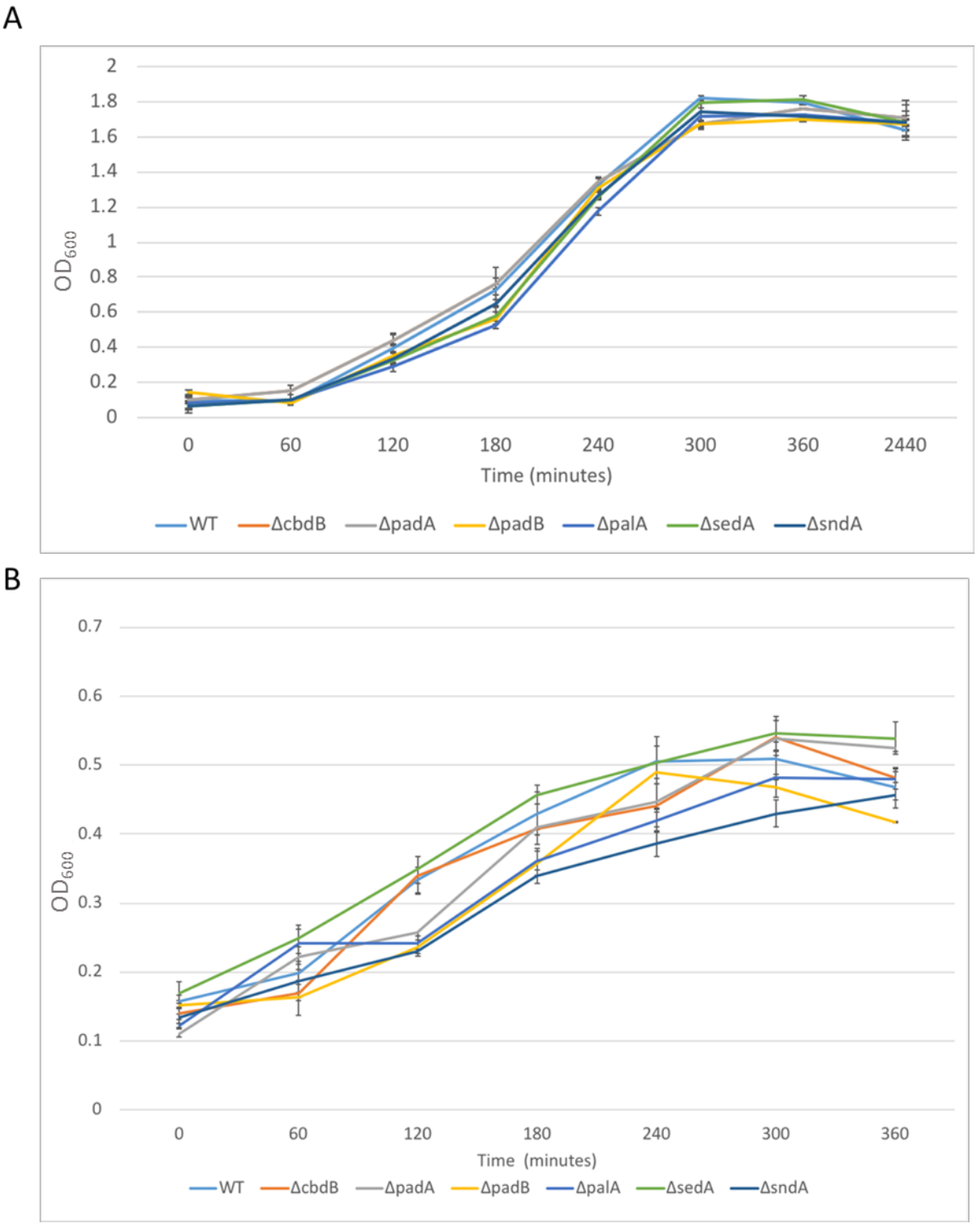

*Figure 4.8 – **Growth curves of S. gordonii strains in BHY and YPTG.** S. gordonii DL1 strains WT, ΔcbdB ΔpadA, ΔpadB, ΔpalA, ΔsedA and ΔsndA were grown at 37 °C in A) BHY or B) YPTG, from OD_{600} = 0.1 until stationary phase was reached; OD_{600} was measured hourly. Data are presented as mean optical density ± SD, n=3. Experiments were performed in triplicate.*

4.3 Hydrophobicity

A variety of bonds can form between bacterial cells and host surfaces or other microbes during biofilm development, and one factor that can affect such interactions is hydrophobicity. To test if expression of any of the target LPxTG proteins influenced cell surface hydrophobicity, a hexadecane assay was performed with the knockout mutants. Bacteria were suspended in an aqueous solution (PBS), then mixed with a non-aqueous solution (hexadecane). Over time, bacteria localised to the phase which resulted in the lowest system energy. By comparing starting optical density with that of the hydrophilic layer at the end of the assay, it was possible to determine the percentage of bacteria which were associated with hexadecane in the hydrophobic layer (% hydrophobicity).

WT *S. gordonii* displayed 54% hydrophobicity (Figure 4.9), which was comparable to the levels of hydrophobicity seen for most of the LPxTG knockout mutants. Only the positive control Δ*cshA* showed a significant reduction relative to WT, exhibiting 26% hydrophobicity (i.e. twice as hydrophilic as WT).

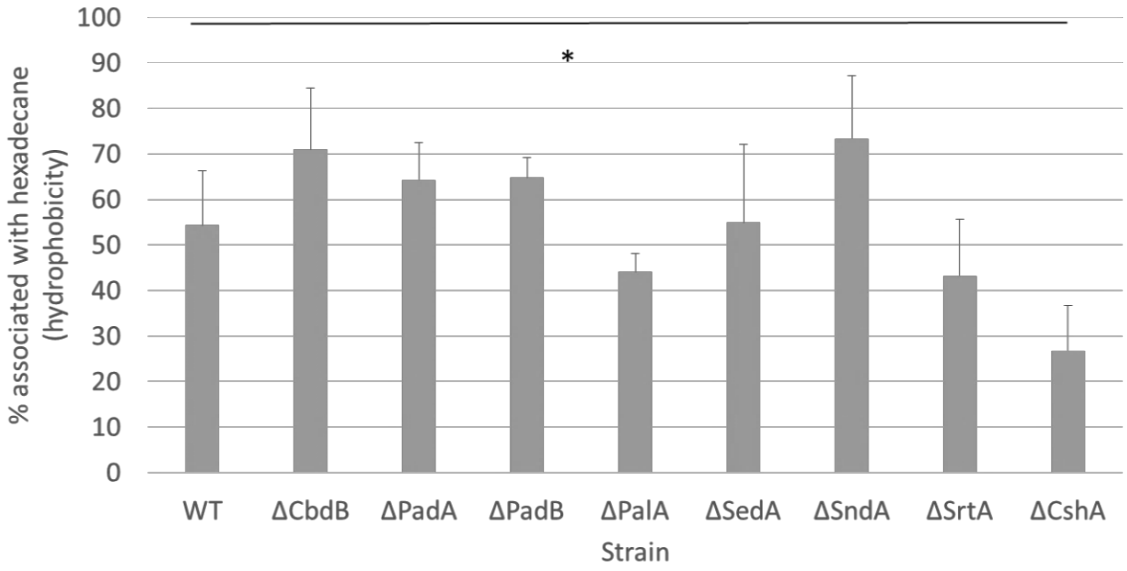

*Figure 4.9 – **Relative hydrophobicity of WT S. gordonii and LPxTG knockout mutants.** S. gordonii strains WT ΔcbdB, ΔpadA, ΔpadB, ΔpalA, ΔsedA, ΔsndA, ΔsrtA and ΔcshA were adjusted to OD_{600} 1 in PBS, then mixed with hexadecane (5:1). Suspensions were vortexed for 10 s then left for 30 min. A spectrophotometer was used to measure OD_{600} of the aqueous phase. % hydrophobicity was calculated as 100 – ((OD_{600} aqueous phase/OD_{600} initial) x 100). Data are presented as % hydrophobicity ± SD; n=3. Experiments were performed in triplicate. A one-way unpaired ANOVA was used to compare mutant strains to WT, with α=0.05. * P<0.05 compared to WT.*

4.4 Coaggregation

Coaggregation is a critical step in accretion of the dental plaque biofilm. *A. oris* is a recognised coaggregation partner of *S. gordonii*, being bound by adhesin SspB (Back *et al.*, 2015). To determine if additional LPxTG proteins were involved, coaggregation assays were performed with the *S. gordonii* knockout mutants and *A. oris*. Suspensions of *S. gordonii* and *A. oris* were mixed, incubated for 30 minutes, and the presence of co-aggregates were then visually scored using a scale of 0-4 developed by Cisar (Cisar *et al.*, 1979). The scale is as follows: 0 = Evenly turbid suspension of bacteria; 1 = Finely dispersed clumps in a turbid background; 2 = Definite clumps of bacteria are easily seen but do not settle immediately and remain in a turbid background; 3 = Clumps settle immediately with a slight turbid background; and 4 = Clumps settle immediately and

supernatant completely clear. The mutant *S. gordonii* strain Δ*sspA/B* was used as a negative control.

It was confirmed that neither *S. gordonii* nor *A. oris* exhibited significant autoaggregation. As anticipated, WT *S. gordonii* and *A. oris* showed significant co-aggregation, forming clumps which immediately settled, leaving a clear suspension (Figure 4.10). A similar coaggregation profile was seen for the majority of LPxTG mutants with *A. oris*, although some residual turbidity could be seen for the suspensions with mutants in PalA and SedA. Mutants lacking SspA/B or SrtA were unable to coaggregate with *A. oris*. This was to be expected, as both *S. gordonii* mutant strains effectively lack SspA/B on the cell surface.

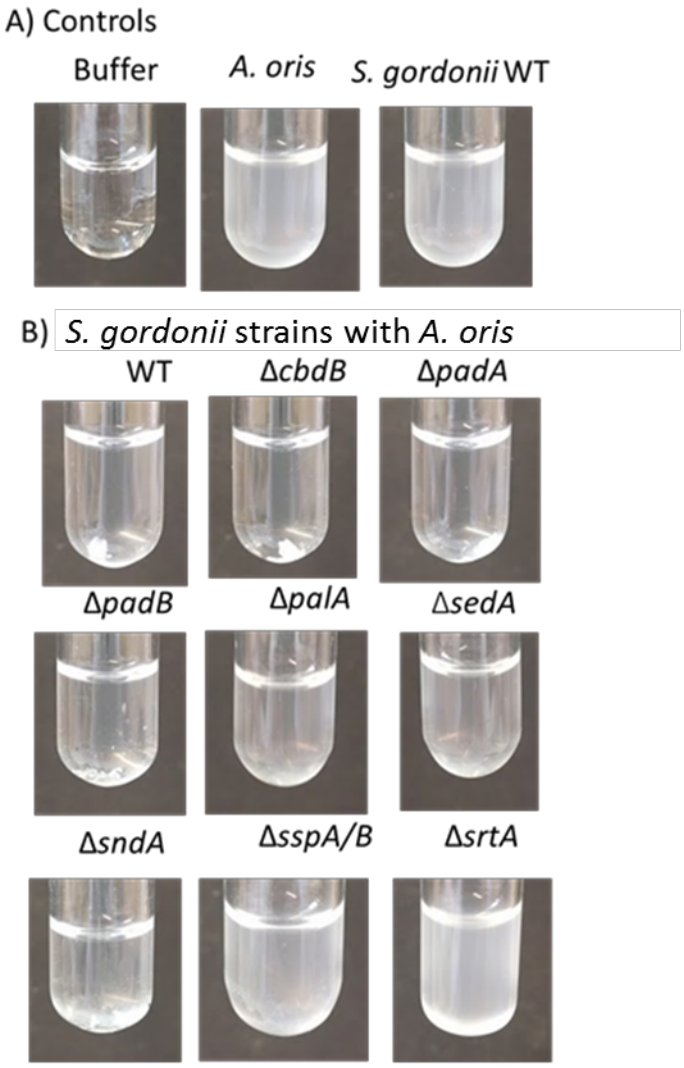

C)

S. gordonii and *A. oris* co-aggregation scores								
Strain of *S. g.*								
WT	ΔcbdB	ΔpadA	ΔpadB	ΔpalA	ΔsedA	ΔsndA	ΔsspA/B	ΔsrtA
4	4	4	4	3/4	3/4	4	0	0

Figure 4.10 – ***Coaggregation profiles for WT S. gordonii and LPxTG knockout mutants with A. oris.*** *S. gordonii strains WT, ΔcbdB, ΔpadA, ΔpadB, ΔpalA, ΔsedA, ΔsndA, ΔsspA/B and ΔsrtA* ***and A. oris were*** *adjusted to* OD_{600} *1 in coaggregation buffer, then mixed (1:1). Suspensions were vortexed for 10 s then left for 30 min. Representative micrographs are shown for A) assay controls with single species or B) assays with both species, and C) coaggregation levels were scored accordingly. Assays were performed in triplicate to n=3.*

4.5 Collagen binding

Type I collagen is a structural, fibrillar protein that is found in human organs, the vasculature and is a common constituent of tissue ECM. The role of *S. gordonii* LPxTG proteins in collagen binding was assessed using collagen-coated plates, with numbers of adherent bacteria determined by viable count. Due to its predicted collagen-binding domain, it was hypothesised that the CbdB mutant strain would exhibit reduced binding relative to WT *S. gordonii*, while the properties of the remaining mutants were unknown. A *Staphylococcus aureus* strain, Col, which is known to have a strong collagen-binding phenotype was used to test this assay (data not shown).

A significant difference in levels of adhesion was also seen for the CbdB mutant strain, which bound to collagen 8-fold more than WT *S. gordonii* (Figure 4.11). This was unexpected, given the presence of a putative collagen-binding domain within CbdB. The other single LPxTG knockout mutants displayed comparable adhesion levels to WT, with the exception of Δ*srtA*, which exhibited a 3-fold reduction in binding to collagen relative to WT.

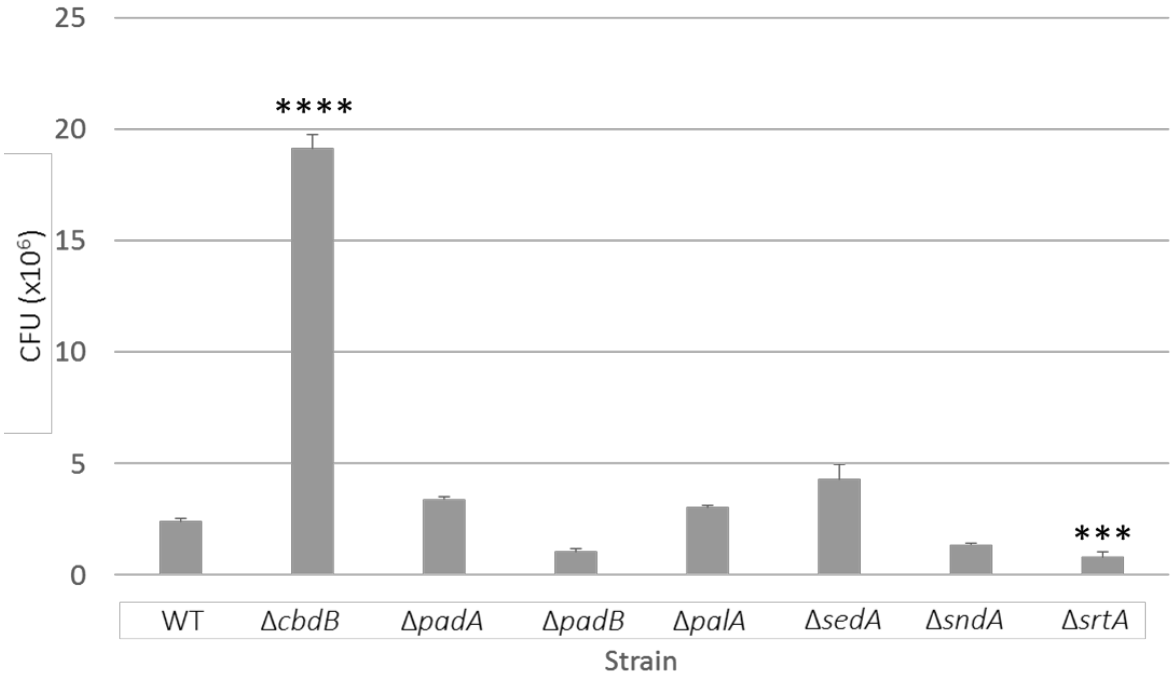

*Figure 4.11 –**S. gordonii ΔcbdB strain has increased collagen binding relative to WT**. S. gordonii strains WT, ΔcbdB, ΔpadA, ΔpadB, ΔpalA, ΔsedA, ΔsndA and ΔsrtA, and Staphylococcus aureus Col (OD_{600} = 1 in TBSC) were incubated in collagen-coated plates for 2 h, then washed with TBSC. Bound bacterial cells were recovered into 0.1% Triton-X100 in TBSC then plated onto agar to determine CFU/ml. Data are presented as mean CFU/ml ± SD; n=3. Experiments were performed in triplicate. A one-way unpaired ANOVA was used to compare each mutant to WT, with α=0.05. *** P<0.0005, **** P<0.0001, compared to WT.*

4.6 Fibronectin binding

S. gordonii is known to bind to fibronectin, so investigations into LPxTG proteins which may facilitate this were undertaken. Both forms of human fibronectin were relevant to these studies: cellular and plasma. Cellular fibronectin acts as a cell scaffold, making 3D structures and helping to organise tissues, and therefore is an important part of the ECM. Plasma fibronectin circulates in blood, where it forms part of the fibrin clot cascade, allowing for tissue repair. It thus has potential to be involved in the pathogenesis of IE.

Of the panel of target LPxTG proteins, PadA and PalA carried domains that were inferred to interact with fibronectin. However, *S. gordonii* Δ*padA* was not included in these studies as it had been characterised previously (Haworth *et al.*,

2017). PalA has domains homologous to SSURE domains, which have been shown in *S. pneumoniae* to bind human fibronectin (Jensch *et al.*, 2010). Mutant strain Δ*srtA* was included as a negative control.

Adhesion of Δ*palA* to cellular fibronectin was reduced by 47% relative to WT (Figure 4.12). By contrast, levels of binding for Δ*palA* and WT to plasma fibronectin were comparable, although these were 2.5-fold lower than determined for cellular fibronectin. Binding levels of Δ*srtA* were comparable for both cellular and plasma fibronectin. These were significantly lower than WT and similar to background levels for BSA.

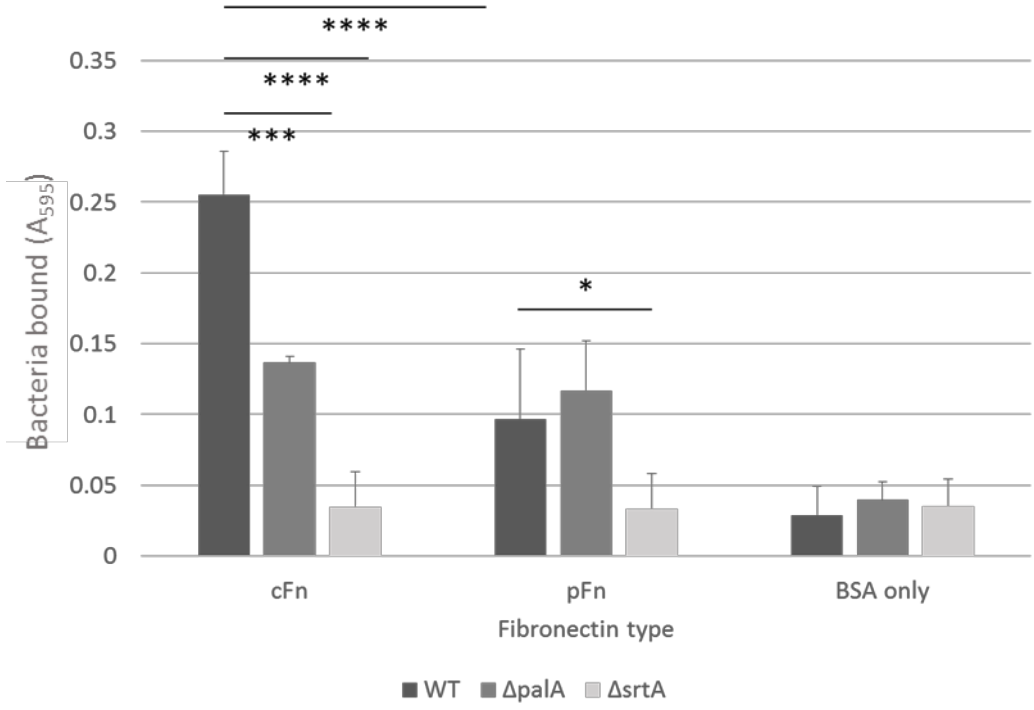

*Figure 4.12 – **PalA binds cellular fibronectin.** S. gordonii strains WT, ΔpalA and ΔsrtA (OD_{600} = 1 in TBSC) were incubated in fibronectin-coated plates for 2 h, then washed with TBSC and fixed with 25% formaldehyde. Bound bacteria were stained with 0.5% crystal violet and levels of biomass quantified following release of the stain with 7% acetic acid and measurement at A_{595}. Data are presented as mean absorbance ± SD; n=3. Experiments were performed in triplicate. A one-way unpaired ANOVA was used, with α=0.05. * P<0.05, *** P<0.0005, **** P<0.0001 compared to WT.*

4.7 Role of LPxTG proteins in biofilm development

The role of the LPxTG proteins in biofilm formation was first investigated by measuring total biomass. Whereas in the previous chapter biofilm formation was investigated under growth conditions specifically optimised to study eDNA strand formation, these studies took a more comprehensive approach and utilised three different media: rich BHY medium, minimal C medium, and nutrient-poor salivary medium.

4.7.1 BHY Medium

Three different time frames were used initially for BHY medium, to investigate the role of each *S. gordonii* LPxTG protein in salivary pellicle adhesion (1 h), early biofilm accretion (6 h) and mature biofilm development (24 h). The sortase A mutant was used as a negative control. However, the growth of reproducible biofilms proved difficult. The biofilms which formed were uneven in terms of thickness, showed a macro swirling appearance and, particularly at 24 h, large segments of biofilm appeared to have been lost (Figure 4.13).

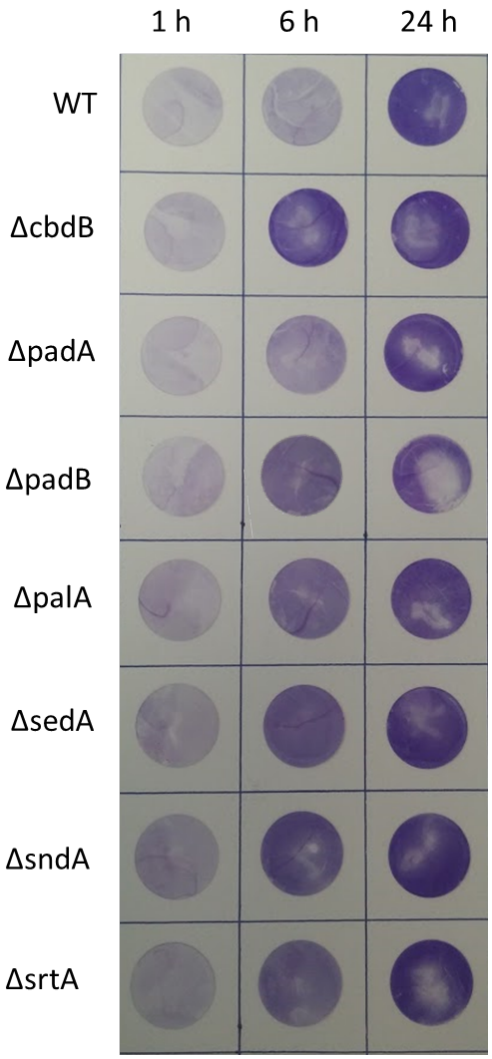

Figure 4.13 – ***S. gordonii WT and LPxTG knockout mutant biofilms grown in BHY show macro swirling and patchy surface.*** *S. gordonii strains WT, ΔcbdB, ΔpadA, ΔpadB, ΔpalA, ΔsedA, ΔsndA and ΔsrtA were adjusted to OD_{600}=0.1 in BHY and incubated on saliva-coated cover slips for 1, 6 or 24 h. Cover slips were washed then stained with 0.25% crystal violet for visualisation.*

4.7.2 C Medium

It was hypothesised that the loss of large patches of biofilm could be due to the use of a rich medium, which led to the formation of biofilms that were unsustainably thick. Studies were therefore repeated using minimal C medium. C medium contains 0.4% sugar, which is in the middle of the range used in Chapter 3 when testing the effects of glucose on eDNA stranding.

First, it was confirmed that all LPxTG knockout mutant strains grew similarly to WT in this growth medium. Bacterial growth (OD_{600}) was measured hourly over the course of 7 h, after which a final time point was taken at 24 h (Figure 4.14). Using regression analysis, all strains were found to grow similarly to WT (data not shown). Cultures grown in C medium peaked at 6 h.

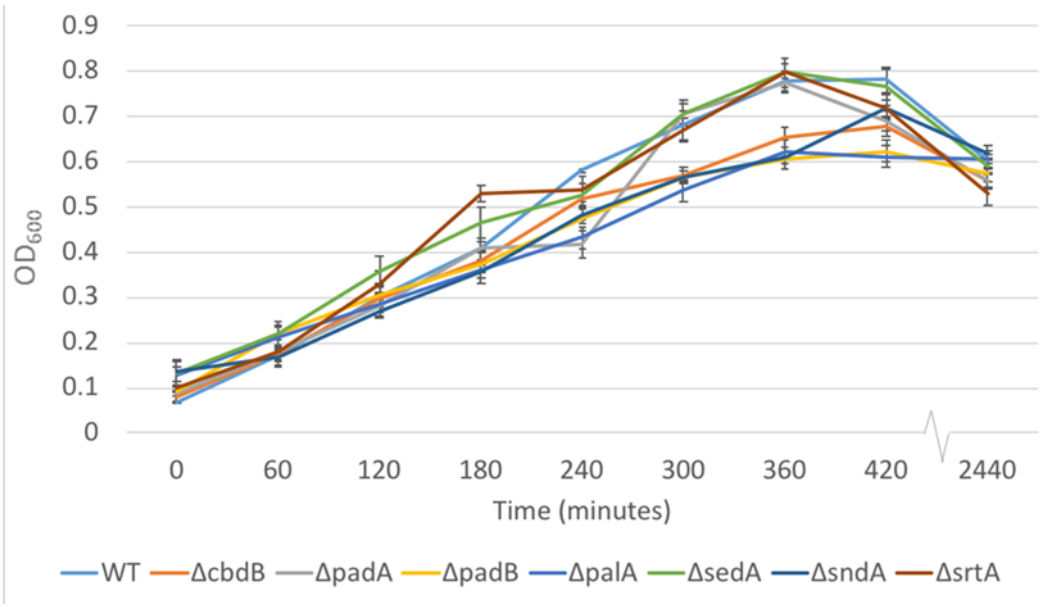

Figure 4.14 - ***Growth curves of WT S. gordonii and LPxTG knockout mutants in C medium.*** *S. gordonii strains WT, Δ**cbdB**, ΔpadA, ΔpadB, ΔpalA, ΔsedA, ΔsndA and ΔsrtA were adjusted to OD_{600} = 0.1 in C medium then incubated at 37 °C for 24 h. OD_{600} was used to measure bacterial growth every 60 min for 7 h, and then a final reading was taken at 24 h. Data are presented as mean absorbance ± SD; n=3. Experiments were performed in triplicate.*

Biofilm growth on saliva-coated glass cover slips was measured at 24 h. All mutants except Δ*cbdB*, Δ*padA* and Δ*padB* exhibited a significantly reduced biomass of 30-50% relative to WT after 24 h (Figure 4.15). Biofilm biomass for the mutant lacking SrtA was 90% lower than WT. These data suggested that PalA, SedA and SndA may all contribute to *S. gordonii* biofilm formation under these conditions.

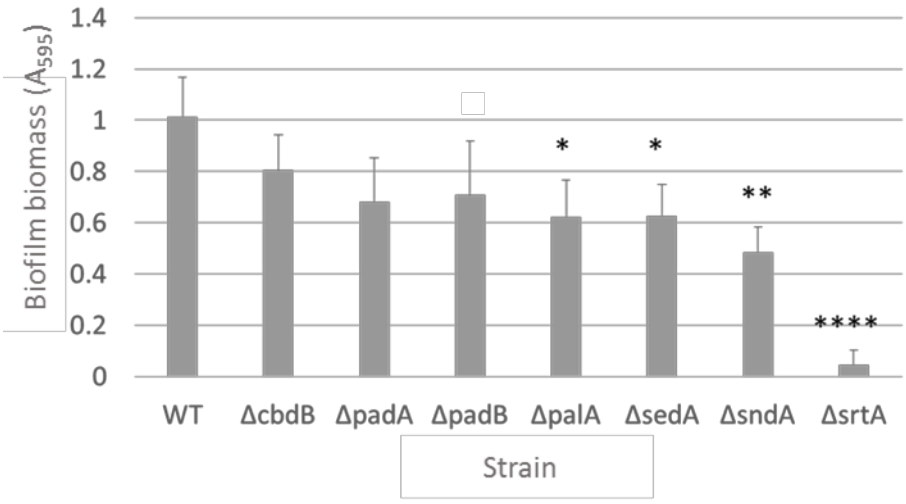

Figure 4.15 – ***S. gordonii ΔpadB, ΔpalA, ΔsedA, ΔsndA and ΔsrtA mutant biofilms grown in C medium are reduced relative to WT.*** *S. gordonii strains WT, ΔcbdB, ΔpadA, ΔpadB, ΔpalA, ΔsedA, ΔsndA and ΔsrtA were adjusted to OD_{600} = 0.1 in C medium and incubated at 37 °C for 24 h on saliva-coated glass-bottomed wells. Biofilms were stained with 0.25% crystal violet, the stain released with acetic acid, and the absorbance measured at A_{595}. Data are presented as absorbance ± SD; n=3. Experiments performed in triplicate. A one-way unpaired ANOVA was used with α=0.05. * P<0.05, ** P<0.005, **** P<0.0001, compared to WT.*

To investigate the architecture of these biofilms in more detail, confocal microscopy with FITC-labelled bacterial cells was undertaken. Volocity was used to analyse confocal micrographs. The intensity threshold was set manually, and then objects which were under 0.5 μm in diameter were excluded. Objects which were closer than 0.5 μm apart were included in the same fragment. This meant that cells and intensities (such as from proteins in the EPS) situated close together were counted as one object. The volume data for these objects were then exported and used to calculate mean biovolume and number of segments in each biofilm. Mutants Δ*padA*, Δ*padB*, Δ*palA*, Δ*sedA* and Δ*sndA* did not differ significantly from WT in terms of biofilm volume, whereas the biovolume for mutant Δ*srtA* was reduced by 52% (Figure 4.16). The biofilm for this mutant also exhibited 11-fold higher segmentation than WT. However, none of the other individual LPxTG knockout mutant strain biofilms were significantly more segmented than WT. The biovolume for the Δ*cbdB* mutant was reduced by 35% relative to WT.

A)

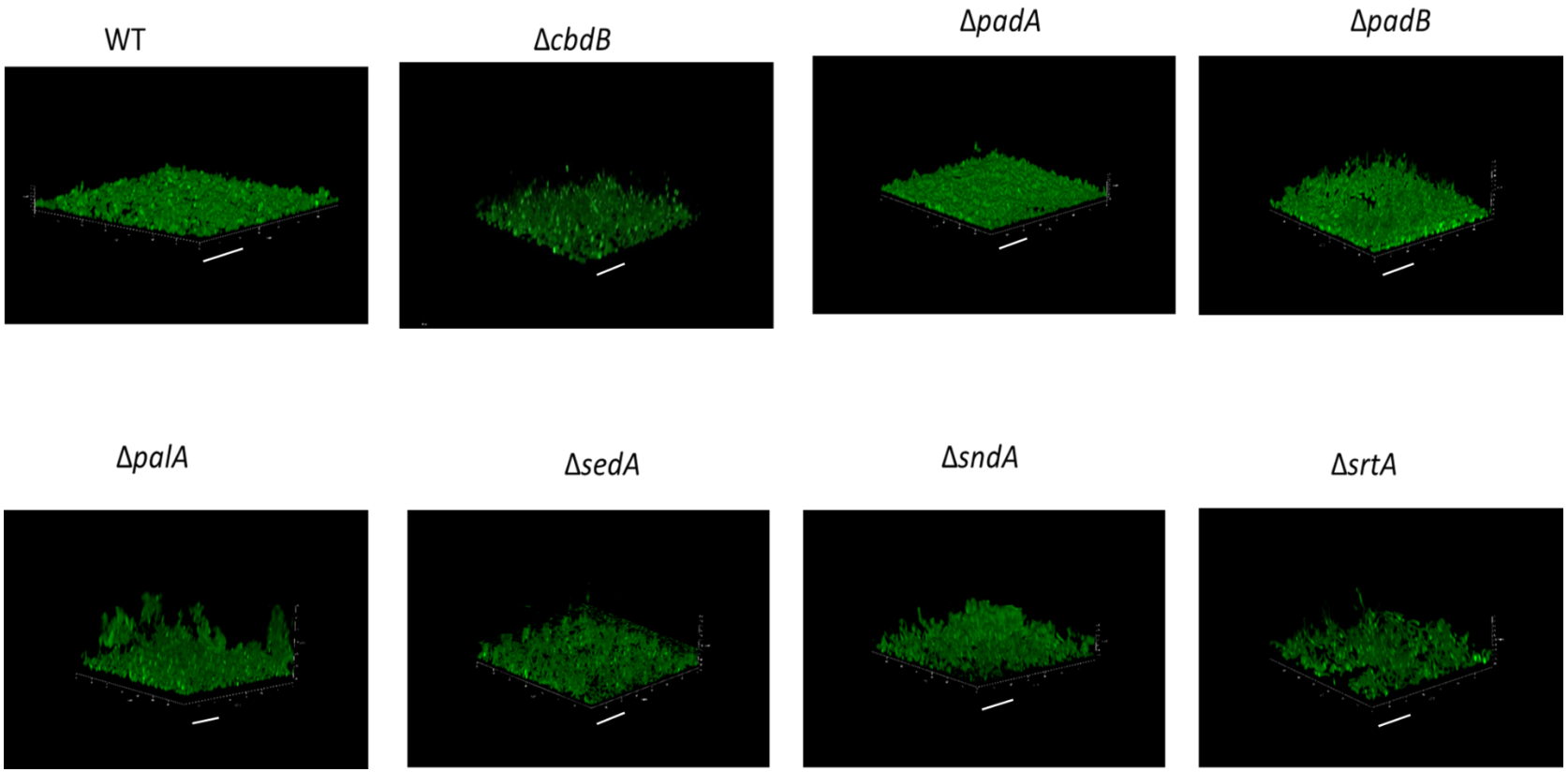

B)

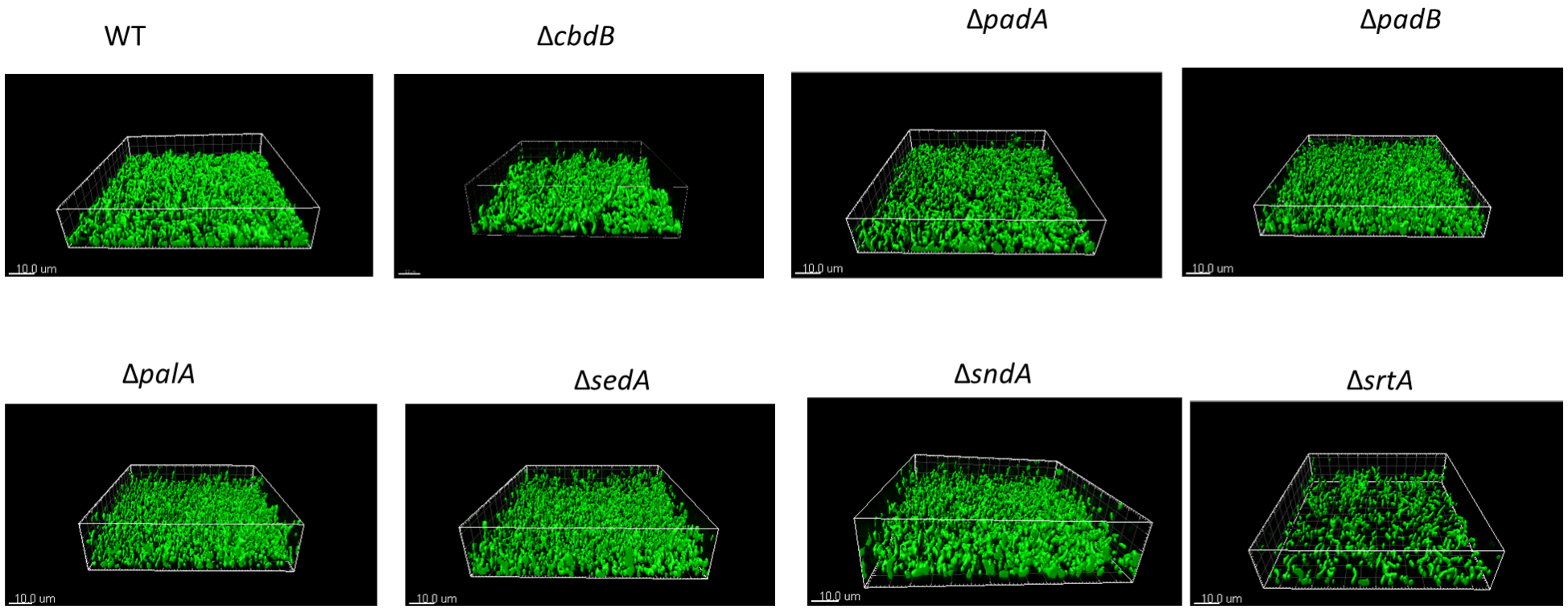

C)

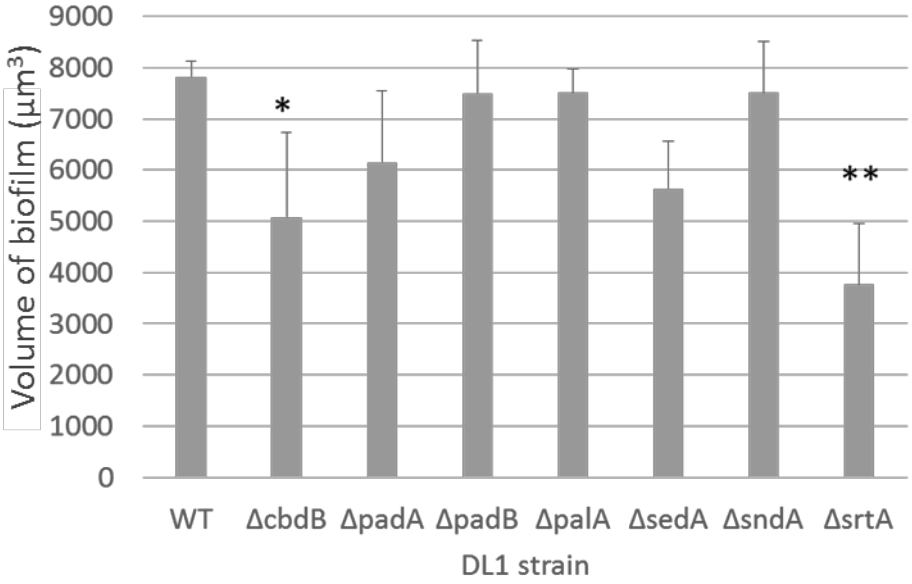

D)

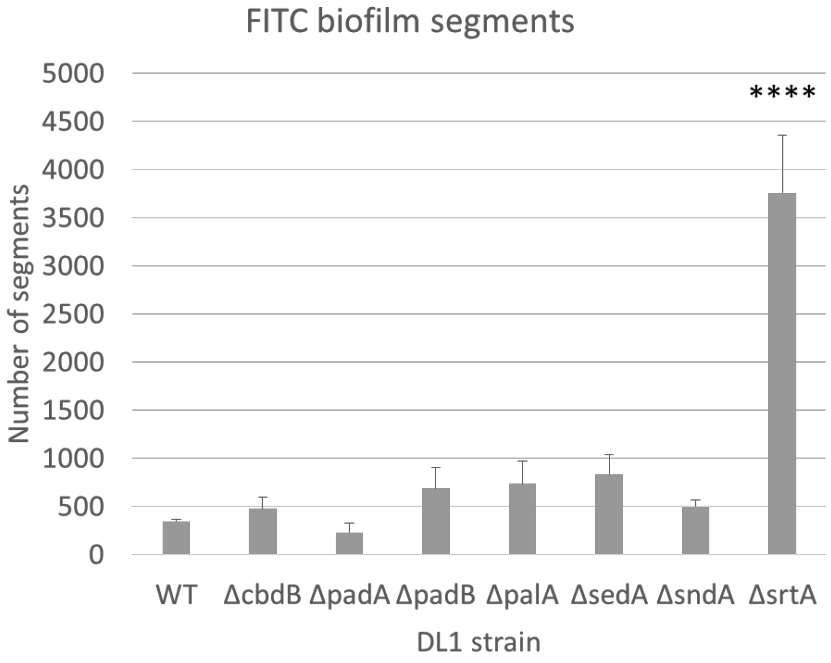

*Figure 4.16 – Confocal **analysis of S. gordonii WT and LPxTG** **mutant biofilms grown in C medium.** S. gordonii strains WT, ΔcbdB, ΔpadA, ΔpadB, ΔpalA, ΔsedA and ΔsndA were labelled with FITC, adjusted to OD_{600} 0.1 in C medium, then incubated in saliva-coated glass-bottomed wells at 37 °C for 24 h. Confocal laser scanning microscopy was used to capture A) micrographs (scale bars = 20 µm), which were then B) analysed using Imaris to determine the volume of the biofilms (scale bars = 10 µm). The C) biovolume and D) segmentation data are presented as mean ± SD; n=3. Experiments were performed in triplicate. A one-way unpaired ANOVA was used to compare mutants to WT, with α=0.05. * P,0.05, ** P<0.005, **** P<0.0001 compared to WT.*

4.7.3 Salivary Medium

Salivary medium is a very minimal medium, comprising just 1% saliva and 0.4% glucose. As might be expected, growth of *S. gordonii* in this medium was slower than seen for the other two media, reaching an optical density of approximately half that reached in C medium over the same time frame. No significant difference was found between WT *S. gordonii* and the LPxTG knockout mutants (Figure 4.17). This was confirmed by regression analysis (not shown).

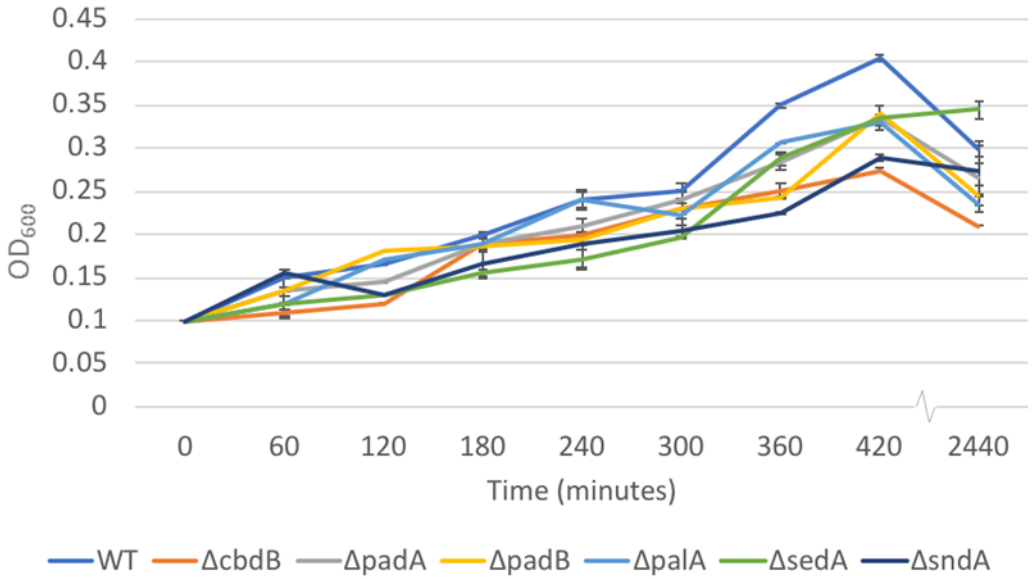

Figure 4.17 – ***Growth curves in salivary media show S. gordonii LPxTG mutants are not retarded in growth relative to WT.*** *S. gordonii strains WT, ΔcbdB, ΔpadA, ΔpadB, ΔpalA, ΔsedA, ΔsndA and ΔsrtA were adjusted to OD_{600} = 0.1 in salivary medium then incubated at 37 °C for 24 h. OD_{600} was used to measure bacterial growth every 60 min for 7 h, and then a final reading was taken at 24 h. Data are presented as mean absorbance ± SD; n=3. Experiments were performed in triplicate.*

Correlating with the planktonic growth profiles, the biomass of biofilms grown in salivary medium was on average much lower (>60%) than that of biofilms grown in C medium. Furthermore, each LPxTG knockout mutant showed a significant reduction of approximately 40% in biomass compared to WT, while a greater reduction of ~70% was seen for the Δ*srtA* mutant (Figure 4.18).

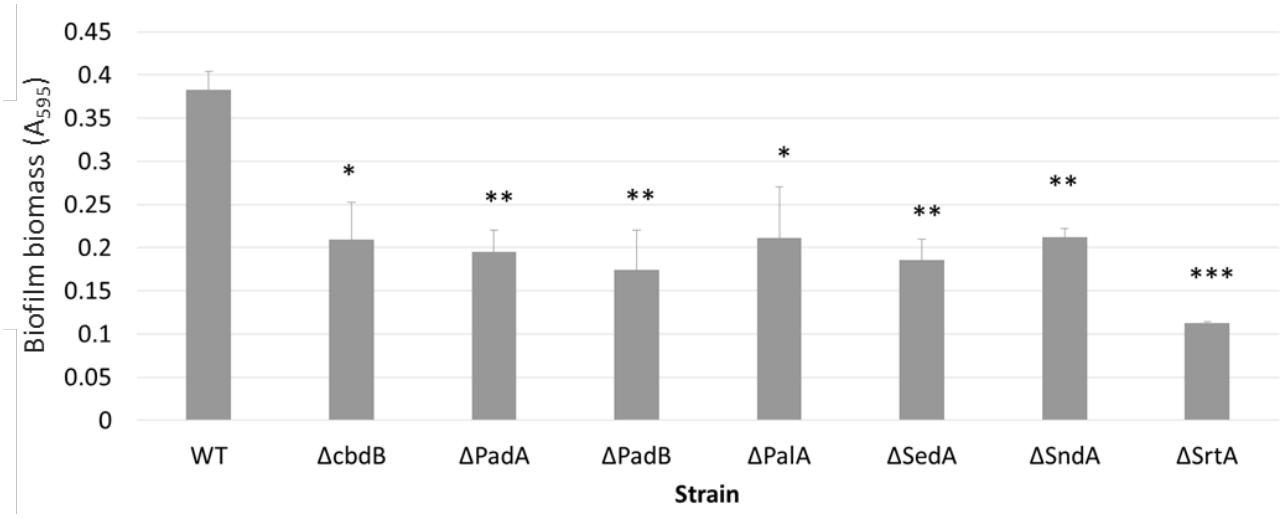

Figure 4.18 – ***S. gordonii WT and LPxTG knockout mutant biofilms grown in salivary medium.*** *S. gordonii WT, ΔcbdB, ΔpadA, ΔpadB, ΔpalA, ΔsedA, ΔsndA and ΔsrtA biofilms were grown in salivary medium at 37 °C for 24 h on saliva-coated glass-bottomed wells. Biofilms were stained with 0.25% crystal violet, the stain released with acetic acid, and the absorbance measured at A_{595}. Data are presented as absorbance ± SD; n=3. Experiments were performed in triplicate. A one-way unpaired ANOVA was used with α=0.05. * P<0.05, ** P<0.005, *** P<0.0005, compared to WT.*

Again, confocal microscopy was utilised to study the architecture of these biofilms in more detail. WT biofilms grown in salivary medium had reduced biovolume of ~45% compared to those grown in C medium, while the number of segments was 3.5-fold lower. Of the LPxTG mutants tested, Δ*cbdB* and Δ*srtA* exhibited an 80% and 98% reduction in biomass, respectively, relative to WT (Figure 4.19). In salivary medium larger cell aggregates were formed, with an average segment size of around 20 µm^3 in C medium and 40 µm^3 in salivary medium. The SrtA mutant formed biofilms containing segments which were 20-fold smaller than their WT counterparts. This suggests that LPXTG surface proteins may be required to form the larger cell aggregates.

Mutant Δ*cbdB* had around 65% of the biovolume of WT *S. gordonii* in C medium, whereas in salivary medium it had only 18%. This suggests that CbdB may have a more important role in biofilm formation under starvation conditions. Whilst the CbdB mutant strain formed biofilms with significantly fewer segments than WT, this corresponded to lower biofilm volume; thus, the average segment size did not differ from WT.

A)

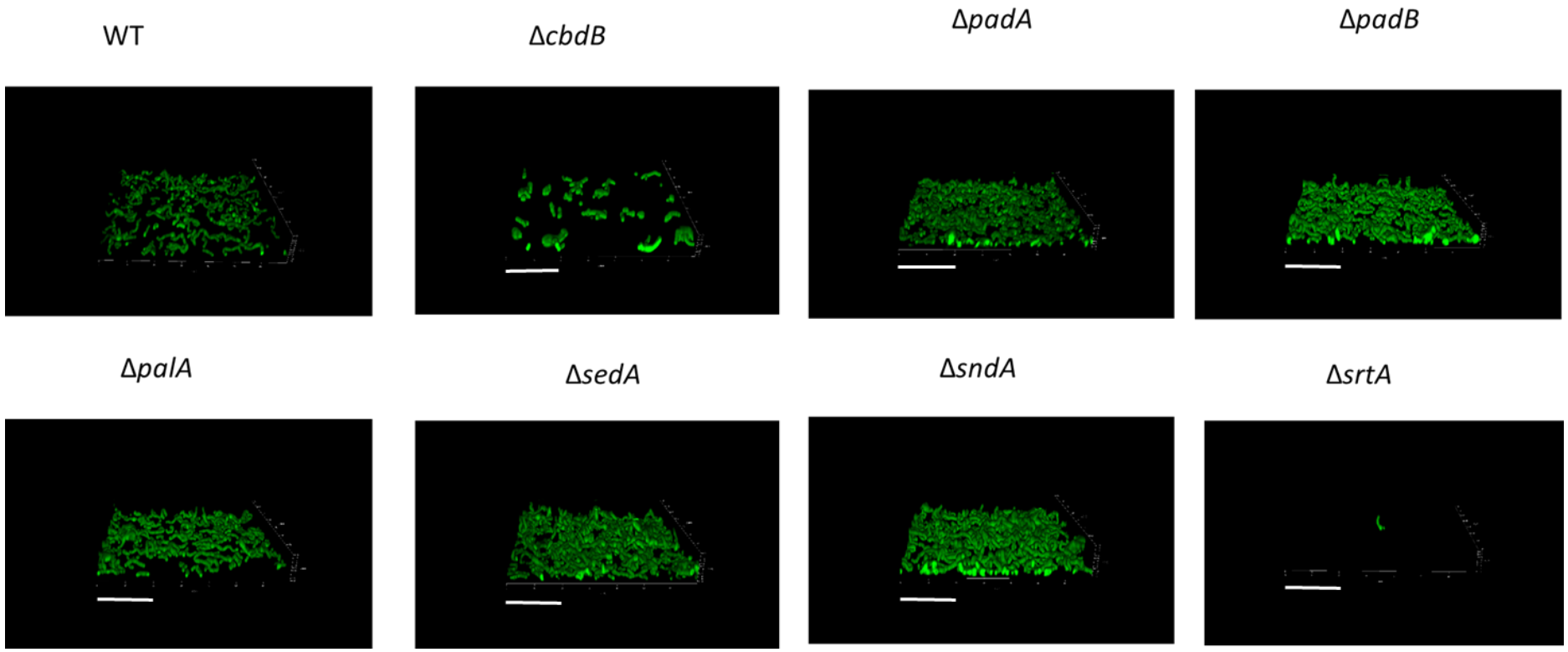

B)

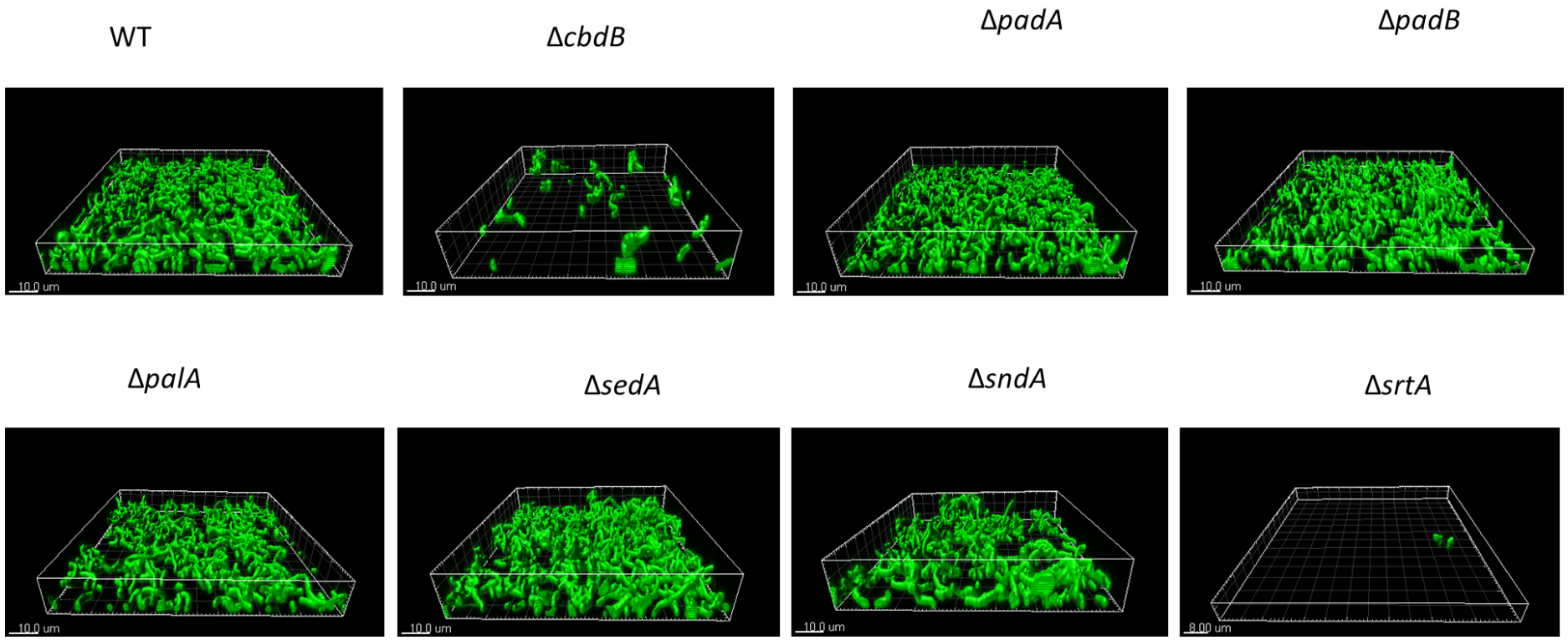
WT
ΔcbdB
ΔpadA
ΔpadB
ΔpalA
ΔsedA
ΔsndA
ΔsrtA
10.0 um
10.0 um
10.0 um
10.0 um
10.0 um
10.0 um
10.0 um
8.00 um

C)

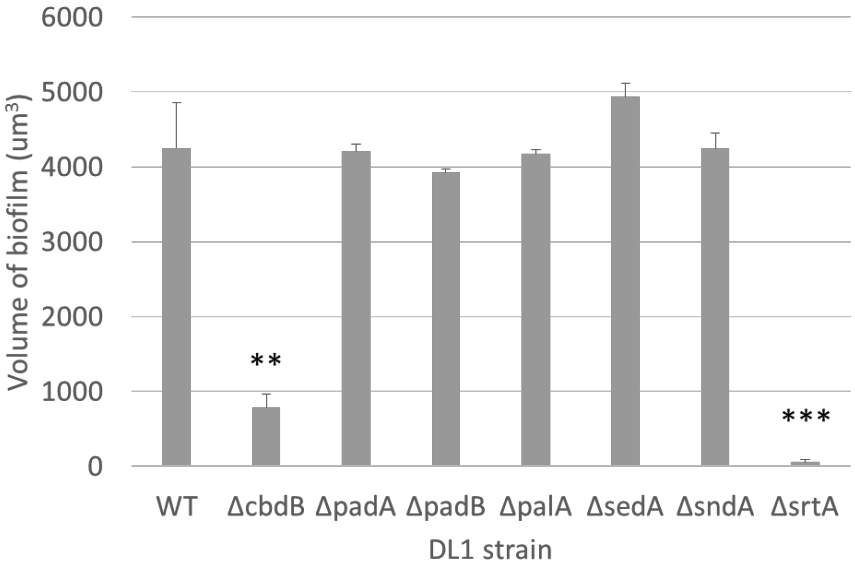

D)

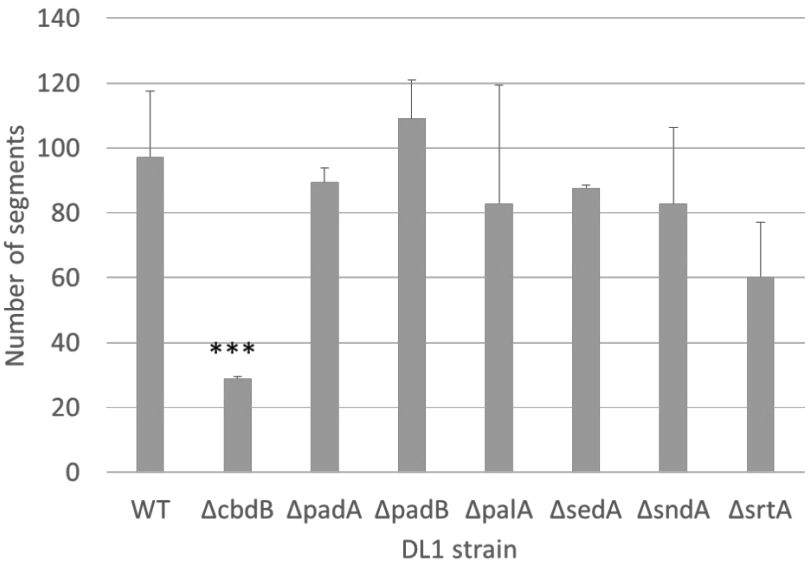

Figure 4.19 – ***Confocal analysis of S. gordonii WT and LPxTG knockout mutant biofilms grown in salivary medium.*** *S. gordonii strains WT, ΔcbdB, ΔpadA, ΔpadB, ΔpalA, ΔsedA, ΔsndA and ΔsrtA were adjusted to OD_{600} 0.1 in salivary medium, then incubated in saliva-coated glass-bottomed wells at 37 °C for 24 h. Confocal laser scanning microscopy was used to capture A) micrographs (scale bars = 20 µm) which were then B) analysed using Imaris to find the volume of the biofilms (scale bars = 10 µm). The C) biovolume and D) segmentation data are presented as mean ± SD; n=3. A one-way unpaired ANOVA was used to compare between treatments of the same strain, with α=0.05. ** P<0.005, *** P<0.0005, compared to WT.*

4.8 Role of LPxTG proteins in eDNA stranding

The potential role of *S. gordonii* LPxTG proteins in eDNA stranding during biofilm formation was investigated using the protocol established in section 3.2. The biomass of each strain grown under the eDNA stranding assay conditions was first measured (Figure 4.20), again using the Δ*srtA* mutant as a negative control. Significantly reduced biomass compared to WT was only seen for the negative control Δ*srtA* strain, which was reduced by approximately 70%. This impairment in biofilm formation was anticipated, as LPxTG surface proteins are known to be involved in *S. gordonii* cell: substratum and cell: cell adhesion.

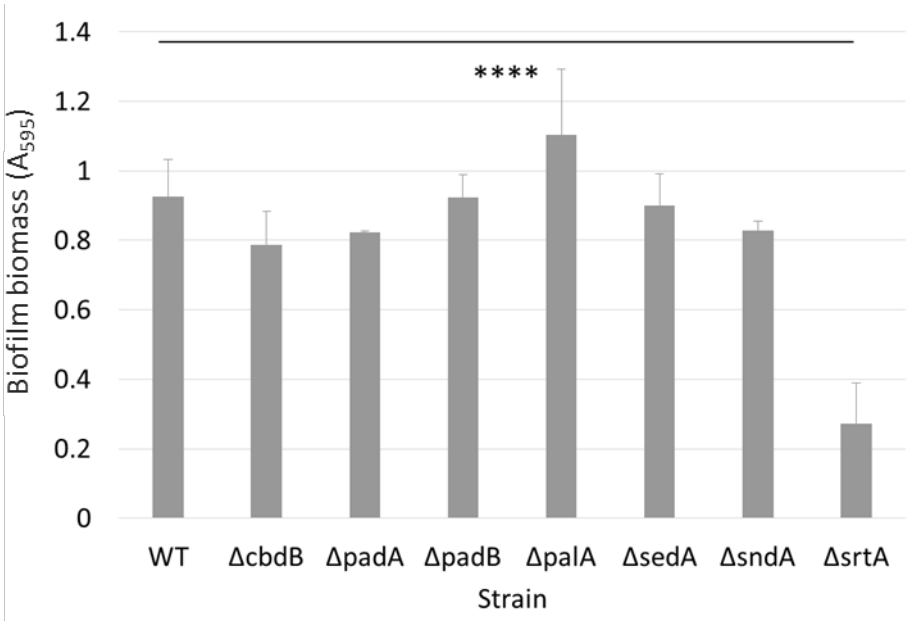

Figure 4.20 - ***Loss of all LPxTG proteins, but not any individual gene tested, reduces S. gordonii biofilm biomass in YPTG****. S. gordonii WT, ΔcbdB, ΔpadA, ΔpadB, ΔpalA, ΔsedA, ΔsndA and ΔsrtA biofilms were grown in YPTG at 37 °C for 5 h on saliva-coated glass-bottomed wells. Biofilms were stained with 0.25% crystal violet, the stain released with acetic acid, and the absorbance measured at A_{595}. Data are presented as absorbance ± SD; n=3. Experiments performed in triplicate. A one-way unpaired ANOVA was used with α=0.05. **** P< 0.0001, compared to WT.*

S. gordonii mutants lacking CbdB, PadA, PadB and PalA produced levels of eDNA stranding that were comparable to those of WT (Figure 4.21). By contrast, despite similar biomass levels, significantly less stranding was detected for Δ*sedA* and Δ*sndA* mutant biofilms, with eDNA levels reduced by 62% compared to WT.

This suggests that whilst eDNA appears to be important in biofilm accretion, loss of eDNA stranding in SedA and SndA mutants does not affect biomass, therefore is compensated for by another, as yet unknown, mechanism. Total eDNA stranding levels were reduced by 78% for Δ*srtA* mutant biofilms relative to WT. However, this correlated directly with the concomitant reduction in biofilm biomass.

A)

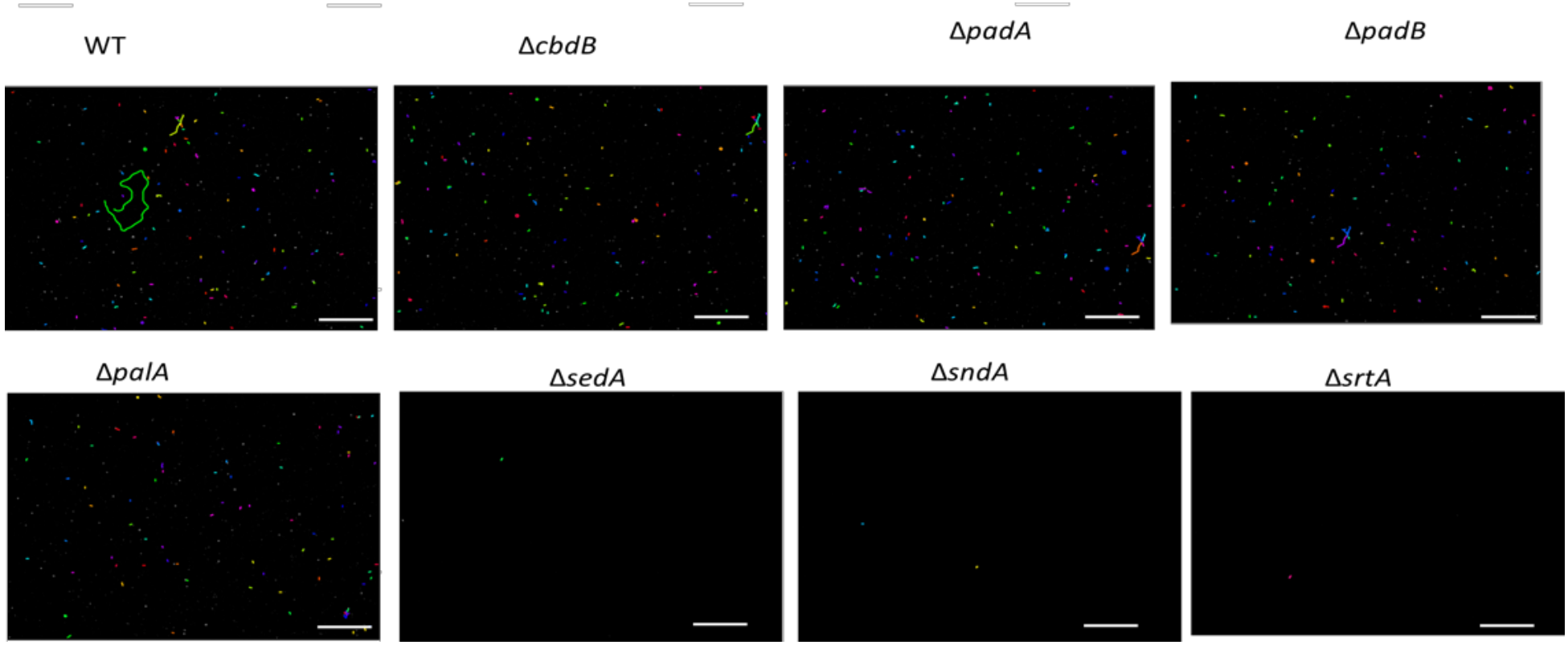

B)

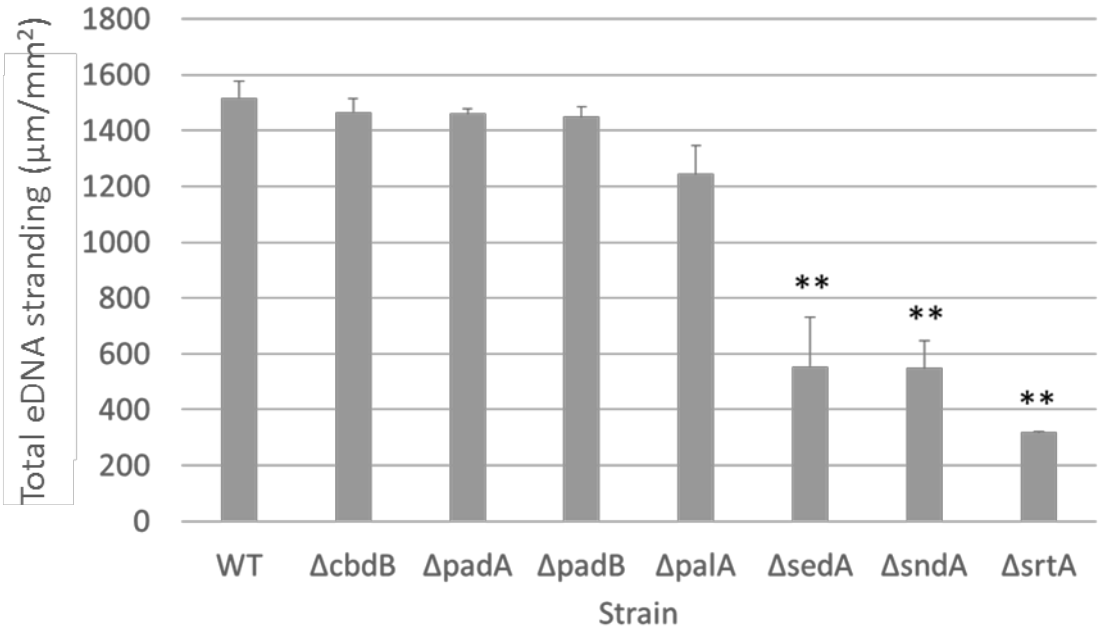

Figure 4.21 – ***S. gordonii ΔsedA, ΔsndA and ΔsrtA biofilms are reduced in eDNA stranding relative to WT.*** *S. gordonii WT, Δ**cbdB**, ΔpadA, ΔpadB, ΔpalA, ΔsedA, ΔsndA and ΔsrtA biofilms were grown in YPTG at 37 °C for 5 h on saliva-coated glass-bottomed wells. Biofilms were stained with TO-PRO3, and eDNA strands were labelled with primary ms anti-ds DNA antibody and secondary gt anti-ms antibody conjugated to Alexa Fluor A594. Biofilms were visualised using widefield microscopy. A) Gallery of images post-ridge finding analysis in MATLAB. Scale bars = 100 µm. B) Quantification of total eDNA stranding. Data are presented as mean total stranding per mm² ± SD; n=3. A one-way unpaired ANOVA was used with α=0.05. ** P<0.005, compared to WT.*

4.9 Extracellular DNase assay

To further explore any potential association between *S. gordonii* LPxTG proteins and eDNA within biofilms, the DNase activity of the LPxTG mutants was investigated, using Δ*srtA* as negative control. *Staphylococccus aureus* was used as a positive control, as this species was known to have strong extracellular DNase activity (Kateete *et al.*, 2010). Bacteria were incubated on DNA-containing agar, DNA was precipitated using HCl, then zones of clearance produced by DNase activity were measured. WT *S. gordonii* generated a zone of clearance on DNase agar of 5.2 mm diameter. The positive control for DNase activity, *Staphylococcus aureus*, generated a zone of clearance with a diameter of 7.8 mm. DNase activity was ablated in Δ*sndA* and Δ*srtA* mutant strains (Figure 4.22).

No other LPxTG mutant strain tested caused a reduction in extracellular DNase activity relative to WT. This implied that LPxTG surface proteins, and specifically SndA, was responsible for all *S. gordonii* extracellular DNase activity. Other components may be involved but if so, it appears that they require SndA for DNase activity.

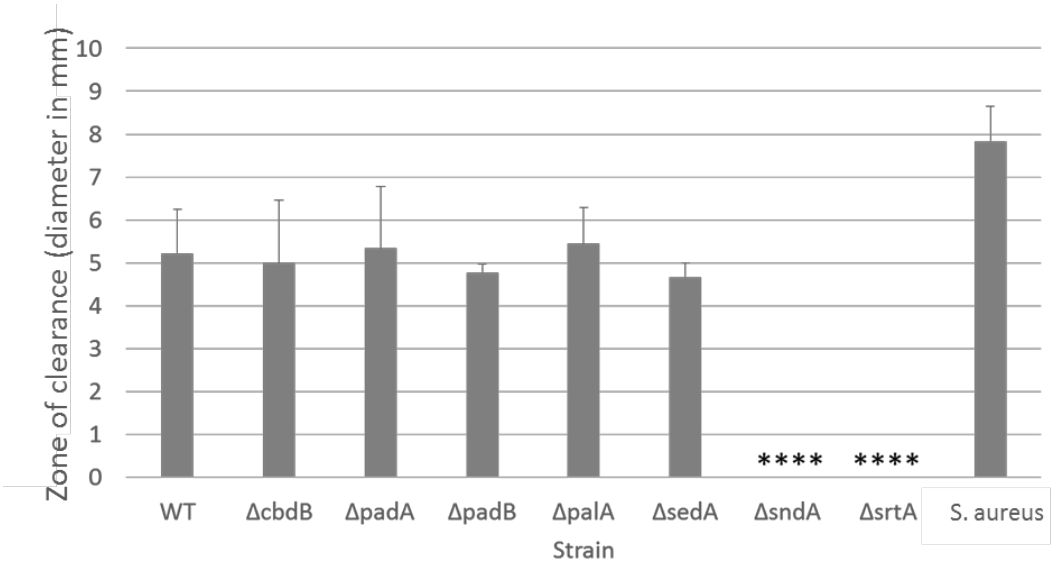

Figure 4.22 ***– Loss of SndA ablates S. gordonii extracellular DNase activity.*** *S. gordonii strains WT, ΔcbdB, ΔpadA, ΔpadB, ΔpalA, ΔsedA, ΔsndA and ΔsrtA, and Staphylococcus aureus were adjusted to OD_{600} = 1 in PBS. 5 mm diameter filter paper circles were inoculated with 2 µl of bacterial suspension and incubated on DNase agar at 37 °C for 16 h. DNA was precipitated with 1 M HCl and zones of clearance measured in mm. Data are presented as mean diameter of clearance ± SD; n=3. Experiments were performed in duplicate. A one-way unpaired ANOVA was used, with α=0.05. **** P<0.0001 compared to WT.*

4.10 Discussion

This work identified 27 LPxTG proteins encoded on the *S. gordonii* genome. The LPxTG protein-encoding genes were found to be distributed evenly across the genome and were not clustered at a specific site. Of these 27 LPxTG proteins, 6 were specifically investigated for their potential role in facilitating *S. gordonii* colonisation and biofilm formation, with a focus on four functional themes: hydrophobicity; coaggregation; ECM binding; biofilm development.

4.10.1 Initial adhesion

Bacterial interactions with salivary pellicle during the initial stages of dental plaque accretion can be influenced by a number of forces, including van der Waals forces and electrostatic interactions. These, in turn, can be affected by the hydrophobicity or hydrophilicity of bacterial surface proteins, which can alter the overall cell surface hydrophobicity. The target LPxTG proteins were therefore investigated in terms of modulating hydrophobicity. LPxTG protein CshA has been implicated in conferring cell surface hydrophobicity (Mcnab *et al.*, 1996) and this was replicated here. However, none of the other LPxTG knockout mutants tested differed from WT, implying that CbdB, PadA, PadB, PalA, SedA or SndA do not directly affect the surface hydrophobicity of *S. gordonii*.

4.10.2 Coaggregation

Coaggregation (coadhesion) is a key driver of dental plaque formation *in vivo*. Ablation of *S. gordonii*: *A. oris* coaggregation following loss of SspA/B was consistent with the known binding of *A. oris* polysaccharide by SspB (Back *et al.*, 2015), but none of the other LPxTG proteins investigated facilitated this coaggregation. However, in this study, only *S. gordonii* coaggregation with *A. oris* was tested. As a pioneer coloniser, *S. gordonii* has capacity to interact with many other bacterial species, SUCH AS to form the polymicrobial communities found within the mouth. It is possible, therefore, that these LPxTG proteins could be involved in coaggregation with other microorganisms, and investigation into these as-yet uncharacterised interactions may be of future interest.

4.10.3 ECM binding

Type I collagen is a host molecule often used to stabilise cell: cell interactions. It is the main protein found in the ECM of human tissues and thus represents a key colonisation target that could be utilised by *S. gordonii* to

associate with the host vasculature or soft (mucosal) tissues. Additionally, type I collagen has been shown to make up 18% of dentin in teeth (Goldberg *et al.*, 2011). *S. gordonii* protein CbdA had already been shown to facilitate *S. gordonii* binding to collagen and was also implicated in persistence within the oral cavity (Moses *et al.*, 2013). Three further 3 potential collagen-binding proteins in *S. gordonii* (CbdB-D) were identified here. Somewhat surprisingly, deletion of CbdB increased the capacity for *S. gordonii* to bind type I collagen. This may indicate that CbdB masks another surface protein which binds collagen. In support of this, adhesion of Δ*srtA* mutant to collagen was 3-fold lower than for WT *S. gordonii*, while Moses *et al.*, 2013 showed only a 2-fold reduction in binding in the absence of CbdA. This implies that *S. gordonii* expresses additional LPxTG protein(s) that adhere to type I collagen that have not yet been characterised. With their putative collagen-binding domains, CbdC or CdbD would be likely candidates.

S. gordonii protein PalA is homologous to SSURE-domain containing *S. pneumoniae* PavB, deletion of which results in impaired binding to fibronectin (Jensch *et al.*, 2010). A similar phenotype was shown here for PalA, although specifically for cellular, not plasma, fibronectin. Cellular fibronectin is found in the ECM and is exposed in damaged tissues, whereas plasma fibronectin is found in the blood. Thus PalA-mediated adhesion to cellular fibronectin may preferentially promote interactions of *S. gordonii* with host mucosal tissues, including damaged heart valves in the initiation of IE. How SSURE domains interact with fibronectin have not yet been determined, but the capacity for PalA to distinguish between the cellular and plasma forms of fibronectin could have important implications, particularly in the context of *S. gordonii* as a causative agent of IE. Direct targeting of cellular fibronectin has also been shown for CshA (Back *et al*., 2017), and so it will be of interest to decipher the interplay and relative contributions of these two adhesins in mediating mucosal tissue interactions of *S. gordonii*, and whether they share a common binding mechanism. Alongside PalA and CshA, *S. gordonii* has several other LPxTG proteins that have been implicated in fibronectin adherence, including PadA and Hsa (Haworth *et al.*, 2017) and FbpA (Christie *et al*., 2002). Loss of all of these

proteins from the Δ*srtA* mutant likely explains why the Δ*srtA* mutant bound fibronectin at an even lower level than the strain lacking PalA alone.

4.10.4 General biofilm formation

It is known that *S. gordonii* can modulate its gene expression profile, including those encoding surface proteins, in response to different environmental conditions (Lui *et al*., 2008), which, in turn, could be expected to affect biofilm development. The role of the target LPxTG proteins in biofilm formation when grown in limiting or minimal media was therefore explored. It was found that Δ*cbdB* biofilm volume and segmentation was lower than that of WT *S. gordonii* when measured using confocal microscopy, possibly implying a role for CbdB in maintaining interbacterial interactions. However, the same effects were not seen when determining biomass by crystal violet stain. It may be that the use of a more sensitive method such as confocal microscopy allowed for the detection of these differences. Alternatively, the action of the different stains used may be responsible; crystal violet stains all components of the biofilm, whereas FITC stains only proteinaceous constituents. Therefore, a reduction may have been seen in CbdB-lacking biofilms relative to WT when measured using FITC if these biofilms differed significantly with respect to non-proteinaceous components. This rationale could also be applied inversely to biofilms formed by mutants Δ*padB*, Δ*palA*, Δ*sedA* and Δ*sndA*, where different outcomes were obtained using the different biofilm analysis techniques. To investigate this further, multiple dyes could be used that target different biofilm constituents to quantify the biofilms using confocal microscopy. For example, a dye such as concanavalin A that reacts with carbohydrates could be used in conjunction with FITC.

A reduction in biofilm-forming capabilities had been reported previously for *S. gordonii* Δ*padA* (Haworth *et al.*, 2017) but was not seen here. However, this may reflect differences in the experimental design e.g. in the previous studies biofilms were grown for 16 h, as opposed to the 5 h used here. Likewise, while G5 domains within *Staphylococcus aureus* surface proteins facilitate biofilm

formation (Bateman *et al.*, 2005), no change in biofilm biomass relative to WT was observed for *S. gordonii* lacking the G5 domain-containing protein PadB. It is possible that the G5 domains in PadB do not function as predicted i.e. do not bind *N*-acetylglucosamine (Bateman *et al.*, 2005), a component of salivary agglutinin (Oho *et al.*, 1998). However, other salivary agglutinin-binding proteins such as GspB and Hsa have already been identified on the surface of *S. gordonii*. These may be able to compensate for the loss of PadB, meaning no effect on phenotype is seen in this assay in the absence of PadB alone.

Further evidence of functional redundancy across the LPxTG proteins of *S. gordonii* comes from the biofilm studies with the Δ*srtA* mutant. For each condition tested, biofilm formation by the Δ*srtA* mutant was significantly impaired relative to WT, but also to the individual LPxTG knockout mutants. This suggests that the LPxTG proteins work collectively to facilitate *S. gordonii* biofilm development. Nonetheless, differences in biofilm biovolume levels between WT and the Δ*srtA* mutant were greatest in salivary medium than C medium WT. This may indicate that the role of LPxTG proteins in *S. gordonii* biofilm formation is particularly critical under very limiting conditions. This could, for example, be due to loss of EPS production under starvation conditions. Given the functional degeneracy seen between LPxTG proteins in *S. gordonii*, future studies into the roles of specific adhesins could benefit from use of a heterologous expression system such as *Lactococcus lactis*. This would allow assessment of function of an individual protein, without potential confounding by the presence of other adhesins.

4.10.5 eDNA stranding in biofilms

Two of the target LPxTG proteins were implicated in eDNA stranding in *S. gordonii* biofilms. Biofilms formed by *S. gordonii* lacking either SedA or SndA showed no change in biomass relative to WT but were significantly reduced in eDNA stranding. This suggested that these proteins may influence eDNA in a way which does not affect biomass, and gave support to the idea that eDNA release

may be an active mechanism. Furthermore, bioinformatic analysis of both proteins indicated they may have potential to interact with DNA.

SedA carries domains with homology to surface exclusion domains, which may have capacity to interact directly with DNA as part of the surface exclusion process. Thus, SedA may also be able to associate with DNA via such domains and this interaction may be important for eDNA stranding.

SndA contains a nuclease domain, shown here to be active and able to cleave DNA. The effects of the Δ*sndA* mutant on eDNA stranding levels were therefore a little surprising. One might have expected that removing a nuclease from the surface of *S. gordonii* would, if anything, increase levels of eDNA. Nonetheless, SndA does have a DNA-binding domain, and it may be this function that is related to its effects on eDNA stranding. It is also possible that the DNase domain of SndA has a role in modelling the eDNA into the constellation-like structures seen across the biofilms.

Attempting to determine the precise roles of SedA and SndA and the mechanism(s) by which they influence eDNA stranding became a focus of the studies presented in Chapter 5.

4.10.6 Summary

Of the 27 LPxTG family proteins identified on the *S. gordonii* genome, 6 were investigated for how they may contribute to *S. gordonii* colonisation and biofilm development. From these studies, PalA was found to bind cellular fibronectin, with potential implications for mucosal tissue interactions and the pathogenesis of IE. SndA was identified as a cell-wall anchored nuclease, and SedA and SndA were both implicated in eDNA stranding during biofilm development.

Chapter 5 Mechanistic basis of *S. gordonii* eDNA production

5.1 Introduction

Experiments in Chapter 3 demonstrated the importance of eDNA stranding in *S. gordonii* biofilms. Disrupting stranding with DNase treatment caused a reduction in overall biomass, suggesting eDNA may have a role as a structural scaffold. The mechanism for eDNA release and strand formation, however, was unknown. Two principal mechanisms of eDNA release have been reported for other bacteria: i) cell lysis, often involving autolytic enzymes, or ii) a lysis-independent, active DNA release. Of specific relevance to *S. gordonii*, Jack et al., 2015, had also shown that the competence (ComCDE) operon of *S. gordonii* facilitated biofilm formation (in mixed species biofilms with *C. albicans),* and bacteria lacking ComCDE appeared to form biofilms with less eDNA (Jack *et al.*, 2015). The effect of the competence system on eDNA stranding had not been quantified, and the mechanism for the change in biofilm biomass was unknown. It was hypothesised, however, that Competence Stimulating Peptide (CSP) may play a role in eDNA release.

The competence operon enables *S. gordonii* to take up DNA from the environment by transformation, and levels of transformation have been shown to be modulated by the concentration of CSP, which is encoded by *comC*. The product, pre-CSP, is cleaved to mature CSP by ComA and then translocated out of the cell through ComAB, where it can be sensed by ComDE, a two-component regulator system (Håvarstein *et al.*, 1996). ComD is the trans-membrane component and autophosphorylates upon detection of CSP, before going on to phosphorylate ComE, the effector. ComE upregulates early competence genes, including activation of ComX (otherwise known as ComR), which induces late competence gene expression, resulting in the ability of the cell to uptake DNA from the environment (Heng *et al.*, 2006) (Figure 5.1).

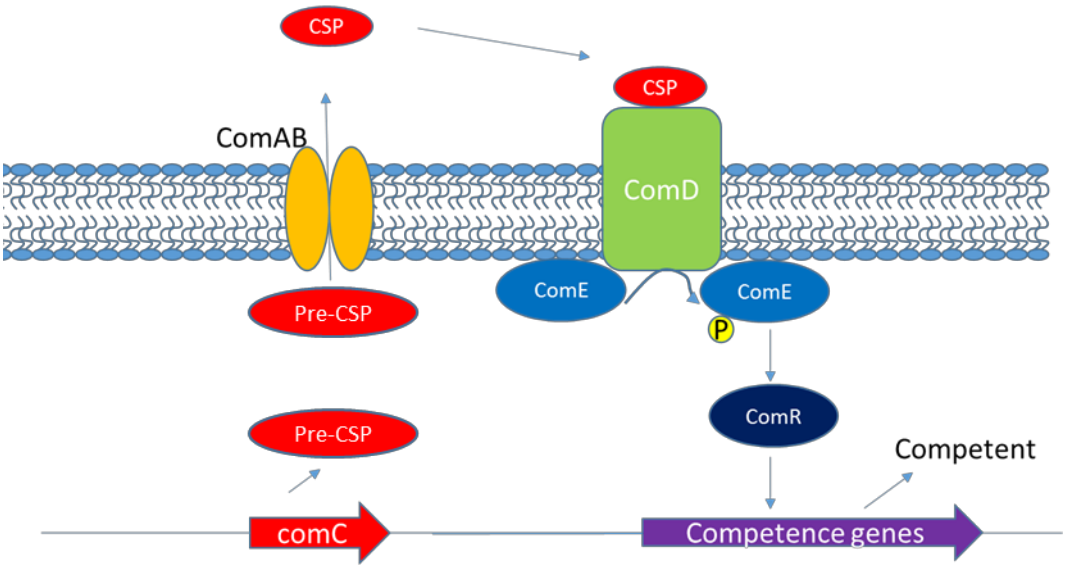

Figure 5.1 - ***S. gordonii competence system.***

Another potential mechanism for eDNA release is autolysis, where cells are killed in a fratricidal or suicidal way via their own enzymatic activity. Two known autolysins in *S. gordonii* are AtlS and competence-regulated LytF. These autolysins respond to oxidative stress, such as that caused by excess hydrogen peroxide, and hydrogen peroxide addition had been shown to increase eDNA production by *S. gordonii* via the actions of LytF (Kreth *et al.*, 2009; Xu & Kreth, 2013).

The studies presented in this chapter aimed to exploit the eDNA quantification tool developed in this project to better understand the roles which the competence operon, lysis and autolysins play in *S. gordonii* eDNA release and biofilm formation. Due to the striking change in eDNA stranding observed for the mutant strains lacking SedA or SndA in Chapter 3, the potential roles for these proteins in eDNA stranding was also further investigated.

5.2 CLSM assessment of eDNA in biofilms

To better explore the role of SedA and SndA in eDNA stranding, complementation of these mutant strains was performed. A double knockout

Δ*sedA* Δ*sndA* mutant was also generated and then complemented with the individual proteins. Alongside these mutants, the *S. gordonii* mutant lacking ComCDE was used to investigate the involvement of the competence pathway in eDNA stranding. The Δ*srtA* strain was used as a negative control.

To further probe eDNA stranding, a new technique was used. Up until this stage, eDNA in biofilms had predominantly been observed in this project using widefield microscopy, where viewing stranding in Z is limited and out of focus light is included. Higher resolution imaging of DNA within biofilms was required to investigate changes in eDNA stranding in the Z plane. Confocal microscopy, which can resolve in Z, was therefore used and data on eDNA position in Z relative to biofilm cells was collected. It was hypothesised that localisation of eDNA within the biofilm may provide information on the source and release mechanism of DNA. For example, if eDNA was at the base of the biofilms, it may suggest a very early release, and if it was on the top of the biofilm, it may suggest a later stage release or that this is eDNA which has been released and bound back to the biofilm. The same biofilm labelling technique was used for confocal microscopy as used previously in widefield microscopy.

Confocal microscopy supported the previous eDNA stranding data analysis: biofilms formed by *S. gordonii* mutant strains Δ*sedA*, Δ*sndA* and Δ*srtA* appeared to produce less eDNA than WT (Figure 5.2). Alike to the single knockout mutants, biofilms of strain Δ*sedA* Δ*sndA* appeared to have less eDNA than WT. By contrast, complementation with SedA or SndA appeared to restore eDNA stranding to near WT levels. Biofilms formed with Δ*comCDE* appear to have less networked DNA than WT, suggesting that the competence system may play a role in eDNA stranding.

Volocity analysis allowed for the quantification of eDNA within biofilms as a proportion of the total volume, and eDNA was found to make up 0.71% of the WT *S. gordonii* biofilm volume. Tilted micrographs also indicated that eDNA was located throughout the biofilms. Confocal micrographs were analysed using Volocity, as described in Materials and Methods, to obtain the Z position of every object (eDNA or bacterial cells) in the biofilm. A box-and-whisker plot was then generated from analysing the average Z position of either eDNA or bacterial cells

within the biofilm (Figure 5.3). It is worth noting that this graph is not intended for comparison between strains directly in terms of Z, as slope on the biofilm plate meant that the Z-stack acquired was slightly different for each biofilm. It was found that the Z position of eDNA was not significantly different to the Z position of cells in all cases, however, in biofilms formed with ΔsedA bacteria, the maximum height at which eDNA stranding was found exceeded the maximum cell height. A potential explanation for this could be that eDNA was bound less well in the absence of SedA, which contains putative DNA binding domains.

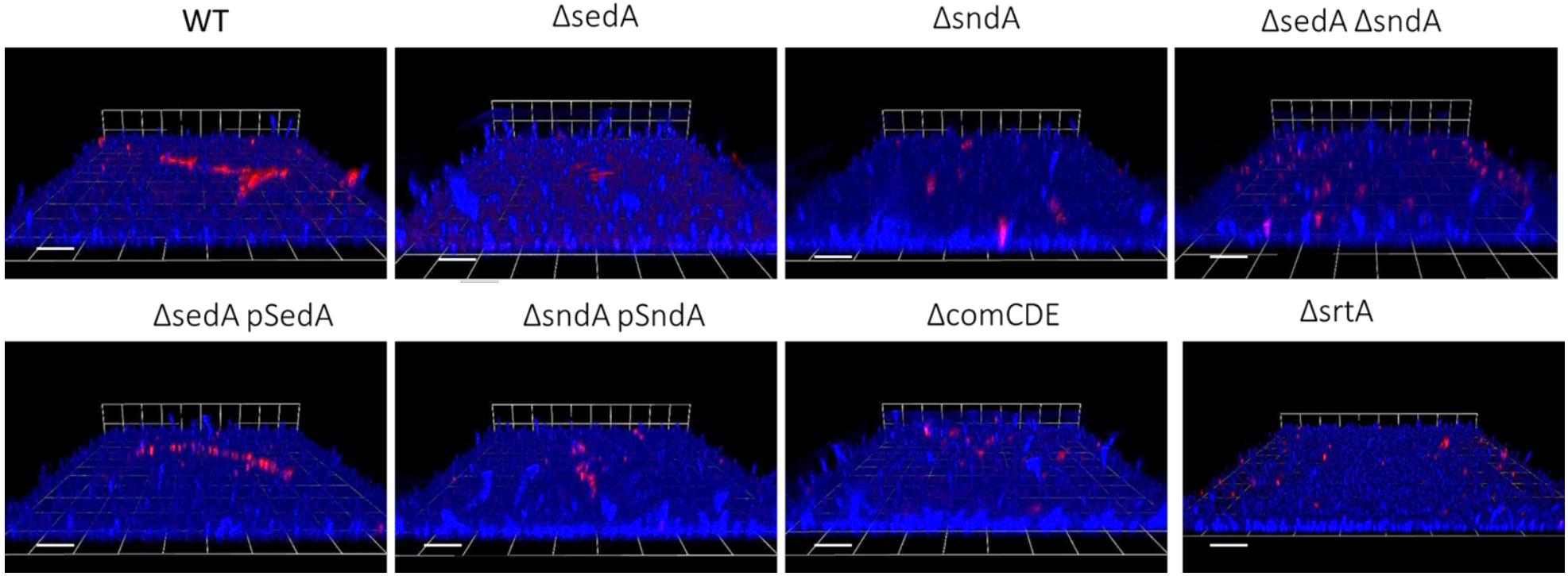

*Figure 5.2 – **eDNA in biofilms as visualised using confocal microscopy**. S. gordonii strains WT, ΔsedA, ΔsndA, ΔsedA ΔsndA, ΔsedA pSedA, ΔsndA pSndA, ΔcomCDE and ΔsrtA were adjusted to OD_{600} = 0.25 in YPTG and incubated at 37 °C, 50 rpm for 5 h on saliva-coated cover slips. Bacterial cells were stained with TO-PRO3 (blue), while eDNA strands were labelled with a mouse anti-dsDNA antibody and a goat anti-mouse Ig antibody conjugated to AlexaFluor 595 (red), and visualised using a confocal laser scanning microscope. A Z-stack of around 10 µm was used to capture each biofilm. Scale bars = 10 µm*

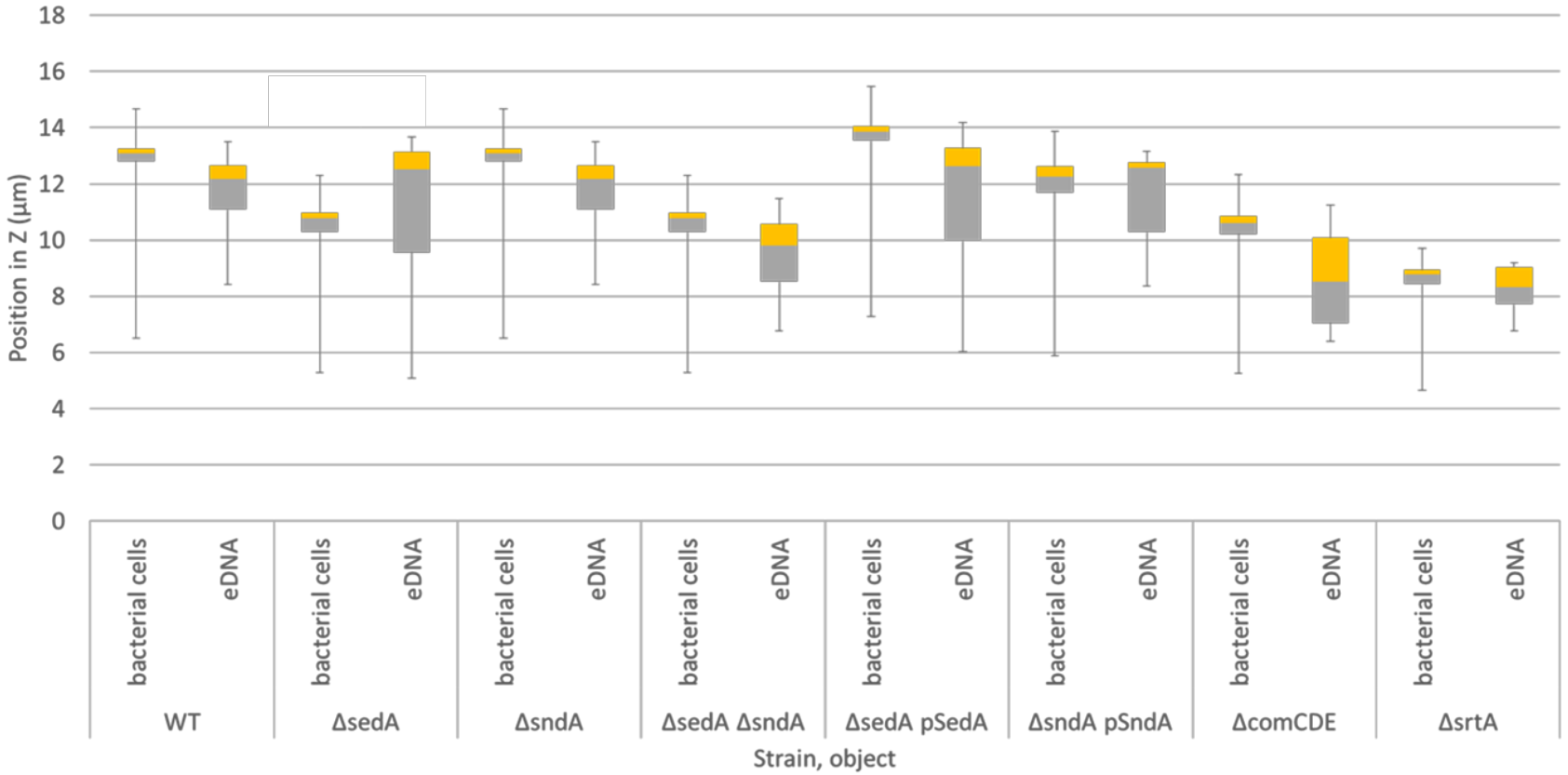

*Figure 5.3 – **eDNA distribution in Z within S. gordonii biofilms**. Micrograph images of biofilms were collected and analysed using Volocity. A box and whisker plot was generated to show the average position in Z of different objects within the biofilm: bacterial cells or eDNA. Data are presented as minimum, first quartile, median, third quartile and maximum. Experiments were performed in triplicate; n=3. An unpaired T-test followed by a Bonferoni multi-comparison correction was used to compare the distribution of bacterial cells and eDNA within each strain, with α=0.05. No significant difference was found.*

5.3 Nuclease activity of mutant strains

Having previously determined the DNase activity of the Δ*sedA* and Δ*sndA* mutants, the activity of the double mutants and complemented strains were investigated. As for the Δ*sndA* mutant, DNase activity was ablated in the double mutant (Figure 5.4). Nuclease activity was restored in Δ*sndA* pSndA and Δ*sedA* Δ*sndA* pSndA mutants, which confirmed successful complementation. Mutants Δ*sndA*, Δ*sedA* Δ*sndA* and Δ*sedA* Δ*sndA* pSedA were all ablated in nuclease activity. All of these strains lack SndA, which supported the hypothesis that SndA is solely required for *S. gordonii* extracellular DNase activity.

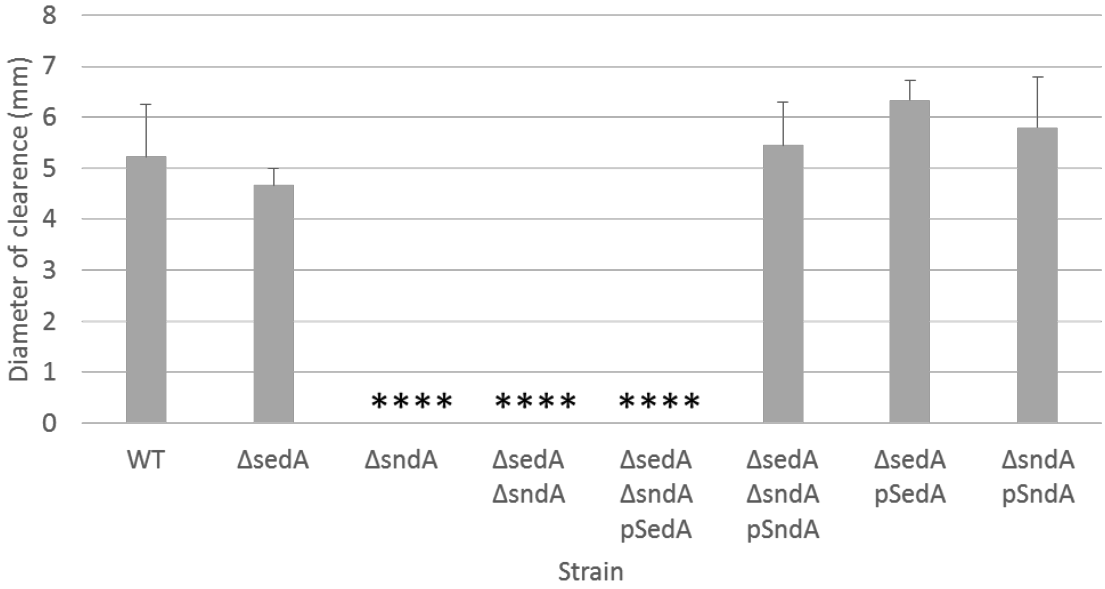

Figure 5.4 – ***Nuclease activity of S. gordonii mutants.*** *S. gordonii strains WT, ΔsedA, ΔsndA, ΔsedA ΔsndA, ΔsedA ΔsndA pSedA. ΔsedA ΔsndA pSndA, ΔsedA pSedA and ΔsndA pSndA were adjusted to OD_{600} = 1 in PBS, then spotted onto 5 mm diameter paper disks on DNase agar. These plates were incubated at 37 °C for 16 h. DNA was precipitated with 1 M HCl and the diameter of clearance was measured. Data are presented as diameter of clearance ± SD; n=3. A one-way unpaired ANOVA was used, with α=0.05. **** P < 0.0001, compared to WT.*

5.4 SedA and SndA mutant stranding

S. gordonii knockout mutants in SedA or SndA had both shown phenotypic differences in eDNA stranding compared to WT. The newly generated SedA and

SndA mutants were investigated in terms of eDNA stranding to further investigate these effects, including the potential for SedA and SndA to exhibit functional cooperativity.

Biofilms formed by the mutant strains were not significantly different in biomass to WT *S. gordonii* (Figure 5.5). This was consistent with what had been found for the bacteria carrying a single SedA or SndA mutation.

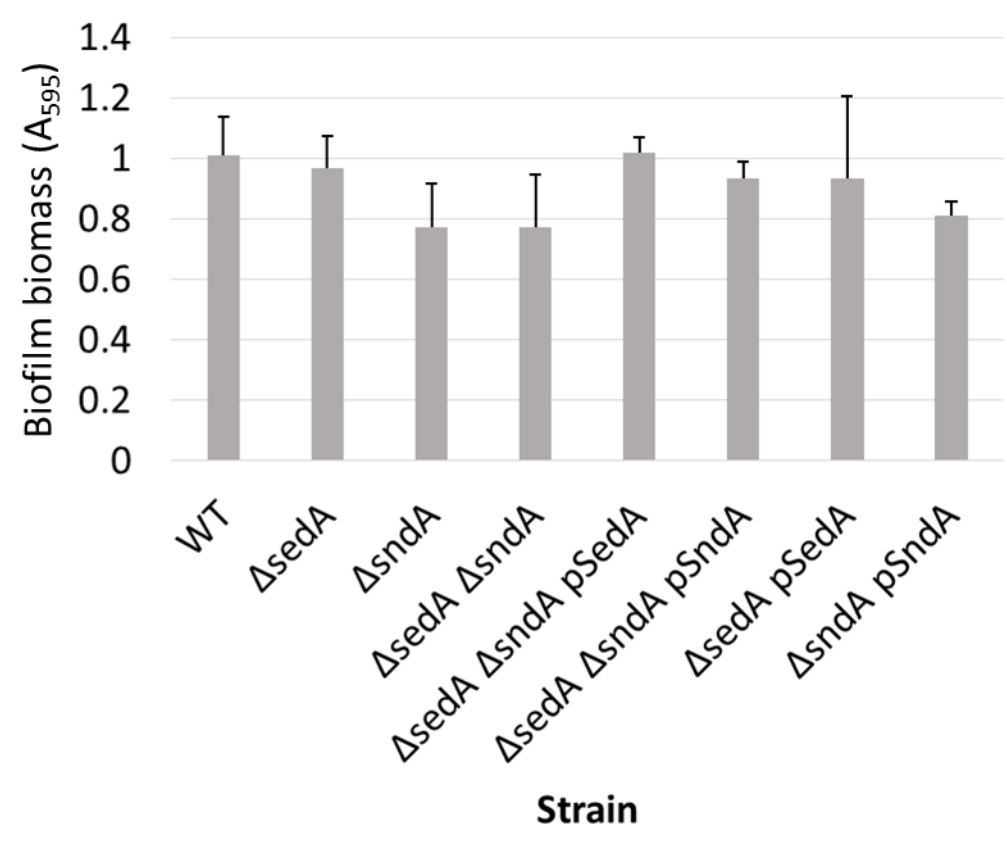

Figure 5.5 - ***Biofilm biomass is not altered in SedA/SndA mutant biofilms relative to WT****. S. gordonii strains WT, ΔsedA, ΔsndA, ΔsedA ΔsndA, ΔsedA ΔsndA pSedA. ΔsedA ΔsndA pSndA, ΔsedA pSedA and ΔsndA pSndA were grown in YPTG at 37 °C for 5 h on saliva-coated glass-bottomed wells. Biofilms were stained with 0.25% crystal violet, the stain released with acetic acid, and the absorbance measured at A_{595}. Data are presented as mean absorbance ± SD; n=3. Experiments performed in triplicate. A one-way unpaired ANOVA was used with α=0.05. No significant difference compared to WT was found.*

As seen before, Δ*sedA* and Δ*sndA* strains were both reduced in eDNA stranding by around two thirds compared to WT. Similar reductions were seen for strains Δ*sedA* Δ*sndA*, Δ*sedA* Δ*sndA* pSedA and Δ*sedA* Δ*sndA* pSndA (Figure 5.6). eDNA stranding was restored to WT levels in both Δ*sedA* pSedA and Δ*sndA*

pSndA strains. Since all mutants which did not have a functioning copy of both SedA *and* SndA were reduced in stranding, it was hypothesised that these proteins work co-operatively to enable eDNA stranding in *S. gordonii*.

A)

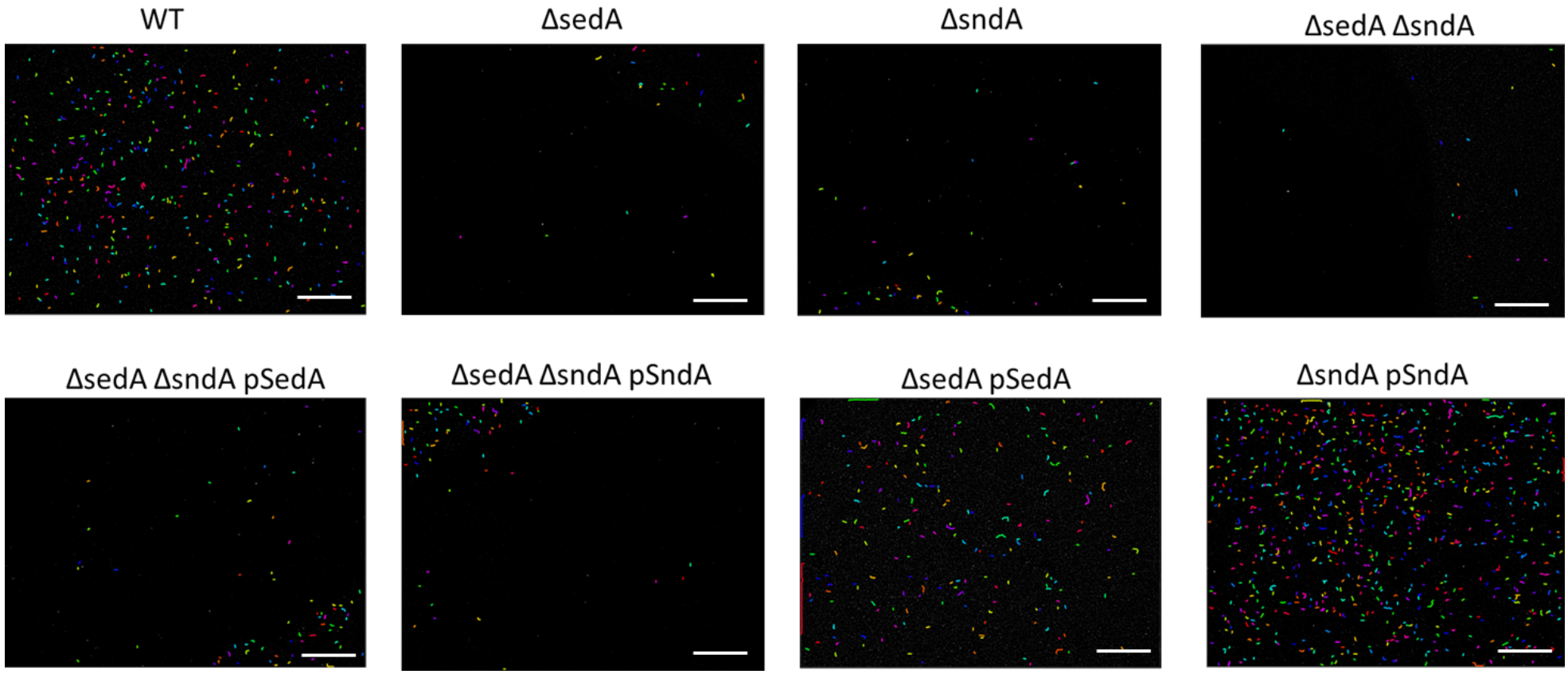
WT
ΔsedA
ΔsndA
ΔsedA ΔsndA
ΔsedA ΔsndA pSedA
ΔsedA ΔsndA pSndA
ΔsedA pSedA
ΔsndA pSndA

B)

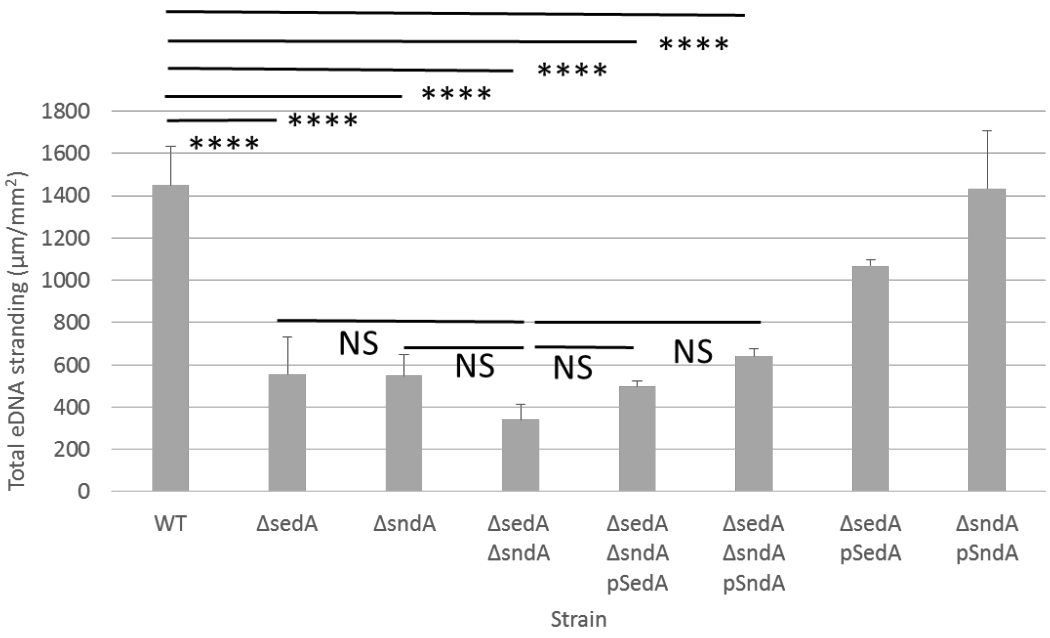

Figure 5.6 – ***eDNA stranding is reduced in biofilms lacking SedA/SndA relative to WT.*** *S. gordonii strains WT, ΔsedA, ΔsndA, ΔsedA ΔsndA, ΔsedA ΔsndA pSedA, ΔsedA ΔsndA pSndA, ΔsedA pSedA and ΔsndA pSndA were used to grow biofilms in YPTG at 37 °C for 5 h on saliva-coated glass-bottomed wells. Biofilms were stained with TO-PRO3, labelled with a ms anti-ds DNA antibody and a gt anti-ms Ig conjugated to AlexaFluor595, and visualised using widefield microscopy. A) Gallery of images post-ridge finding analysis in MATLAB. Scale bars = 100 µm. B) Quantification of total eDNA stranding. Data are presented as mean total stranding per mm² ± SD; n=3. A one-way unpaired ANOVA was used with α=0.05. **** P<0.0001.*

A potential mechanism by which SedA and SndA might affect eDNA stranding would be if these proteins influenced *S. gordonii* cell lysis. This was investigated using an ATP determination assay. This was considered sensitive enough to measure the small-scale sub-population lysis events that might be responsible for eDNA stranding, with the amount of ATP measured in the biofilm supernatant proportional to the number of cells lysed.

Biofilms were first treated with mutanolysin, which lyses Gram-positive cells, to confirm that the assay was working as anticipated. Treatment with 500 U/ml mutanolysin caused an increase of around 50% in extracellular ATP

concentration – this correlated to around 30% lysed cells, when CFUs were counted (Figure 5.7).

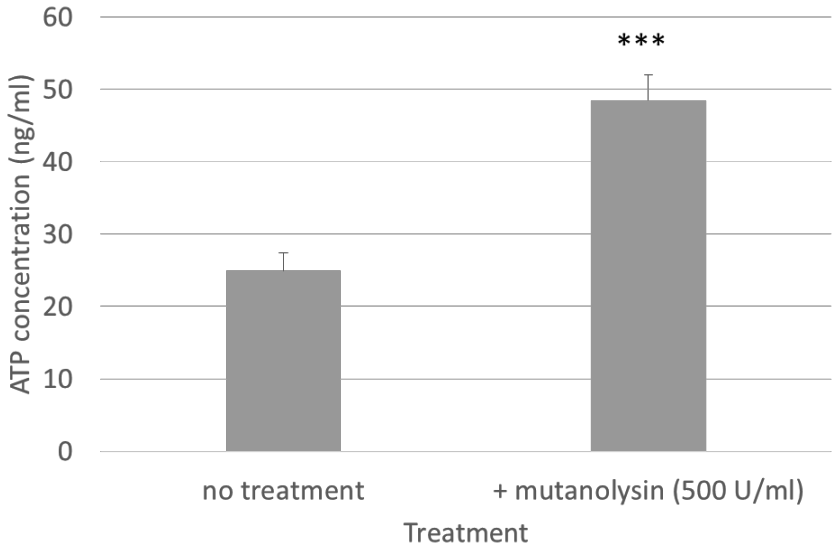

Figure 5.7 – ***Mutanolysin treatment of S. gordonii biofilm results in increased extracellular ATP.*** *S. gordonii biofilms were grown in YPTG with no treatment or 50 U/ml mutanolysin and incubated at 37 °C for 5 h on saliva-coated glass-bottomed wells. Biofilm supernatant was removed and mixed with Standard Reaction Solution (ATP determination assay (Invitrogen)). Luminescence was measured in a plate reader. A standard curve of ATP concentration was performed alongside, against which luminescence units could be converted into ATP concentration. Data are displayed as mean ATP concentration (ng/ml) ± SD; n=3. Experiments were performed in triplicate. An unpaired T-test was used with α=0.05. *** P<0.0005, compared to no treatment.*

None of the SedA or SndA mutant biofilms differed in levels of extracellular ATP compared to WT *S. gordonii* (Figure 5.8), implying that there were no significant differences with regards to cell lysis events.

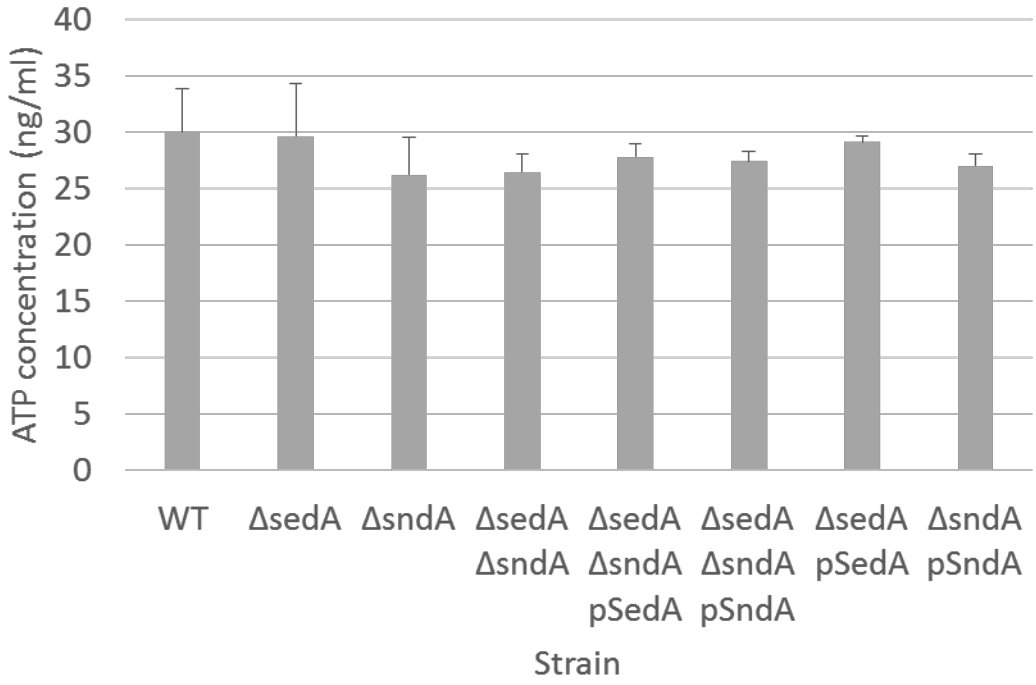

Figure 5.8 - ***Loss of SedA or SndA does not affect cell lysis within biofilms****. S. gordonii strains WT, ΔsedA, ΔsndA, ΔsedA ΔsndA, ΔsedA ΔsndA pSedA, ΔsedA ΔsndA pSndA, ΔsedA pSedA and ΔsndA pSndA were grown in YPTG and incubated at 37 °C for 5 h on saliva-coated glass-bottomed wells. Biofilm supernatant was removed and used to calculate levels of ATP, using an ATP determination assay (Invitrogen) in which luminescence units were converted into ATP concentration. Data are displayed as mean ATP concentration (ng/ml) ± SD; n=3. Experiments were performed in triplicate. A one-way ANOVA was used with α=0.05. No significant difference was found compared to WT untreated.*

5.5 Direct interactions of SedA/SndA with DNA

SedA and SndA both have putative DNA-interacting domains, as identified using bioinformatics. It was possible, therefore, that SedA and SndA facilitated eDNA stranding via direct binding to DNA and additionally, that this interaction may be co-operative, as it appeared to be based on the eDNA stranding data. To explore this possibility in more detail, the ability of the SedA/SndA mutant *S. gordonii* strains to bind double-stranded DNA (dsDNA) was investigated. The effects of the *comCDE* mutation on DNA binding were also determined, and strain Δ*srtA* was used as a control. A DNA kit was used, in which a cell-impermeable fluorophore specific to dsDNA fluoresces upon binding, which can then be detected on a fluorescence microtitre plate reader.

In the first instance, planktonic bacterial cultures were grown for 5 hours (to match the time period of the biofilm studies), and levels of dsDNA within the extracellular milieu or bound to the bacterial cells were measured (Figure 5.9). Mutants lacking either SedA, SndA or SrtA bound approximately 40% less DNA than WT *S. gordonii*, while the complemented strains Δ*sedA* pSedA and Δ*sndA* pSndA, and strain Δ*comCDE,* were comparable to WT. These effects were inverted for the levels of dsDNA found within the extracellular milieu. This implied that the bacterial strains were *producing* the same quantity of DNA but *binding/retaining* different amounts, and supported the notion that both SedA and SndA were needed for *S. gordonii* to maximise DNA binding. No difference was found between strains which lacked one of either SedA or SndA and those which lacked both. This implied that these proteins may work co-operatively to bind DNA, and supported the theory of co-operation developed from the eDNA stranding data.

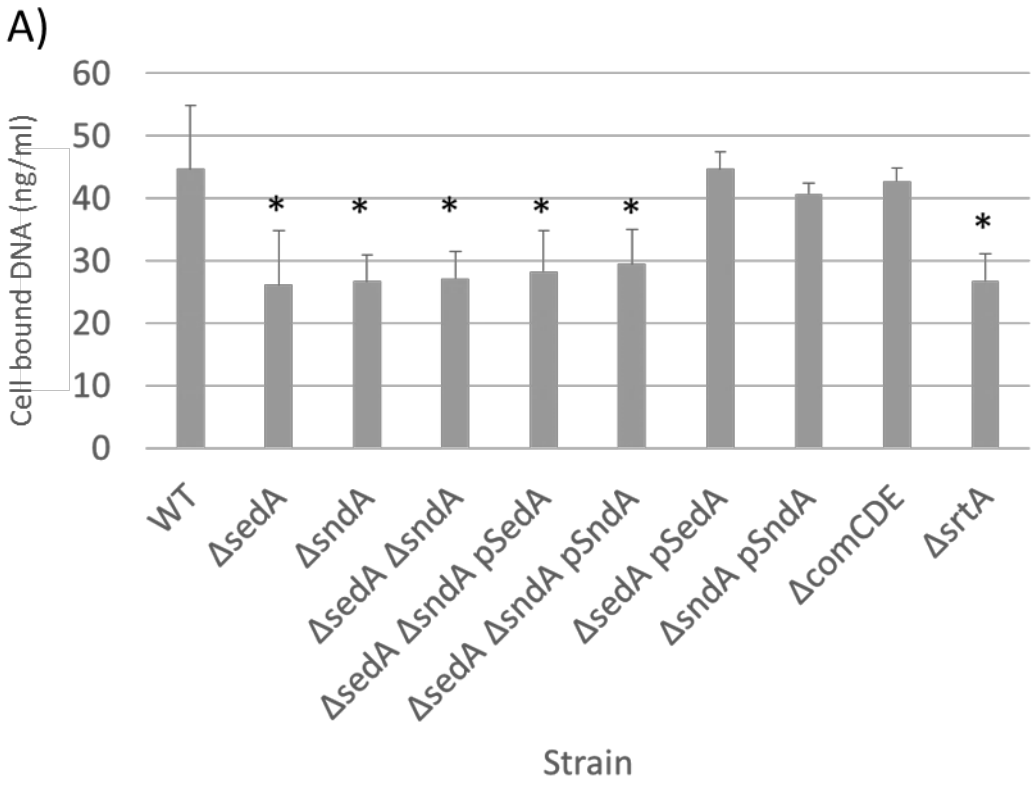

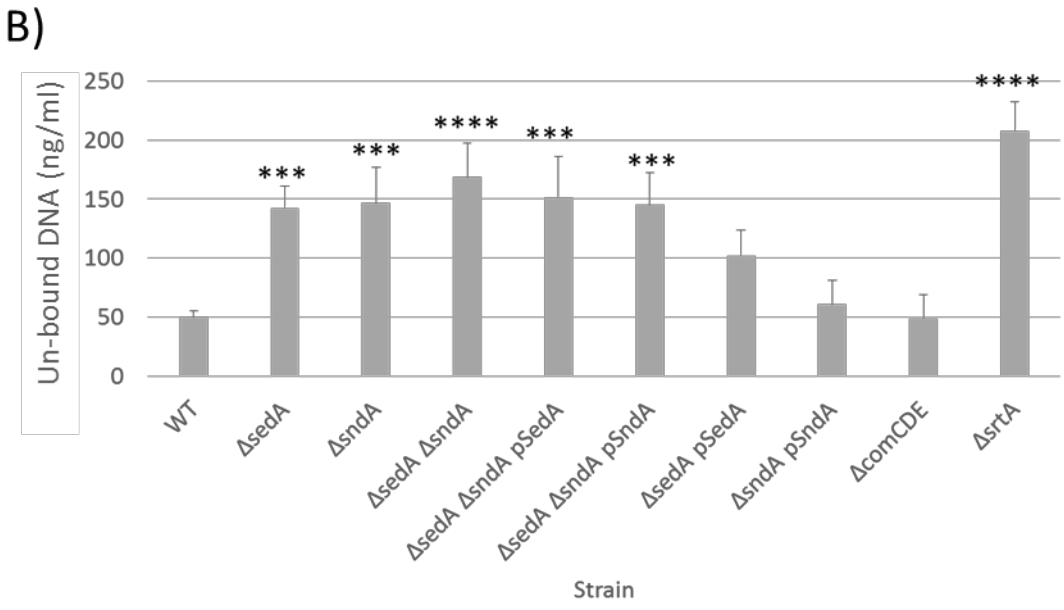

Figure 5.9 – ***Loss of SedA or SndA decreases the amount of DNA produced and bound to cells in planktonic culture.*** *S. gordonii strains WT, ΔsedA, ΔsndA, ΔsedA ΔsndA, ΔsedA ΔsndA pSedA, ΔsedA ΔsndA pSndA, ΔsedA pSedA, ΔsndA pSndA, ΔcomCDE and ΔsrtA were adjusted to OD_{600} = 0.25 in YPTG and incubated at 37 °C for 5 h. A) Bacterial cells (and associated DNA) were pelleted at 8,000 rpm for 3 min, then resuspended in PBS, while B) supernatants were collected into fresh tubes. A Quant-it PicoGreen kit was used to measure levels of dsDNA. Data are displayed as mean DNA concentration ± SD; n=3. Experiments were performed in triplicate. A one-way unpaired ANOVA was used, with α=0.05. * P<0.05, *** P<0.0005, **** P<0.0001.*

Similar studies were then performed under biofilm conditions. In general, these data mirrored those from the planktonic cultures. Mutant biofilms lacking either SedA, SndA or SrtA exhibited less bound DNA than WT *S. gordonii*, but had significantly higher levels of dsDNA within the extracellular milieu (Figure 5.10). The largest difference compared to WT was seen for Δ*srtA* biofilms, which showed a 3.8-fold increase in unbound DNA. This indicates the importance of LPxTG proteins in binding DNA. The Δ*comCDE* mutant had significantly reduced levels of dsDNA within its biofilm but was comparable to WT with regards to dsDNA within the surrounding environment. This implied that, specifically under biofilm conditions, the Δ*comCDE* mutant produced less eDNA than WT *S. gordonii* or that the *comCDE* operon may be behaving differently under biofilm vs planktonic conditions in a way which influences eDNA release.

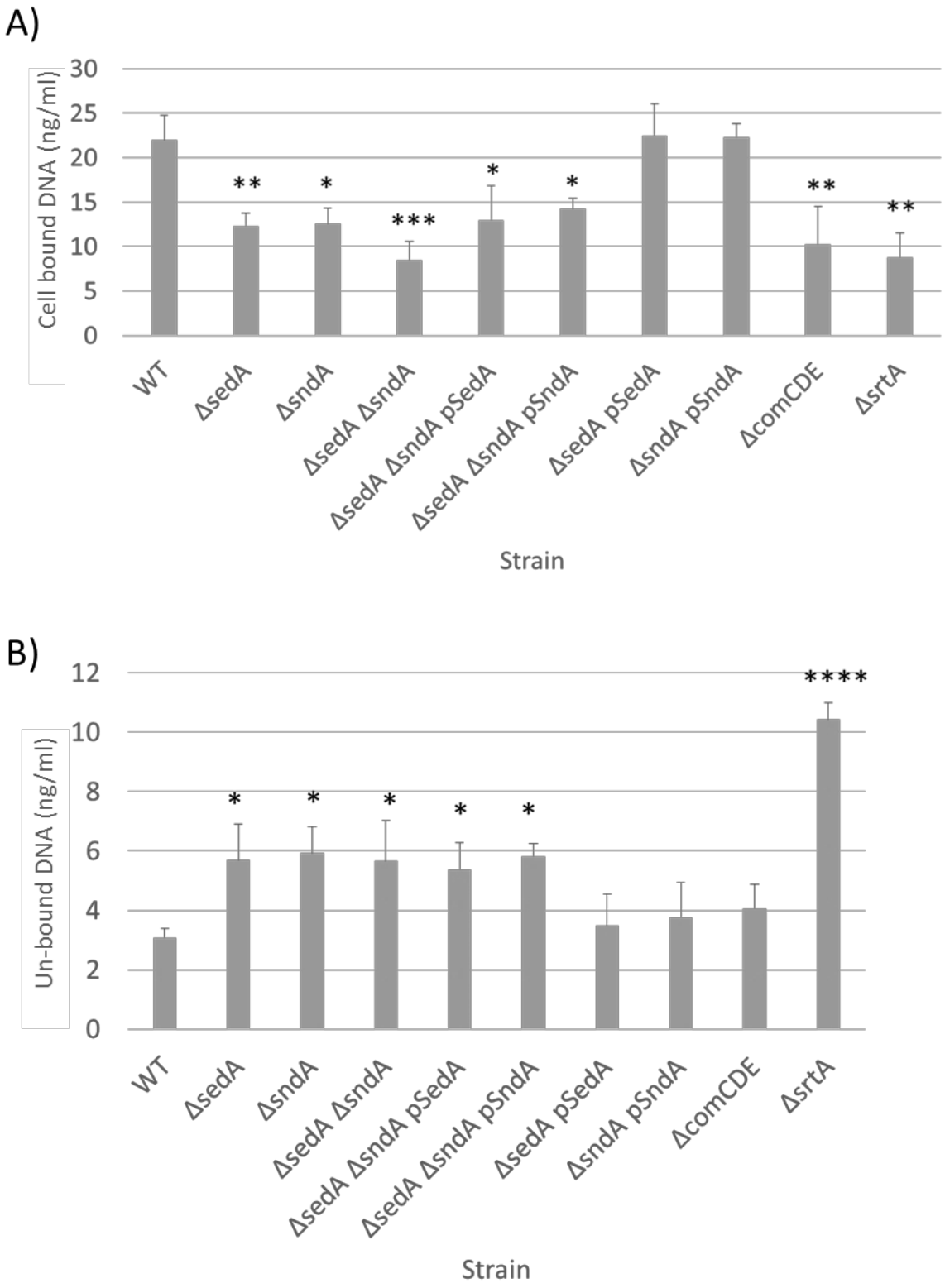

Figure 5.10 – ***Effects of SedA, SndA or ComCDE mutations on levels of dsDNA produced under biofilm conditions.*** *S. gordonii strains WT, ΔsedA, ΔsndA, ΔsedA ΔsndA, ΔsedA ΔsndA pSedA, ΔsedA ΔsndA pSndA, ΔsedA pSedA, ΔsndA pSndA, ΔcomCDE and ΔsrtA were adjusted to OD_{600} = 0.25 in YPTG and incubated at 37 °C for 5 h on saliva-coated glass cover slips. A Quant-it PicoGreen kit was then used to measure levels of*

*dsDNA either A) associated with the biofilm or B) in the extracellular milieu. Data are displayed as mean DNA concentration ± SD; n=3. Experiments were performed in triplicate. A one-way unpaired ANOVA was used, with α=0.05. * P<0.05, ** P<0.005, *** P<0.0005, **** P<0.0001.*

The preceding assays monitored the capacity of the different *S. gordonii* strains to bind gDNA that had been released during growth. To test the full potential of *S. gordonii* and its surface proteins to bind DNA, a final set of studies were performed using exogenous dsDNA. It was hypothesised that this approach may reveal greater phenotypic differences, as the amount of DNA available to bind would no longer be a limiting factor. DNA binding was adjusted for the differing amounts of eDNA produced by each strain. A dsDNA concentration of 1 µg/ml was found to be the saturation point for WT *S. gordonii*, above which no further increases in DNA binding were seen (data not shown).

The loss of either SedA or SndA resulted in a significant reduction in DNA binding capacity of *S. gordonii*, ranging from a 12-fold reduction to ablation (Figure 5.11). DNA binding was comparable to that of WT for strains Δ*sedA* pSedA, Δ*sedA* pSndA and Δ*comCDE*. Taken together, these data provide strong evidence that both SedA and SndA are required to enable *S. gordonii* to bind optimally to exogenous dsDNA, while the reduction of eDNA levels resulting from the *comCDE* mutation appear to be biofilm-specific.

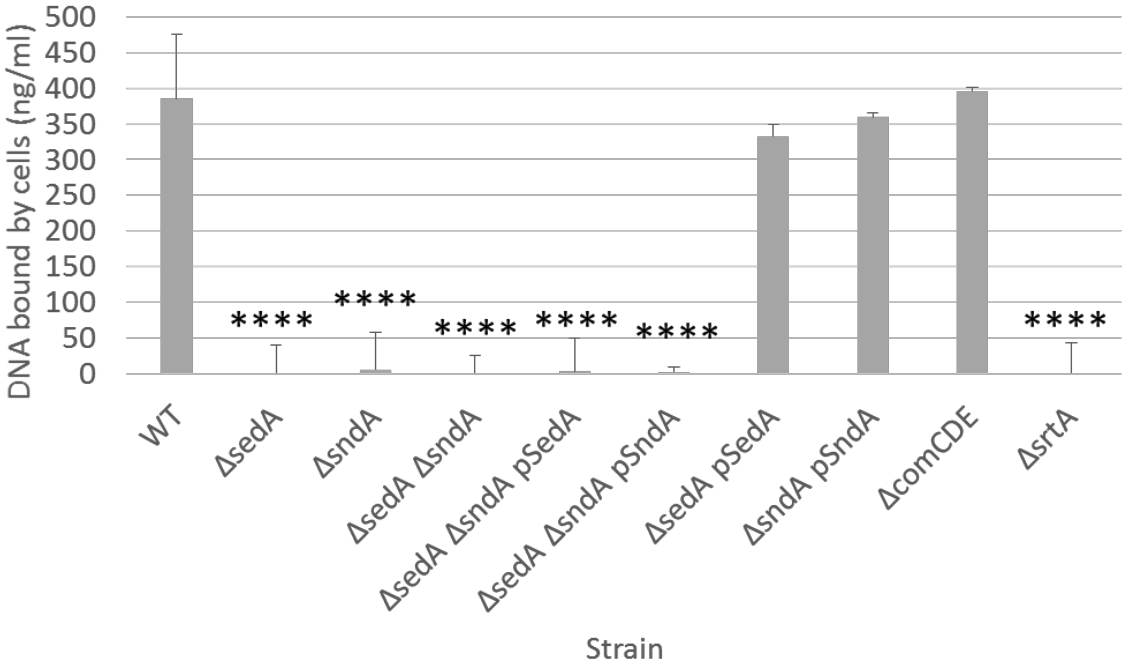

Figure 5.11 – ***Effects of SedA, SndA or ComCDE mutations on planktonic S. gordonii binding to exogenous dsDNA****. S. gordonii strains WT, ΔsedA, ΔsndA, ΔsedA ΔsndA, ΔsedA ΔsndA pSedA, ΔsedA ΔsndA pSndA, ΔsedA pSedA, ΔsndA pSndA, ΔcomCDE and ΔsrtA were adjusted to OD_{600} = 0.25 in YPTG containing 1 µg/ml lambda phage dsDNA and incubated at 37 °C for 5 h. Bacterial cells (and associated DNA) were pelleted at 8,000 g for 3 min, then resuspended in PBS. A Quant-it PicoGreen kit was used to measure levels of bound dsDNA. Data are displayed as mean DNA concentration ± SD; n=3. Experiments were performed in triplicate. A one-way unpaired ANOVA was used, with α=0.05. **** P<0.0001.*

It was clear from the studies above that SedA and SndA could bind directly to dsDNA and that this may relate to their apparent association with eDNA stranding in *S. gordonii* biofilms. However, another process that involves the capacity to bind exogenous DNA is transformation. To determine if SedA or SndA may also be involved in this mechanism, competence assays were performed using the SedA and SndA mutants, and with Δ*srtA* and Δ*comCDE* as control strains. As *S. gordonii* is naturally competent, these assays were performed with or without stimulation from exogenous CSP. In the absence of exogenous CSP, the rate of transformation was found to be reduced by 8-fold relative to WT *S. gordonii* for all strains lacking SndA but not SedA (Figure 5.12). As expected, Δ*srtA* and Δ*comCDE* mutants were also impaired in transformation capacity. Addition of exogenous CSP increased the transformation efficiency of the *S. gordonii* strains overall (with the exception of Δ*comCDE*). However, the

same trend was seen, with all mutants lacking SndA exhibiting a significantly reduced transformation frequency compared to WT. These data imply that SndA is involved in transformation. Whether or not this relates to its capacity to bind dsDNA, its DNase activity, or another function altogether, remains to be determined.

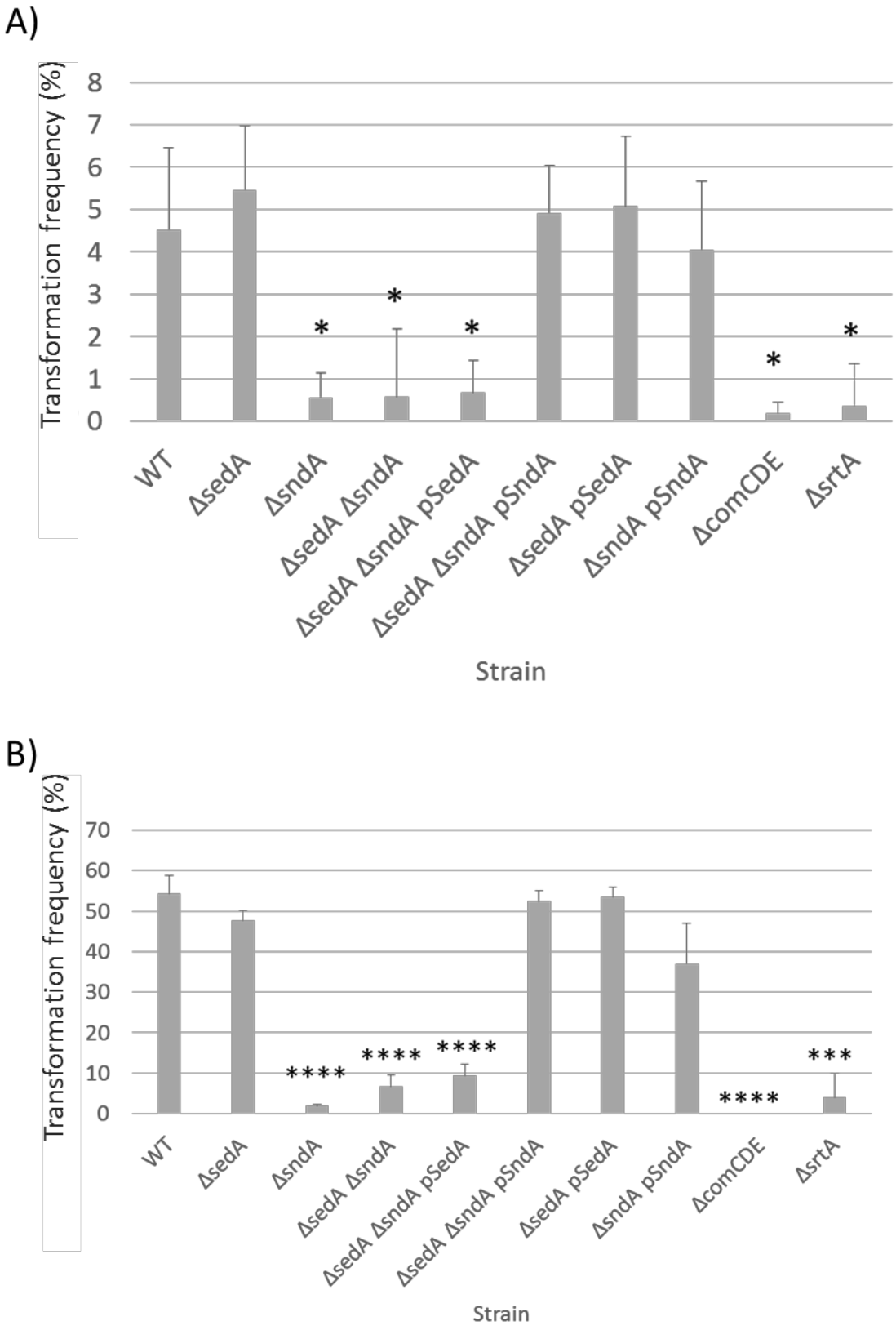

Figure 5.12 – ***Mutants lacking SndA are reduced in transformation capabilities relative to WT****. S. gordonii strains WT, ΔsedA, ΔsndA, ΔsedA ΔsndA, ΔsndA ΔsedA pSedA, ΔsndA ΔsedA pSndA, ΔsedA pSedA, ΔsndA pSndA, ΔcomCDE and ΔsrtA were grown overnight and sub-cultured 1:100 into BHY:FCS:Glc and incubated for 5 h at 37 °C. Cultures were sub-cultured again A) without or B) with 5 µg/ml CSP and incubated for a further 1 h, after which 0 or 1 µg/ml of plasmid DNA was added. Cultures were incubated for a further 3 h, then plated onto selective agar and incubated for 16 h. Colonies were counted, and the transformation*

*frequency calculated. Data are presented as transformation frequency (%) ± SD; n=3. Experiments were performed in triplicate. A one-way unpaired ANOVA was used with α=0.05. * P<0.05, *** P<0.0005, **** P<0.0001 compared to WT.*

5.6 Relationship between the competence pathway and eDNA

5.6.1 Role of CSP

It was clear from studies performed here that the competence (ComCDE) pathway modulated levels of eDNA within *S. gordonii* biofilms, and supported the work of Jack et al. (2015) in implicating CSP in this process. To explore a potential mechanistic basis for this in more detail, *S. gordonii* mutants lacking expression of ComC or ComCDE were used in the eDNA stranding quantification assays, and exposed to exogenous CSP or a scrambled peptide control. ComC is the precursor of CSP and ComDE is the canonical CSP transporter. Thus *S. gordonii* Δ*comC* does not produce CSP but can respond to it, while *S. gordonii* Δ*comCDE* can neither produce nor respond to CSP. Scrambled CSP (sCSP) was used as a control to show that it was specific recognition of CSP that was mediating any effects, rather than a response to addition of any peptide to the biofilm.

Biomass levels were comparable between WT *S. gordonii* and Δ*comC* and Δ*comCDE* mutants, with or without the addition of exogenous CSP or sCSP (Figure 5.13).

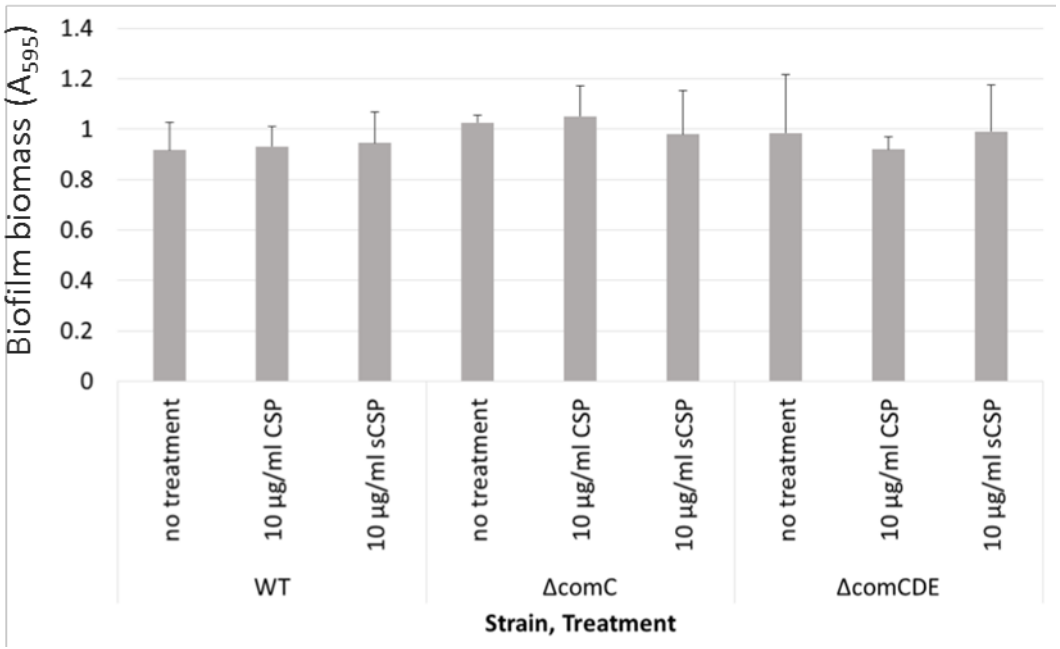

Figure 5.13 - ***Loss of ComC/DE does not affect biofilm biomass relative to WT****. S. gordonii WT, ΔcomC or ΔcomCDE strains were grown at 37 °C in YPTG on saliva-coated glass cover slips for 5 h in the presence of 0 (no treatment) or 10 µg/ml CSP or sCSP. Biofilms were stained with 0.25% crystal violet, the stain released with acetic acid, and the absorbance measured at A_{595}. Data are presented as mean absorbance ± SD; n=3. A one-way unpaired ANOVA was used with α=0.05. No significant difference was found compared to WT.*

In contrast to biomass, which was not altered, ΔcomC biofilms were significantly reduced in eDNA stranding compared to WT biofilms (

Figure 5.14). This reduction was restored to WT levels with supplementation of exogenous CSP, but not sCSP. The same pattern was also seen in ΔcomCDE biofilms, implying that the effects of CSP on eDNA stranding were occurring independently of the canonical ComDE TCSS. Addition of CSP or sCSP to WT biofilms did not cause a significant change in eDNA stranding levels (

Figure 5.14).

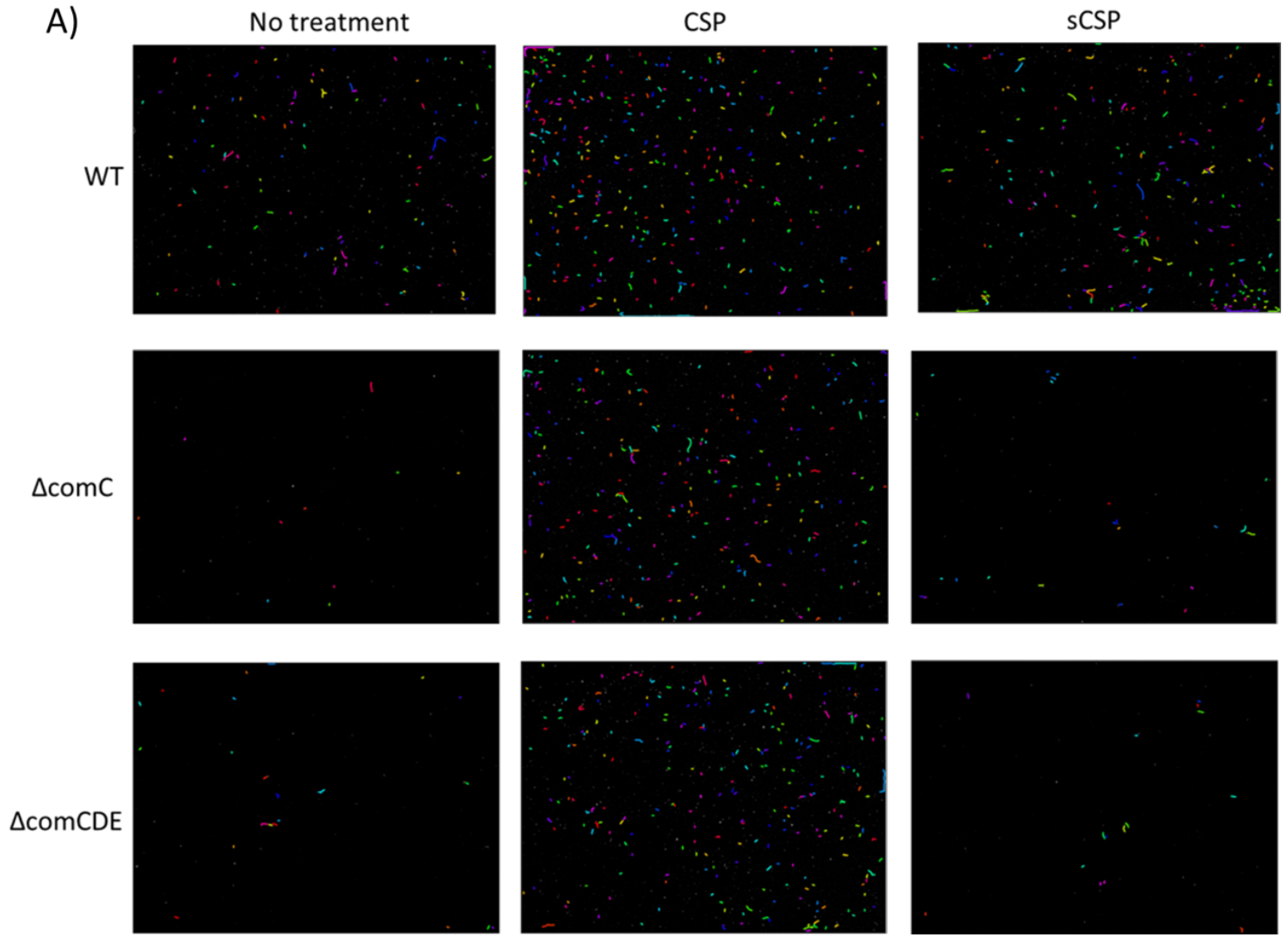
A)
No treatment
CSP
sCSP
WT
ΔcomC
ΔcomCDE

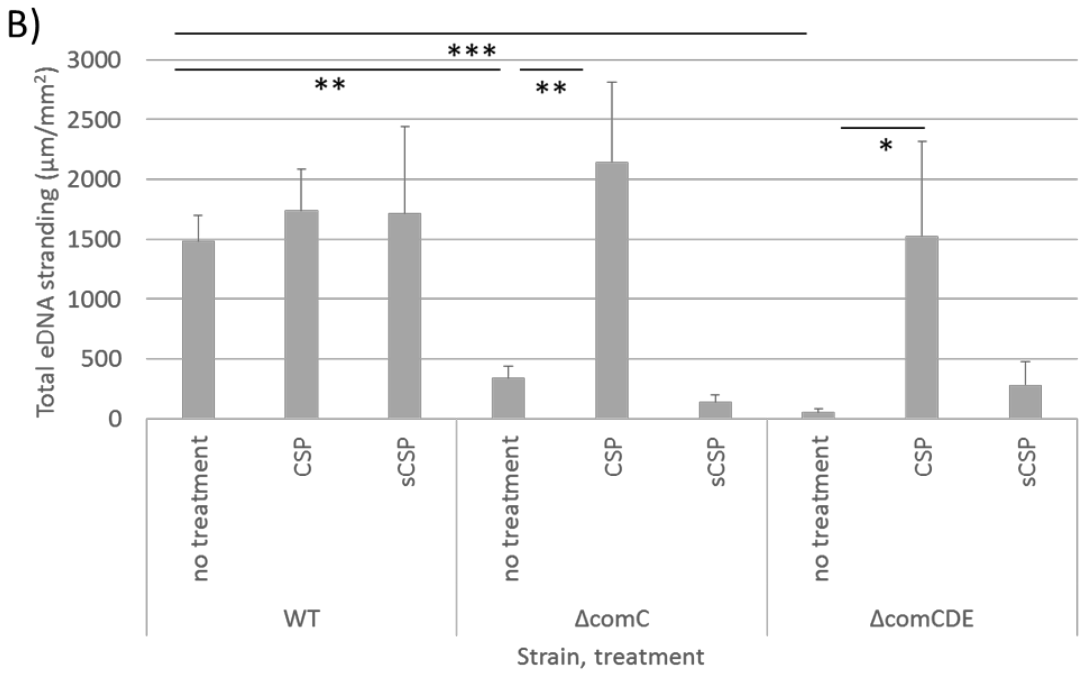

*Figure 5.14 – **CSP affects eDNA stranding in S. gordonii biofilms.** S. gordonii WT, ΔcomC and ΔcomCDE strains were grown at 37 °C in YPTG on saliva-coated glass cover slips for 5 h with 0 (no treatment) or 10 µg/ml CSP or sCSP. Biofilms were stained with TO-PRO3, labelled with a ms anti-ds DNA antibody and a gt anti-ms Ig conjugated to AlexaFluor595, and visualised using widefield microscopy. A) Gallery of images post-ridge finding analysis in MATLAB. Scale bars = 100 µm. B) Quantification of total eDNA stranding. Data are presented as mean total stranding per mm² ± SD; n=3. Experiments were performed in triplicate. A one-way unpaired ANOVA was used with α=0.05. * P<0.05, ** P<0.005, *** P<0.0005.*

It was clear from studies performed here that CSP could modulate levels of eDNA within *S. gordonii* biofilms. To further explore the specificity of the CSP effect on eDNA stranding in *S. gordonii* biofilms, CSPs derived from S. *pneumoniae* and *S. mutans* were also tested. Addition of these CSPs caused no significant differences in biofilm biomass for WT *S. gordonii* or Δ*comC* strain (Figure 5.15).

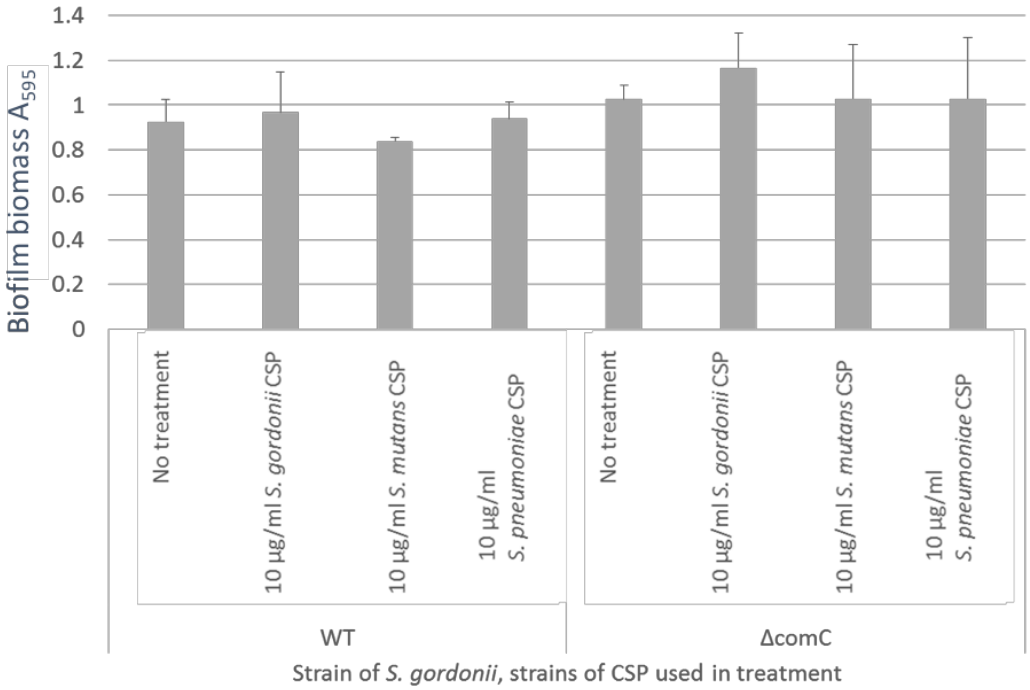

Figure 5.15 - ***CSPs derived from different streptococcal species have no effect on biofilm biomass****. S. gordonii WT or ΔcomC were grown in YPTG with no treatment or 10 µg/ml CSP from either S. gordonii, S. mutans or S. pneumoniae at 37 °C for 5 h on saliva-coated glass-bottomed wells. Biofilms were stained with 0.25% crystal violet, the stain released with acetic acid, and the absorbance measured at A_{595}. Data are presented as mean absorbance ± SD; n=3. Experiments performed in triplicate. A one-way unpaired ANOVA was used with α=0.05. No significant difference was found compared to WT untreated.*

WT *S. gordonii* biofilms did not display altered stranding with addition of CSP derived from any of the streptococcal strains tested. By contrast, the impaired eDNA stranding seen with the Δ*comC* mutant could be restored to WT levels with the addition of *S. gordonii* and *S. pneumoniae* CSP. Addition of *S. mutans* CSP increased eDNA stranding compared to untreated Δ*comC* biofilms but did not restore stranding to WT levels (Figure 5.16).

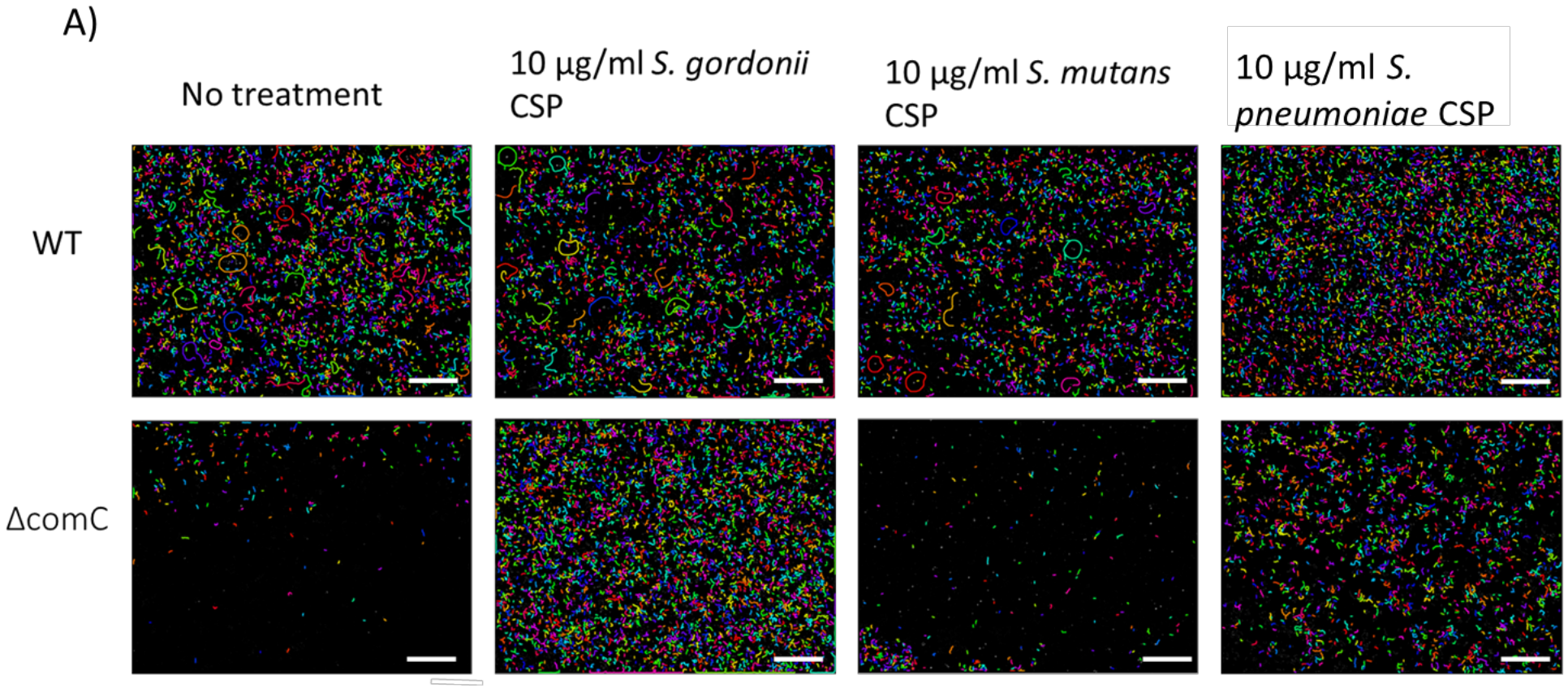
A)
No treatment
10 µg/ml S. gordonii CSP
10 µg/ml S. mutans CSP
10 µg/ml S. pneumoniae CSP
WT
ΔcomC

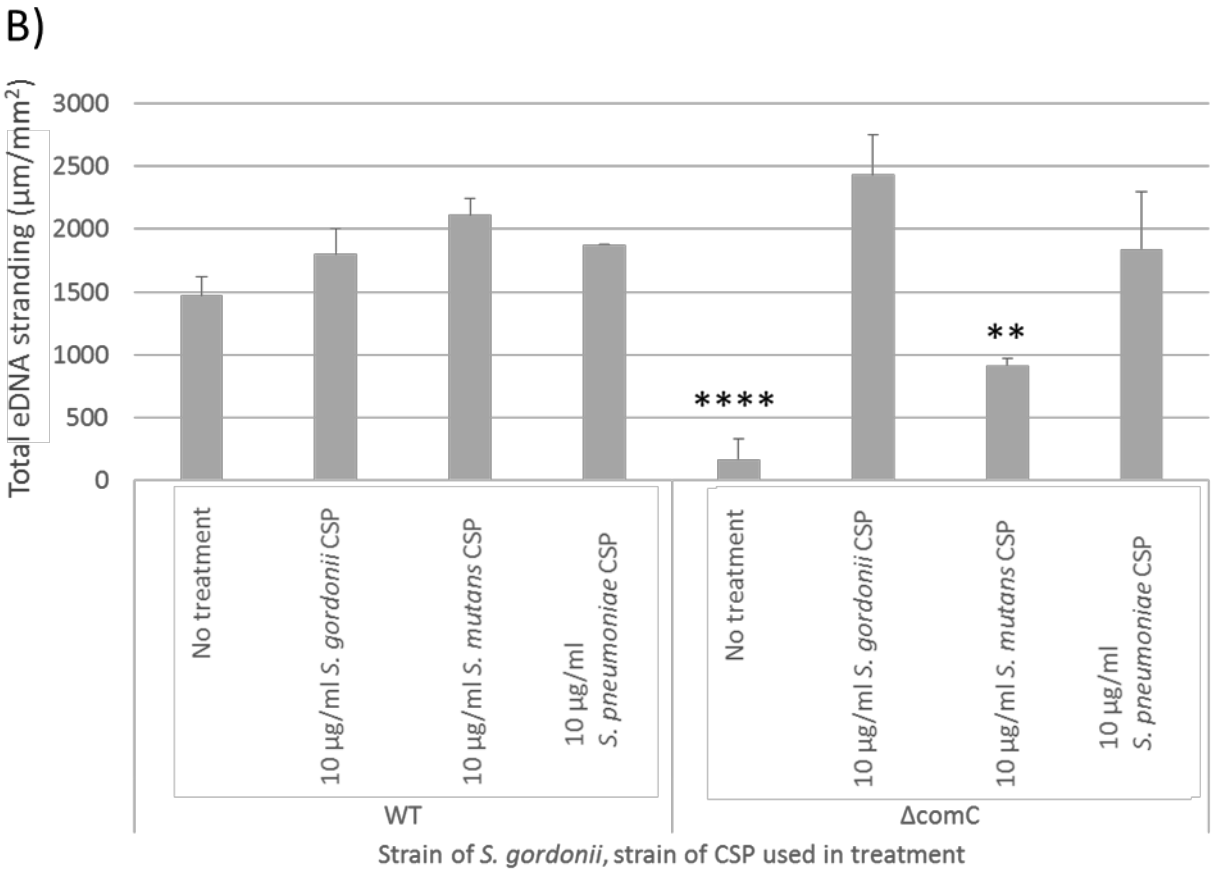

Figure 5.16 – ***S. gordonii and S. pneumoniae CSP can restore eDNA stranding in S. gordonii ΔcomC mutant biofilms****. S. gordonii strains WT and ΔcomC were adjusted to OD_{600} = 0.25 in YPTG supplemented with 10 µg/ml CSP derived from S. gordonii, S. mutans or S. pneumoniae and grown at 37 °C for 5 h on saliva-coated glass-bottomed wells. Biofilms were stained with TO-PRO3, labelled with a ms anti-ds DNA antibody, then a gt anti-Ig antibody conjugated to Alexafluor594, and biofilms were visualised using widefield microscopy. A) Gallery of images post-ridge finding analysis in MATLAB. Scale bars = 100 µm. B) Quantification of total eDNA stranding. Data are presented as mean total eDNA stranding per mm^2 ± SD; n=3. A one-way unpaired ANOVA was used with α=0.05. ** P<0.005, **** P<0.0001, compared to WT no treatment.*

Investigations into the effects of *S. gordonii* CSP on eDNA stranding continued by testing a wider range of CSP concentrations, to establish if CSP affected stranding in a dose-dependent manner. CSP concentrations used (1-50 µg/ml) represented a range of concentrations around that used to induce competence in *S. gordonii* (5 µg/ml). No significant differences in biofilm biomass were seen between WT *S. gordonii* and the Δ*comC* mutant across the CSP concentration range 1-10 µg/ml. However, the highest CSP concentration tested, 50 µg/ml, caused an 8-fold reduction in biomass compared to untreated biofilms for both WT and Δ*comC* strains (Figure 5.17).

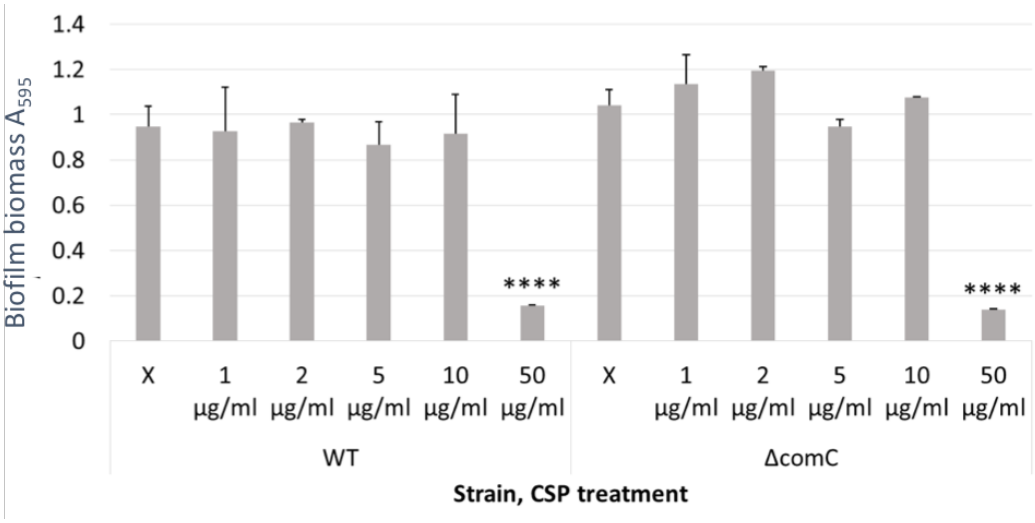

Figure 5.17 – ***Dose-dependent effects of CSP on S. gordonii biofilm biomass****. S. gordonii strains WT and ΔcomC were grown in YPTG with 0, 1, 2, 5, 10 or 50 µg/ml CSP at 37 °C for 5 h on saliva-coated glass-bottomed wells. Biofilms were stained with 0.25% crystal violet, the stain released with acetic acid, and the absorbance measured at A_{595}. Data are presented as mean absorbance ± SD; n=3. Experiments performed in triplicate. A one-way unpaired ANOVA was used with α=0.05. **** P<0.0001.*

The same parameters were then used to test the effects of CSP on eDNA stranding. Addition of CSP did not alter eDNA stranding in WT biofilms, except for the highest concentration, which caused a reduction in stranding (Figure 5.18). The reduction in stranding was proportional to the loss of biomass seen at this same concentration of CSP. As seen before, biofilms lacking ComC had significantly less eDNA stranding than WT, despite having comparable biomass. Supplementation of CSP at levels equal to or above 2 µg/ml restored eDNA stranding to WT levels. Regression analysis was used to determine the effect of CSP supplementation on eDNA stranding was dose dependent (P<0.005; Figure 5.19). Similar to the effects seen in WT, eDNA stranding was low in Δ*comC* biofilms supplemented with 50 µg/ml CSP, in line with the reduction in biomass due to the apparent toxicity of excess CSP.

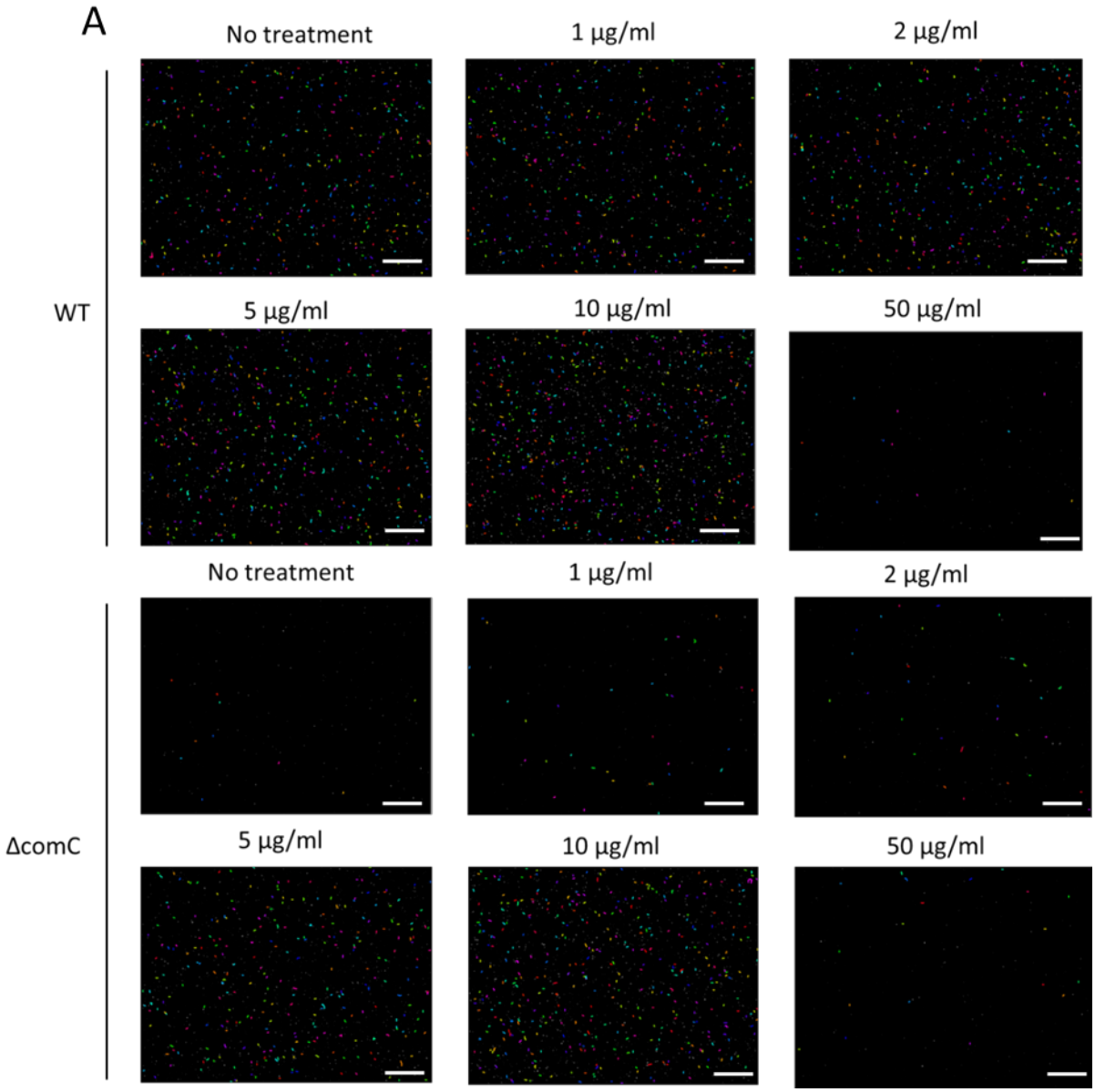
A
No treatment
1 µg/ml
2 µg/ml
WT
5 µg/ml
10 µg/ml
50 µg/ml
No treatment
1 µg/ml
2 µg/ml
ΔcomC
5 µg/ml
10 µg/ml
50 µg/ml

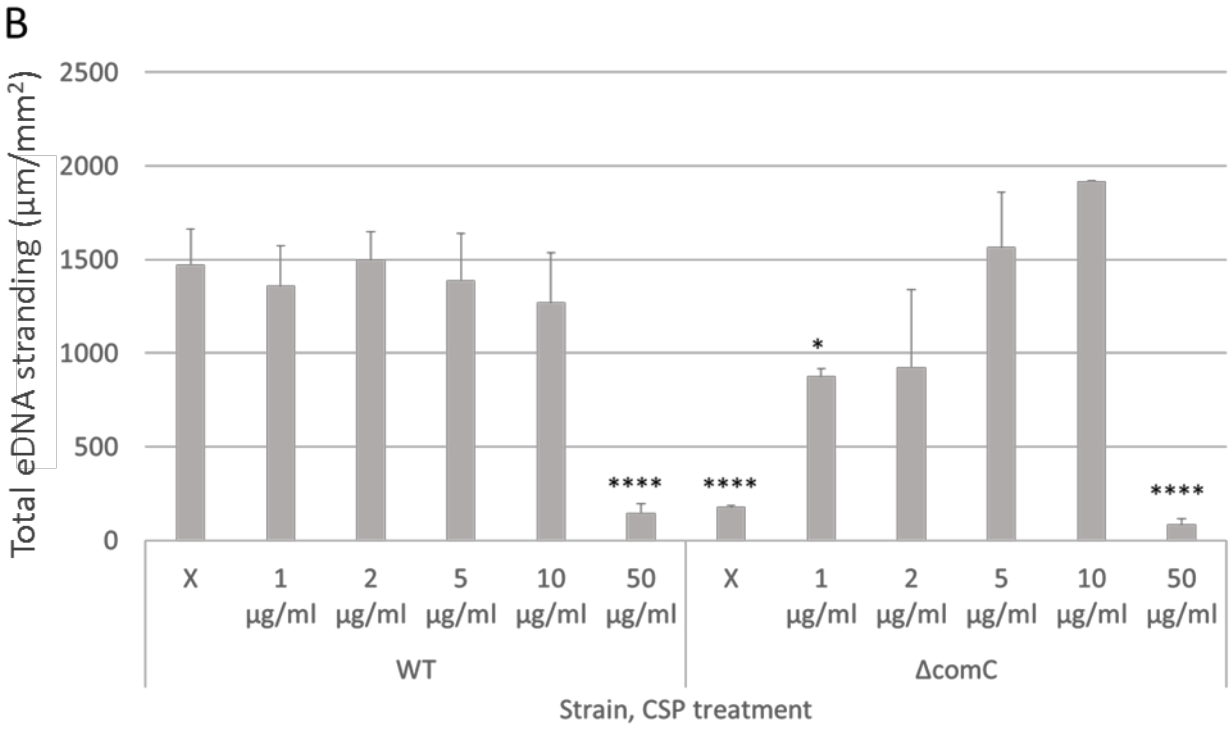

*Figure 5.18 – **Dose-dependent effects of S. gordonii CSP on eDNA stranding**. S. gordonii strains WT and ΔcomC were adjusted to OD_{600} = 0.25 in YPTG supplemented with 0, 1, 2, 5, 10 or 50 µg/ml CSP, and incubated at 37 °C for 5 h on saliva-coated glass-bottomed wells. Biofilms were stained with TO-PRO3, labelled with a ms anti-ds DNA antibody, then gt anti-ms Ig antibody conjugated to AlexaFluor 594 and visualised using widefield microscopy. A) Gallery of images post- ridge finding analysis in MATLAB. Scale bars = 100 µm. B) Quantification of total eDNA stranding. Data are presented as mean total eDNA stranding per mm² ± SD; n=3. Experiments were performed in triplicate. A one-way unpaired ANOVA was used with α=0.05. * P<0.05, **** P<0.0001.*

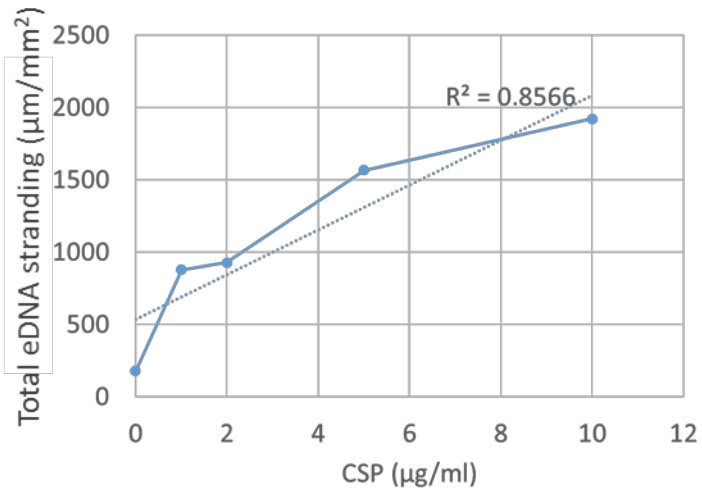

*Figure 5.19 - **Regression analysis of CSP vs. total eDNA stranding in ΔcomC strains.***

5.6.2 Mechanism of CSP detection

The capacity for *S. gordonii* CSP to induce eDNA stranding was clear, but as CSP also mediated its effects in the absence of canonical TCSS ComDE, its mode of detection was unknown. One potential alternative system was the Hpp (Hexa-heptapeptide permease) system in *S. gordonii*. Hpp is an Opp transporter system. Such systems function as oligopeptide permeases (Doeven *et al.*, 2005) and, of particular relevance to this project, the Hpp system of *S. gordonii* had previously been associated with competence development. Mutants lacking a functional Hpp system had been found to be reduced in transformation efficacy (Jenkinson *et al.*, 1996). To investigate if the Hpp system of *S. gordonii* was linked to the CSP effects on eDNA stranding, three mutant strains were generated: Δ*hppA*, Δ*comC* Δ*hppA* and Δ*hppA* Δ*comCDE*.

Investigations began by testing the effects of CSP on eDNA stranding in the HppA mutant biofilms. As shown in Figure 5.20, deletion of HppA had no effect on biofilm biomass relative to WT *S. gordonii*, and this was not affected by addition of exogenous CSP.

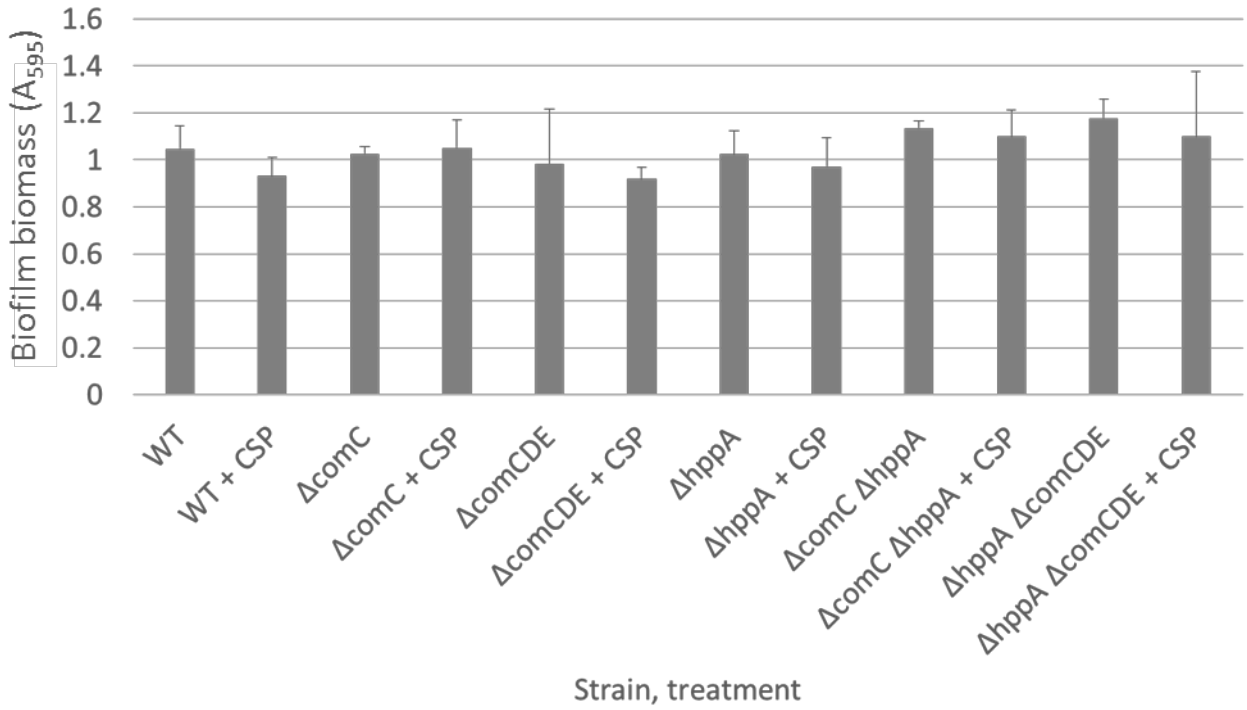

Figure 5.20 - ***Deletion of hppA does not affect biofilm biomass.*** *S. gordonii strains WT, ΔcomC, ΔcomCDE, ΔhppA, ΔcomC ΔhppA and ΔhppA ΔcomCDE were grown in YPTG with no treatment or 10 µg/ml CSP at 37 °C for 5 h on saliva-coated glass-bottomed wells. Biofilms were stained with 0.25% crystal violet, the stain released with acetic acid, and the absorbance measured at A_{595}. Data are presented as mean absorbance ± SD; n=3. Experiments performed in triplicate. A one-way unpaired ANOVA was used with α=0.05. No significant difference was found compared to WT untreated biofilms.*

In contrast to the lack of effect on biomass, Δ*hppA* mutant biofilms exhibited 50% less eDNA stranding than WT biofilms, similar to the Δ*comC* and Δ*comCDE* mutant biofilms (Figure 5.21). However, while exogenous CSP restored eDNA stranding to WT levels for Δ*comC* and Δ*comCDE* mutant biofilms, CSP had no effect on mutants lacking *hppA*. These data implied that it may be the Hpp system that is responsible for detection of CSP and its subsequent effects on eDNA stranding.

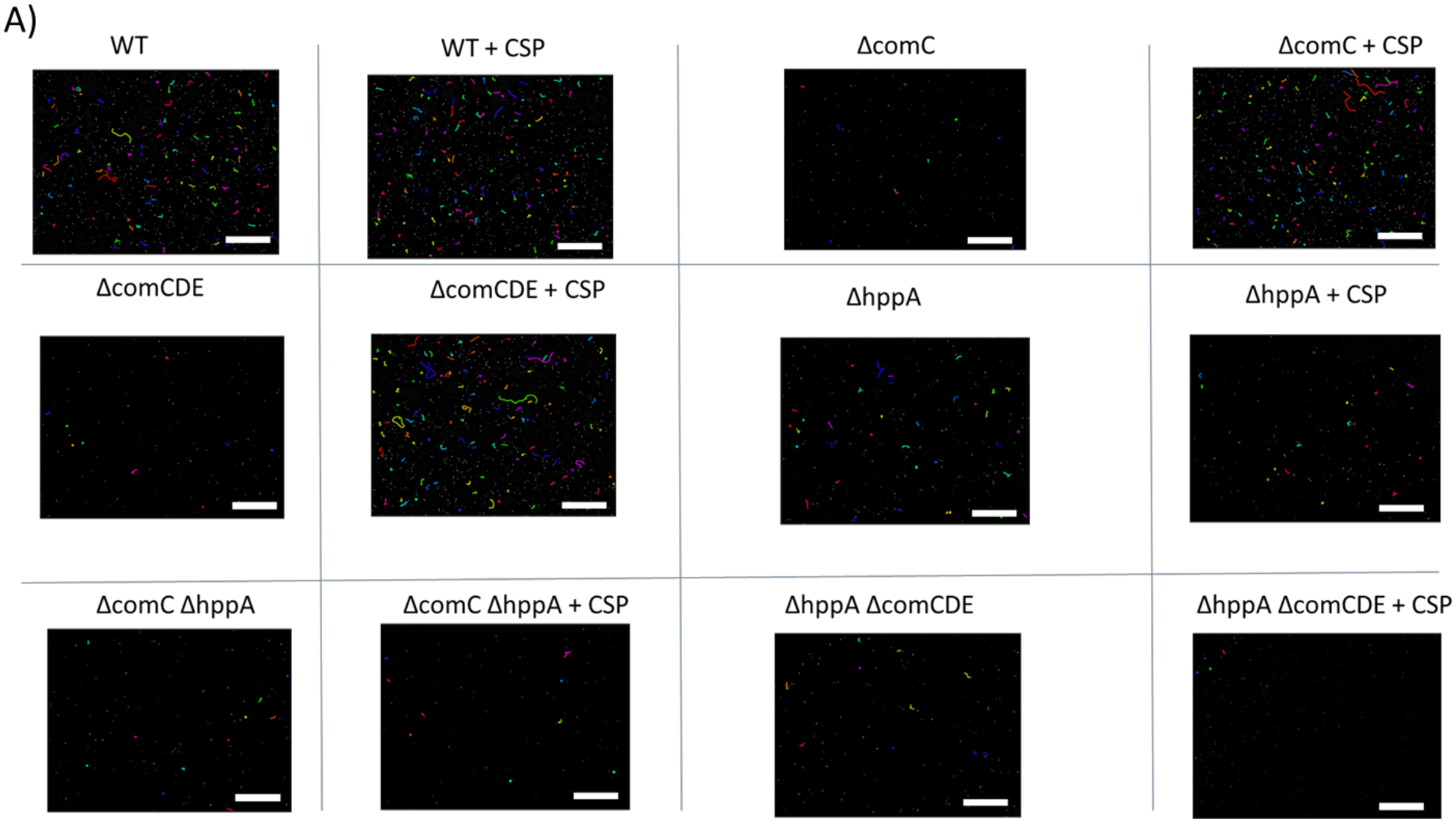
A)
WT
WT + CSP
ΔcomC
ΔcomC + CSP
ΔcomCDE
ΔcomCDE + CSP
ΔhppA
ΔhppA + CSP
ΔcomC ΔhppA
ΔcomC ΔhppA + CSP
ΔhppA ΔcomCDE
ΔhppA ΔcomCDE + CSP

B)

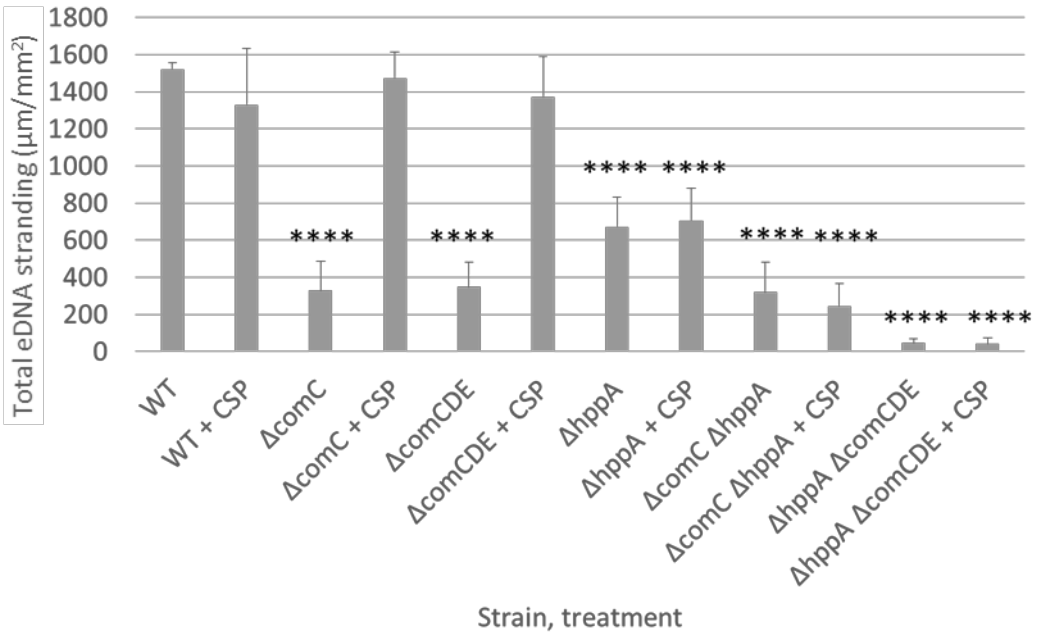

Figure 5.21 – ***Loss of HppA prevents restoration of stranding in ΔcomC mutants by CSP.*** *S. gordonii strains WT, ΔcomC, ΔcomCDE, ΔhppA, ΔcomC ΔhppA and ΔhppA ΔcomCDE were grown in YPTG with no treatment or 10 µg/ml CSP and incubated at 37 °C for 5 h on saliva-coated glass-bottomed wells. Biofilms were stained with TO-PRO3, labelled with a ms anti-ds DNA antibody then a gt anti-ms Ig antibody conjugated to Alex594, and visualised using widefield microscopy. A) Gallery of images post-ridge finding analysis in MATLAB. Scale bars = 100 µm. B) Quantification of total eDNA stranding. Data are presented as mean total eDNA stranding per mm² ± SD; n=3. Experiments were performed in triplicate. A one-way unpaired ANOVA was used with α=0.05. **** P<0.0001, compared to WT no treatment.*

5.6.3 Effects on cell lysis

A final area of investigation was how the effects of CSP on eDNA stranding may be related to induction of cell lysis. This was tested using an ATP determination assay. Extracellular ATP concentrations were reduced by 85-95% for the Δ*comC*, Δ*comCDE* and Δ*hppA* mutants relative to WT *S. gordonii* (Figure 5.22). This implies that reduced eDNA stranding in these mutants may result from a lower level of cell lysis within the biofilm populations. Addition of CSP to WT biofilms had no significant effect on extracellular ATP concentration. No effect of CSP was seen with the Δ*comCDE* and Δ*hppA* mutants either. However, ATP levels from the Δ*comC* biofilms were restored to WT with the addition of exogenous CSP. Taken together, these data implied that, across a certain

concentration range, CSP can induce cell lysis, but that both ComDE and HppA may be involved in its detection to mediate these effects. However, the enhanced eDNA stranding seen with the Δ*comCDE* mutant in the presence of exogenous CSP does not seem to result from a significant increase in cell lysis.

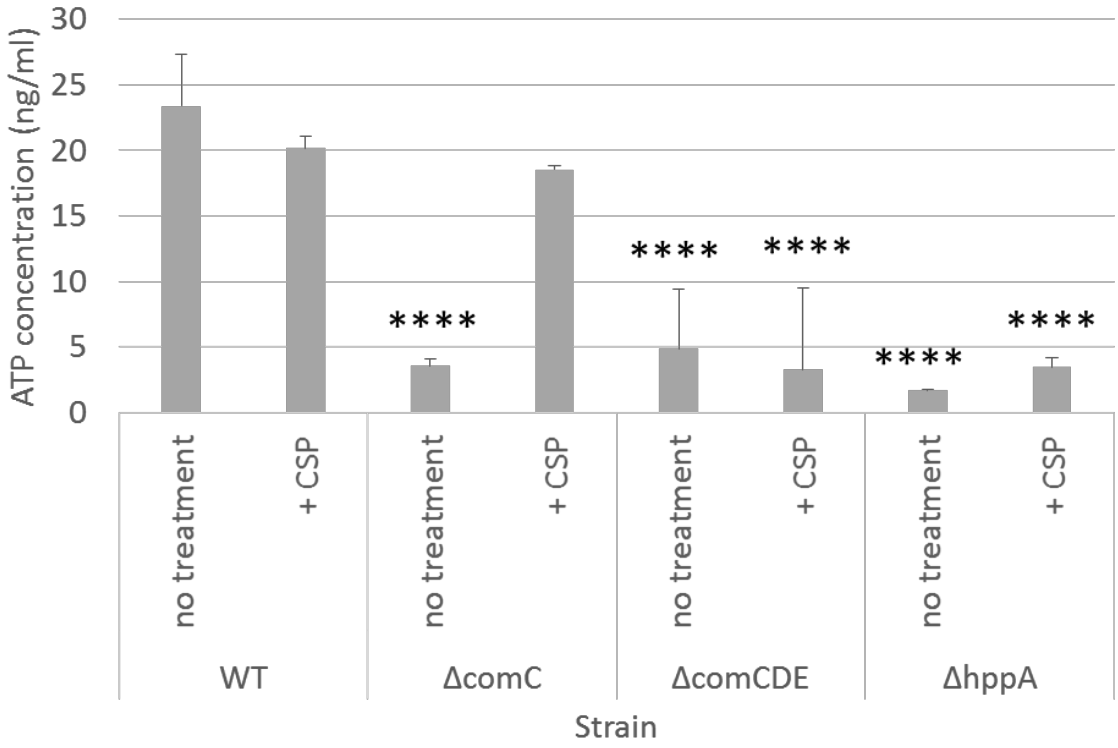

Figure 5.22 – ***CSP and receptors for CSP affects cell lysis over a defined concentration range.*** *S. gordonii strains WT, ΔcomC, ΔcomCDE and ΔhppA were grown in YPTG supplemented with 0 or 10 μg/ml CSP and incubated at 37 °C for 5 h on saliva-coated glass-bottomed wells. Biofilm supernatant was removed and used to calculate levels of ATP, using an ATP determination assay (Invitrogen) in which luminescence units were converted into ATP concentration. Data are displayed as mean ATP concentration (ng/ml) ± SD; n=3. Experiments were performed in triplicate. A one-way ANOVA was used with α=0.05. **** P<0.0001, compared to WT untreated.*

5.7 Role of H_2O_2 in eDNA stranding

It had previously been shown that H_2O_2 can induce eDNA release by *S. gordonii* (Itzek *et al*., 2011), but its effect on eDNA stranding and role in eDNA release was unknown. It was hypothesised that reactive oxygen species (ROS) may be influencing cell lysis and consequently eDNA stranding in *S. gordonii.*

Superoxide dismutase treatment was first used to investigate this, because it neutralises a wide array of ROS. A concentration of 10 µg/ml was chosen for treatment. This was 10-fold higher than that used for catalase by (Kreth et al., 2008), with the view to exceeding the reducing power needed (without knowing the activity units of this enzyme). Superoxide dismutase treatment did not affect *S. gordonii* biofilm biomass (Figure 5.23), but 10 µg/ml superoxide dismutase caused a 5-fold reduction in total eDNA stranding compared to WT (Figure 5.24), implicating ROS in eDNA stranding.

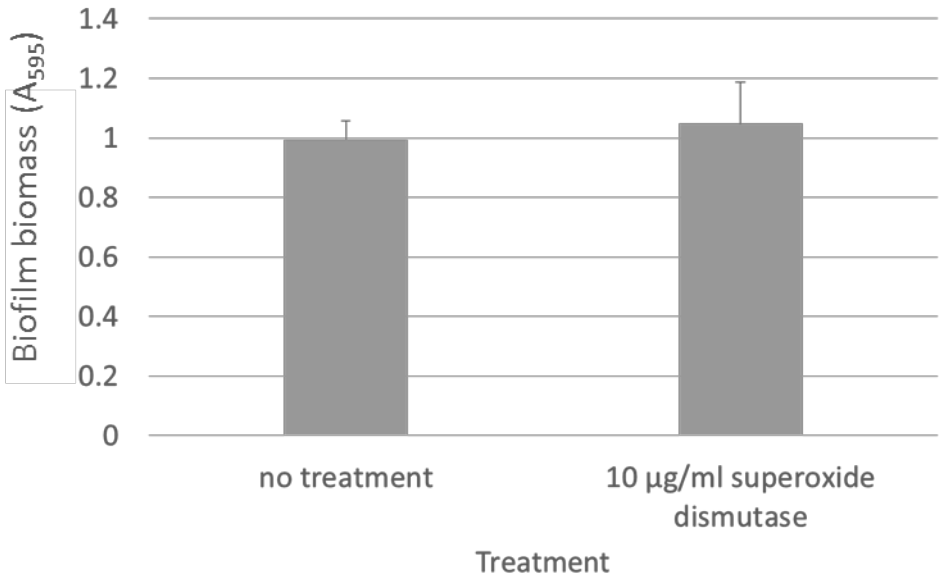

Figure 5.23 – ***Superoxide dismutase treatment does not affect biofilm biomass****. S. gordonii WT biofilms were grown in YPTG with 0 or 10 µg/ml superoxide dismutase at 37 °C for 5 h on saliva-coated glass-bottomed wells. Biofilms were stained with 0.25% crystal violet, the stain released with acetic acid, and the absorbance measured at A_{595}. Data are presented as mean absorbance ± SD; n=3. Experiments performed in triplicate. A one-way unpaired ANOVA was used with α=0.05. No significant difference was found compared to no treatment.*

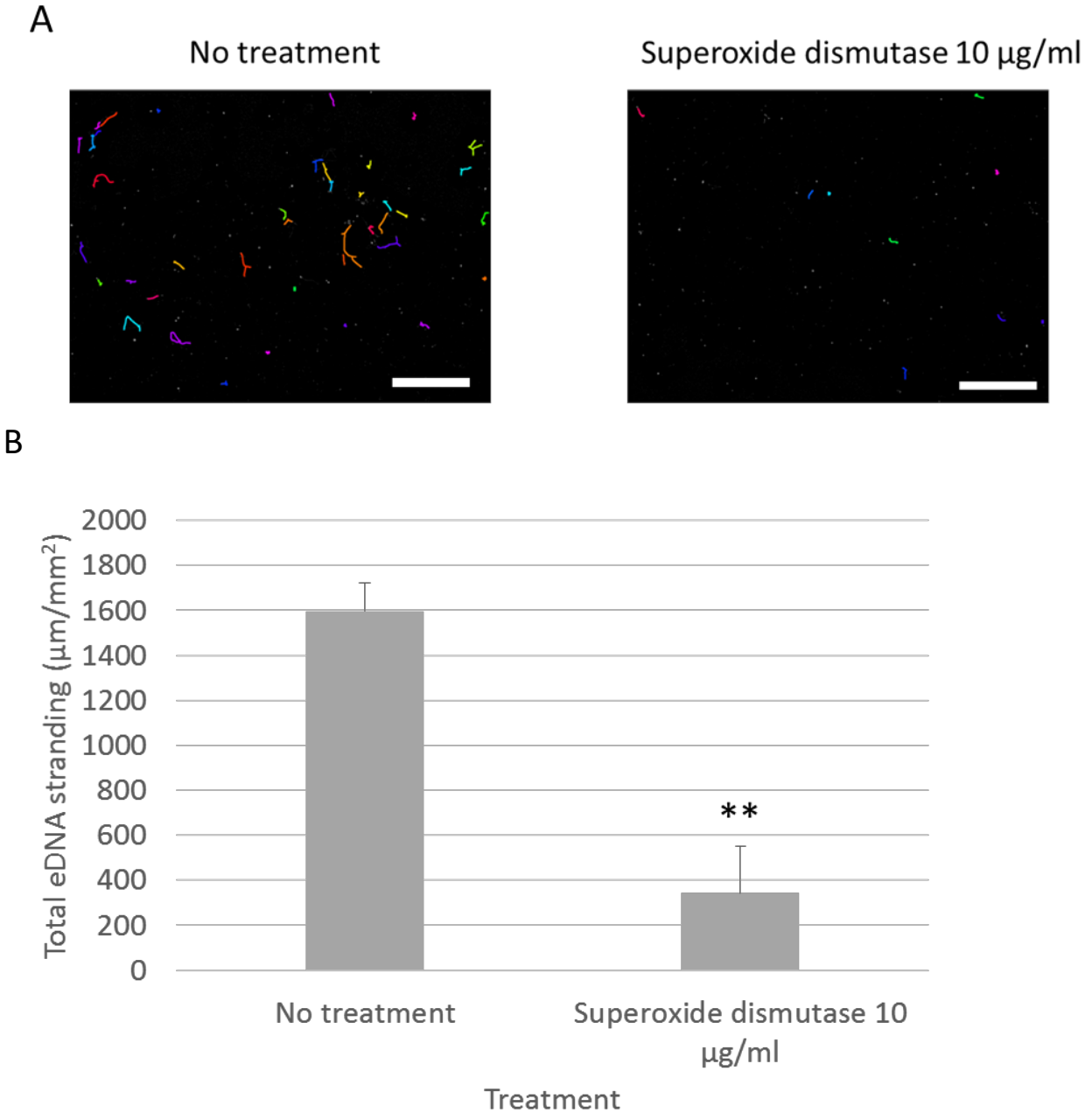

*Figure 5.24 - **Superoxide dismutase treatment significantly reduces eDNA stranding**. S. gordonii was adjusted to OD_{600} = 0.25 in YPTG supplemented with 0 or 10 µg/ml superoxide dismutase and incubated at 37 °C for 5 h on saliva-coated glass-bottomed wells. Biofilms were stained with TO-PRO3, labelled with a ms anti-ds DNA antibody, followed by a gt anti-ms Ig antibody conjugated to Alexafluor 594, and visualised using widefield microscopy. A) Gallery of images post-ridge finding analysis in MATLAB. Scale bars = 100 µm. B) Quantification of total eDNA stranding. Data are presented as mean total eDNA stranding per mm^2 ± SD; n=3. Experiments were performed in triplicate. A one-way unpaired ANOVA was used with α=0.05. ** P<0.005, compared to no treatment.*

To determine if the ROS that were affecting eDNA stranding included H_2O_2, biofilms were treated with catalase, which neutralises H_2O_2. A range of

catalase concentrations were used, based on that used for superoxide dismutase, to investigate whether any effects on eDNA stranding were dose-dependent. Catalase treatment did not affect biofilm biomass (Figure 5.25).

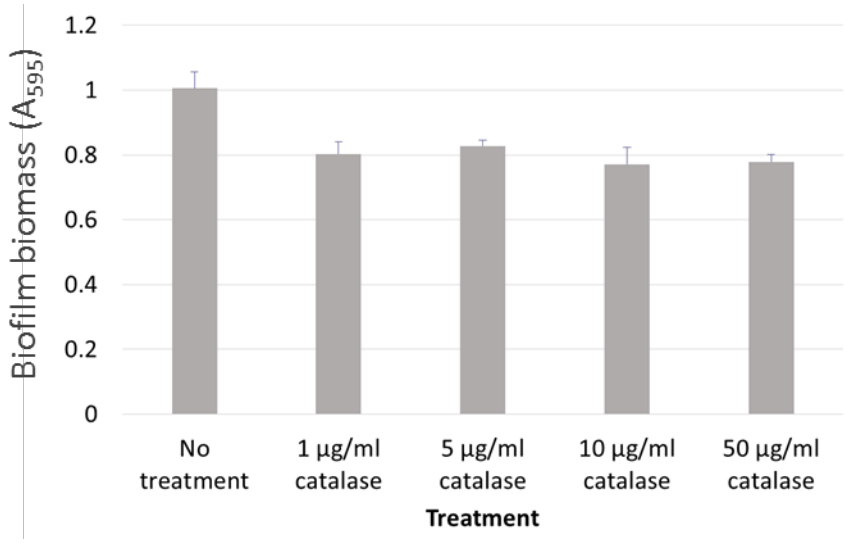

Figure 5.25 - ***Catalase treatment does not affect biofilm biomass.*** *S. gordonii WT biofilms were grown in YPTG with 0, 1, 5, 10 or 50 µg/ml catalase at 37 °C for 5 h on saliva-coated glass-bottomed wells. Biofilms were stained with 0.25% crystal violet, the stain released with acetic acid, and the absorbance measured at A_{595}. Data are presented as mean absorbance ± SD; n=3. Experiments performed in triplicate. A one-way unpaired ANOVA was used with α=0.05. No significant difference was found compared to no treatment.*

By contrast, 50 µg/ml catalase treatment reduced total eDNA stranding by 50% compared to WT (Figure 5.26). This implied that H_2O_2 can induce eDNA stranding, although it may not be the reactive oxygen species involved.

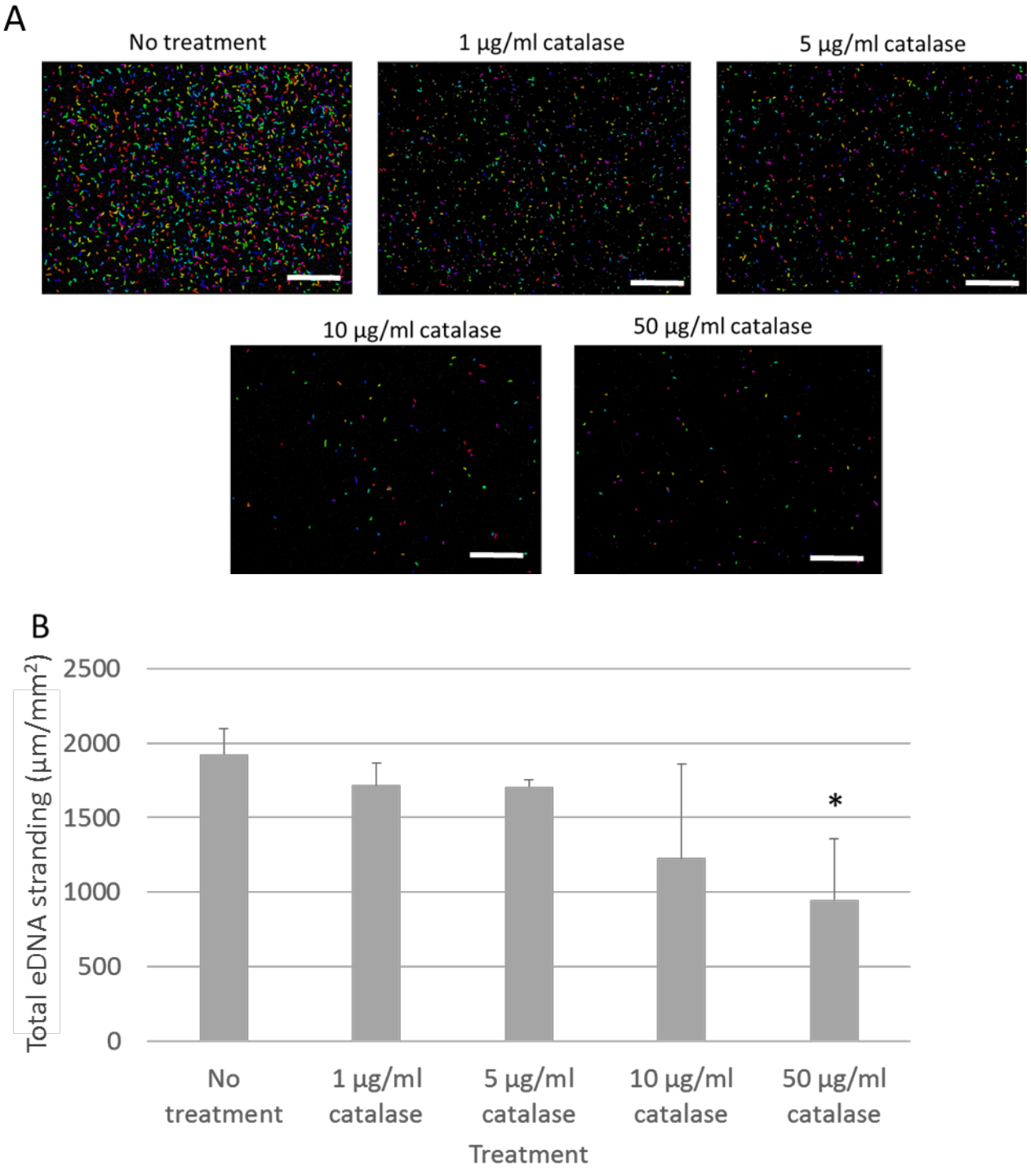

*Figure 5.26 - **Catalase treatment reduces eDNA stranding.** S. gordonii was adjusted to OD_{600} = 0.25 in YPTG supplemented with 0, 1, 5, 10 or 50 µg/ml catalase and incubated at 37 °C for 5 h on saliva-coated glass-bottomed wells. Biofilms were stained with TO-PRO3, labelled with an anti-ds DNA antibody and visualised using widefield microscopy. A) Gallery of images post-ridge finding analysis in MATLAB. Scale bars = 100 µm. B) Quantification of total eDNA stranding. Data are presented as mean total eDNA stranding per mm^2 ± SD; n=3. Experiments were performed in triplicate. A one-way unpaired ANOVA was used with α=0.05. * P<0.05, compared to no treatment.*

H_2O_2 influences eDNA release in *S. gordonii* via a mechanism that is linked with the competence pathway (Xu & Kreth, 2013). Having shown in this work that both H_2O_2 and CSP modulate eDNA stranding, the effects of simultaneous catalase addition and CSP supplementation on eDNA stranding were tested using WT and Δ*comC S. gordonii* strains, to investigate if these components and their effects on eDNA stranding may be interlinked. No effects on biofilm biomass were seen when catalase and CSP treatments were used together (Figure 5.27).

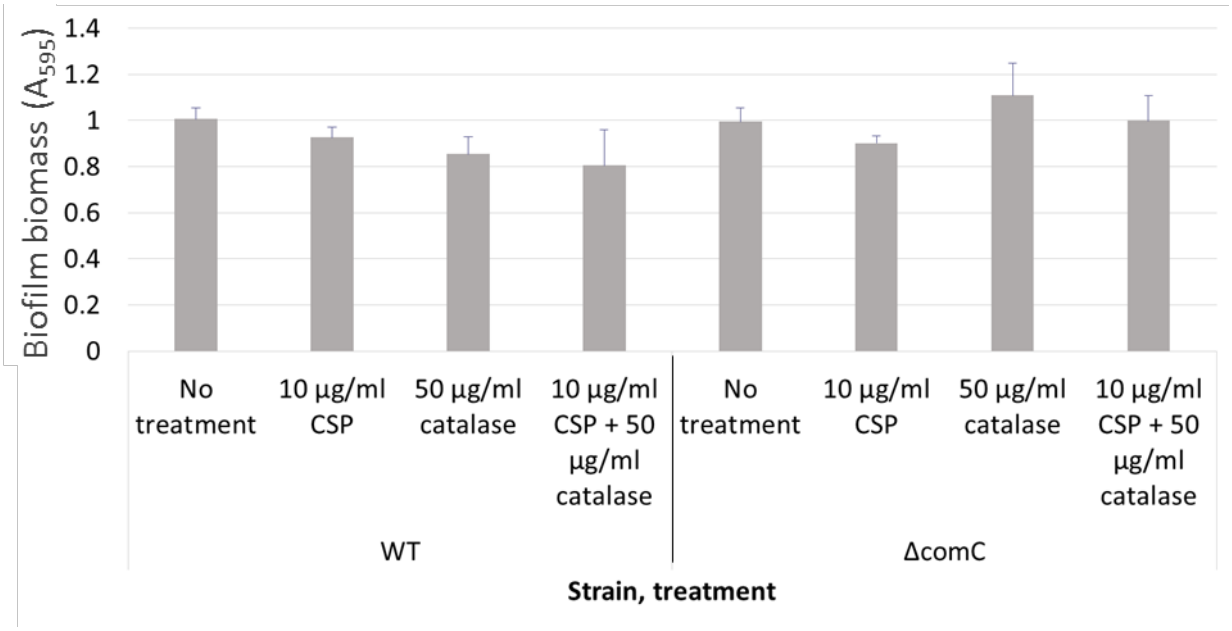

Figure 5.27 – ***Combined CSP and catalase treatments do not affect biofilm biomass.*** *S. gordonii WT and ΔcomC biofilms were grown in YPTG with no treatment, 10 µg/ml CSP, 50 µg/ml catalase or both at 37 °C for 5 h on saliva-coated glass-bottomed wells. Biofilms were stained with 0.25% crystal violet, the stain released with acetic acid, and the absorbance measured at A_{595}. Data are presented as mean absorbance ± SD; n=3. Experiments performed in triplicate. A one-way unpaired ANOVA was used with α=0.05. No significant difference was found compared to no treatment.*

As seen before, catalase treatment of WT *S. gordonii* reduced eDNA stranding by 60%, but this effect was reversed by the addition of CSP (Figure 5.28). Addition of catalase to Δ*comC* biofilms significantly reduced levels of eDNA stranding relative to the untreated control. However, once again this could be overcome by addition of CSP, which promoted levels of eDNA stranding to those seen with CSP treatment alone. Taken together, these data suggested that CSP mediates its effects via an independent, more dominant pathway to that of H_2O_2,

or that CSP targets downstream of H_2O_2 in a pathway that modulates eDNA stranding.

A)

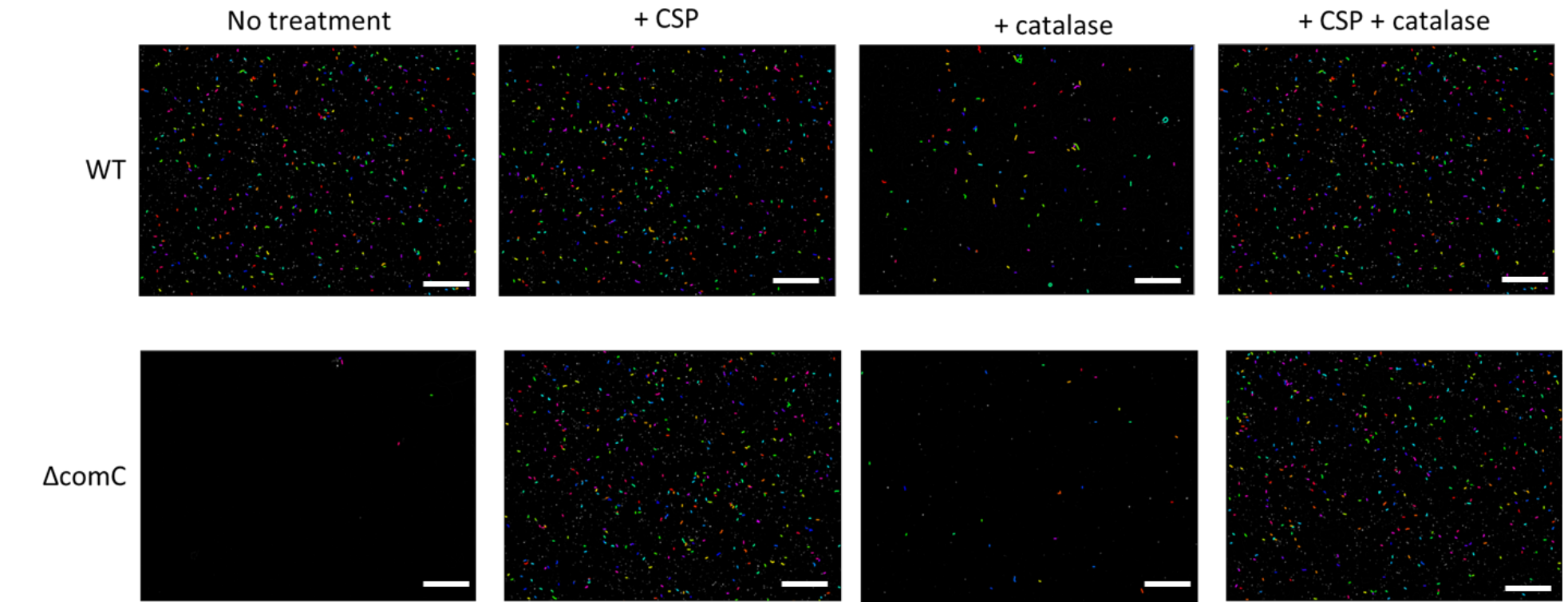

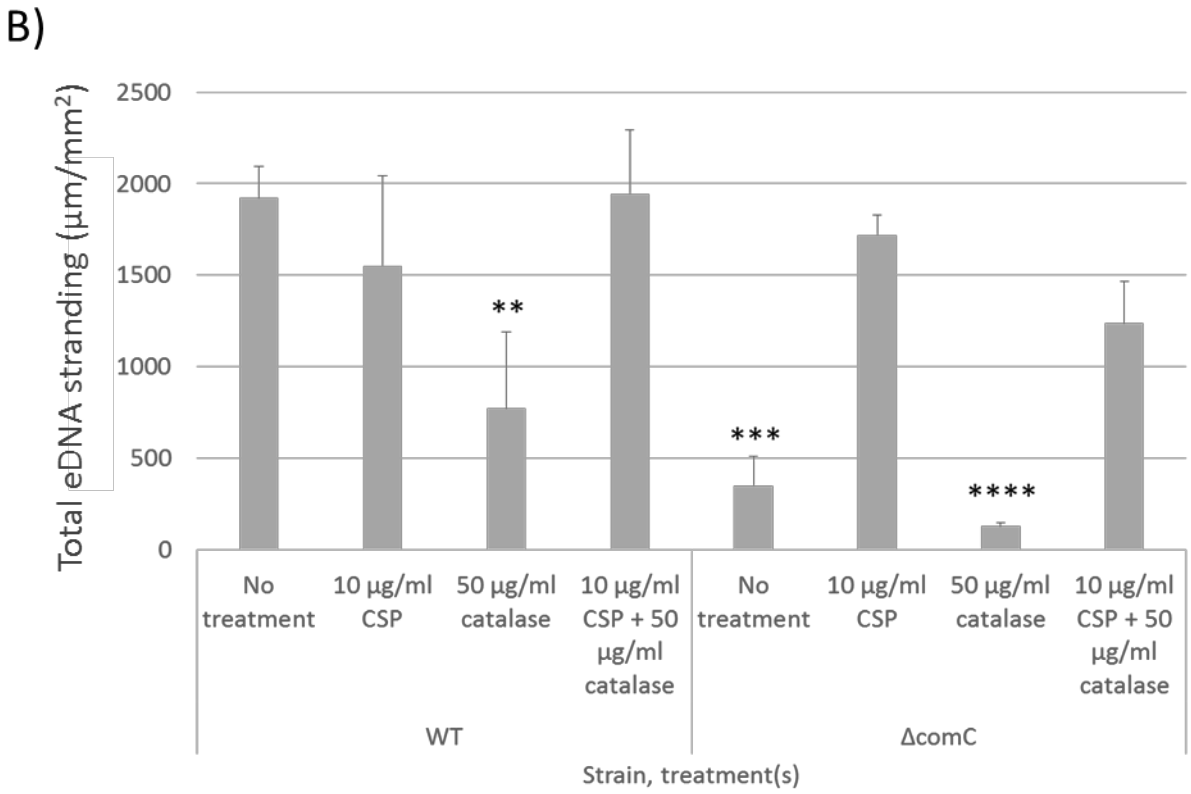

*Figure 5.28 – **CSP can restore eDNA stranding in catalase-treated biofilms**. S. gordonii strains WT and ΔcomC were adjusted to OD_{600} = 0.25 in YPTG supplemented with 10 µg/ml CSP, 50 µg/ml catalase or both, or no treatment control, and incubated at 37 °C for 5 h on saliva-coated glass-bottomed wells. Biofilms were stained with TO-PRO3, labelled with a ms anti-ds DNA antibody, then a gt anti-ms Ig antibody conjugated to Alexafluor A594, and visualised using widefield microscopy. A) Gallery of images post-ridge finding analysis in MATLAB. Scale bars = 100 µm. B) Quantification of total eDNA stranding. Data are presented as mean total eDNA stranding per mm² ± SD; n=3. Experiments were performed in triplicate. A one-way unpaired ANOVA was used with α=0.05. ** P<0.005, *** P<0.0005, **** P<0.0001, compared to WT no treatment.*

5.8 Role of autolysins in eDNA stranding

Autolysins are proteins which control cell lysis in response to cell signals. Two such proteins in S. gordonii are AtlS and competence-regulated LytF, and both had been previously associated with hydrogen peroxide levels and eDNA release (Xu & Kreth, 2013). Studies were therefore performed to investigate the potential role of these two autolysins in the eDNA stranding phenomenon. Mutants Δ*atlS* and Δ*lytF* were generated, and investigated for levels of eDNA stranding in biofilms. Neither mutant differed significantly from WT *S. gordonii* in terms of biofilm biomass (Figure 5.29).

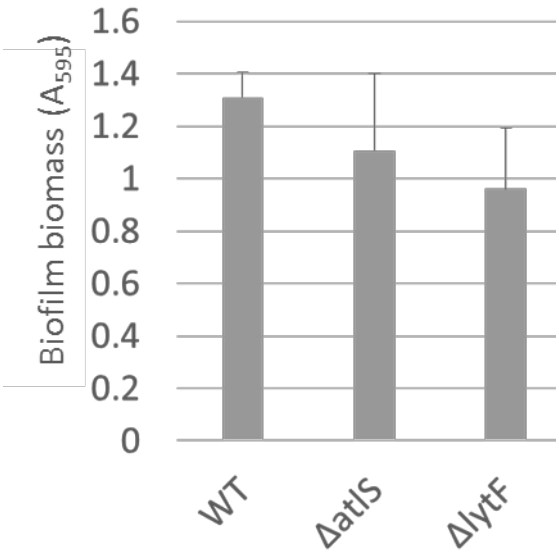

Figure 5.29 - ***Mutation of AtlS or LytF does not affect biofilm biomass.*** *S. gordonii WT, ΔatlS and ΔlytF biofilms were grown in YPTG at 37 °C for 5 h on saliva-coated glass-bottomed wells. Biofilms were stained with 0.25% crystal violet, the stain released with acetic acid, and the absorbance measured at A_{595}. Data are presented as mean absorbance ± SD; n=3. Experiments performed in triplicate. A one-way unpaired ANOVA was used with α=0.05. No significant difference was found compared to WT.*

However, eDNA stranding was reduced by two thirds for the Δ*atlS* mutant biofilms compared to WT, while eDNA stranding of the Δ*lytF* mutant biofilms was half that of WT (Figure 5.30). Taken together, these data suggested that both AtlS and LytF autolysins were associated with eDNA stranding in *S. gordonii* biofilms.

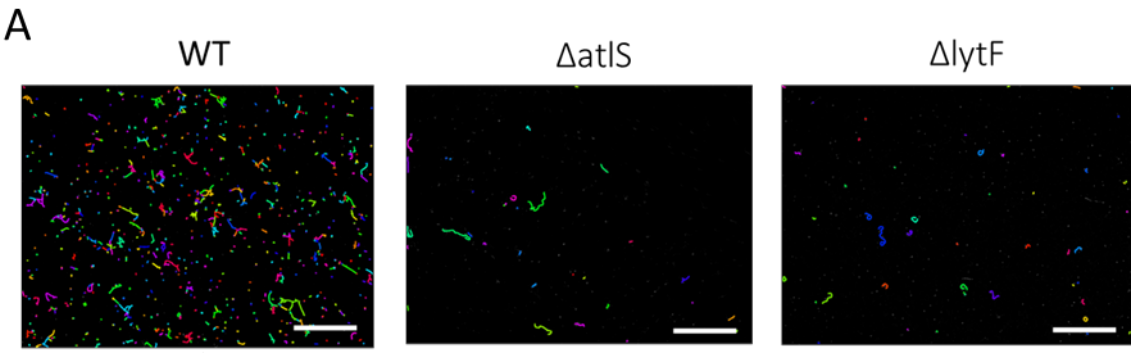

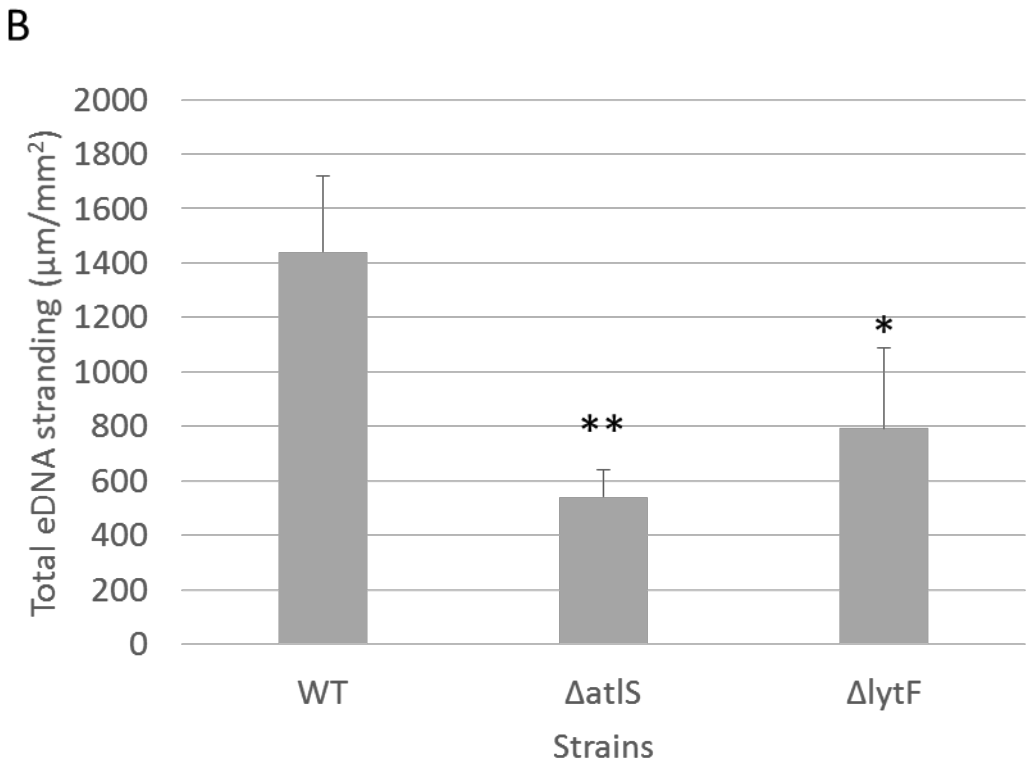

*Figure 5.30 – **AtlS and LytF mutants are reduced in eDNA stranding relative to WT**. S. gordonii strains WT, ΔatlS and ΔlytF were adjusted to OD_{600} = 0.25 in YPTG and incubated at 37 °C for 5 h on saliva-coated glass-bottomed wells. Biofilms were stained with TO-PRO3, labelled with a ms anti-ds DNA antibody followed by a gt anti-ms Ig antibody conjugated to Alexafluor 594, and visualised using widefield microscopy. A) Gallery of images post-ridge finding analysis in MATLAB. Scale bars = 100 µm. B) Quantification of total eDNA stranding. Data are presented as mean total eDNA stranding per mm² ± SD; n=3. Experiments were performed in triplicate. A one-way unpaired ANOVA was used with α=0.05. * P<0.05, ** P<0.005, compared to WT.*

The previous study by (Xu & Kreth, 2013) proposed that AtlS indirectly affects eDNA release in *S. gordonii* by affecting levels of H_2O_2, whilst LytF is directly responsible for the eDNA release. This was based, in part, on the finding that the Δ*atlS* mutant was inducible for eDNA release by addition of exogenous H_2O_2, while the Δ*lytF* mutant was not. Similar studies were performed here to investigate the effects with regards to eDNA stranding, and any association with CSP-mediated induction of eDNA release. The concentration of H_2O_2 used was based on the amount of H_2O_2 that would be neutralised by the 50 µg/ml catalase used in previous assays. Addition of neither CSP nor H_2O_2 affected the biofilm biomass of the ΔatlS or ΔlytF mutants relative to WT (Figure 5.31).

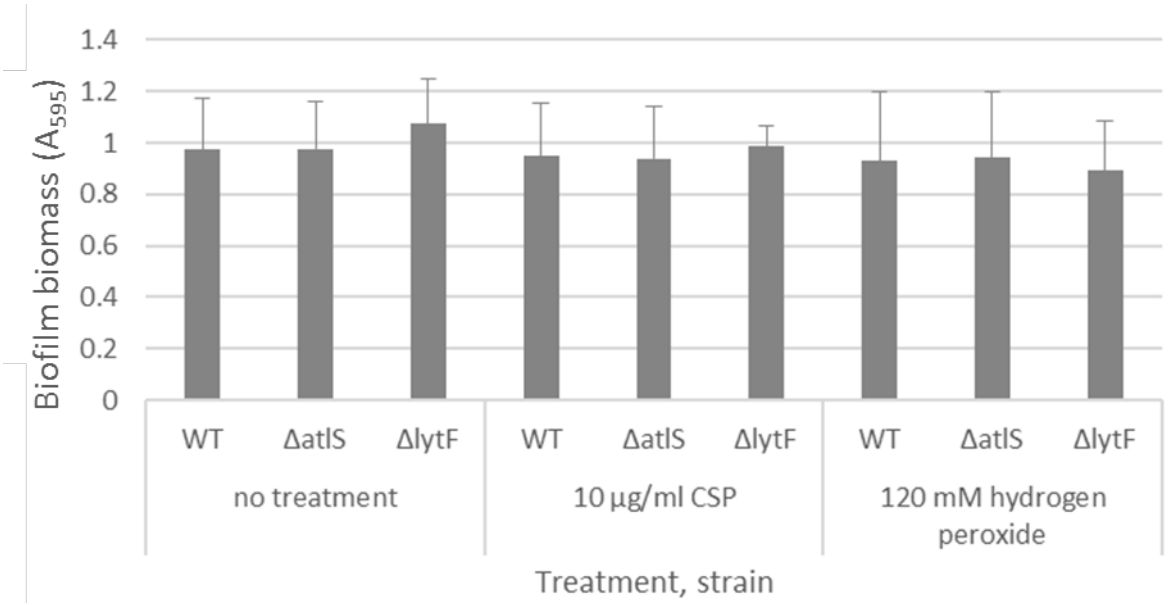

Figure 5.31 - ***CSP and hydrogen peroxide addition do not affect WT, ΔatlS or ΔlytF biofilm biomass****. S. gordonii WT, ΔatlS and ΔlytF biofilms were grown in YPTG with no treatment, 10 µg/ml CSP or 120 mM H_2O_2 at 37 °C for 5 h on saliva-coated glass-bottomed wells. Biofilms were stained with 0.25% crystal violet, the stain released with acetic acid, and the absorbance measured at A_{595}. Data are presented as mean absorbance ± SD; n=3. Experiments performed in triplicate. A one-way unpaired ANOVA was used with α=0.05. No significant difference was found compared to WT.*

CSP did not restore eDNA stranding to WT levels in the AtlS or LytF mutants (Figure 5.32). However, while treatment of the biofilms with H_2O_2 had no effect on the levels of eDNA stranding in Δ*lytF* mutant biofilms, it did restore eDNA stranding to WT levels for the Δ*atlS* mutant biofilms, and promoted eDNA stranding in WT biofilms.

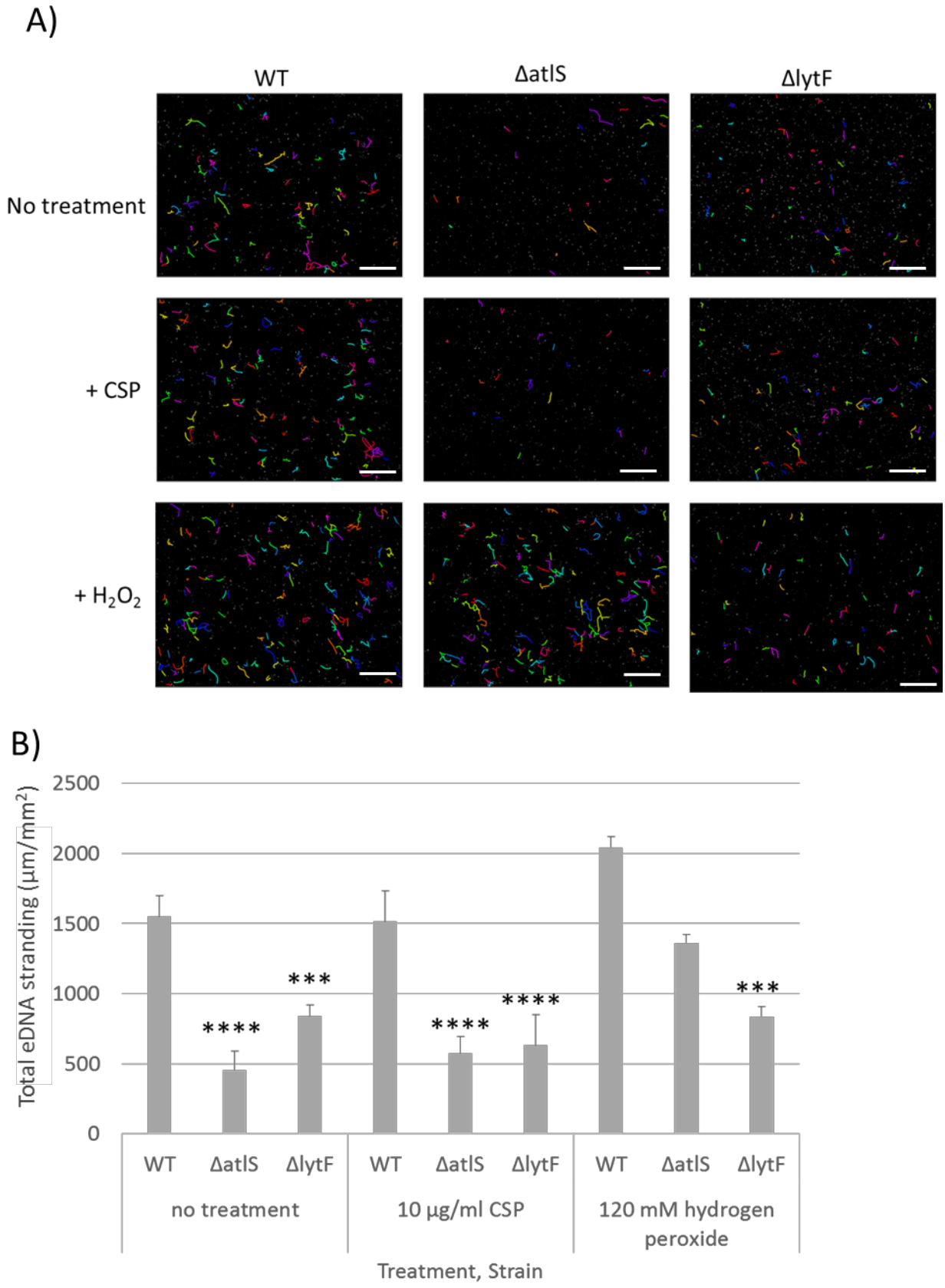

*Figure 5.32 – **Hydrogen peroxide treatment restores eDNA stranding in ΔatlS biofilms**. S. gordonii strains WT, ΔatlS and ΔlytF were adjusted to OD_{600} = 0.25 in YPTG with no treatment, 10 µg/ml CSP or 120 mM H_2O_2*

*and incubated at 37 °C for 5 h on saliva-coated glass-bottomed wells. Biofilms were stained with TO-PRO3, labelled with an anti-ds DNA antibody and visualised using widefield microscopy. A) Gallery of images post-ridge finding analysis in MATLAB. Scale bars = 100 µm. B) Quantification of total eDNA stranding. Data are presented as mean total eDNA stranding per mm² ± SD; n=3. Experiments were performed in triplicate. A one-way unpaired ANOVA was used with α=0.05. *** P<0.0005, **** P<0.0001, compared to WT no treatment.*

If addition of exogenous H_2O_2 modulated levels of eDNA stranding by promoting cell lysis via the autolysins AtlS and LytF (as indicated by eDNA stranding assays), it was anticipated that such effects would be detectable by ATP release assay. This was confirmed, as exogenous H_2O_2 treatment approximately doubled the concentration of extracellular ATP in WT *S. gordonii* and Δ*atlS* biofilms, while no response was seen for the Δ*lytF* mutant (Figure 5.33).

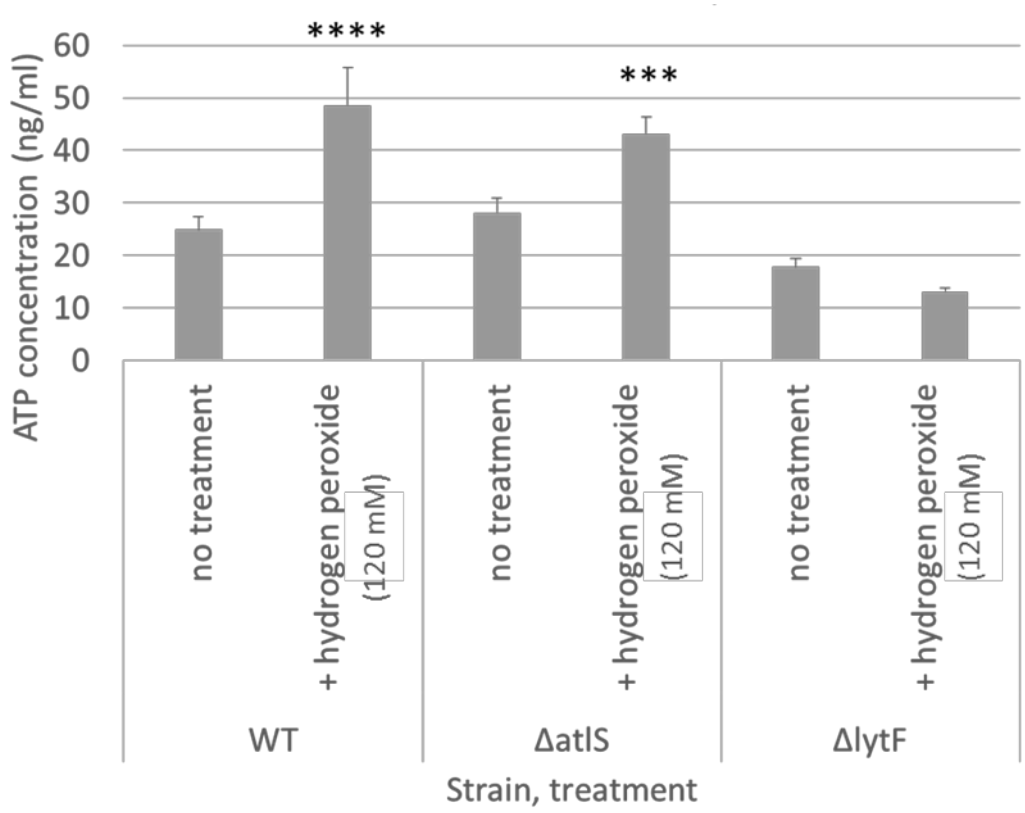

Figure 5.33 – ***Hydrogen peroxide does not induce cell lysis in LytF mutant biofilms.*** *S. gordonii strains WT, ΔatlS and ΔlytF were grown in YPTG supplemented with 0 or 120 mM hydrogen peroxide and incubated at 37 °C for 5 h on saliva-coated glass-bottomed wells. Biofilm supernatant was removed and used to calculate levels of ATP, using an ATP determination assay (Invitrogen) in which luminescence units were converted into ATP concentration. Data are displayed as mean ATP concentration (ng/ml) ± SD; n=3. Experiments were performed in triplicate. A one-way ANOVA was used with α=0.05. *** P<0.0005, **** P<0.0001, compared to WT untreated.*

Together, these data provided further support for the mechanism proposed by (Xu & Kreth, 2013) i.e. AtlS modulates levels of H_2O_2 , while LytF mediates H_2O_2-induced eDNA release. However, the lack of response of either autolysin mutant to CSP implied that both autolysins were also associated with the CSP-mediated eDNA stranding mechanism. This may have been anticipated for LytF, which is known to be active during competence development (Berg *et al.*, 2012), but the interplay with AtlS (and the Hpp system) also remained to be fully understood. One possibility that was explored was if CSP signalling via Hpp upregulated expression of both AtlS and LytF. As AtlS and LytF are both murein hydrolases which facilitate cell lysis by digesting peptidoglycan, zymography was used to test their activity. This method uses SDS- or native-PAGE in which the gels contain bacterial cell lysate. Any autolytic activity by the samples loaded onto the gels, following a protein re-folding step, will therefore result in degradation of the peptidoglycan within the gel, which appears as a clear band against a translucent background.

In the first instance, the appearance of the AtlS and LytF mutants on zymograms compared to WT *S. gordonii* was determined, using three different cell preparation techniques. As seen in Figure 5.34, methods A and C yielded similar results, whilst method B did not show any enzymatic activity. AtlS activity was found at 130 kDa, consistent with the literature (Liu & Burne, 2011), for WT and Δ*lytF* mutant, as would be expected. However, no visible LytF activity was detected across any of the samples. Bands of clearance have been previously reported at 60 and 30 kDa corresponding to LytF activity (Berg *et al.*, 2012), and so these would have been expected in the WT and Δ*atlS* samples. Further attempts to optimise the zymograms, including native PAGE approaches and analysis of *S. gordonii* spent media (since LytF can be secreted), failed to result in visible LytF activity. This approach was therefore only used to explore the effects of CSP on AtlS activity. Method C of cell preparation was selected for these future studies.

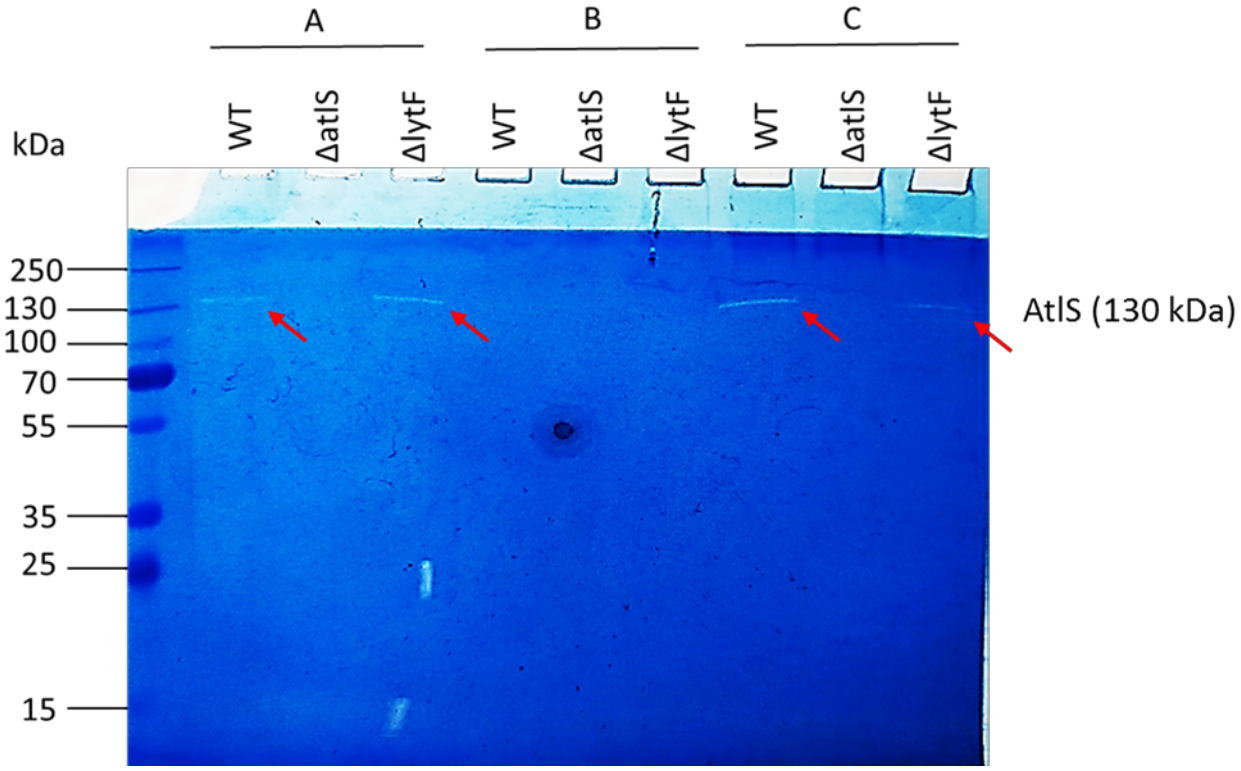

Figure 5.34 – ***Autolytic activity of S. gordonii using different cell preparation methods.*** *S. gordonii cell pellets were heat killed and added to a 10% SDS-PAGE separating gel. S. gordonii strains WT, ΔatlS and ΔlytF were adjusted to OD_{600} = 0.25 in YPTG and incubated at 37 C for 5 h. A) Cells were pelleted, B) cells were lysed with Triton-X100, cell debris pelleted, and the supernatant used, or C) cells were incubated for 7 h before pelleting. These heat-killed samples were then run on the prepared SDS-PAGE gel, incubated in refolding buffer and then stained with methylene blue for visualisation of autolytic activity. Clear bands labelled with arrows represent autolytic activity.*

No difference was seen in AtlS activity with CSP supplementation of WT or Δ*lytF* mutant biofilms (Figure 5.5). The Δ*comC* mutant displayed no visible AtlS activity but this could be reversed by addition of exogenous CSP (Figure 5.36). No autolytic activity was detected for the Δ*comCDE* mutant, with or without CSP addition. By contrast, the Δ*hppA* mutant exhibited AtlS activity, both with and without exogenous CSP supplementation. These data suggested that CSP, over a certain concentration range, can induce AtlS activity and that this occurs via the canonical receptor ComDE. However, AtlS activity does not appear to be responsible for the eDNA stranding effects mediated by CSP via the Hpp system.

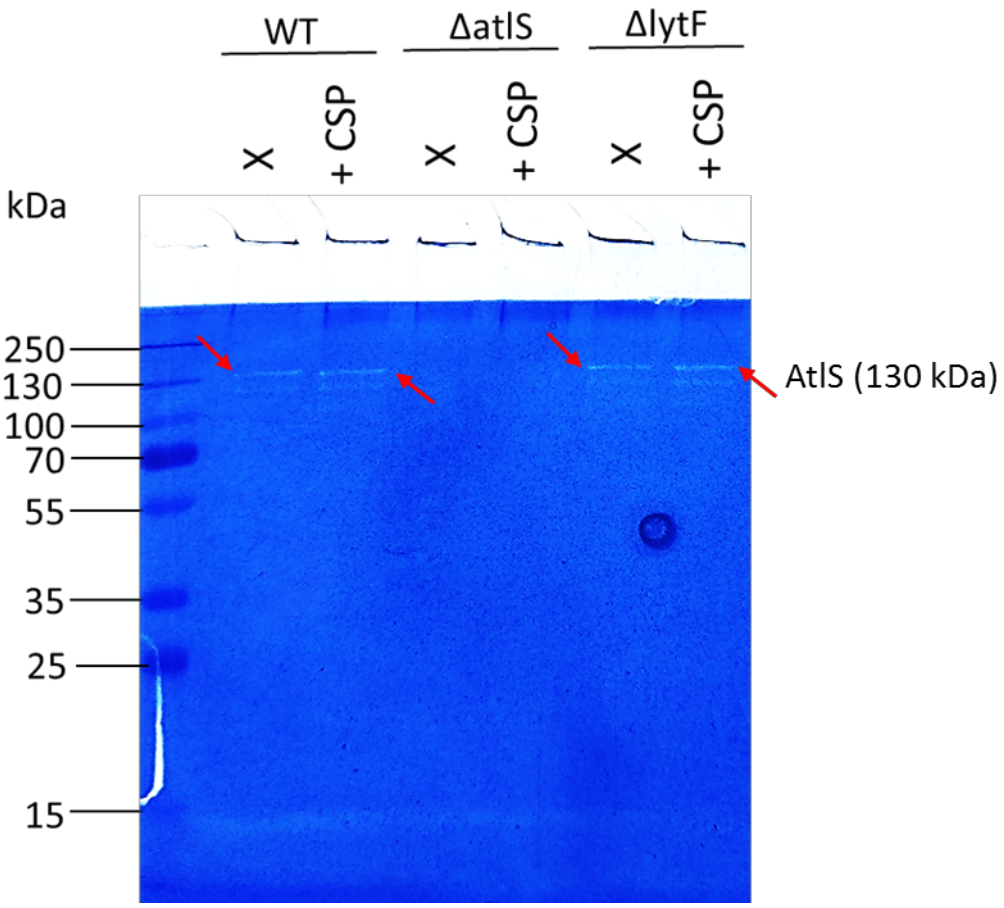

Figure 5.35 – ***CSP addition does not significantly alter autolytic activity of AtlS.*** *S. gordonii cell pellets were heat killed and added to a 10% SDS-PAGE separating gel. S. gordonii strains WT, ΔatlS and ΔlytF were adjusted to OD600 = 0.25 in YPTG with 0 or 10 μg/ml CSP and incubated at 37 C for 7 h. Cells were pelleted, heat killed, and run on the prepared SDS-PAGE gel, before being incubated in refolding buffer and then stained with methylene blue for visualisation of autolytic activity. Clear bands labelled with arrows represent autolytic activity.*

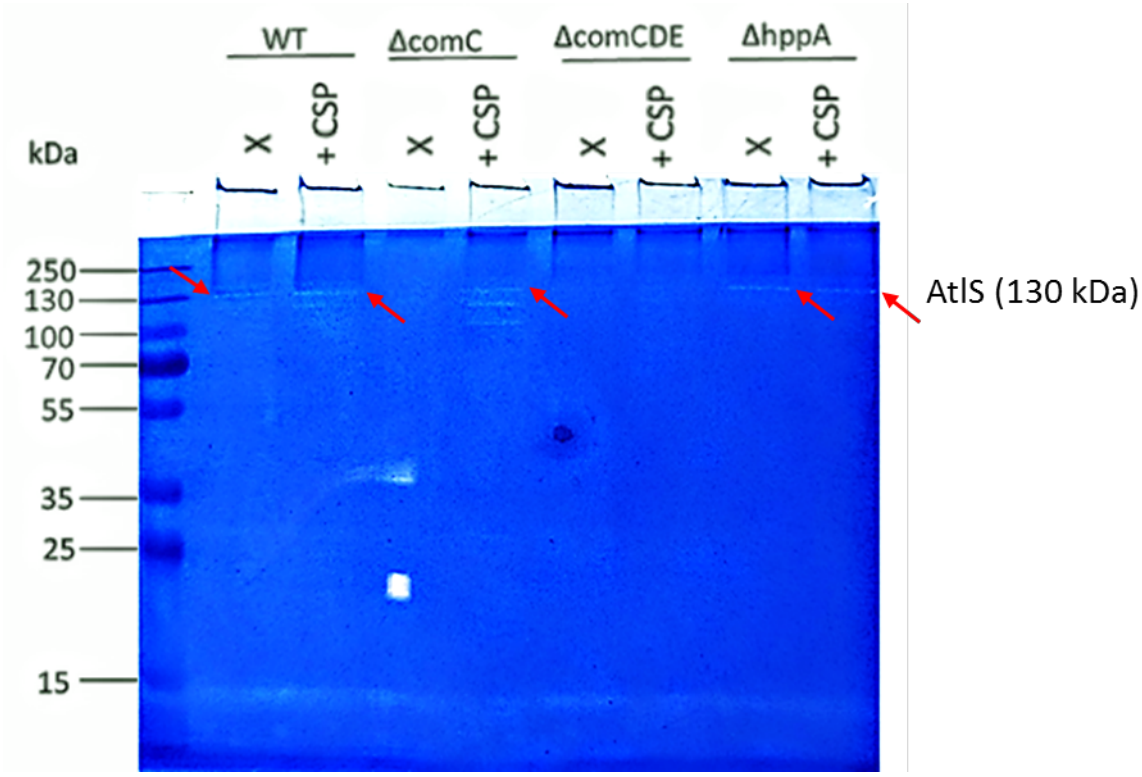

*Figure 5.36 – **CSP signals via ComDE to alter AtlS activity**. S. gordonii cell pellets were heat killed and added to a 10% acrylamide SDS-PAGE separating gel. S. gordonii strains WT, ΔcomC, ΔcomCDE and ΔhppA were adjusted to OD_{600} = 0.25 in YPTG with 0 or 10 μg/ml CSP and incubated at 37 C for 7 h. Cells were pelleted, heat killed, and run on the prepared SDS-PAGE gel, before being incubated in refolding buffer and then stained with methylene blue for visualisation of autolytic activity. Clear bands labelled with arrows represent autolytic activity.*

5.9 Discussion

5.9.1 SedA/SndA and eDNA stranding

eDNA stranding assays in Chapter 4 implied that LPxTG proteins SedA and SndA were important in eDNA stranding. This was confirmed here through testing a wider range of knockout and complemented mutants. Furthermore, the data suggested that SedA and SndA may function co-operatively with regards to their eDNA stranding effects, since no additive effect was seen with the Δ*sedA* Δ*sndA* double mutant. Neither protein seemed to affect the susceptibility of *S. gordonii* to cell lysis, and only SndA exhibited DNase activity. However, both

SedA and SndA modulated the capacity for *S. gordonii* to bind exogenous DNA under both planktonic and biofilm conditions. This correlates with the presence of predicted DNA-binding domains in both proteins and suggests that this may be the mechanism by which these proteins can influence eDNA stranding. The distinct 'constellation-like' pattern of eDNA stranding implies that the eDNA strands may be held at anchor points across the biofilm, and this may be a role performed by SedA and SndA. In support of this, a direct correlation was found by regression analysis ($P<0.0001$; Figure 5.37) between the capacity for *S. gordonii* strains to bind dsDNA and the levels of eDNA stranding.

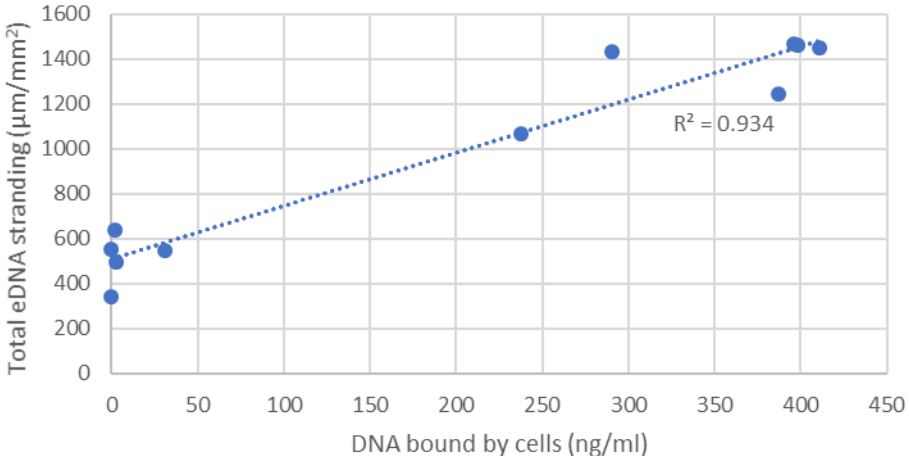

Figure 5.37 – ***Regression analysis of DNA binding vs. eDNA stranding in SedA and SndA mutants.***

Given the apparent co-operativity between SedA and SndA, it is possible that these proteins co-localise on the surface of *S. gordonii* to form functional DNA-binding sites, or that engagement of both proteins with DNA is required to enable *S. gordonii* to effectively hold dsDNA at its cell surface. Future studies could explore such possibilities. Direct protein interaction supports the idea that eDNA stranding is an active phenomenon. Interestingly, as no further reduction was seen in Δ*srtA* biofilms, SedA and SndA proteins may be the only LPxTG family DNA-binding proteins on *S. gordonii* that affect eDNA stranding in biofilms.

Another observation of note from these studies was that SndA influenced the transformation efficiency of *S. gordonii*. As for eDNA stranding, it is perhaps

paradoxical that loss of an exonuclease would diminish uptake of extracellular DNA. For instance, in some bacteria, such as *Campylobacter jejuni*, transformation is reduced by extracellular DNase activity (Gaasbeek *et al.*, 2009).

A potential explanation is that DNA is cleaved into smaller pieces to be more easily uptaken by the bacteria. Whilst the exact mechanism for DNA uptake in Gram-positive bacteria is still under investigation, the binding of DNA, DNA fragmentation and then internalisation have been proposed as three stages which occur - it is this DNA fragmentation stage in which SndA may be involved. In *S. pneumoniae*, DNA fragmentation occurs at the cell surface and increases the rate of transformation (Muschiol *et al.*, 2015). Furthermore, loss of DNase reduces transformation because entry of DNA into the cell is prevented (Lacks & Greenberg, 1976), which supports the finding of reduced transformation in SndA-lacking *S. gordonii* cells. To further investigate this, in the first instance, targeted mutagenesis of the DNase or DNA-binding domains of SndA could be performed, to determine which domain or if both are required for the effects on transformation (and eDNA stranding).

5.9.2 Competence and eDNA stranding

It had been shown previously that *S. gordonii* mutants lacking ComC appeared to produce less eDNA in biofilms, implicating CSP in this process, but this had not been quantified (Jack *et al.*, 2015). This work is supported and further developed here, as it was shown that biofilms of *S. gordonii* Δ*comC* and Δ*comCDE* strains are impaired relative to WT with regards to eDNA stranding levels, and that this defect can be restored upon addition of exogenous CSP in a dose-dependent manner. However, induction of eDNA stranding with CSP was not seen in WT biofilms. As WT *S. gordonii* will produce CSP during growth, unlike the Δ*comC* and Δ*comCDE* mutants, this implied that CSP induces eDNA stranding but that, once a threshold concentration is CSP reached (likely around 2 μg/ml based on the results in Figure 5.18), no further influence on eDNA stranding can be seen.

Induction of eDNA stranding was a specific response, as no effect was seen using a scrambled version of the CSP. However, eDNA stranding was promoted, to varying degrees, by the CSPs of *S. pneumoniae* and *S. mutans* also, despite these CSPs not sharing sequence homology to *S. gordonii* CSP. This was unexpected as for competence, the response is CSP pherotype specific (Li *et al.*, 2001). Such discrepancy may relate to the fact that detection of CSP for induction of eDNA stranding was also found to be independent of TCSS ComDE and rather appeared to be performed by the Hpp system. Jenkinson *et al*. (1996) linked the Hpp system with competence in *S. gordonii*, which would support these findings that Hpp is an alternative system that can detect and respond to CSP. Other mechanisms for competence induction in streptococcal species have been identified which do not follow the canonical ComCDE pathway, showing that induction of competence can be mediated by alternative pathways. For example, *Streptococcus thermophilus* and *Streptococcus salivarius* possess the ComRS rather than ComCDE system, which exploits an Opp system to import the CSP equivalent, known as XIP (Fontaine *et al.*, 2010; Gardan *et al.*, 2009).

5.9.3 Cell lysis and eDNA stranding

In *S. pneumoniae*, eDNA has been shown to be released via a sub-population lysis event (Steinmoen et al., 2003). In contrast, for other bacteria such as *E. faecalis*, a lysis-independent mechanism of eDNA release has been proposed (Barnes *et al.*, 2012). From the data presented here it is clear that H_2O_2 can induce *S. gordonii* eDNA stranding in a LytF-dependent manner and that this process is associated with release of intracellular ATP. This was confirmed by regression analysis linking H_2O_2 with eDNA stranding ($P<0.05$;
Figure 5.20), and ATP release with eDNA stranding for the AtlS and LytF knockout strains ($P<0.0005$; Figure 5.39).

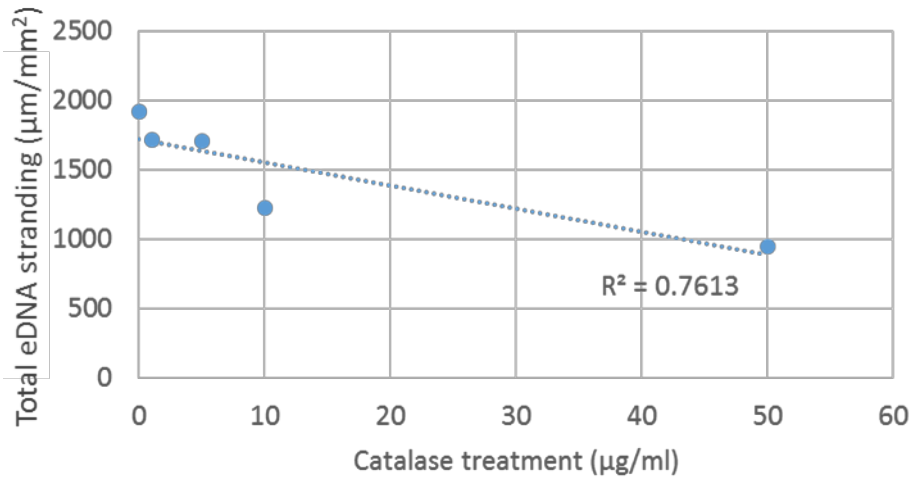

Figure 5.20 – ***Regression analysis of catalase treatment vs. eDNA stranding.***

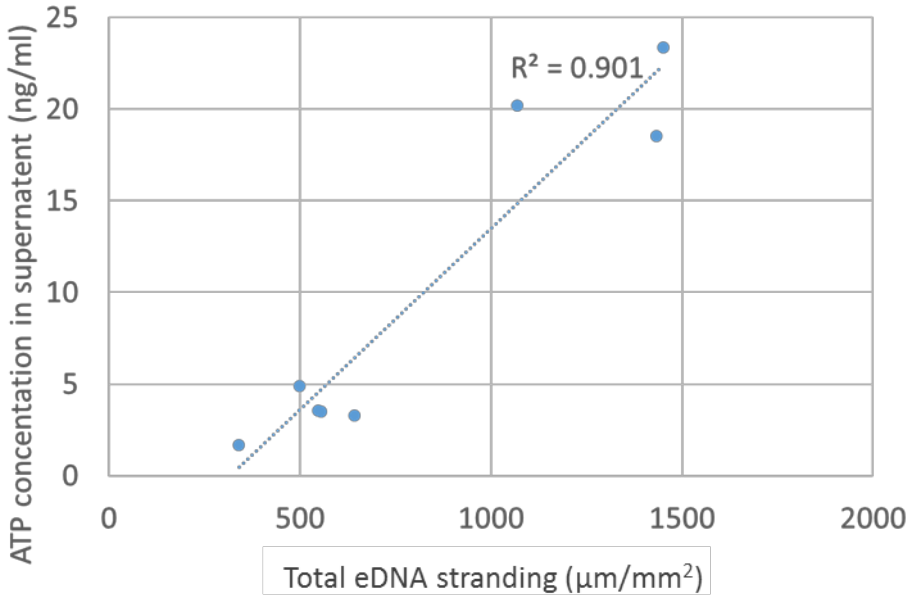

Figure 5.39 - ***Regression analysis of eDNA stranding vs. ATP concentration in supernatant in ΔatlS and ΔlytF.***

Release of intracellular ATP was also seen during CSP induction of eDNA stranding by the *S. gordonii* Δ*comC* mutant, for which the mechanism, at least in part, seemed to relate to upregulation of AtlS activity following signalling via ComDE, which would in turn result in elevated levels of H_2O_2. These data support the mechanism of eDNA release proposed by (Xu & Kreth, 2013). Nonetheless, for this and our own studies, it was also noted that minimal cell lysis was detectable. Thus, it remains to be determined if LytF mediates its effects via lysis

of a very small sub-population of cells or via a process that allows DNA release but without complete cell lysis.

Alongside this stress-induced eDNA release mechanism, these studies provided strong evidence that CSP can also induce eDNA stranding via a process that is independent of H_2O_2 levels, and is specifically mediated by CSP detection via the Hpp system. Moreover, this seems to be the dominant pathway for the eDNA stranding reported here, and both the AtlS and LytF autolysins were implicated. Using zymography, there was no evidence that CSP signalling via Hpp could upregulate AtlS activity. However, it is possible that the assay was not sensitive enough to measure changes in autolysis with this concentration of CSP. Furthermore, to obtain sufficient biomass, these assays were performed under planktonic conditions, and it is quite possible that the eDNA stranding effects are specific to the biofilm environment. Determining the precise relationship between CSP, Hpp and the AtlS and LytF autolysins will be the focus of future studies.

5.9.4 Summary

These studies have identified two major factors that can influence levels of eDNA stranding in *S. gordonii* biofilms:

1. LPxTG proteins SedA and SndA appear to function co-operatively in promoting eDNA stranding, most likely due to their capacity to bind dsDNA on the surface of bacterial cells
2. CSP is able to induce eDNA stranding. This can occur via:
    a. a stress-induced pathway following signalling via ComDE that involves hydrogen peroxide/AtlS and LytF-mediated cell lysis
    b. signalling via the Hpp system involving an as yet unknown mechanism that appears to be associated with autolysins AtlS and LytF

Chapter 6 - Discussion

6.1 LPxTG proteins in *S. gordonii* colonisation and pathogenesis

Infections by Gram positive bacteria pose a major health burden (Willems *et al.,* 2012) and one genus of these bacteria, streptococci, are prominent members of the oral microbiota. *Streptococcus gordonii* was chosen for investigation in this project as it is an early coloniser of the clean tooth surface (Li *et al.,* 2004) and readily forms biofilms on salivary pellicle (Cook *et al*., 1998). To facilitate colonisation of the oral cavity, bacteria must adhere tightly to host surfaces to resist shear forces and prevent washing away by saliva (Nobbs *et al*., 2009). Bacteria, including *S. gordonii*, then form biofilms which increase bacterial persistence (Balaban *et al*., 2004), a process which involves production of extracellular material - the EPS (Jack *et al*., 2015). The emphasis of this project was to investigate novel proteins on the surface of *S. gordonii* which may act as adhesins and contribute to biofilm formation, and study the mechanism which allows for the formation of a major component of the EPS: eDNA.

LPxTG protein are a large family of adhesins found in Gram-positive bacteria. The sequence LPxTG is used to target the proteins to the surface and for covalent attachment to peptidoglycan for external display. In this project LPxTG proteins were analysed using bioinformatics – this study identified genes which encoded 27 LPxTG motif-containing proteins, using the genomic sequence of *S. gordonii*. Six proteins were chosen for further investigation: CbdB, PadA, PadB, PalA, SedA and SndA. Based on bioinformatics, these proteins were hypothesized to bind to host or biofilm components. The loss of each proteins individually from a bacteria resulted in disrupted biofilm formation, which demonstrates the importance of surface proteins in colonisation and pathogenesis. It would be interesting to investigate whether they are present on the cell surface constitutively. To investigate the presence of the proteins at the cell surface and how this changes over time, antibodies tagged with a

fluorophore or nano gold (Winkler *et al.,* 1995) could be added to fixed biofilms grown to different ages, then visualised and quantified using microscopy. Alternatively, an enzyme-linked immunosorbent assay system could be used. In this system, antibodies to the surface protein of interest can be coupled with an enzyme, for instance a phosphatase. Following washing, and upon the addition of a substrate, for example phosphate, enzymatic activity could be measured using a microtitre plate reader – this would be proportional to the amount of surface protein present (Burkovsk, 1997). If these systems revealed temporal differences in proteins at the cell surface, it would be of interest to investigate what cell signals control this.

As this project became more focussed on role and mechanism of eDNA stranding, interesting phenotypes for proteins such as CbdB and PalA were not pursued further, which present exciting opportunities for further research. CbdB, was selected for investigation due to the potential to bind collagen, based on the homology shared with Cnm, a collagen binding protein in *S. mutans* (Abranches *et al*., 2011). Cnm is a colonisation and major virulence factor (Avilés-Reyes *et al.*, 2014), so this was hypothesised to be the case for CbdB. However, this study found bacteria lacking CbdB were *more* able to bind collagen. CbdB may therefore be masking another collagen binding protein in *S. gordonii*. Future work could investigate whether CdbB is masking a collagen binding protein with known collagen binding activity such as CbdA or alternative protein, including two proteins which have been hypothesised to bind collagen based on bioinformatics: CbdC and CbdD. First, assessment of whether CbdC and CbdD bind collagen could be performed using the same assay used to test CbdB in this work. CbdB could be isolated by transforming the CbdB-lacking mutant with a construct which encodes for CdbB with a hexa-His tag, allowing for nickel ion column purification. A cell wall preparation could be used in a pull-down assay to find if CbdB is binding to any proteins on the surface of the bacterium. If CbdB is binding to and masking a collagen binding protein, CbdA for example, addition of exogenous CbdB may prevent *S. gordonii* adhesion to collagen-containing surfaces (such as soft oral tissues). This could occur by CbdB binding to and occluding the collagen binding site on CbdA. CbdB was also required to form

cohesive biofilms under the conditions tested in this study. An explanation for how CbdB could perform both of these roles is by binding to a collagen-binding protein on the surface of another bacteria, thus stabilising the biofilm architecture. To test this, FRET could be used. For instance, CbdB coupled to a donor molecule could be expressed in a *S. gordonii* Δ*cbdA* Δ*cbdB* strains and CbdA coupled to an acceptor molecule could be expressed in Δ*cbdA* Δ*cbdB*. If these strains were mixed, it would be possible to infer direct interaction of CbdB and (for example) CbdA based on changes in fluorescence. Comparing the interaction of these strains to the interaction between Δ*cbdA* Δc*bdB* bacteria would show what the result of the activity of CbdB is. Blocking this interaction with a rationally designed small molecule inhibitor may result in less cohesive biofilms, which in turn require less antibiotic to reach the minimum inhibitory concentration (MIC). However, because *S. gordonii* typically participates in multi-species biofilms *in vivo*, it is not known whether disruption of the cohesion of this species alone would result in an oral biofilm which is more readily penetrable.

This study found that PalA binds cellular, but not plasma fibronectin. Cellular fibronectin makes up part of the human extracellular matrix and basement membrane and is an insoluble glycoprotein dimer, whereas plasma fibronectin is found in the blood and used in wound healing, and is a soluble disulphide linked dimer (To & Midwood, 2011). In the oral environment, *S. gordonii* may encounter cellular fibronectin in damaged or degraded tissues, which presents opportunity for plaque accretion at these sites. PalA is a potential microbial surface component recognizing adhesive matrix molecules (MSCRAMM). *S. gordonii* binds to damaged heart values in infective endocarditis. The cellular fibronectin binding ability of PalA potentially implicates it in the pathogenesis of *S. gordonii*. This would be consistent with other SSURE domain-containing proteins, for example, PavB in *Streptococcus pneumoniae* (Jensch *et al*., 2010). This protein shares homology with PalA and is a colonisation and infection factor in mice. To investigate if PalA binds fibronectin via the SSURE domain, Δ*palA* could be transformed with a construct encoding PalA lacking the SSURE domain, and adhesion to fibronectin could be assessed in comparison to a complemented Δ*palA*. PalA and CshA share the same specificity of binding

cellular, but not plasma, fibronectin. *S. gordonii* can also bind fibronectin via FbpA (Christie *et al.*, 2002) and MsrA (Giomarelli *et al.*, 2006). Has can also bind fibronectin. This is an example where adhesins initially appear redundant. However, it is hypothesised that these five proteins, each of which are encoded within different loci, allow *S. gordonii* to mediate the interaction it makes with fibronectin at different points in its life cycle. This could be investigated using real-time PCR, with primers based on the genes encoding these four proteins used to amplify RNA gathered from different ages of biofilms i.e. adhesion, early, mid and late stages. Additionally, quantitative PCR could also be used to find different levels of expression between these proteins in biofilms derived from oral or cardiac environments. If one of these proteins was implicated during infective endocarditis, there is an opportunity for the development of a therapeutic agent which would disrupt this interaction, therefore reducing *S. gordonii* colonisation and subsequent pathogenesis.

6.2 eDNA stranding in *S. gordonii* biofilms

DNA is a recently recognised component of the biofilm EPS. This study found eDNA constitutes 0.7% of the *S. gordonii* biofilm by volume (Section 5.2). Disruption of eDNA with DNase caused a reduction of over 50% in biomass. Taken together, this supports the long-held hypothesis that eDNA is contributing prominently to biomass and by providing a structural scaffold which facilitates biofilm accretion. eDNA in Gram positive bacteria has been associated with the precursor stages of biofilm development: bacterial adhesion and aggregation (Das *et al.*, 2010). As a structural scaffold, eDNA facilitates the formation of robust biofilms. Additionally, binding to an existing eDNA network facilitates incorporation of new bacteria into the biofilm (Rocco *et al.*, 2018).

This study has led to the development of a novel methodology for quantification of eDNA stranding within biofilms. Previously, eDNA was measured in several different ways. Total eDNA concentration was measured, which also includes DNA which is not networked and may have resulted from

random lysis. It is hypothesised that this type of “loose” DNA is not integral to biofilm formation. Some analysis of DNA had been performed using microscopy, where relative eDNA between two biofilms could be assessed qualitatively e.g. in Jack *et al*., 2015. However, because this is qualitative, there can be no comparison between studies. Furthermore, this method does not discriminate between lysed unnetworked DNA and eDNA strands. Total fluorescence could be measured, but this has the same problems in interpreting eDNA data gathered from concentration. The methodology developed in this work is uniquely capable of discriminating between loose, unnetworked DNA and eDNA strands. It has allowed eDNA strands to be measured quantitively for the first time. This methodology can be used in other work and will enable comparison between studies.

This methodology allowed for the discrimination between different eDNA strands, therefore measurement of the length and frequency of individual stranding events for the first time. This allowed the mechanism behind stranding to be probed. Stranding varied more in frequency of events than in length of individual strands. For example, mutant strains tested in this project varied by 106% in frequency, and by only 16% in terms of strand length. This implies that the control on the eDNA stranding system takes place at the point of eDNA release. The theory of controlled eDNA release led to the development of a hypothesis whereby an actively-controlled sub-population lysis event was the source of eDNA for strands.

Using this assay, it was found that degradation of eDNA strands by DNase treatment during biofilm formation resulted in biofilms with lower biomass. However, other factors, for instance loss of surface proteins, caused a reduction in eDNA stranding but no effect on biomass. Whilst the former finding supports the hypothesis that eDNA stranding is required for biofilm formation, the latter appears to contradict this. A possible explanation for this apparent contradiction would be the presence of a feedback mechanism which detects and relays when eDNA is not bound, triggering an alternative, and as yet unknown, pathway which facilitates accretion of biomass in the absence of eDNA (Figure 6.1). However, another possibility simpler explanation for this dichotomy is that eDNA

stranding is not directly linked to biofilm accretion and instead serves another role within the biofilm.

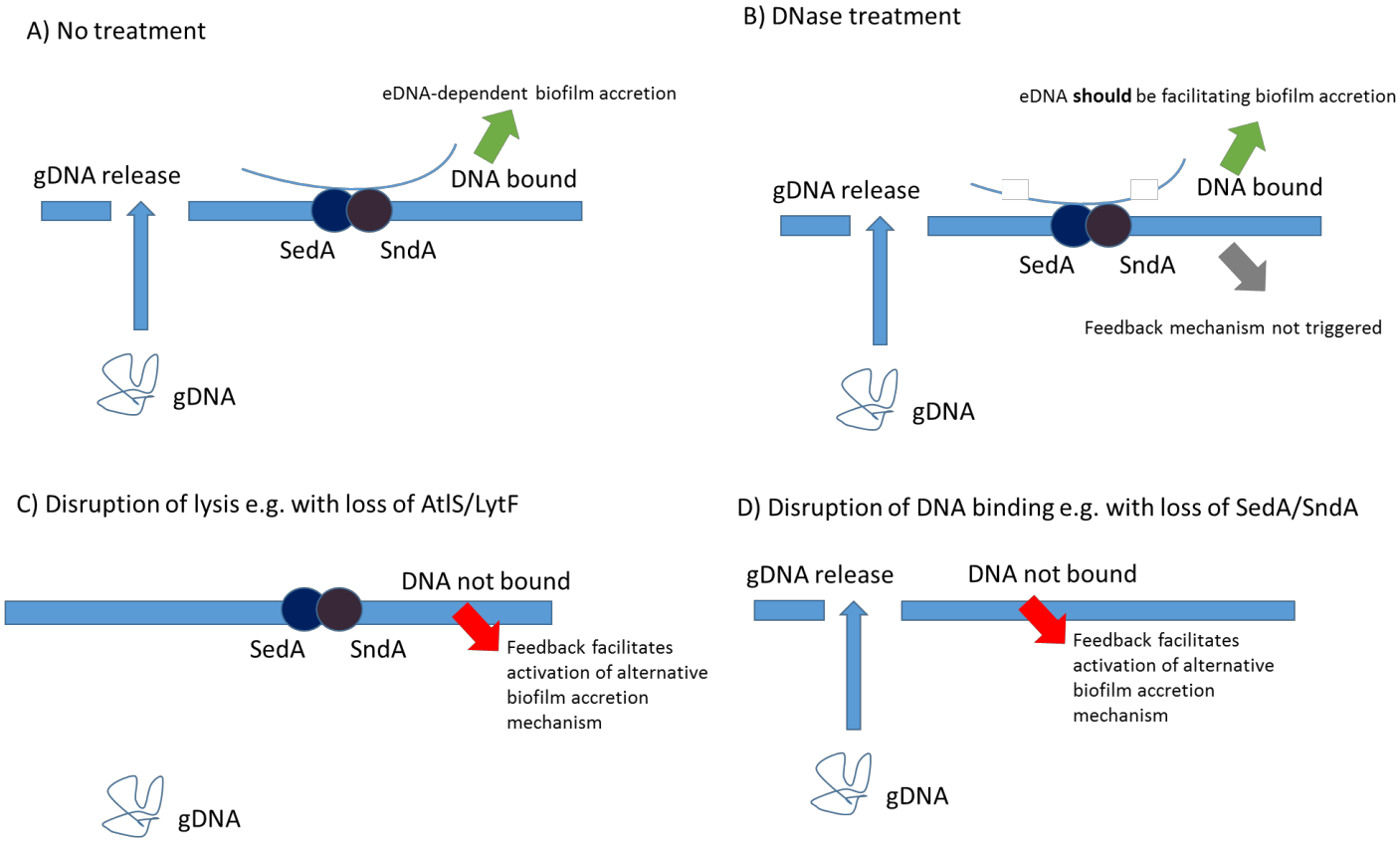

Figure 6.1 – Hypothesis of a feedback mechanism which activates an alternative pathway for biofilm accretion upon the sensing of the absence of eDNA binding. Such a system would allow B) DNase treatment to affect biofilm biomass, whilst allowing C&D) loss of proteins implicated in eDNA stranding not to affect biomass.

Potential roles for eDNA stranding were discussed in Section XX. If DNA is not acting as a structural scaffold to facilitate biofilm accretion, it may be facilitating resistance to shear flow. To test this, first the amount of eDNA stranding produced by biofilms grown under different amounts of shear in flow cells could be measured. Next, the ability of biofilms with low and high eDNA and their ability to resist shear forces could be investigated, to infer if eDNA is involved in the biofilm resistance to flow. Investigations into the ability of another oral bacterium, *S. mutans*, to resist flow, have been carried out in the literature, focussing on the role of EPS production (Hwang *et al.,* 2014). However, as far as we know, no work has yet looked specifically at eDNA (a component of EPS) in relation to shear forces, and therefore would be of future interest.

Another facet of the structure of DNA which may be important in streptococcal biofilms is the ability of DNA to sequester metal ions and modulate resistance to antibiotics, as observed in *Pseudomonas aeruginosa* (Mulcahy et al., 2008). Future work could investigate is this antibiotic resistance of eDNA persists in S. gordonii biofilms, and if so, whether biofilms with reduced eDNA (such as those lacking SedA and SndA) are more susceptible to antibiotic treatment.

It was hypothesised that DNA, as a major component of eDNA strands, may be used to in genetic exchange. This work has not found evidence to support eDNA being used for genetic transfer: biofilms lacking SedA, which have lower eDNA stranding, had similar transformation frequency compared to wild type biofilms.

eDNA also has the potential to be used as a nutrient store. In this work into the potential eDNA was found to be reduced in biofilms grown with limiting glucose. To further elucidate if eDNA has a role of nutrient store, biofilms could be grown under limiting glucose with and without the addition of exogenous DNA. If biomass accretion is higher in glucose limited biofilms with addition of eDNA, eDNA may be being used as an alternative nutrient source.

Whilst previously proteins thought to be associated with eDNA stranding were implicated by qualitative assessment of changes to the apparent eDNA

stranding, the method developed here allowed for the eDNA strand specific effects of bacterial proteins to be measured, allowing for a more rigorous assessment of their contribution to this phenomenon. This work has investigated monospecies *S. gordonii* biofilms, but we expect this methodology to be highly transferrable to other systems, such as other single species or multispecies biofilms *in vitro*, as well as biofilms which are grown *in vivo*.

Two *S. gordonii* LPxTG motif-containing surface proteins have been implicated in DNA binding and eDNA stranding: SedA and SndA. It is hypothesised that these proteins act as anchor points for eDNA strands, to facilitate the distinctive "constellation" shapes observed in eDNA stranding. SndA contains an OB-fold which may interact with DNA (Flynn & Zou, 2010). SedA contains a surface exclusion domain, which is hypothesised to interact with DNA to fulfil its function. Prior work in other species has implicated DNA binding proteins in eDNA networks. For instance, Huβ, a DNABII protein of *P. gingivalis* (Tjokro *et al*., 2014), has been found to provide structure to the biofilms, with loss of this action resulting in a 75% reduction in biomass (Rocco *et al.*, 2017). However, the effect of extracellular HUβ on eDNA stranding in *P. gingivalis* biofilms has not yet been investigated - using the methodology developed to analyse eDNA stranding within this project, this affect could be quantified. *S. gordonii* also expresses the DNABII family protein αHU_{Sg}, which has been implicated in biofilms (Rocco *et al.*, 2017). The presence of another DNA binding protein may explain why removal of SedA/SndA does not ablate eDNA stranding, and why ΔsrtA mutants are further reduced in DNA binding compared to SedA SndA double mutants. DNA-binding proteins have also been implicated in the pathogenesis of oral biofilms. *P. gingivalis* enters pre-formed communities which are formed by coloniser species such as *S. gordonii* (Rocco *et al.*, 2018). Disruption of the eDNA network in these coloniser species, may prevent disease-associated organisms from entering the biofilms.

Having implicated SedA and SndA in DNA binding, it would now be interesting to discern the mechanism for this interaction. First, the mutant strains could be complemented with plasmids encoding SedA or SndA lacking either the MnuA-like domain or OB-fold, or the surface exclusions domain,

respectively. Next, site-directed mutagenesis could be used to probe the specific areas of the protein which bind DNA. Characterisation of the interaction these proteins make with DNA could be undertaken further if the nuclease activity of DNase was inhibited. Each protein could be crystallised with DNA. X-ray crystallography could be used to solve the structure of the proteins bound to DNA. This may allow for the generation of a small molecule inhibitor designed to disrupt the protein: bacterial interaction. This is hypothesised to result in biofilms which display a similar phenotype to Δ*sedA* or Δ*sndA* biofilms: reduced eDNA stranding. These biofilms may then be easier to disrupt, for example, with mechanical force or antimicrobial treatment.

SedA and SndA have only been hypothesised to interact based on disruption of activity being the same in single or double mutants. By expressing and purifying these proteins, it would be possible to determine if this interaction continues when the proteins are not anchored to the cell surface. FRET could be used to establish if these proteins make a short-range physical interaction, which may be involved in their co-operative behaviour. Cis-membrane FRET analysis has successfully identified short-range interactions between surface components in the literature (Lin *et al.,* 2014). Is such an interaction is occurring, in addition to looking into which domains bind DNA, research could be conducted into which domains interact with one another. However, these proteins may not make a physical interaction to function co-operatively, for example, they may each perform a different step which is required to fulfil their role.

SndA is the first extracellular DNase identified in *S. gordonii* and is required for all extracellular DNase activity. The *S. gordonii* genome comprises 2,196,662 nucleotides (Vickerman *et al.*, 2007). A single nucleotide is 0.33 nm in length within the DNA helix (Wilkins *et al.*, 1953), meaning the length of the whole *S. gordonii* genome is around 724 µm, much greater than the average length of eDNA in individual stranding events: 40 µm. A possible function of the extracellular DNase SndA is cleaving DNA to form the smaller length eDNA strands observed.

Another potential role for SndA is cleaving eDNA to allow *S. gordonii* to use the phosphate and sugar which comprise the DNA backbone as a nutrient

source. Of note, SndA is found in an operon which also contains two nutrient source proteins (PTS transporter unit and α-amylase). The presence of these genes in the same operon may indicate that these proteins are used simultaneously to provide *S. gordonii* with the necessary nutrient supply.

SndA shares homology with three cell wall anchored endonucleases, all of which have been implicated in immune subversion, virulence and persistence by cleavage of neutrophil extracellular traps: SWAN in *S. sanguinis*, EndA of *S. pneumoniae* (Zhu *et al.*, 2013), and MnuA of *Mycoplasma bovis* (Mitiku *et al.*, 2018). In systemic disease such as infective endocarditis clearance of the causative organism by the immune system is of paramount importance to the prevention and resolution of disease. *S. gordonii* can evade the immune system (Cho *et al.*, 2013; Ji & Choi, 2013). *S. sanguinis* lacking SWAN has been shown to be cleared more quickly by the immune system in mice (due to impaired NET degradation). Investigation into whether *S. gordonii* can degrade NETs to escape from neutrophils and whether this uses SndA, and if this can be prevented to reduce infective endocarditis disease burden, may be of future interest. The same methodology as used in Morita *et al*., 2014, could be used to investigate if SndA has a similar effect to SWAN on neutrophil NETs: human blood neutrophil clearance of bacterial infection and investigation of NETs degradation using microscopy. If this is the case, development of a therapeutic against the endonuclease activity of SndA may result in biofilms which are cleared more completely by the immune system, reducing bacteraemia and potentially infective endocarditis. Development of therapeutics against EndA to reduce the virulence of *S. pneumoniae* has begun (Peterson *et al.*, 2013 (B)).

SndA was also implicated in bacterial competence. SndA may degrade DNA to facilitate transformation – it shares 30% homology to EndA in *S. pneumoniae*, a surface bound endonuclease which fragments DNA prior to internalisation (Muschiol *et al.*, 2015). Unlike EndA, SndA has additionally been implicated in DNA binding.

Competence is the uptake of DNA from the environment. Stranding is also a process which involves extracellular DNA, so the effect of the competence system on stranding was investigated. In this project CSP was found to increase

eDNA stranding, however, this was found to be independent of the canonical receptor ComDE. Opp systems are a family of ATP-binding cassette oligopeptide permeases. A member of this family in *S. gordonii*, Hpp, has previously been associated with competence (Jenkinson *et al.*, 1996). In this study, a component of Hpp system (HppA) was found to influence eDNA stranding, furthermore, HppA was found to be required for the effect CSP had on eDNA stranding.

HppA determines the selectivity of the system by recognising and delivering peptides to the membrane complex (Doeven *et al.*, 2005). It forms part of the heterotrimeric membrane protein HppAGH (Jenkinson *et al.*, 1996). Disruption of HppA alone is likely to disrupt the function of the entire system. HppAGH has so far been demonstrated to be a hexa-hepta peptide permease (Jenkinson *et al.*, 1996). *S. gordonii* CSP is 19 amino acids in length (Håvarstein *et al.,* 1996). It is possible that extracellular interaction causes signal transduction which alters eDNA stranding, without requiring CSP entry to the cell. However, in other bacteria such as *L. lactis,* Opp family proteins are permeases to peptides between 4 and 35 amino acids in length (Detmers *et al.*, 2000). In this system, the whole peptide does not enter the recognition site of OppA (homologous to HppA in *S. gordonii*), despite the recognition site controlling the specificity in terms of peptide length. This presents a possible method whereby only part of the CSP sequence is recognised by HppA, but all of it may be translocated through the protein channel. Alternatively, CSP may be cleaved to a shorter length peptide prior to translocation into the cell through the Hpp system. To test this, peptides could be generated which are 7 amino acids long, which cover the length of CSP. This set of peptides could be added to Δ*comC* biofilms and the eDNA produced measured by the quantification technique devised in this work. If any of these 7 amino acid peptides cause restoration in stranding, the Hpp system is likely acting as a hexa-hepta peptide permease to fragments of CSP.

Further investigation was carried out into the mechanism of CSP (via Hpp) to induce eDNA stranding. One process of interest has been linked with eDNA release and competence: autolysis. Autolysins AtlS and LytF have been shown to be associated with eDNA release (Xu & Kreth, 2013). In this study AtlS and LytF mutants were found to have reduced eDNA stranding. These autolysins have also

been associated with competence. LytF is a competence regulated murein hydrolase (Berg *et al.*, 2012). Its expression is induced by ComX, a competence-specific sigma factor (Luo & Morrison, 2003). To confirm the link between ComX and LytF in eDNA stranding, a ΔcomX knock-out mutant could be generated. This is hypothesised to prevent activation of LytF, and therefore reduce eDNA stranding to ΔlytF levels.

Itzek *et al.*, 2011 showed hydrogen peroxide triggered eDNA release, and Xu & Kreth, 2013 showed this was LytF dependent. The work in this project has built on this, showing eDNA stranding in *S. gordonii* was modulated by hydrogen peroxide and that this required LytF. AtlS expression is upregulated by CSP (Liu & Burne, 2011). AtlS activity then induces expression of SpxB, which increases intracellular hydrogen peroxide concentration, activating LytF (Xu & Kreth, 2013). This study indicated there is a CSP-dependent DNA release event which requires autolysins AtlS and LytF, as a key part of the eDNA stranding mechanism. Because signalling via ComDE is known not to affect eDNA stranding, the alternative CSP sensor, the Hpp system, was also implicated. Xu & Kreth, 2013, also showed LytF was active only in a subpopulation of cells, which supports the theory of a sub-population event, such as lysis or alteration to the bacterial cell wall, through which gDNA can pass. An interesting question yet to be addressed is why LytF is only active in a subpopulation of cells, when all cells were thought to be exposed to similar conditions from the milieu? However, recent work has found that the different conditions experiences by cells within a single biofilm result in different bacterial phenotypes (Carvalho *et al.,* 2017).

This work found removing components now implicated upstream from eDNA stranding, such as ROS, CSP, CSP receptors, autolysins and DNA binding proteins, affects eDNA stranding but does not have an affect on biomass. When eDNA stranding is targeted directly, by DNase treatment, both eDNA stranding and biomass are reduced. This difference appears to undermine the role for eDNA in biofilm accretion. However, it is possible that when targeting upstream processes of eDNA stranding, the bacteria is able to sense this disruption and thus utilizes alternative systems to facilitate biofilm accretion. When DNase is

used, it is possible the bacteria cannot sense eDNA stranding has been disrupted, therefore will not induce alternative biofilm accretion pathways.

The schematic shown in Figure 6.2 summarises the effects seen with CSP on eDNA stranding during this project. Combined with the other data from these studies, we propose the mechanism illustrated in Figure 6.3 for eDNA stranding in *S. gordonii*, in which the Hpp system acts as a receptor for the CSP system. The autolysis pathway is then activated. AtlS expression is increased, which induces SpxB to create hydrogen peroxide, which activates LytF to degrade peptidoglycan. This leads to gDNA release and eDNA stranding - competence is not affected. DNA binding proteins SedA and SndA are implicated in binding to DNA to form enable strand formation once gDNA is outside of the cell. CSP signal transduction with ComDE is via autolysin activity of AtlS and LytF (which is fed into by hydrogen peroxide, a marker of oxidative stress). This results in cell lysis but does not affect eDNA stranding. Although the competence pathway and eDNA stranding pathway are both stimulated by CSP and involve the autolysins AtlS and LytF, they have different receptors and appear to have distinct functions. They also potentially occur during different phases of biofilm maturity. The mechanism behind the separation of these pathways is of great future interest.

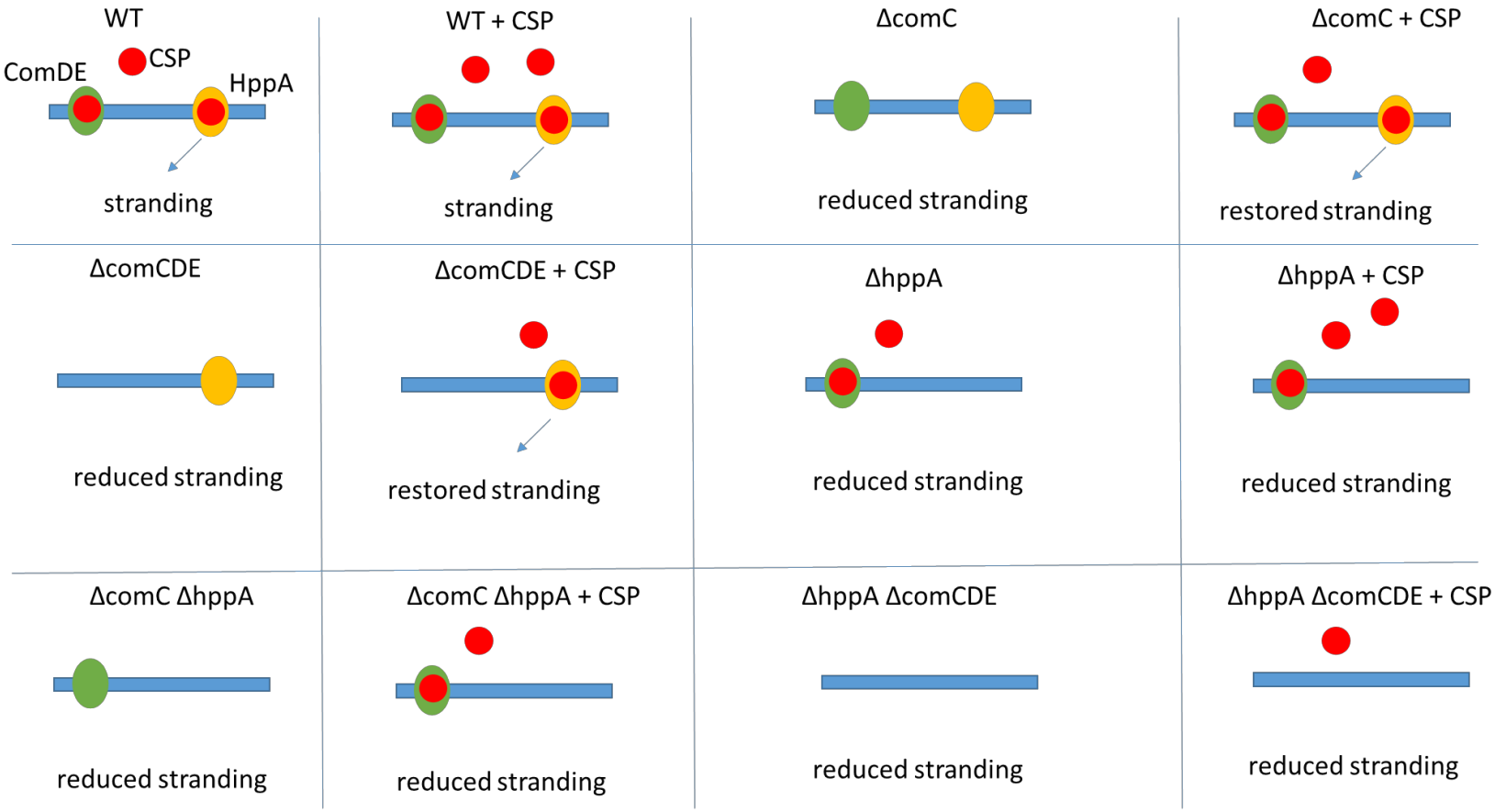

Figure 6.2 - Schematic summarising the effects of CSP on eDNA stranding – The input of mutant organism and addition of exogenous CSP change the components of the surface of S. gordonii (represented by blue line). By monitoring the effect on eDNA stranding of removal of the Com or Opp systems, a mechanism which uses both of these surface components was generated (Figure 6.2).

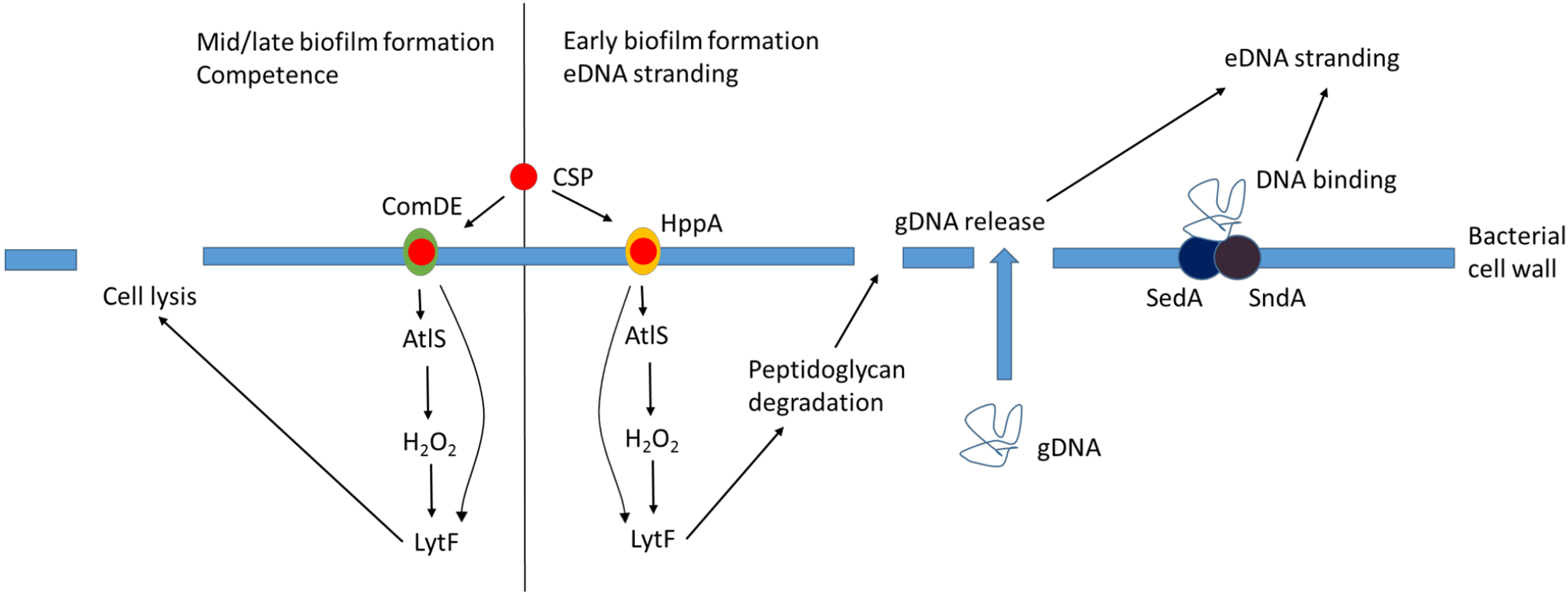

Figure 6.3 – Proposed eDNA stranding mechanism. The interaction of CSP and ComCDE, its affect on cell lysis and transformation is upheld in mature biofilms. In early biofilms however, the predominating mechanism which influences eDNA stranding is proposed to be via an alternative receptor system, Hpp. A similar downstream pathway via autolysins AtlS and LytF are hypothesised to affect the integrity of the membrane, causing cell lysis in late biofilms, and gDNA release, potentially via cell lysis, in early biofilms. Genomic DNA is then held at the surface by surface anchored SedA and SndA in a way which facilitates eDNA stranding.

6.3 Wider/future perspectives

eDNA contributes to the stability of oral biofilms (Schlafer *et al.*, 2017). This work has confirmed this in monospecies *S. gordonii* biofilms. In the context of the mouth, *S. gordonii* participates in multispecies interactions to form plaque. Future work could investigate the presence of eDNA strands in a multispecies biofilm, using the eDNA stranding measurement technique developed here. eDNA in biofilms has been found in biofilms formed by the salivary microcosm *in vitro*, as well as in subgingival plaque *in vivo* (Rostami *et al*., 2017). However, eDNA stranding was not measured quantitively preceding the development of the novel eDNA stranding technique in this work. A starting point for the examination of eDNA in multispecies biofilms would repeat the experiments of Rostami *et al.*, 2017, using the methodology developed here. This could probe the relative abundance of eDNA strands formed both *in vivo* from bacteria in the salivary microcosm and in different locations of oral biofilms *in vitro*, for instance sub gingival plaque vs plaque on dental implant abutments. Also of interest is the amount of eDNA each species of the biofilm contributes to the matrix. As eDNA stranding is found during early biofilm formation, it is hypothesised that colonisers such as *S. gordonii* may contribute more DNA to a mixed species biofilm than bacteria which join later, for instance, *P. gingivalis*. To test this, quantitative PCR could be used. A sensitive method such as this would allow for the detection of very small amounts of DNA. Following extraction of eDNA from a multispecies biofilms as in Section 3.2, primers against 16S rRNA specific to each organism in the biofilm could be used to determine the relative contribution each organism is making to the eDNA stranding network. This has the potential to inform which species DNA-targeted treatment strategies could focus on.

Many therapeutic strategies to disrupt eDNA networks focus on degradation of the DNA network using DNase. A DNA-degrading protein, NucB of *Bacillus licheniformis* (Nijland *et al*., 2010), appears to disrupt multispecies biofilms *in vitro* (Rostami *et al.*, 2017). The effect on eDNA stranding has not yet

been quantified – the eDNA stranding quantification technique could be used to achieve this. This would also help inform suitable concentration of NucB required to treat biofilms. One caveat to attempting DNase treatment of plaque would be the finding of Rostami *et al*., 2017, supported in this work, that post-treatment with DNase does not affect biofilm biomass. This means that if oral biofilms were collected and post-treated with DNase, no disruption may be seen. For this reason, continual exposure to DNase, and disruption of pre-existing biofilms may be required for DNase treatment to be effective. Therefore, a DNase containing-toothpaste which would allow for regular exposure to DNase, coupled with the mechanical disruption of biofilms from brushing, may result in lower biofilm formation. A standard technique which could be used for the quantification of the effect of an oral treatment on plaque accretion is plaque scoring (Claydon & Addy, 1995). Furthermore, oral plaque could be collected and the eDNA stranding quantification method used to confirm disruption of DNA networks within these biofilms. Plaque accretion is a risk factor for periodontal disease and dental caries, so a treatment of this nature has the potential to reduce oral disease. Oral diseases are found globally and affect between 20 and 50% of the population. Periodontal disease is also associated with poor outcomes in cardiovascular disease, diabetes and pregnancy (Nazir *et al*., 2017).

eDNA networks, as a major component of the EPS, contribute to biofilm stability, and therefore are hypothesised to shield bacteria from antimicrobials. DNase treatment can disrupt biofilms and when used in co-therapy with antibiotics, can increase their efficacy between 2- and 15-fold (Tetz *et al.*, 2009). This may allow for a reduction in antibiotic usage, which may help to combat rising antibiotic resistance. However, an abiotic mouth may not be healthy, with *S. gordonii* carriage known to modulate the mouth towards oral health.

Infective endocarditis treatment, on the other hand, relies on antibiotics and would also be aided by biofilm disruption. *S. gordonii* can colonise damaged aortic valves, which can cause infective endocarditis – this has around an 18% mortality rate at discharge (Wallace *et al.*, 2002). Dental surgeries are a risk factor for infective endocarditis - antibiotics have therefore been trailed as a prophylaxis following dental surgery, and whilst rates of bacteraemia reduced,

no strong evidence as found for reduction of infective endocarditis (Cahill *et al.*, 2017). This study has reinforced the importance of DNA in *S. gordonii* biofilms. Potentially, DNase: antibiotic co-therapy, as currently seen in cystic fibrosis treatment (Yang *et al*., 2010), could be used to treat infective endocarditis. Cystic fibrosis biofilms are particularly rich in DNA (around 2%), but this project has reinforced the effectiveness of DNase usage to disrupt biofilms with a lower DNA composition, i.e. *S. gordonii* at 0.7%. Biofilms could be harvested from IE patients and the novel eDNA quantification method used to find the amount of eDNA stranding within these biofilms. A model biofilm which produces the same amount of DNA could then be used to test the amount of DNase required for biofilm disruption. Intravenous DNase could be used as a prophylaxis in oral surgery to reduce risk of biofilm formation, and therefore thrombus formation to prevent infective endocarditis.

Currently, the recommended treatment of streptococcal infective endocarditis (IE) is four weeks of penicillin with two weeks of gentamycin (Gould *et al.*, 2012). Unfortunately, longer use of gentamycin is associated with nephrotoxicity (Mingeot-Leclercq & Tulkens, 1999). Vancomycin may be given instead of penicillin in two cases: if the patient is allergic to penicillin (around 10% of people), or if the streptococcal strain is resistant to penicillin. Recently 25% of streptococcal disease-causing strains are have been found to be resistant to penicillin, and a further 25% resistant to penicillin and one other antibiotic (Gaude *et al*., 2013). If DNase was used in co-therapy with antibiotics, a lower dosage of antibiotic may be required, reducing the risk of increasing bacterial antibiotic resistance from drug overuse. Furthermore, the treatment of IE may be shorted by DNase treatment, which may reduce the nephrotoxicity associated with long or high exposure to aminoglycosides such as gentamycin. Because DNase has already been approved for medical usage in therapeutics such as Pulmozyme (cystic fibrosis treatment), less testing would be required for a change-of-use, compared to a completely new drug. This project has identified another DNase, SndA, which may be suitable for use in the treatment of IE. A caveat to the usage of DNase in general is the potential for them to degrade NETs, which are important feature of the innate immune system.

These treatments rely on disruption of the DNA network by treatment with DNase. However, a less investigated route of disrupting eDNA networks is by targeting DNA-binding proteins. Huβ is a *P. gingivalis* DNAIIB family DNA binding protein. Antibodies were produced which were directed against this protein. These blocked the Huβ: DNA interaction. This resulted in *P. gingivalis* being unable to bind to eDNA networks in pre-formed Streptococcal biofilms (Rocco *et al*., 2018). A similar strategy could be used to developed therapeutic agent against *S. gordonii* biofilms. This project has identified SedA and SndA as DNA-binding proteins. If an antiserum was developed against these proteins, it may block DNA binding activity. These proteins are hypothesised to form anchor points on the cell to allow for an eDNA network to be formed, so blocking this may disrupt the network. It also has the potential to disrupt stranding by inhibition of the DNase activity SndA possesses. This activity is hypothesised to be used to remodel strands to form the eDNA network. The effects of antibodies on eDNA stranding could be quantified using the methodology developed in this work. If antisera was found to be successful at disrupting the eDNA network in *S. gordonii* biofilms, it could be investigated if this results in biofilms which are more easily disrupted by flow or therapeutic agents. The antisera could be given intravenously to treat biofilms formed in infective endocarditis. This strategy of treatment would be advantageous compared to DNase treatment, as the antibodies would not be capable of NETs degradation.

6.4 Conclusions

Through this work, a new tool for quantification of eDNA within biofilms has been developed that, in turn, has led to a greater understanding of the mechanism of eDNA stranding within *S. gordonii* biofilms. The role of eDNA stranding as a structural scaffold has been supported, and CSP has been shown to be a trigger for this process, providing evidence for an active eDNA release mechanism. The predominant CSP signalling pathway associated with eDNA stranding was shown to occur through the Hpp system via the autolysin pathway, involving AtlS and LytF. Two *S. gordonii* cell wall-anchored proteins, SedA and

SndA, have been identified which also modulate eDNA stranding levels. These proteins work co-operatively and most likely mediate their effects through direct binding to the eDNA strands. As a nuclease, SndA also has the potential to remodel eDNA strands, and was implicated in facilitating *S. gordonii* transformation. Expanding our knowledge of the mechanism of eDNA stranding in *S. gordonii* may help to elucidate this process in other bacterial species and could be used in the future to develop therapies that disrupt eDNA stranding as a strategy to combat biofilm-related diseases.

Chapter 7 Appendices

7.1 eDNA analysis code

7.1.1 Stack splitter (FIJI)

```
macro"StackSplit" {
run("Bio-Formats Macro Extensions");
inputDir = getDirectory("Choose a Source Directory");
inputFormat=newArray(".lif",".tif",  ".jpg", ".gif", ".png", ".pgm", ".bmp", ".fits",
".txt",  ".raw");
Dialog.create("Select options");
Dialog.addChoice("Input image type: ", inputFormat, "lif");
Dialog.addCheckbox("Select different output directory", true);
Dialog.show();
inputFormat= Dialog.getChoice();


if( Dialog.getCheckbox())
{
  outputDir = getDirectory("Choose an Output Directory");
}
else
{
  outputDir = inputDir;
}

fileList=getFileList(inputDir);

for(i=0; i<(fileList.length);i++)
{
print(fileList[i]);
if(endsWith(fileList[i],""+inputFormat+""))
{
filePath=inputDir+fileList[i];
print(filePath);

Ext.setId(filePath);
Ext.getCurrentFile(file);
print(file);
Ext.getSeriesCount(seriesCount);
```

```
print(seriesCount);

for(s=1; s<=seriesCount;s++)
{

run("Bio-Formats Importer", "open=["+filePath+"] color_mode=Default
split_channels view=Hyperstack stack_order=XYCZT use_virtual_stack
series_list="+s);
name=getTitle;
print(name);

NameLength=lengthOf(name);
Sub=substring(name,NameLength-3,NameLength);
name2=replace(name,Sub,"");
print(name2);
name3=replace(name2,"/"," - ");
numberOfImages=nImages;
print(numberOfImages);

if (numberOfImages==1){

saveAs("Tiff", outputDir+name3+"_Series-00"+s+".tif");
run("Close All");
}

if (numberOfImages==2){
selectWindow(name2+ "C=0");
saveAs("Tiff", outputDir+name3+"_Series-00"+s+".tif");
run("Close All");
//selectWindow(name2+"C=1");
//run("Close");
}
if (numberOfImages==3){
selectWindow(name2+"C=0");
saveAs("Tiff", outputDir+name3+"_Series-00"+s+".tif");
run("Close All");
//selectWindow(name2+"C=1");
//run("Close");
//selectWindow(name2+"C=2");
//run("Close");
}



}
}
}
```

}

7.1.2 eDNA strand identification (MATLAB)

```
clc
clear all
close all
%REMEMBER TO CHANGE xlsread1 folder!

% Parameters to edit-----------------------------------------
ThreshArea=25%25;%adaptive threshold search area
Filter=5;%after thresholding, objects smaller than this will be removed
Filter2=50;
circularityThresh = 0.99; %Set between 0 and 1, 1 = perfect circle
spotArea=500; %Max spot area (pixels)
filamentArea=0.5; % minimum filament size (pixels)
PlottingVar={'Condition 1','Condition 2','Condition 3'} %Names to plot
pixelSize=0.46;%0.2776; 0.46 for 20x lens no binning...
sol=0.6;
saveFolder = ''
excelFileNameOut=''
%-----------------------------------------------------------------


%Main Programme ---------------------------------------------------
MeanSpot=[];
filesMaster=[];

for bigExcel=1:length(PlottingVar)
   excelData=[];
   PV=strcat('*',PlottingVar(bigExcel),'*')
   files = dir(char(PV));
   filesMaster={filesMaster, files}
   for file = files'
      close all
      data=bfopen(file.name);
      im=data{1,1};
      I = imread(file.name); %Read in image and plot original
      [pathstr,name,ext] = fileparts(file.name);
      %[token, remain] = strtok(name, '_');
      %remain=remain(2:end-5);
      %name=strcat(token,'_',remain);
      [sizeX,sizeY]=size(I);
```

```
    % Create binary image
    focused=fstack(im);
    %focused2=imadjust(focused);
%       se=strel('disk', 50);
%       focused2 = imtophat(focused2,se);
%


    %focused=uint16(focused);
    %gaussFilt=fspecial('gaussian',[3 3], 0.5);
    %focusedtest = imfilter(focused,gaussFilt,'replicate');

    %cleanIm=noisecomp(focused,2,6,2,8,0);
    %background = imopen(focused,strel('disk',25));
    %focused2 = focused - background;

%       invert=imcomplement(focused);
%        h=fspecial('log', [5 5], 0.5);
%       logFocused=imfilter(invert,h,'replicate');
%


    h=fspecial('gaussian', [700 700], 5);
    longGauss=imfilter(focused,h,'replicate');
    bkSub=focused-longGauss;

    %mask=adaptivethreshold(bkSub,ThreshArea,-0.01,0);
    %mask = bwmorph(mask,'bridge');
    %mask = adaptivethresh(logFocused,200,-500);
    %mask=adaptivethreshold(focused,ThreshArea,-0.0065,0);
    mask=adaptivethreshold(bkSub,ThreshArea,-0.01,0);
    %level=graythresh(logFocused);
    %mask=im2bw(focused,level/50);

    mask = bwmorph(mask,'bridge');
    mask=bwareaopen(mask,Filter);
    se=strel('disk',1);
    mask=imclose(mask,se);

    mask=imdilate(mask,se);
    mask=imerode(mask,se);
    mask = bwmorph(mask,'bridge');
    mask=bwareaopen(mask,Filter2);
    se=strel('disk',3);
    mask=imclose(mask,se);
```

```
%       [B,L] = bwboundaries(mask,'noholes'); % find boundaries, label binary
image
%       stats = regionprops(L, 'All');


      cc = bwconncomp(mask);
      stats2 = regionprops(cc, 'Area','Eccentricity', 'Centroid', 'Solidity');
      idx = find([stats2.Solidity] < sol);
      BW2 = ismember(labelmatrix(cc), idx);
      %figure, imshow(BW2);
      statsFiltered=stats2(find([stats2.Solidity]<sol));

      skel=bwmorph(BW2, 'skel',Inf);
      skel=bwmorph(skel, 'spur', 6);
      merged=imfuse(focused,skel);


%       figure,imshow(label2rgb(labelmatrix(cc), @jet, [.5 .5 .5]))
%       hold on
%       for k = 1:length(statsFiltered)
%          metric = statsFiltered(k).Solidity;
%          % display the results
%          metric_string = sprintf('%2.2f',metric);
%          % mark objects above the threshold with a black circle
%          centroid = statsFiltered(k).Centroid;
%          plot(centroid(1),centroid(2),'ko');
%          text(centroid(1)-3,centroid(2)+3,metric_string,'Color','y',...
%             'FontSize',10,'FontWeight','bold');
%       end
%       hold off



      %Rescale pixels to microns
      for i=1:length(statsFiltered)
         statsFiltered(i).Area=pixelSize*(statsFiltered(i).Area);
      end

      %label filaments figure
      figure;
      tempIm=im2double(merged);

      for i=1:length(idx);
         filamentnumber=idx(i);
         filamentnumber_string = sprintf('%d',filamentnumber);
         centroidFilament=statsFiltered(i).Centroid;
         H=vision.TextInserter(filamentnumber_string);
```

```
            H.Color=[1,1,1];
            H.FontSize=12;
            H.Location=centroidFilament;
            tempIm=step(H,tempIm);

        end

        filamentName=strcat(name,'_filaments.tif');
        imwrite(tempIm,strcat(saveFolder,filamentName));

        %Saving and exporting data

        c=cell(1,length(idx));
        for t=1:length(idx)
            c(t)=cellstr(name)
        end
        TF=isempty(statsFiltered);
        if TF==0;

        filamentexport=struct2table(statsFiltered);
        tableFilamentIndex=table(idx.');
        filamentexport=[tableFilamentIndex filamentexport];

        filamentexport2=[c.' filamentexport]
        excelData=[excelData;filamentexport2];
        end

    end
    close all
    writetable(excelData,excelFileNameOut,'sheet',char(PlottingVar(bigExcel)));
end

%Plotting Graphs & saving data
Mean=zeros(1);
SD=zeros(1);
SE=zeros(1);
anovaData=[];
groupSize=[];
Excel = actxserver ('Excel.Application');

%File='O:\Documents\User Data\Debbie\Filament
measurment\test\2016_01_12_Filaments_new_output.xls'
File=fullfile(pwd,excelFileNameOut);
if ~exist(File,'file')
    ExcelWorkbook = Excel.Workbooks.Add;
    ExcelWorkbook.SaveAs(File,1);
    ExcelWorkbook.Close(false);
```

```
end
Excel.Workbooks.Open(File);

for j=1:length(PlottingVar)
   [stauts,sheets]=xlsfinfo(excelFileNameOut);
   startIndex = regexpi(sheets,PlottingVar(j));
   emptyCells = cellfun('isempty', startIndex);

   readInList=[];
   for i=1:length(sheets)
      if emptyCells(i)==0
         readInList=[readInList,sheets(i)]
      end
   end
   tic
   tempData=[];
   for i=1:length(readInList)
      tempData= [tempData; xlsread1(excelFileNameOut,char(readInList(i)),'C:C')];
      anovaData=[anovaData;
xlsread1(excelFileNameOut,char(readInList(i)),'C:C')];
   end
   toc
   groupSize=[groupSize length(tempData)];


   Mean(j)= mean(tempData);
   Median(j)= median(tempData);
   SD(j)= std(tempData);
   SE(j)=Mean(j)/sqrt(length(tempData));
   total(j)=sum(tempData);
   %scaledTotal(j)=total(j)/(length(filesMaster(j))/8.9638);%10.9329??
   scaledTotal(j)=total(j)/(length(unique(excelData.Var1_1))/8.9638);
end

figure
bar(Mean,'stacked','FaceColor',[0.5,0.5,1],'EdgeColor',[0.5,0.5,0.5])
hold on
errorbar(Mean,SE,'--k');
hold off
xlabel('Data group');
ylabel('Mean filament length (Microns)');

figure
bar(total, 'stacked','FaceColor',[0.5,1,0.5],'EdgeColor',[0.5,0.5,0.5])
xlabel('Data group');
ylabel('Total filament length (Microns)');
```

```
figure
bar(scaledTotal, 'stacked','FaceColor',[1,0.5,0.5],'EdgeColor',[0.5,0.5,0.5])
xlabel('Data group');
ylabel('Total filament length per unit area (microns/mm^2) ');

a=1;
b=0;
c=[];
counter=[];
qcount=[];
group=ones([length(anovaData),1]);


for q=1:length(groupSize)
   qcount=[qcount, q];
   for k=a:(a+groupSize(q)-1)
      counter=[counter k];
      group(k)=q*group(k);
   end
   a=a+groupSize(q);
   c=[c a];

end


[p,table,stats2]=anova1(anovaData,group);
c = multcompare(stats2);
figure();
box=boxplot(anovaData,group,'colorgroup',group,'labels',PlottingVar,'widths',0.5
,'symbol','k+','notch','on','factorseparator',1);
xlabel('Condition');
ylabel('Filament Length (Microns)');

Excel.ActiveWorkbook.Save;
Excel.Quit
Excel.delete
clear Excel
```

7.1.3 Data consolidation (MATLAB)

```
>> dist_per_px=0;letter=['A','B','C','D'];
for j=1:length(letter)
for i=1:6
```

```
excelData=[];
well=strcat('*well_',letter(j),mat2str(i),'*','.xlsx');
files=dir(well);
for k=1:length(files)
if dist_per_px ~= 0
tempData=xlsread(char(files(k).name),'Contours','E');
else
try;tempData=xlsread(char(files(k).name),'Contours','A:B');catch;end
end
excelData=[excelData;tempData];
end
if ~isempty(excelData)
xlswrite(strcat(['030317_rearranged_',strrep(well,'*','')]),excelData,'Contour
Lengths');
end
end
end
end
```

7.2 Mutant strain sequencing

7.2.1 ΔcbdB

Upstream of *cbdB* locus

```
1    GGAAGCGGAT TATGGGACCA ACAATATAAG AAAAACCACT TTAGCAAGGA CTATTTTAAG
61   GATGCTACTG TTGATCTTGG AGAAATTGAG GCGGCAGTTC CAGCGGGCGT CAAAGAAAAG
121  GAATTGAAAT TCCTCTGGGA TGGTAAATTC TACGCCTTGA CTTTTAGGAA ATAAATCATT
181  CGAACCGGAT ATTTTTCCGG TTTTTTTGTA GCATTTTGGA CCCAAAAAGT CAGAAGAAAT
241  TTGATTTAGT AGCACCAAAT TTAATTTGAA AGTTAATGTA ATTATTTGTT CAATGCTAGC
301  AAGTTAATGA AAATTGAATG AATATTAAAA AAAGACTGAT TACGTATGGT CTTTTTATTG
361  ATAGTATGGT AGAATGAAGG CGTAATGTAT CTATAAAAAT GTTTGCTTTT TTGTAAAGGT
421  AAACACTGAT AAGATGGGGA AATCAGTTAG TATACAATTA CATTGTACAT TCAAAACTGA
481  ATATTATGAG AAAGGAAGAT TGCATGAATA CATACGAACA AATTAATAAA GTGAAAAAAA
541  TACTTCGGAA ACATTTAAAA AATAACCTTA TTGGTACTTA CATGTTTGGA TCAGGAGTTG
601  AGAGTGGACT AAAACCAAAT AGTGATCTTG ACTTTTTAGT CGTCGTATCT GAACCATTGA
661  CAGATCAAAG TAAAGAAATA CTTATACAAA AAATTAGACC TATTTCAAAA AAAATAGGAG
721  ATAAAAGCAA CTTACGATAT ATTGAATTAA CAATTATTAT TCAGCAAGAA ATGGTACCGT
781  GGAATCATCC TCCCAAACAA GAATTTATTT ATGAGA
```

Downstream of *cbdB* locus

TTACAAGCAAAACGAAAAAATAAAAGAATATACGGAAATTATGACTTAGAGGAATTACTACCTGATATTCC
ATTTTCTGATGTGAGAAGAGCCATTATGGATTCGTCAGAGGAATTAATAGATAATTATCAGGATGATGAA
ACCAACTCTATATTAACTTTATGCCGTATGATTTTAACTATGGACACGAGTAAAATCATACCAAAAGATATT
GCGGGAAATGCAGTGGCTGAATCTTCTCCATTAGAACATAGGGAGAGAATTTTGTTAGCAGTTCGTAGTT
ATCTTGGAGAGAATATTGAATGGACTAATGAAAATGTAAATTTAACTATAAACTATTTAAATAACAGATTA
AAAAAATTATAAAACAAGAAACAAGTGTCAATGAAAATTGACGCTTGTTTTTTTATGTTTTGTACTTTTTAT
CAGAAATAAGCGACAGAACTGATCGGATAGAGATGACCGATAGCTTAGTAAGATTCTATGATTCTCCTAAT
TTTAGAAAAATCACTCATAAATATGAAAACGGCTTCATTCGTATTGAGATTATCCAACTTGTTTTATAAAAT
AAGGTGAAGAAAACTATAGGAATAGCTTGCTTCTATAAAATTGGAAGCGGTTACTTAGTGGAGGACCTTA
TGGAAAAAGGATATTGGAATCGTAAAAGAGTCTATAGCATCCGGAAATTTACTGTTGGTGCATGCTCAGT
GCTTATTGGAACTTGTGCAGTTTTGTTTGGAGCTAGTCTTTCTGCAGGAAATCCTGTTTATGCGGAAGAAG
TGGCCGTTAACGCTAGTGCTGAAAGCGTCAAAGAAGAAGGAATGATTGAGGAAGAGAACTCTGATAAAG
TAGTTGCCACTAGTGAATTGTCTGAGG

7.2.2 ΔpadA

Upstream of *padA* locus

ATGTGTATTTTGAATGGTTTACCAGCAAAACGAAAAAATAAAAGAATATACGGAAATTATGACTTAGAGG
AATTACTACCTGATATTCCATTTTCTGATGTGAGAAGAGCCATTATGGATTCGTCAGAGGAATTAATAGAT
AATTATCAGGATGATGAAACCAACTCTATATTAACTTTATGCCGTATGATTTTAACTATGGACACGAGTAAA
ATCATACCAAAAGATATTGCGGGAAATGCAGTGGCTGAATCTTCTCCATTAGAACATAGGGAGAGAATTTT
GTTAGCAGTTCGTAGTTATCTTGGAGAGAATATTGAATGGACTAATGAAAATGTAAATTTAACTATAAACT
ATTTAAATAACAGGTTGAAAAAATTATAATGTAAGATAGTCCAGGAGAGCTATGCTCTTCTGGTTACTATC
GTATTATTAGGAAAAAGATTAAAGGAAAATCATTATGGATAGAAAAAAGTTAATTAAGTTAGGAATCTCA
TTGCTAGCTGTTAATGCTTTGGGAGCAGTAGCCGTTTATAAATATCCTGAGCTGACACATGTACCTACTGTC
TATGCATAGGAAGTGCCTGGCGAGGATGAAGAAATTCCAGATGCATCTGAAGCGGAGGCGGCAGAGCAC
TTTAAGGGATCTGATGGATTAGTTTGCTTAACTGATCAATGAATTGAATCCAGATGATAAAAATTCTTTCGA
AAGATTAGTAGCCATGCTTTGCAAAATACAGAAAGGAACCATACTACTGCAGTATATGTCGATCACAGTTA
TAATGGAGAGAAAAGGTTCCGCCCAGGCTGACCCCCCCCTCCCAAGATTAGTTTATTTTTTTGACGGAGGG
CCTACGAGTCGGTGTATAGCGAACATCGTCTTCCTGTGGAGTGTAGAGTTTAGATAGTTACCTATCTACTTT

TTCCTGCCCTCACTCGAGCATCCACCGAAGCTGACGTCCAGCTACAGCATAGAGGAGAGAGAACGCAGTA
CTGTCCCTGTCCTTTCTACTTGCTAAGAGCAGCAGGATACGTATCCCCT

Downstream of *padA* locus

1 CGTAAAATCA TACCAAAAGA TATTGCGGGA AATGCAGTGG CTGAATCTTC TCCATTAGAA
61 CATAGGGAGA GAATTTTGTT AGCAGTTCGT AGTTATCTTG GAGAGAATAT TGAATGGACT
121 AATGAAAATG TAAATTTAAC TATAAACTAT TTAAATAACA GGTTGAAAAA ATTATAATGT
181 AAGATAGTCC AGGAGAGCTA TGCTCTTCTG GTTACTATCG TATTATTAGG AAAAAGATTA
241 AAGGAAAATC ATTATGGATA GAAAAAAGTT AATTAAGTTA GGAATCTCAG TGCTAGCTGT
301 TAATGCTTTG GGAGCAGTAG CCGTTTATAA ATATCCTGAG CTGACACATG TCCCTACTGT
361 CTATGCAGAG GAAGTGCCTG GTGAGGATGA AGAAATTCCA GATGCATCTG AAGCGCAAGC
421 AGCAGCGAAC TTTAAAAATC AAATGGATGA GTTTGAAAAA GCAATCAATG AATTCAATCC
481 AGATGATTCA GATACTAAGG AAAGTTTGCA GTATGCTTTG GAAGATGCAG AAGGGTACCA
541 TACTACTGCA GTTAATGCGA TCAAGAGCGA AGAAGGTAAG AAAGGTTTTG CCAAGTATGA
601 AGCTCGTTAC CAAGCTTTAA AAGCAAAAGC TCAAGCCCTT CTAAACGGTG AATCACCAAA
661 ACCTCAACCA GAGATTACGA CTCAGGACGT TACAGTCAAA GAACCAATCC TTTATGGATC
721 TTCAACCGTG CAAAATCCAG CTTTACCAAA AGGCACAAGA AACACAAAAG TTCAAGGTGT
781 CAATGGTGAA AAGGAAGTAA CCTACACAAT CACTTTAACA GATGGCAAGG AAACAGGCCG
841 TGTGAAAAAG TCTG

7.2.3 ΔpadB

Upstream of *padB* locus

1 TGATTCCCGA AATATAGGCT ACTGTAACCT TCAACGATAA ACCGAAAGTA ACGAATACAG
61 TAAACGTTTA TCCGCCAGAG CCAACTACAC CGCCGCAAAC ACCACCGCAT ACACCACCGA
121 CAACACCGGG TACGCCGCCA CCAACAACCC CAGATACGCC ACCAGCGCCT AAGGGTGACT
181 TGCCACCGGC ACCAACACCA GAGCCAGAAA AACCTAAGAA TATCTTGCCA AAAACAGGTA
241 CTTCTGCTAC TATGGTAAAT GAGGTGATTA TCGGAATGAT CCTTGTGCTG ATGGGACTTC
301 TTTTGAGAAG AAAACCAAAG CATTAATGTA AGATAGTCCA GGAGAGCTAT GCTCTTCTGG
361 TTACTATCGT ATTATTAGGA AAAAGATTAA AGGAAAATCA TTATGGAAAA ATCATTATGA
421 ATACATACGA ACAAATTAAT AAAGTGAAAA AAATACTTCG GAAACATTTA AAAAATAACC
481 TTATTGGTAC TTACATGTTT GGATCAGGAG TTGAGAGTGG ACTAAAACCA AATAGTGATC
541 TTGACTTTTT AGTCGTCGTA TCTGAACCAT TGACAGATCA AAGTAAAGAA ATACTTATAC
601 AAAAAATTAG ACCTATTTCA AAAAAAATAG GAGATAAAAG CAACTTACGA TATATTGAAT
661 TAACAATTAT TATTCAGCAA GAAATGGTAC CGTGGAATCA TCCTCCCAAA CAAGAATTTA
721 TTTATGAGAA GTACAGCTC

Downstream of *padB* locus

1 ATAGGGAGAG AATTTTGTTA GCAGTTCGTA GTTATCTTGG AGAGAATATT GAATGGACTA
61 ATGAAAATGT AAATTTAACT ATAAACTATT TAAATAACAG ATTAAAAAAA TTATAAGAAT
121 TAGCTTGAAA ATTAGGTTGA AAAAATAGAA GGCATTTGTC TTTAATTCTA CTGCTTTTCT
181 CAAAACAGAG GATTAGTAAA AATGCTATAA AAAGAGGCTG AGAGAATATC TCAGCCTCTT
241 TTTGAACCCT AACTTAAGAG ATAGGCTTAA AATCTAGCGT CAAATGAAAA GAAAAAAGCC
301 CGATCTTACG AGCTTTGTGT TCAGATGCTT CCTGATAAAT CAGGTTATAT AAGGCGGTAG
361 ACGGATTTGA ACCGACGATC AAGCTTTTGC AGAGCCGTGC CTTACCACTT GGCTATACCG
421 CCTCAACCTT TACTATTTTA CCTTAAAAAA GGACTTTCGT CAATACACTT GATTCTAAGA
481 AAATGAAATA ATACTGAAAA TCAGAAAAAT AAATGCTGAT AAAATCAAGG TTTTCGAGGA
541 AAAATAAAGC AAAAGAGCTT GTCAAATCCT TGAAATTCTG TTATCATAAT AGATGCCGTG
601 CAAATGGCAA AATACTCATT TTAGATG

7.2.4 ΔpalA

Upstream of *palA* locus

1 CCTGTCAAAA ATTGGTATGC AAGTGACAGT TGCGCTAGTG ACTTTGATTG CTCTTGCAAG
61 CATTTTGGGC TCTTTATTCA AAGTCAAGGA AGTTATGGAT ACAATAAATA CTTTGCCTTT
121 TTCACAAGCT TCTCTGCCTT GGCTACTTCC AGCTCTTTTA GGAATTATTT TGTCACTCAT
181 TTTGCCTGAT AAACAAAAGA GTGAATCTTT TGAAATTGAA GCATAAAAAC TTAAATTCAT
241 CACGATAGTG ATGGATTTTT TTGTTGAGTG TCAACAGTAG AAGATGTTTT ATAATTAAAT
301 ACGAACACAA AGCAATTTGG TGGCTTCTGT TAACCTTTGT TAAGAGATAT AATGTTTTTT
361 AGTTCCAGAT TATATTCTTG GAGAATAGCT AGTATATATA AAGTGTAGAA GCTTATTCTC
421 CTATTTTTTG ATGGGTGAAA AAAATATAAG TATTTTATAA GAAGGATTTA AGAAAAAATT
481 TAACTTTTTC TTATTCCTTT TTAATTTTAT GATTTTATAC TAGAGTCATA AAAAATATAA
541 GGAGGATCCT ATGAATACAT ACGAACAAAT TAATAAAGTG AAAAAAATAC TTCGGAAACA
601 TTTAAAAAAT AACCTTATTG GTACTTACAT GTTTGGATCA GGAGTTGAGA GTGGACTAAA
661 ACCAAATAGT GATCTTGACT TTTTAGTCGT CGTATCTGAA CCATTGACAG ATCAAAGTAA
721 AGAAATACTT ATACAAAAAA TTAGACCTAT TTCAAAAAAA ATAGGAGATA AAAGCAACTT
781 ACGATATATT GAATTAACAA TTATTATTCA GCAAGAAATG GTACCGTGGA ATCATCCTCC
841 CAAACAAGAA TTTATTTATG GAGAATGGTT ACAAGAGCTT TATG

Downstream of *palA* locus

1 GAACAAGGAT ACATTCCTCA GAAGGAATTA AATTCAGATT TAACCATAAT GCTTTACCAA
61 GCAAAACGAA AAAATAAAAG AATATACGGA AATTATGACT TAGAGGAATT ACTACCTGAT
121 ATTCCATTTT CTGATGTGAG AAGAGCCATT ATGGATTCGT CAGAGGAATT AATAGATAAT
181 TATCAGGATG ATGAAACCAA CTCTATATTA ACTTTATGCC GTATGATTTT AACTATGGAC
241 ACGAGTAAAA TCATACCAAA AGATATTGCG GGAAATGCAG TGGCTGAATC TTCTCCATTA
301 GAACATAGGG AGAGAATTTT GTTAGCAGTT CGTAGTTATC TTGGAGAGAA TATTGAATGG
361 ACTAATGAAA ATGTAAATTT AACTATAAAC TATTTAAATA ACAGATTAAA AAAATTATAA
421 GATTCAAATC ATTTAAAAAT TAGTAAAAAT AGTGTTATAC TAAAGCCAGT CTAACACTGT

481 TTTTATCAGG AGATAGTCAA ATGGAAAAGA CAATTTTACT TGTTGATGAT GAGGTGGATA
541 TCCTAGATAT CCAAAAACGT TATCTTTTGC AGGCTGGTTA CCAAGTTTTA GTGGCTCATG
601 ATGGATTGGA AGGTTTAGAA CTTTTCAAAA AAAAATCCGT TGACCTAATC ATCACAGATA
661 TCATGATGCC AAATATGGAT GGTTATGATT TTATCAGTGA GGTTCAGTAT TTAGCTCCTG
721 ATCAACCTTT TCTTTTTACA ACCGCTAAGA CCAGCGAGCA GGACAGGATT TATGGATTGA
781 GCTTGGGAGC AGATGATTTT ATCGCGAAAC CCTTTAGCCC TCGAGAGTTA GTTTAAGAGT
841 CAATAACATC TTGCGTCGTC TTCAGCGTGG GGACGAGACA GAACAAATTG AGCTCGGTGA
901 TTTAGTTATG AATCATGTGA CTCATGAGGT TCGTATTGGA GATCAATTTC TAGAATTAAC
961 AGTGAAATCC TTTGAACTAC TCTGGATATT AGCCAGTAAT CCTGAGAGAG TG

7.2.5 ΔsedA

Upstream of *sedA* locus

1 AAACAAGAAA AAATTCTGCT AGTTCATGGC CGTGGCTTCA ATTGGAAGGA TCCTGATCAT
61 TTCCGAATTG TATATTTGCC ACGTGTGGAT GAATTGGCCC AAGTGCAAGA AAAAATGACT
121 CGTTTCTTGC AACAATACCG GCGCTAATTG AATTAATAAA AGTCAAAAGA AGAATGAAAT
181 GTTCTTCTTT TTTTGTTGTT TAAATGGAAT AAGGCTAAAT TATTGTATCA GATGGTTTCT
241 AAATTAACCT TTTAAGTTAA ATAGTTCTAA TTATAAAATT GTTAAAAAAA TGAAATAAAT
301 GACATAAAAG CAGATCTAAA AAAATGGGAG TGGAAATTAT GTTTGTTTTT ATCAAGTTTT
361 CATATTTTTT TTATGTAACA TTTTAATGAC AAAGTTTTCG ATTCTCTTGT TTGAAGTCCA
421 AATGAACCTC ATAGCCACTT TTCTGTCAAA TCTAAAGATG GTAGAATAAT TCCATCATTA
481 TTTTACCAAT GATGAAAAGA TTTAAACACA AAGGAGAGTT TTTATGAATA CATACGAACA
541 AATTAATAAA GTGAAAAAAA TACTTCGGAA ACATTTAAAA AATAACCTTA TTGGTACTTA
601 CATGTTTGGA TCAGGAGTTG AGAGTGGACT AAAACCAAAT AGTGATCTTG ACTTTTTAGT
661 CGTCGTATCT GAACCATTGA CAGATCAAAG TAAAGAAATA CTTATACAAA AAATTAGACC
721 TATTTCAAAA AAAATAGGAG ATAAAAGCAA CTTACGATAT ATTGAATTAA CAATTATTAT
781 TCAGCAAGAA ATGGTACCGT GGAATCATCC TCCCAAACAA GAATTTATTT ATGAGA

Downstream of *sedA* locus

TAATGCTTTACCAAGCAAAACGAAAAAATAAAAGAATATACGGAAATTATGACTTAGAGGAATTACTACCT
GATATTCCATTTTCTGATGTGAGAAGAGCCATTATGGATTCGTCAGAGGAATTAATAGATAATTATCAGGA
TGATGAAACCAACTCTATATTAACTTTATGCCGTATGATTTTAACTATGGACACGAGTAAAATCATACCAAA
AGATATTGCGGGAAATGCAGTGGCTGAATCTTCTCCATTAGAACATAGGGAGAGAATTTTGTTAGCAGTT
CGTAGTTATCTTGGAGAGAATATTGAATGGACTAATGAAAATGTAAATTTAACTATAAACTATTTAAATAA
CAGATTAAAAAAATTATAAATTTTTGAAGAAGCTATAGATATAGTAAATAAGATAATAGGCCGGAAGTTA
GGGTGAGATAAGCTCCTAACTTCCTTTTATTTTTCACAAAAAAAGCGTTGAAATCCCAATAAATTTAAATCA
GGACCTCGCACTATTTTCAAAAAAATCTTGGTTTTGAAGGAACTAAAATCGTTTTTGGGATAAATTGTAAA
GAATTATTATTCAATAGGCAATTTTCAGATAATTATTGAAATTTCTGTCAATTTATGATATAATCAATCGGA
CTAAATGCGAGGTGGCTTATGGCACATTTATTAGAAAAAACAAGAAAAATTACATCTATTTTGAAGCGCTC
TGAAGAGCAACTTCAAGAAGAGTTGCCATACAATGACATTACAAGACAGTTAGCAGAAATTATGGACTGT
AATGCTTGTTTGT

7.2.6 ΔsndA

Upstream of *sndA* locus

1 ATGCTACACG ACTAGTTAGC GATAGAGTAG CTGCTCCAGC CGATACTAGA GAATATAATT
61 TAATATCACC ATAACAGCCT GTGCGGCGCC AGACACGCCA GATACGAGGA GTTAATAGCT
121 TTTATTACTG ATTCTCCAGA CGAGTAACTA TATTTTTTTT ATTTGTGGCG AGATATGTTT
181 GTTTGGGGGG CCGTGGGTTT TTTTTATACA CAGAAAAAAT ATGCCTTGCG TAAGGAACTG
241 CCCATCATAG CAGAAGGTAG CTATCAGCCA GCCTATGAGG ACAGTCCTCA GGTCTATGCC
301 TTTGAGCGGG AGTGGCAAGG ACAAAAGCTT TTGGTTTTGA ATAATTTTTA TATGGATCCA
361 ATTACAGTGG ATATCTTACC AGATTATCAA ACTGGTCAGG TCCTTTTATC CAATTACGGC
421 AGGACTCAGA TTGATCATAT TCTGACTCTA CAACCGTATG AAACGCTAGC TATTCTTGTT
481 AATTAAAAAT ACTATTTTGC AGTGAGGAAA GTTGATTTTT AGATATCGGT TTTCTTCACT
541 GTTTTTATAT ATTGACTGAT TTATCAAAAC TTATAACAGA AATGGAAGTA TGCATGAGTT
601 TAAGAAAACG TTTGCGAAAA TATTATTTTT TCTATATAAT ATAAACAGTA TAGTAATTAA
661 GTTTCATTAG GAAAAGGAGA ACTTTATGAA TACATACGAA CAAATTAATA AAGTGAAAAA
721 AATACTTCGG AAACATTTAA AAAATAACCT TATTGGTACT TACATGTTTG GATCAGGAGT
781 TGAGAGTGGA CTAAAACCAA ATAGTGATCT TGACTTTTTA GTCGTCGTAT CTGAACCATT
841 GACAGATCAA AGTAAAGAAA TACTTATACA AAAAATTAGA CCTATTTCAA AAAAAATAGG
901 AGATAAAAGC AACTTACGAT ATATTGAATT AACAATTATT ATTCAGCAAG AAATGGTACC
961 GTGGAATCAT CCTCCCAAAC AAGAATTTAT TTATGAGAAT GTACAAGAGC GCTCA

Downstream of *sndA* locus

TATGCTTTACCAAGCAAAACGAAAAAATAAAAGAATATACGGAAATTATGACTTAGAGGAATTACTACCTG
ATATTCCATTTTCTGATGTGAGAAGAGCCATTATGGATTCGTCAGAGGAATTAATAGATAATTATCAGGAT
GATGAAACCAACTCTATATTAACTTTATGCCGTATGATTTTAACTATGGACACGAGTAAAATCATACCAAAA
GATATTGCGGGAAATGCAGTGGCTGAATCTTCTCCATTAGAACATAGGGAGAGAATTTTGTTAGCAGTTC
GTAGTTATCTTGGAGAGAATATTGAATGGACTAATGAAAATGTAAATTTAACTATAAACTATTTAAATAAC
AGATTAAAAAAATTATAACCTAGAGTAAGCTCTAAACATCTTCGACACTCATCTATTCTTAGCAGAATAAGT
ATTTTGGGTTGAAAATAAAGTGACAGTAGTAGTTCATCATATCAACTATGATCTGCCTCTTGAGCTGAAGT
ATCGGATGCTTAAGATAGACTCGCTATATCTTCTTATGGTAATCAGTGGATCAATAAAATGATCCAGTTTGC
CATAAGATTGATATAGCTTTTTATTTTGAGTTTGTTTGAAGATAGGTGCCTAGCAAAAGAGCTCTTTGTGAA
AGCAATTTAGAAAATGCTTGAAAATCCAAGGAAATTATTTTATAATGAAGTGATAGTTTTGTTATAAAACG
ATCCTGTTGTTGTATATTTTTTTTGGAAAAGGAGATGATAAAATGAATAAAAAAATCTTGATGATGATTTTT
CTTCCCCTAACTCTACTATTCAGTCTATTTGTTACTCAAGGAAACAAGGTCTTTGCTACAGAACATGGAGAT
GTCATTACTCGGATGTATCTGACAGATAGTAAAGGAAACGAGCTCACTTCTTCTAATGTTGATCAGTGGCA
AGAATTTCGTATTAATGTGGAGTTTAAATTACACA

Chapter 8 References

Aas JA, Paster BJ, Stokes LN, Olsen I, Dewhirst FE. 2005. Defining the normal bacterial flora of the oral cavity. J Clin Microbiol 43:5721-5732.

Abranches J, Miller JH, Martinez AR, Simpson-Haidaris PJ, Burne RA, Lemos JA. 2011. The collagen-binding protein Cnm is required for *Streptococcus mutans* adherence to and intracellular invasion of human coronary artery endothelial cells. Infect Immun.;79(6):2277-2284.

Achtman M, Kennedy N, Skurray R. 1977. Cell--cell interactions in conjugating Escherichia coli: role of traT protein in surface exclusion. Proc Natl Acad Sci U S A 74:11:5104-8

Andrian E, Qi G, Wang J, Halperin SA, Lee SF. 2012. Role of surface proteins SspA and SspB of *Streptococcus gordonii* in innate immunity. Microbiology. 158(Pt 8):2099-106.

Ali Mohammed MM, Nerland AH, Al-Haroni M, Bakken V. 2013. Characterization of extracellular polymeric matrix, and treatment of *Fusobacterium nucleatum* and *Porphyromonas gingivalis* biofilms with DNase I and proteinase K. J Oral Microbiol. 5: 2000-2297.

Alkhawam, H, Sogomonian, R, Zaiem, F, Vyas, N, El-Hunjul, M, Jolly, J, Al-Khazraji, A. & Ashraf, A. .2016. Morbidity and mortality of infective endocarditis in a hospital system in New York City serving a diverse urban population. J Investig Med, 64: 1118-23.

Ashwinkumar Subramenium G, Viszwapriya D, Iyer PM, Balamurugan K, Karutha Pandian S. 2015. covR Mediated Antibiofilm Activity of 3-Furancarboxaldehyde Increases the Virulence of Group A *Streptococcus*. PLoS One, 10:5:e0127210.

Avilés-Reyes A, Miller JH, Simpson-Haidaris PJ, Lemos JA, Abranches J. 2014. Cnm is a major virulence factor of invasive *Streptococcus mutans* and part of a conserved three-gene locus. Mol Oral Microbiol. 29:1:11-23.

Back CR, Douglas SK, Emerson JE, Nobbs AH, Jenkinson. 2015. *Streptococcus gordonii* DL1 adhesin SspB V-region mediates coaggregation via receptor polysaccharide of *Actinomyces oris* T14V. Mol Oral Microbiol 30:5:411-24.

Back CR, Sztukowska M, Till M, Lamont R, Jenkinson H, Nobb A, Race P. 2017. The *Streptococcus gordonii* Adhesin CshA Protein Binds Host Fibronectin via a Catch-Clamp Mechanism. J Biol Chem. 292:5:1538-1549.

Bae T, Schneewind O. 2003. The YSIRK-G/S motif of staphylococcal protein A and its role in efficiency of signal peptide processing. J Bacteriol, 185:9:2910-9.

Balaban, NQ, Merrin, J, Chait, R, Kowalik, L & Leibler, S. 2004. Bacterial persistence as a phenotypic switch. Science, 305: 1622-5.

Baliga S, Muglikar S, Kale R. 2013. Salivary pH: A diagnostic biomarker. J Indian Soc Periodontol. 17:4: 461-5.

Bamford CV, d'Mello A, Nobbs AH, Dutton LC, Vickerman MM, Jenkinson HF. 2009. *Streptococcus gordonii* modulates Candida albicans biofilm formation through intergeneric communication. Infect Immun, 77:9:3696-704.

Bao, K, Bostanci, N, Thurnheer, T & Belibasakis, GN. 2017. Proteomic shifts in multi-species oral biofilms caused by *Anaeroglobus geminatus*. Scientific Reports volume 7, Article number: 4409.

Barnes AM, Ballering KS, Leibman RS, Wells CL, Dunny GM. 2012. *Enterococcus faecalis* produces abundant extracellular structures containing DNA in the absence of cell lysis during early biofilm formation. MBio. 3:4:e00193-12,

Bateman A, Holden M, Yeats C. 2005. The G5 domain: a potential N-acetylglucosamine recognition domain involved in biofilm formation. Bioinformatics, 21:8:1301-3.

Bensing BA, Sallam PM. 2002. An accessory sec locus of *Streptococcus gordonii* is required for export of the surface protein GspB and for normal levels of binding to human platelets. Mol Microbiol. 44:4:1081-94.

Bensing BA, Gibson BW, Sullam PM. 2004. The *Streptococcus gordonii* Platelet Binding Protein GspB Undergoes Glycosylation Independently of Export. Journal of Bacteriology. 186(3):638-645.

Berg K, Ohnstad H, Havarstein L. 2012. LytF, a novel competence-regulated murein hydrolase in the genus *Streptococcus*. J Bacteriol, 194:3:627-35.

Blesa A, Berenguer J. 2015. Contribution of vesicle-protected extracellular DNA to horizontal gene transfer in Thermus spp. Int Microbiol, 18:3:177-87.

Boström M, Deniz V, Franks GV, Ninham BW. 2006. Extended DLVO theory: electrostatic and non-electrostatic forces in oxide suspensions. Adv Colloid Interface Sci, 123-126:5-15.

Brackman G, Breyne K, De Rycke R, Vermote A, Van Nieuwerburgh F, Meyer E, Van Calenbergh S, Coenye T. 2016. The Quorum Sensing Inhibitor Hamamelitannin Increases Antibiotic Susceptibility of *Staphylococcus aureus* Biofilms by Affecting Peptidoglycan Biosynthesis and eDNA Release. Sci Rep, 6:20321.

Bradshaw D, Marsh P. 1998. Analysis of pH–Driven Disruption of Oral Microbial Communities in vitro. Caries Res. 32:456-462

Brandt T, Breitenstein S, von der Hardt H, Tümmler B. 1995. DNA concentration and length in sputum of patients with cystic fibrosis during inhalation with recombinant human DNase. Thorax, 5:8:880-2.

Burkovski A. 1997. Rapid detection of bacterial surface proteins using an enzyme-linked immunosorbent assay system. J Biochem Biophys Methods. 34(1):69-71.

Cabral DJ, Wurster JI, Flokas ME, Alevizakos M, Zabat M, Korry BJ, Rowan AD, Sano WH, Andreatos N, Ducharme RB, Chan PA, Mylonakis E, Fuchs BB, Belenky P. 2017. The salivary microbiome is consistent between subjects and resistant to impacts of short-term hospitalization. Sci Rep 7:1:11040.

Cahill TJ, Dayer M, Prendergast B, Thornhill M. 2017. Do patients at risk of infective endocarditis need antibiotics before dental procedures? Bmj, 358:j3942.

Carrolo M, Frias MJ, Pinto FR, Melo-Cristino J, Ramirez M. 2010. Prophage spontaneous activation promotes DNA release enhancing biofilm formation in *Streptococcus pneumoniae*. PLoS One, 5:12:e15678.

Cavalcanti IM, Del Bel Cury AA, Jenkinson HF, Nobbs AH. 2017. Interactions between *Streptococcus oralis*, *Actinomyces oris*, and *Candida albicans* in the development of multispecies oral microbial biofilms on salivary pellicle. Mol Oral Microbiol, 32:1:60-73.

Cekici, A, Kantarci, A, Hasturk, H & Van Dyke, TE. 2014. Inflammatory and immune pathways in the pathogenesis of periodontal disease. Periodontol 2000. 2014 Feb; 64(1): 57–80.

Chaudhuri B, Rojek J, Vickerman MM, Tanzer JM, Scannapieco FA. 2007. Interaction of Salivary alpha-Amylase and Amylase-Binding-Protein A (AbpA) of *Streptococcus gordonii* with Glucosyltransferase of *S. gordonii* and *Streptococcus mutans*. BMC Microbiology. 7:60.

Chen CY, Ezzeddine N, Shyu AB. 2008. Messenger RNA half-life measurements in mammalian cells. Methods Enzymol. 448:335-357.

Cho 1, Arimoto T, Igarashi T, Yamamoto M. 2013. Involvement of lipoprotein PpiA of *Streptococcus gordonii* in evasion of phagocytosis by macrophages. Mol Oral Microbiol, 28:5:379-91.

Christie J, McNab R, Jenkinson HF. 2002. Expression of fibronectin-binding protein FbpA modulates adhesion in *Streptococcus gordonii*. Microbiology, 148:6:1615-25.

Cisar JO, Kolenbrander PE, McIntire FC. 1979. Specificity of coaggregation reactions between human oral streptococci and strains of *Actinomyces viscosus* or *Actinomyces naeslundii*. Infect Immun, 24:3:742-52.

Claessen D, Rozen DE, Kuipers OP, Søgaard-Andersen L, van Wezel GP. 2014. Bacterial solutions to multicellularity: a tale of biofilms, filaments and fruiting bodies. Nat Rev Microbiol, 12:2:115-24.

Collins LM, Dawes C. 1987. The surface area of the adult human mouth and thickness of the salivary film covering the teeth and oral mucosa. J Dent Res, 66:8:1300-2.

Conrad A, Suutari MK, Keinänen MM, Cadoret A, Faure P, Mansuy-Huault L, Block JC. 2003. Fatty acids of lipid fractions in extracellular polymeric substances of activated sludge flocs. Lipids, 38:10:1093-105.

Cook, GS, Costerton, JW, Lamont, RJ. 1998, Biofilm formation by *Porphyromonas gingivalis* and *Streptococcus gordonii*. Journal of Periodontal Research, 33: 323-327.

Cramer GW, Bosso JA. 1996. The role of dornase alfa in the treatment of cystic fibrosis. Ann Pharmacother, 30:6:656-61.

Czaikoski PG, Mota JM, Nascimento DC, Sônego F, Castanheira FV, Melo PH, Scortegagna GT, Silva RL, Barroso-Sousa R, Souto FO, Pazin-Filho A, Figueiredo F, Alves-Filho JC, Cunha FQ. 2016. Neutrophil Extracellular Traps Induce Organ Damage during Experimental and Clinical Sepsis. PLoS One, 11:2:e0148142.

D'Urzo N, Martinelli M, Pezzicoli A, De Cesare V, Pinto V, Margarit I, Telford JL, Maione D. 2014. Acidic pH strongly enhances in vitro biofilm formation by a subset of hypervirulent ST-17 *Streptococcus agalactiae* strains. Appl Environ Microbiol, 80:7:2176-85.

Dani S, Prabhu A, Chaitra KR, Desai NC, Patil SR, Rajeev R. 2016. Assessment of *Streptococcus mutans* in healthy versus gingivitis and chronic periodontitis: A clinico-microbiological study. Contemp Clin Dent. India, v.7, 2016. p.529-34.

Das T, Sharma PK, Busscher HJ, van der Mei HC, Krom BP. 2010. Role of extracellular DNA in initial bacterial adhesion and surface aggregation. Appl Environ Microbiol, 76:10:3405-8.

Davies, DG, Parsek, MR, Pearson, JP, Iglewski, BH, Costerton, JW & Greenberg, EP. 1998. The involvement of cell-to-cell signals in the development of a bacterial biofilm. Science, 280: 295-8.

Dyke K. G., Jevons M. P., Parker M. T. 1966. Penicillinase production and intrinsic resistance to penicillins in *Staphylococcus aureus*. Lancet 1:835–838

De Furio M, Ahn SJ, Burne RA, Hagen SJ. 2017.Oxidative Stressors Modify the Response of *Streptococcus mutans* to Its Competence Signal Peptides. Appl Environ Microbiol, 83:22.

Decker EM, Klein C, Schwindt D, von Ohle C. 2014. Metabolic activity of *Streptococcus mutans* biofilms and gene expression during exposure to xylitol and sucrose. Int J Oral Sci, 6:4:195-204.

DeDent A, Bae T, Missiakas DM, Schneewind O. 2008. Signal peptides direct surface proteins to two distinct envelope locations of *Staphylococcus aureus*. Embo j, 27:20:2656-68.

DeFrancesco AS, Masloboeva N, Syed AK, DeLoughery A, Bradshaw N, Li G, Gilmore MS, Walker S, Losick R. 2017. Genome-wide screen for genes involved in eDNA release during biofilm formation by *Staphylococcus aureus*. Proc Natl Acad Sci U S A, 114:29:E5969-e5978.

Detmers FJM, Lanfermeijer FC, Abele R, Jack RW, Tampé R, Konings WN, Poolman B. 2000. Combinatorial peptide libraries reveal the ligand-binding mechanism of the oligopeptide receptor OppA of *Lactococcus lactis*. Proc Natl Acad Sci U S A, 97:23:12487-92.

Devaraj A, Justice SS, Bakaletz LO, Goodman SD. 2015. DNABII proteins play a central role in UPEC biofilm structure. Mol Microbiol, 96:6:1119-35.

Dewhirst FE, Chen T, Izard J, Paster BJ, Tanner AC, Yu WH, Lakshmanan A, Wade WG. 2010. The human oral microbiome. J Bacteriol, 192:19:5002-17.

Doern CD, Roberts AL, Hong W, Nelson J, Lukomski S, Swords WE, Reid SD. 2009. Biofilm formation by group A *Streptococcus*: a role for the streptococcal regulator of virulence (Srv) and streptococcal cysteine protease (SpeB). Microbiology, 155:1:46-52.

Doeven MK, Kok L, Poolman B. 2005. Specificity and selectivity determinants of peptide transport in *Lactococcus lactis* and other microorganisms. Mol Microbiol, 57:3:640-9.

Donlan RM, Costerton JW. 2002. Biofilms: survival mechanisms of clinically relevant microorganisms. Clin Microbiol Rev 15:2:167-93.

Dorkhan M, Svensater G, Davies JR. 2013. Salivary pellicles on titanium and their effect on metabolic activity in *Streptococcus oralis*. BMC Oral Health, 13:32.

Duong F, Wickner W. 1997. The SecDFyajC domain of preprotein translocase controls preprotein movement by regulating SecA membrane cycling. Embo j, 16:16:4871-9.

Egland PG, Du LD, Kolenbrander PE. 2001. Identification of Independent *Streptococcus gordonii* SspA and SspB Functions in Coaggregation with Actinomyces naeslundii. Infect Immun, 69:2001:7512-6.

Egland PG, Palmer RJ, Kolenbrander PE. 2004. Interspecies communication in *Streptococcus gordonii-Veillonella atypica* biofilms: signalling in flow conditions requires juxtaposition. Proc Natl Acad Sci U S A, 101:48:16917-22.

Engen SA, Rørvik GH, Schreurs O, Blix IJ, Schenck K. 2017. The oral commensal *Streptococcus mitis* activates the aryl hydrocarbon receptor in human oral epithelial cells. Int J Oral Sci, 9:3:145-50.

Facklam R. 2002. What Happened to the Streptococci: Overview of Taxonomic and Nomenclature Changes. Clin Microbiol Rev, 15:2002:613-30.

Fang J, Wei Y. 2011. Expression, purification and characterization of the *Escherichia coli* integral membrane protein YajC. Protein Pept Lett, 18:6:601-8.

Feigelman R, Kahlert CR, Baty F, Rassouli F, Kleiner RL, Kohler P, Brutsche MH, von Mering C. 2017. Sputum DNA sequencing in cystic fibrosis: non-invasive access to the lung microbiome and to pathogen details. Microbiome London, 5.

Fernández-Piñar R, Cámara M, Dubern JF, Ramos JL, Espinosa-Urgel M. 2011. The *Pseudomonas aeruginosa* quinolone quorum sensing signal alters the multicellular behaviour of *Pseudomonas putida* KT2440. Res Microbiol, 162:8:773-81.

Fernandez, CE, Aspiras, MB, Dodds, MW, Gonzalez-Cabezas, C & Rickard, AH. 2017. The effect of inoculum source and fluid shear force on the development of in vitro oral multispecies biofilms. J Appl Microbiol, 122: 796-808.

Ferrer MD, Mira A. 2016. Oral Biofilm Architecture at the Microbial Scale. Trends Microbiol, 24:4:246-248.

File, TM, Jr. (2004) *Streptococcus pneumoniae* and community-acquired pneumonia: a cause for concern. Am J Med, 117 Suppl 3A: 39s-50s.

Fitzgerald, JR, Foster, TJ & Cox, D. 2006. The interaction of bacterial pathogens with platelets. Nat Rev Microbiol, 4: 445-57.

Flemming HC, Wingender J. 2010. The biofilm matrix. Nat Rev Microbiol, 8:9:623-33.

Flemming HC, Wingender J, Szewzyk U, Steinberg P, Rice SA, Kjelleberg S. 2016. Biofilms: an emergent form of bacterial life. Nat Rev Microbiol, 14:9:563-75.

Flynn RL, Zou L. 2010. Oligonucleotide/oligosaccharide-binding fold proteins: a growing family of genome guardians. Crit Rev Biochem Mol Biol. 45(4):266-275.

Fontaine L, Boutry C, de Frahan MH, Delplace B, Fremaux C, Horvath P, Boyaval P, Hols P. 2010. A novel pheromone quorum-sensing system controls the development of natural competence in *Streptococcus thermophilus* and *Streptococcus salivarius*. J Bacteriol, 192:5:1444-54.

Forssten SD, Bjorklund M, Ouwehand AC. 2010. *Streptococcus mutans*, Caries and Simulation Models. Nutrients 2:290-8.

Foster TJ, Geoghegan JA, Ganesh VK, Höök M. 2014. Adhesion, invasion and evasion: the many functions of the surface proteins of *Staphylococcus aureus*. Nat Rev Microbiol. 12(1):49-62.

Frencken JE, Sharma P, Stenhouse L, Green D, Laverty D, Dietrich T. 2017. Global epidemiology of dental caries and severe periodontitis - a comprehensive review. J Clin Periodontol, 44 Suppl 18:S94-s105.

Frenkel ES, Ribbeck K. 2015. Salivary Mucins Protect Surfaces from Colonization by Cariogenic Bacteria. Applied and Environmental Microbiology. 81:1:332-338.

Gaasbeek EJ, Wagenaar JA, Guilhabert MR, Wösten MM, van Putten JP, van der Graaf-van Bloois L, Parker CT, van der Wal FJ. 2009. A DNase encoded by integrated element CJIE1 inhibits natural transformation of *Campylobacter jejuni*. J Bacteriol, 191:7:2296-306.

Gardan R1, Besset C, Guillot A, Gitton C, Monnet V. 2009. The oligopeptide transport system is essential for the development of natural competence in *Streptococcus thermophilus* strain LMD-9. J Bacteriol, 191:14:4647-55.

Gaude S. 2013. Rising bacterial resistance to beta-lactam antibiotics: Can there be solutions? H, J. Journal of Dr NTR University of Health Sciences 2: 4-9.

Giomarelli B, Visai L, Hijazi K, Rindi S, Ponzio M, Iannelli F, Speziale P, Pozzi G. 2006. Binding of *Streptococcus gordonii* to extracellular matrix proteins. FEMS Microbiol Lett, 265:2:172-7.

Gloag ES, Turnbull L, Huang A, Vallotton P, Wang H, Nolan LM, Mililli L, Hunt C, Lu J, Osvath SR, Monahan LG, Cavaliere R, Charles IG, Wand MP, Gee ML, Prabhakar R, Whitchurch CB. 2013. Self-organization of bacterial biofilms is facilitated by extracellular DNA. Proc Natl Acad Sci U S A, 110:28:11541-6.

Goldberg M, Kulkarni AB, Young M, Boskey A. 2011. Dentin: structure, composition and mineralization. Front Biosci (Elite Ed), 3:711-35.

Goodman SD, Obergfell KP, Jurcisek JA, Novotny LA, Downey JS, Ayala EA, Tjokro N, Li B, Justice SS, Bakaletz LO. 2011. Biofilms can be dispersed by focusing the immune system on a common family of bacterial nucleoid-associated proteins. Mucosal Immunol, 4:6:625-37.

Gould FK, Denning DW, Elliott TS, Foweraker J, Perry JD, Prendergast BD, Sandoe JA, Spry MJ, Watkin RW. 2012. Guidelines for the diagnosis and antibiotic treatment of endocarditis in adults: a report of the Working Party of the British Society for Antimicrobial Chemotherapy. J Antimicrob Chemother, 67:2:269-89.

Green ER, Mecsas J. 2016. Bacterial Secretion Systems – An overview Microbiol Spectr, 4:1.

Guo L, He X, Shi W. 2014. Intercellular communications in multispecies oral microbial communities. Front Microbiol, 5:328.

Gunput ST, Wouters D, Nazmi K, Cukkemane N, Brouwer M, Veerman EC & Ligtenberg, AJ. 2016. Salivary agglutinin is the major component in human saliva that modulates the lectin pathway of the complement system. Innate Immun, 22: 257-65.

Hall-Stoodley L, Nistico L, Sambanthamoorthy K, Dice B, Nguyen D, Mershon WJ, Johnson C, Hu FZ, Stoodley P, Ehrlich GD, Post JC. 2008. Characterization of biofilm matrix, degradation by DNase treatment and evidence of capsule downregulation in *Streptococcus pneumoniae* clinical isolates. BMC Microbiol, 8:173.

Hanahan D. 1983. Studies on transformation of *Escherichia coli* with plasmids. J Mol Biol, 166:4:557-80.

Hannig, M. 2002. The protective nature of the salivary pellicle. International Dental Journal Volume 52 (S5)417-423.

Hans R, Thomas S, Garla B, Dagli RJ, Hans MK. 2016. Effect of Various Sugary Beverages on Salivary pH, Flow Rate, and Oral Clearance Rate amongst Adults. Scientifica (Cairo). 2016:5027283.

Harmsen M, Lappann M, Knochel S, Molin S. 2010. Role of extracellular DNA during biofilm formation by *Listeria monocytogenes*. Appl Environ Microbiol. 76(7):2271-2279.

Havarstein LS, Gaustad P, Nes IF, Morrison DA. 1996. Identification of the streptococcal competence-pheromone receptor. Mol Microbiol. 21(4):863-869.

Haworth JA, Jenkinson HF, Petersen HJ, Back CR, Brittan JL, Kerrigan SW, Nobbs AH. 2017. Concerted functions of *Streptococcus gordonii* surface proteins PadA and Hsa mediate activation of human platelets and interactions with extracellular matrix. Cell Microbiol, 19:1.

Hedge MN, Sajnani AR. 2017. Salivary Proteins—A Barrier on Enamel Demineralization: An in vitro Study. Int J Clin Pediatr Dent, 10:1:10-3.

Hendrickx AP, Budzik JM, Oh SY, Schneewind O. 2011. Architects at the bacterial surface - sortases and the assembly of pili with isopeptide bonds. Nat Rev Microbiol, 9:3:166-76.

Heng N, Tagg JR, Tompskins GR. 2006. Identification and characterization of the loci encoding the competence-associated alternative sigma factor of *Streptococcus gordonii*. FEMS Microbiol Lett 259:1:27-34.

Heo SM, Ruhl S, Scannapieco FA. 2013. Implications of salivary protein binding to commensal and pathogenic bacteria. J Oral Biosci, 55:4:169-74.

Heo SM, Choi KS, Kazim LA. 2013. Host Defense Proteins Derived from Human Saliva Bind to *Staphylococcus aureus*. Infection and Immunity. 81(4):1364-1373

Hodges NA, Gordon CA. 1991. Protection of *Pseudomonas aeruginosa* against ciprofloxacin and beta-lactams by homologous alginate. Antimicrob Agents Chemother.35(11):2450-2452.

Hoiby N, Bjarnsholt T, Moser C. 2017. Diagnosis of biofilm infections in cystic fibrosis patients. Apmis. 125(4):339-343.

Holland TL, Baddour L M, Bayer AS, Hoen B, Miro JM & Fowler VG, Jr. 2016. Infective endocarditis. Nat Rev Dis Primers. 2: 16059.

Hope CK & Wilson M. 2006. Biofilm structure and cell vitality in a laboratory model of subgingival plaque. J Microbiol Methods, 66: 390-8.

Hostacká A, Ciznár I, Stefkovicová M. 2010. Temperature and pH affect the production of bacterial biofilm. Folia Microbiol (Praha), 55:1:75-8.

Horstkotte D, Task Force M, Follath F, Gutschik E, Lengyel M, Oto A, Pavie A, Soler-Soler J, Thiene G, von Graevenitz A, Priori SG. 2015. ESC Guidelines for the management of infective endocarditis. European Heart Journal, 36(44)3075–3128.

How KY, Song KP, Chan KG. 2016. *Porphyromonas gingivalis*: An Overview of Periodontopathic Pathogen below the Gum Line. Frontiers in Microbiology. 7:53.

Huang R, Li M, Gregory R. 2011. Bacterial interactions in dental biofilm. Virulence. 2(5)435–444.

Huang X, Browngardt CM, Jiang M, Ahn SJ, Burne RA, Nascimento MM. 2018. Diversity in Antagonistic Interactions between Commensal Oral Streptococci and *Streptococcus mutans*. Caries Res, 52:1-2:88-101.

Hubrich F, Juneja P, Müller M, Diederichs K, Welte W, Andexer JA. 2015. Chorismatase Mechanisms Reveal Fundamentally Different Types of Reaction in a Single Conserved Protein Fold. J Am Chem Soc, 137:34:11032-7.

Humphrey SP, Williamson RT. 2001. A review of saliva: normal composition, flow, and function. J Prosthet Dent, 85:2:162-9.

Humphries J, Xiong L, Liu J, Prindle A, Yuan F, Arjes HA, Tsimring L, Süel GM. 2017. Species-independent attraction to biofilms through electrical signalling. Cell, 168:1-2:200-209.

Hung CS, Henderson JP. 2009. Emerging concepts of biofilms in infectious diseases. Mo Med 106:4:292-6.

Huttenhower C. 2012. Structure, function and diversity of the healthy human microbiome. Nature 486:7402:207-14.

Hwang G, Klein MI & Koo H. 2014. Analysis of the mechanical stability and surface detachment of mature *Streptococcus mutans* biofilms by applying a range of external shear forces. Biofouling, 30: 1079-91.

Håvarstein LS, Gaustad P, Nes IF, Morrison DA. 1996. Identification of the streptococcal competence-pheromone receptor. Mol Microbiol, 21:4:863-9.

Ileri M, Alper A, Senen K, Durmaz T, Atak R, Hisar I, Yetkin E, Turhan H, Demirkan D. 2003. Effect of infective endocarditis on blood coagulation and platelet activation and comparison of patients with to those without embolic events. Am J Cardiol, 91:6:689-92.

Im GJ, An YS, Choi J, Song JJ, Chae SW, Jung HH. 2015. Analysis of Bacterial Biofilms on a Cochlear Implant Following Methicillin-Resistant *Staphylococcus Aureus* Infection. J Audiol Otol, 19:3:172-7.

Iorgulescu, G. 2009. Saliva between normal and pathological. Important factors in determining systemic and oral health. J Med Life. 2(3):303-7.

Ito T, Ichinosawa T, Shimizu T. 2017. Streptococcal adhesin SspA/B analogue peptide inhibits adherence and impacts biofilm formation of *Streptococcus mutans*. PLoS ONE 12(4): e0175483.

Itzek A, Zheng L, Chen Z, Merritt J, Kreth J. 2011. Hydrogen Peroxide-Dependent DNA Release and Transfer of Antibiotic Resistance Genes in *Streptococcus gordonii*. J Bacteriol. 193:6912-22.

Jack AA, Daniels DE, Jepson MA, Vickerman MM, Lamont RJ, Jenkinson HF, Nobbs AH. 2015. *Streptococcus gordonii* comCDE (competence) operon modulates biofilm formation with *Candida albicans*. Microbiology, 161:2:411-21.

Jakubovics NS, Gill SR, Iobst SE, Vickerman MM, Kolenbrander PE. 2008. (A) Regulation of gene expression in a mixed-genus community: stabilized arginine biosynthesis in *Streptococcus gordonii* by coaggregation with *Actinomyces naeslundii*. J Bacteriol, 190:10:3646-57.

Jakubovics NS, Gill SR, Vickerman MM, Kolenbrander PE. 2008. (B) Role of hydrogen peroxide in competition and cooperation between *Streptococcus gordonii* and *Actinomyces naeslundii*. FEMS Microbiol Ecol, 66:3:637-44.

Jarvill-Taylor KJ, VanDyk C, Minion FC. 1999. Cloning of *mnuA*, a membrane nuclease gene of *Mycoplasma pulmonis*, and analysis of its expression in *Escherichia coli*. J Bacteriol, 181:6:1853-60.

Jenkinson HF, Baker RA, Tannock GW. 1996. A binding-lipoprotein-dependent oligopeptide transport system in *Streptococcus gordonii* essential for uptake of hexa- and heptapeptides. J Bacteriol, 178:1:68-77.

Jensch I, Gámez G, Rothe M, Ebert S, Fulde M, Somplatzki D, Bergmann S, Petruschka L, Rohde M, Nau R, Hammerschmidt S. 2010. PavB is a surface-exposed adhesin of *Streptococcus pneumoniae* contributing to nasopharyngeal colonization and airways infections. Mol Microbiol, 77:1:22-43.

Ji S, Choi Y. 2013. Innate immune response to oral bacteria and the immune evasive characteristics of periodontal pathogens. J Periodontal Implant Sci, 43:1:3-11.

Johnson BP, Jensen BJ, Ransom EM, Heinemann KA, Vannatta KM, Egland KA, Egland PG. 2009. Interspecies Signaling between *Veillonella atypica* and *Streptococcus gordonii* Requires the Transcription Factor CcpA. J Bacteriol, 191:5563-5.

Jones EA, McGillivary G, Bakaletz LO. 2013. Extracellular DNA within a nontypeable *Haemophilus influenzae*-induced biofilm binds human beta defensin-3 and reduces its antimicrobial activity. J Innate Immun, 5:1:24-38.

Jung CJ, Hsu RB, Shun CT, Hsu CC, Chia JS. 2017. AtlA Mediates Extracellular DNA Release, Which Contributes to *Streptococcus mutans* Biofilm Formation in an Experimental Rat Model of Infective Endocarditis. Infect Immun, 85:9.

Kang HJ, Coulibaly F, Clow F, Proft T, Baker EN. 2007. Stabilizing isopeptide bonds revealed in gram-positive bacterial pilus structure. Science, 318:5856:1625-8.

Kang HJ, Paterson NG, Gaspar AH, Ton-That H, Baker EN. 2009. The *Corynebacterium diphtheriae* shaft pilin SpaA is built of tandem Ig-like modules with stabilizing isopeptide and disulfide bonds. Proc Natl Acad Sci U S A, 106:40:16967-71.

Kang M, Ko YP, Liang X, Ross CL, Liu Q, Murray BE, Höök M. 2013. Collagen-binding Microbial Surface Components Recognizing Adhesive Matrix Molecule (MSCRAMM) of Gram-positive Bacteria Inhibit Complement Activation via the Classical Pathway. J Biol Chem. 288:20520-31.

Kaplan, J. B. 2010. Biofilm Dispersal. J Dent Res. 89(3): 205–218.

Kaspar J, Underhill SAM, Shields RC, Reyes A, Rosenzweig S, Hagen SJ, Burne RA. 2017. Intercellular communication via the *comX*-Inducing Peptide (XIP) of *Streptococcus mutans*. J Bacteriol, 00404-1.

Kateete DP, Kimani CN, Katabazi FA, Okeng A, Okee MS, Nanteza A, Joloba ML, Najjuka FC. 2010. Identification of *Staphylococcus aureus*: DNase and Mannitol salt agar improve the efficiency of the tube coagulase test. 9:23:1476-0711.

Kato Y, Nishiyama K, Tokuda H. 2003. Depletion of SecDF-YajC causes a decrease in the level of SecG: implication for their functional interaction FEBS Lett 550:1-3:114-8 .

Kavita K, Mishra A, Jha B. 2013. Extracellular polymeric substances from two biofilm forming *Vibrio* species: characterization and applications. Carbohydr Polym, 94:2:882-8.

Kawamura Y, Hou XG, Sultana F, Miura H, Ezaki T. 1995. Determination of 16S rRNA sequences of *Streptococcus mitis* and *Streptococcus gordonii* and phylogenetic relationships among members of the genus *Streptococcus*. Int J Syst Bacteriol, 45:2:406-8.

Keane C, Petersen HJ, Tilley D, Haworth J, Cox D, Jenkinson HF, Kerrigan SW. 2013. Multiple sites on *Streptococcus gordonii* surface protein PadA bind to platelet GPIIbIIIa. Thromb Haemost, 110:6:1278-1287.

Kerrigan SW, Jakubovics NS, Keane C, Maguire P, Wynne K, Jenkinson HF, Cox D. 2007. Role of *Streptococcus gordonii* surface proteins SspA/SspB and Hsa in platelet function. Infect Immun, 75:12:5740-7.

Keynan, Y & Rubinstein E. 2013. Pathophysiology of Infective Endocarditis. Curr Infect Dis Rep. 15(4):342-6.

Khemaleelakul S, Baumgartner JC, Pruksakom S. 2006. Autoaggregation and coaggregation of bacteria associated with acute endodontic infections. J Endod, 32:4:312-8.

Kilian M, Chapple IL, Hannig M, Marsh PD, Meuric V, Pedersen AM, Tonetti MS, Wade WG, Zaura E. 2016. The oral microbiome - an update for oral healthcare professionals. Br Dent J, 221:10:657-666.

A-Reum K, Moon-Jin J, Yong-Soon A, Mi-Na K, Sung-Im K, Do-Seon L. 2015. The interactive effect of these bacterial substrates on the growth of *Streptococcus gordonii*, *Fusobacterium nucleatum* and *Porphyromonas gingivalis*. Journal of dental hygiene science. 15:209-219.

Kim AR, Ahn KB, Kim HY, Seo HS, Yun CH, Han SH. Serine-rich Repeat Adhesin Gordonii Surface Protein B is Important for *Streptococcus gordonii* Biofilm Formation. J Endod, v. 42, n. 12, p. 1767-1772, Dec 2016. ISSN 0099-2399.

Kilian M, Chapple IL, Hannig M, Marsh PD, Meuric V, Pedersen AM, Tonetti MS, Wade W. & Zaura E. 2016. The oral microbiome - an update for oral healthcare professionals. Br Dent J, 221: 657-66.

Kim AR, Ahn KB, Kim HY, Seo HS, Yun CH, Han SH. 2018. *Streptococcus mutans* extracellular DNA levels depend on the number of bacteria in a biofilm. Sci Rep, 8:1:13313.

Kindblom C, Davies JR, Herzberg MC, Svensater G & Wickstrom C. 2012. Salivary proteins promote proteolytic activity in *Streptococcus mitis* biovar 2 and *Streptococcus mutans*. Mol Oral Microbiol, 27: 362-72.

Kleerebezem M, Quadri LE, Kuipers OP, de Vos WM. 1997. Quorum sensing by peptide pheromones and two-component signal-transduction systems in Gram-positive bacteria. Mol Microbiol, 24:5:895-904.

Kolenbrander PE, Palmer RJ Jr, Periasamy S, Jakubovics NS. 2010. Oral multispecies biofilm development and the key role of cell-cell distance. Nat Rev Microbiol, 8:7:471-80.

Komatsuzawa H, Ohta K, Sugai M, Fujiwara T, Glanzmann P, Berger-BächiB, Suginaka H. 2000. Tn551-mediated insertional inactivation of the *fmtB* gene encoding a cell wall-associated protein abolishes methicillin resistance in *Staphylococcus aureus*. J Antimicrob Chemother, 45:4:421-31.

Konstan MW, Ratjen T. 2012. Effect of dornase alfa on inflammation and lung function: potential role in the early treatment of cystic fibrosis. J Cyst Fibros, 11:2:78-83.

Koo H, Xiao J, Klein MI, Jeon JG. 2010. Exopolysaccharides produced by *Streptococcus mutans* glucosyltransferases modulate the establishment of microcolonies within multispecies biofilms. J Bacteriol, 192:12:3024-32.

Kreth J, Merritt J. Qi F. 2009. Bacterial and host interactions of oral streptococci. DNA Cell Biol, 28:8:397-403.

Kreth J, Vu H, Zhang Y, Herzberg MC. 2009. Characterization of hydrogen peroxide-induced DNA release by *Streptococcus sanguinis* and *Streptococcus gordonii*. J Bacteriol, 191:20:6281-91

Kreth J, Zhang Y, Herzberg MC. 2008. Streptococcal antagonism in oral biofilms: *Streptococcus sanguinis* and *Streptococcus gordonii* interference with Streptococcus mutans. J Bacteriol, 190:13:4632-40.

Krzyściak W, Pluskwa KK, Jurczak A, Kościelniak D. 2013. The pathogenicity of the *Streptococcus* genus. Eur J Clin Microbiol Infect Dis, 32:11:1361-76.

Lacks S, Greenberg B. 1976. Single-strand breakage on binding of DNA to cells in the genetic transformation of *Diplococcus pneumoniae*. J Mol Biol, 101:2:255-75.

Lamont R, El-Sabaeny A, Park Y, Cook G, Costerton J, Demuth D. 2002. Role of the *Streptococcus gordonii* SspB protein in the development of *Porphyromonas gingivalis* biofilms on streptococcal substrates. Microbiology 148:6:1627-1636.

Langdon A, Crook N, Dantas G. 2016. The effects of antibiotics on the microbiome throughout development and alternative approaches for therapeutic modulation. Genome Med, 8:1:39.

Lapaglia C, Hartxell P. 1997. Stress-Induced Production of Biofilm in the Hyperthermophile *Archaeoglobus fulgidus*. Appl Environ Microbiol, 63:8:3158-63.

Lebeaux D, Ghigo JM, Beloin C. 2014. Biofilm-related infections: bridging the gap between clinical management and fundamental aspects of recalcitrance toward antibiotics. Microbiol Mol Biol Rev. 78(3):510-543.

Lee N, Kim WY. 2017. Microbiota in T-cell homeostasis and inflammatory diseases. Exp Mol Med, 49:5:e340.

Lethem MI, James SL, Marriott C, Burke JF. 1990. The origin of DNA associated with mucus glycoproteins in cystic fibrosis sputum. Eur Respir J, 3:1:19-23.

Levdikov VM, Blagova E, Young VL, Belitsky BR, Lebedev A, Sonenshein AL, Wilkinson AJ. 2017. Structure of the Branched-chain Amino Acid and GTP-sensing Global Regulator, CodY, from *Bacillus subtilis*. J Biol Chem 292:7:2714-2728.

Li J, Helmerhorst EJ, Leone CW, Troxler RF, Yaskell T, Haffajee AD, Socransky SS & Oppenheim FG. 2004. Identification of early microbial colonizers in human dental biofilm. J Appl Microbiol, 97: 1311-8.

Li T, Zhai S, Xu M, Shang M, Gao Y, Liu G, Wang Q, Zheng L. 2016. SpxB-mediated H_2O_2 induces programmed cell death in *Streptococcus sanguinis*. J Basic Microbiol, 56:7:741-52.

Li YH, Lau PC, Lee JH, Ellen RP, Cvitkovitch DG. 2001. Natural Genetic Transformation of *Streptococcus mutans* Growing in Biofilms. J Bacteriol, 183:897-908.

Li Y-H & Tian X. 2012. Quorum sensing and bacterial social interactions in biofilms. Sensors (Basel). 2012;12(3):2519-38.

Liao S, Klein MI, Heim KP, Fan Y, Bitoun JP, Ahn SJ, Burne RA, Koo H, Brady LJ, Wen ZT. 2014. *Streptococcus mutans* extracellular DNA is upregulated during growth in biofilms, actively released via membrane vesicles, and influenced by components of the protein secretion machinery. J Bacteriol, 196:13:2355-66.

Liljemark WF, Bloomquist CG, Bandt CL, Pihlstrom BL, Hinrichs JE, Wolff LF. 1993. Comparison of the distribution of *Actinomyces* in dental plaque on inserted enamel and natural tooth surfaces in periodontal health and disease. Oral Microbiol Immunol, 8:1:5-15.

Lima BP, Shi W, Lux R. 2017. Identification and characterization of a novel *Fusobacterium nucleatum* adhesin involved in physical interaction and biofilm formation with *Streptococcus gordonii*. Microbiologyopen, 6:3.

Limoli DH, Jones CJ, Wozniak DJ. 2015. Bacterial Extracellular Polysaccharides in Biofilm Formation and Function. Microbiol Spectr, 3:3.

Lin W, Du Y, Zhu Y, Chen X. 2014. A cis-membrane FRET-based method for protein-specific imaging of cell-surface glycans. J Am Chem Soc. 136(2):679-687.

Liu J, Prindle A, Humphries J, Gabalda-Sagarra M, Asally M, Lee DY, Ly S, Garcia-Ojalvo J, Süel GM. 2015. Metabolic co-dependence gives rise to collective oscillations within biofilms. Nature, 523:7562:550-4.

Liu J, Sun L, Liu W, Guo L, Liu Z, Wei X, Ling J. 2017. A Nuclease from *Streptococcus mutans* Facilitates Biofilm Dispersal and Escape from Killing by Neutrophil Extracellular Traps. Front Cell Infect Microbiol, 7:97.

Lui U, Burne RA. 2011. The major autolysin of *Streptococcus gordonii* is subject to complex regulation and modulates stress tolerance, biofilm formation, and extracellular-DNA release. J Bacteriol, 193:11:2826-37.

Lockhart PB, Brennan MT, Thornhill M, Michalowicz BS, Noll J, Bahrani-Mougeot FK & Sasser HC. 2009. Poor oral hygiene as a risk factor for infective endocarditis–related bacteremia. J Am Dent Assoc. 140(10): 1238–1244.

Loesche WJ, Gusberti F, Mettraux G, Higgins T & Syed S. 1983. Relationship between oxygen tension and subgingival bacterial flora in untreated human periodontal pockets. Infect Immun, 42: 659-67.

Loo CY, Corliss DA, Ganeshkumar N. 2000. *Streptococcus gordonii* biofilm formation: identification of genes that code for biofilm phenotypes. J Bacteriol, 182:5:1374-82.

Luo P, Mossiron DA. 2003. Transient association of an alternative sigma factor, ComX, with RNA polymerase during the period of competence for genetic transformation in *Streptococcus pneumoniae*. J Bacteriol, 185:1:349-58.

Lopez D, Vlamakis H, Kolter R. 2010. Biofilms. Cold Spring Harb Perspect Biol, 2.

Ma L, Jackson KD, Landry RM, Parsek MR & Wozniak DJ. 2006. Analysis of Pseudomonas aeruginosa conditional psl variants reveals roles for the psl

polysaccharide in adhesion and maintaining biofilm structure post attachment. J Bacteriol, 188: 8213-21.

Majerczyk CD, Sadykov MR, Luong TT, Lee C, Somerville GA, Sonenshein AL. 2008. *Staphylococcus aureus* CodY negatively regulates virulence gene expression. J Bacteriol. 190(7):2257-65

Marcotte H & Lavoie MC. 1998. Oral microbial ecology and the role of salivary immunoglobulin A. Microbiol Mol Biol Rev, 62: 71-109.

Martí S, Rodríguez-Baño J, Catel-Ferreira M. 2011. Biofilm formation at the solid-liquid and air-liquid interfaces by *Acinetobacter* species. BMC Res Notes. 4:5.

McCoy JG, Levn EJ, Zhou M. 2015. Structural insight into the PTS sugar transporter EIIC. Biochim Biophys Acta, 1850:3:577-85.

McCrate OA, Zhou X, Reichhardt C, Cegelski L. 2013. Sum of the parts: composition and architecture of the bacterial extracellular matrix. J Mol Biol, 425:22:4286-94.

McNab R, Forbes H, Handley PS, Loach DM, Tannock GW, Jenkinson HF. 1999. Cell wall-anchored CshA polypeptide (259 kilodaltons) in *Streptococcus gordonii* forms surface fibrils that confer hydrophobic and adhesive properties. J Bacteriol, 181:10:3087-95.

McNab R, Holmes AR, Clarke JM, Tannock GW, Jenkinson HF. 1996. Cell surface polypeptide CshA mediates binding of *Streptococcus gordonii* to other oral bacteria and to immobilized fibronectin. Infect Immun, 64:10:4204-10.

Mehta D, Satyanarayana T. 2016. Bacterial and Archaeal α-Amylases: Diversity and Amelioration of the Desirable Characteristics for Industrial Applications. Front Microbiol, 7:1129.

Merritt J, Niu G, Okinaga T, Qi F. 2009. Autoaggregation Response of *Fusobacterium nucleatum*. Appl Environ Microbiol, 75:7725-33.

Metzgar D, Zampolli A. 2011. The M protein of group A *Streptococcus* is a key virulence factor and a clinically relevant strain identification marker. Virulence, 2:5:402-12.

Miller MB, Basser BL. 2001. Quorum sensing in bacteria. Annu Rev Microbiol, 55:165-99.

Mingeot-LeClerq MP, Tulkem PM. 1999. Aminoglycosides: nephrotoxicity. Antimicrob Agents Chemother, 43:5:1003-12.

Mitiku F, Hartley CA, Sansom FM, Coombe JE, Mansell PD, Beggs DS, Browning GF. 2018. The major membrane nuclease MnuA degrades neutrophil extracellular traps induced by *Mycoplasma bovis*. Vet Microbiol, 218:13-19.

Mohammed WK, Krasnogor N, Jakubovics NS. 2018. *Streptococcus gordonii* Challisin protease is required for sensing cell--cell contact with *Actinomyces oris*. FEMS Microbiol Ecol, 94:5.

Montanaro L, Poggi A, Visai L, Ravaioli S, Campoccia D, Speziale P, Arciola CR. 2011. Extracellular DNA in biofilms. Int J Artif Organs, 34:9:824-31.

Montelongo-Jauregui D, Srinivasan A, Ramasubramanian AK, Lopez-Ribot JL. 2016. An In Vitro Model for Oral Mixed Biofilms of *Candida albicans* and *Streptococcus gordonii* in Synthetic Saliva. Front Microbiol, 12:7:686.

Mori H, Ito K. 2001.The Sec protein-translocation pathway. Trends Microbiol, 9:10:494-500.

Moore RJ, Watts JT, Hood JA & Burritt DJ. 1999. Intra-oral temperature variation over 24 hours. Eur J Orthod, 21: 249-61.

Moscoso M, Garcia E, Lopez R. 2006. Biofilm formation by *Streptococcus pneumoniae*: role of choline, extracellular DNA, and capsular polysaccharide in microbial accretion. J Bacteriol, v. 188:22:7785-95.

Moses PJ, Power DA, Jesionowski AM, Jenkinson HF, Pantera EA Jr, Vickerman MM. 2013. *Streptococcus gordonii* collagen-binding domain protein CbdA may enhance bacterial survival in instrumented root canals ex vivo. J Endod, 39:1:39-43.

Murzin AG. 1993. OB (oligonucleotide/oligosaccharide binding)-fold: common structural and functional solution for non-homologous sequences. EMBO J, 12:3:861-7.

Mulcahy H, Charron-Mazenod L & Lewenza S. 2008. Extracellular DNA chelates cations and induces antibiotic resistance in *Pseudomonas aeruginosa* biofilms. PLoS Pathog, 4: e1000213.

Muschiol S, Balaban M, Normark S, Henriques-Normark B. 2015. Uptake of extracellular DNA: competence induced pili in natural transformation of *Streptococcus pneumoniae*. Bioessays, 37:4:426-35,.

Muto Y, Goto S. 1986 Transformation by Extracellular DNA Produced by *Pseudomonas aeruginosa*. Microbiology and Immunology: J-Stage. 3:621-628.

Natale P, Bruser T, Driessem AJ. 2008. Sec- and Tat-mediated protein secretion across the bacterial cytoplasmic membrane--distinct translocases and mechanisms. Biochim Biophys Acta, 1778:9:1735-56.

Navarre WW, Schneewind O. 1994. Proteolytic cleavage and cell wall anchoring at the LPxTG motif of surface proteins in gram-positive bacteria. Mol Microbiol, 14:1:115-21.

Nazir MA. 2017. Prevalence of periodontal disease, its association with systemic diseases and prevention. Int J Health Sci (Qassim), 11:2:72-80.

Nijland R, Hall MJ, Burgess JG. 2010. Dispersal of biofilms by secreted, matrix degrading, bacterial DNase. PLoS One, 5:12:e15668.

Nobile CJ, Johnson AD. Candida albicans Biofilms and Human Disease. Annu Rev Microbiol. 2015;69:71-92.

Nobbs AH, Lamont RJ, Jenkinson HF. 2009. *Streptococcus* adherence and colonization. Microbiol Mol Biol Rev, 73:3:407-50.

Nobbs AH, Shearer BH, Drobni M, Jepson MA & Jenkinson HF. 2007. Adherence and internalization of *Streptococcus gordonii* by epithelial cells involves beta1 integrin recognition by SspA and SspB (antigen I/II family) polypeptides. Cell Microbiol, 9: 65-83.

Nobbs AH, Vajna RM, Johnson JR, Zhang Y, Erlandsen SL, Oli MW, Kreth J, Brady LJ, Herzberg MC. 2007 (A). Consequences of a *sortase A* mutation in *Streptococcus gordonii*. Microbiology, 15:12:4088-97.

Nobbs A. 2017. Getting to the heart of the matter: Role of *Streptococcus mutans* adhesin Cnm in systemic disease. Virulence. 8(1):1-4.

O'Toole GA, Stewart PS. 2005. Biofilms strike back. Nat Biotechnol, 23:11:1378-9.

Ogawa T, Kono Y, McGhee ML, McGhee JR, Roberts JE, Hamada S, Kiyono H. 1991. *Porphyromonas gingivalis*-specific serum IgG and IgA antibodies originate from immunoglobulin-secreting cells in inflamed gingiva. Clin Exp Immunol, 83:2:237-44.

Oho T, Yu H, Yamashita Y, Koga T. 1998. Binding of salivary glycoprotein-secretory immunoglobulin A complex to the surface protein antigen of *Streptococcus mutans*. Infect Immun, 66:1:115-21.

Okshevsky M, Meyer RL. 2015. The role of extracellular DNA in the establishment, maintenance and perpetuation of bacterial biofilms. Crit Rev Microbiol, 41:3:341-52.

Pachori A, Kambalimath H, Maran S, Niranjan B, Bhambhani G & Malhotra G. 2018. Evaluation of Changes in Salivary pH after Intake of Different Eatables and Beverages in Children at Different Time Intervals. Int J Clin Pediatr Dent. 11(3):177-182.

Pakula R, Walczak W. 1963. On the nature of the competence of transformable streptococci. J Gen Microbiol 31, 125–133.

Park JH, Lee J-K, Um H-S, Chang B-S. & Lee S-Y. 2014. A periodontitis-associated multispecies model of an oral biofilm. J Periodontal Implant Sci. 44(2): 79–84.

Park J, Shokeen B, Haake S, and Lux R. 2016. Characterization of Fusobacterium nucleatum ATCC 23726 adhesins involved in strain-specific attachment to *Porphyromonas gingivalis*. Int J Oral Sci, 8:3:138-44.

Peng X, Zhang Y, Bai G, Zhou X, Wu H. 2016. Cyclic di-AMP mediates biofilm formation. Mol Microbiol, 99:5:945-59.

Petersen HJ, Keane C, Jenkinson HF, Vickerman MM, Jesionowski A, Waterhouse JC, Cox D, Kerrigan SW. 2010. Human platelets recognize a novel surface protein, PadA, on *Streptococcus gordonii* through a unique interaction involving fibrinogen receptor GPIIbIIIa. Infect Immun, 78:1:413-22.

Peterson BW, van der Mei HC, Sjollema J, Busscher HJ, Sharma PK. 2013. (A) A distinguishable role of eDNA in the viscoelastic relaxation of biofilms. MBio, 4:5:e00497-13.

Peterson EJ, Kireev D, Moon AF, Midon M, Janzen WP, Pingoud A, Pedersen LC, Singleton SF. 2013. (B) Inhibitors of *Streptococcus pneumoniae* surface endonuclease EndA discovered by high-throughput screening using a PicoGreen fluorescence assay. J Biomol Screen, 8:3:247-57.

Pettersson GB, Hussain ST, Shrestha NK, Gordon S, Fraser TG, Ibrahim KS, Blackstone EH. 2014. Infective endocarditis: an atlas of disease progression for describing, staging, coding, and understanding the pathology. J Thorac Cardiovasc Surg, 147:4:1142-1149.e2.

Prindle A, Liu J, Asally 2, Ly S, Garcia-Ojalvo J, Süel GM. 2015. Ion channels enable electrical communication in bacterial communities. Nature, 527:7576:59-63.

Podbielski A, Spellerberg B, Woischnik M, Pohl B, Lütticken R. 1996. Novel series of plasmid vectors for gene inactivation and expression analysis in group A streptococci (GAS). Gene 177:1–2:137-147.

Pudakalkatii PS, Baheti S. 2015. Correlation of salivary immunoglobulin A against lipopolysaccharide of *Porphyromonas gingivalis* with clinical periodontal parameters. In: (Ed.). Contemp Clin Dent. India 6:305-8.

Puttaswamy KA, Puttabudhi JH & Raju S. 2017. Correlation between Salivary Glucose and Blood Glucose and the Implications of Salivary Factors on the Oral Health Status in Type 2 Diabetes Mellitus Patients. J Int Soc Prev Community Dent. 7(1):28-33.

Rajendran R, Williams C, Lappin DF, Millington O, Martins M, Ramage G. 2013. Extracellular DNA release acts as an antifungal resistance mechanism in mature *Aspergillus fumigatus* biofilms. Eukaryot Cell, 12:3:420-9.

Ramboarina S, Garnett JA, Zhou M, Li Y, Peng Z, Taylor JD, Lee WC, Bodey A, Murray JW, Alguel Y, Bergeron J, Bardiaux B, Sawyer E, Isaacson R, Tagliaferri C, Cota E, Nilges M, Simpson P, Ruiz T, Wu H, Matthews S. 2010. Structural insights into serine-rich fimbriae from Gram-positive bacteria. J Biol Chem, 285:42:32446-57.

Ras M, Lefebvre D, Derlon N, Paul E, Girbal-Neuhauser E. 2011. Extracellular Polymeric Substances diversity of biofilms grown under contrasted environmental conditions. Water Res. 45(4):1529-1538.

Resch U, Tsatsaronis JA, Le Rhun A1, Stübiger G, Rohde M, Kasvandik S, Holzmeister S, Tinnefeld P, Wai SN, Charpentier E. 2016. A Two-Component Regulatory System Impacts Extracellular Membrane-Derived Vesicle Production in Group A *Streptococcus*. MBio, 7:6.

Ribeiro SM, Felício MR, Boas EV, Gonçalves S, Costa FF, Samy RP, Santos NC, Franco OL. 2016. New frontiers for anti-biofilm drug development. Pharmacol Ther, 160:133-44.

Ricker A, Vickerman M, Dongari-Bagtzoglou A. 2014. *Streptococcus gordonii* glucosyltransferase promotes biofilm interactions with *Candida albicans*. J Oral Microbiol, v. 6.

Rocco CJ, Bakaletz LO, Goodman SD. 2018. Targeting the HUbeta Protein Prevents *Porphyromonas gingivalis* from Entering into Preexisting Biofilms. J Bacteriol, 200:11.

Rocco CJ, Davey ME, Bakaletz LO, Goodman SD. 2016. Natural antigenic differences in the functionally equivalent extracellular DNABII proteins of bacterial biofilms provide a means for targeted biofilm therapeutics. Mol Oral Microbiol, 322:118-130.

Rohde H, Burandt EC, Siemssen N, Frommelt L, Burdelski C, Wurster S, Scherpe S, Davies AP, Harris LG, Horstkotte MA, Knobloch JK, Ragunath C, Kaplan JB, Mack D. 2007. Polysaccharide intercellular adhesin or protein factors in biofilm accumulation of *Staphylococcus epidermidis* and *Staphylococcus aureus* isolated from prosthetic hip and knee joint infections. Biomaterials, v. 28:9:1711-20.

Rosan B, Lamont RJ. 2000. Dental plaque formation. Microbes Infect, 2:13:1599-607.

Rostami N, Shields RC, Yassin SA, Hawkins AR, Bowen L, Luo TL, Rickard AH, Holliday R, Preshaw PM, Jakubovics NS. 2017. A Critical Role for Extracellular DNA in Dental Plaque Formation. J Dent Res, v. 96:2:208-216.

Rudiger SG, Carlen A, Meurman JH, Kari K. & Olsson J. 2002. Dental biofilms at healthy and inflamed gingival margins. J Clin Periodontol, 29: 524-30.

Sadler JE. 1998. Biochemistry and genetics of von Willebrand factor. Annu Rev Biochem, 67:395-424.

Sandal I, Hong W, Swords WE & Inzana TJ. 2007. Characterization and Comparison of Biofilm Development by Pathogenic and Commensal Isolates of *Histophilus somni*. J Bacteriol. 189(22): 8179–8185.

Sands KM, Twigg JA, Lewis MA, Wise MP, Marchesi JR, Smith A, Wilson MJ, Williams DW. 2016. Microbial profiling of dental plaque from mechanically ventilated patients. J Med Microbiol, 65:2:147-59.

Sass V, Pag U, Tossi A, Bierbaum G, Sahl HG. 2008. Mode of action of human beta-defensin 3 against *Staphylococcus aureus* and transcriptional analysis of responses to defensin challenge. Int J Med Microbiol, 298:78:619-33.

Schild S, Tamayo R, Nelson EJ, Qadri F, Calderwood SB, Camilli A. 2007. Genes induced late in infection increase fitness of *Vibrio cholerae* after release into the environment. Cell Host Microbe, 2:4:264-77.

Schlafer S, Meyer RL, Dige I, Regina VR. 2017. Extracellular DNA Contributes to Dental Biofilm Stability. Caries Res, 51:4:436-442.

Schneewind O, Missiakas D. 2014. Sec-secretion and sortase-mediated anchoring of proteins in Gram-positive bacteria. Biochim Biophys Acta, 1843:8:1687-97.

Shen Y, Zhang H, Xu X, Lin X. 2015. Biofilm formation and lipid accumulation of attached culture of *Botryococcus braunii*. Bioprocess Biosyst Eng, 38:3:481-8.

Shockman GD, Daneo-Moore L, Kariyama R, Massidda O. 1996. Bacterial walls, peptidoglycan hydrolases, autolysins, and autolysis. Microb Drug Resist, 2:1:95-8

Shopova I, Bruns S, Thywissen A, Kniemeyer O, Brakhage AA, Hillmann F. 2013. Extrinsic extracellular DNA leads to biofilm formation and colocalizes with matrix polysaccharides in the human pathogenic fungus *Aspergillus fumigatus*. Front Microbiol, 4:141.

Shu M, Wong L, Miller JH, Sissons CH. 2000. Development of multi-species consortia biofilms of oral bacteria as an enamel and root caries model system. Arch Oral Biol, 45:1:27-40.

Silverman RJ, Nobbs AH, Vickerman MM, Barbour ME, Jenkinson HF. 2010. Interaction of *Candida albicans* cell wall Als3 protein with *Streptococcus gordonii* SspB adhesin promotes development of mixed-species communities. Infect Immun, 78:11:4644-52.

Smeesters PR, McMillan DJ, Sriprakash KS. 2010. The streptococcal M protein: a highly versatile molecule. Trends Microbiol, 18:6:275-82.

Song T, Duperthuy M, Wui SN. 2016. Sub-Optimal Treatment of Bacterial Biofilms. Antibiotics (Basel), 5:2.

Southern P, Horbul J, Maher D & Davis DA. 2008. *C. albicans* colonization of human mucosal surfaces. PLoS One 30;3(4):e2067.

Steenackers HP, Parijs I, Dubey A, Foster KR, Vanderleyden J. 2016. Experimental evolution in biofilm populations. FEMS Microbiol Rev, 403:373-97.

Steinmoen H, Knutsen E, Hararstein LS. 2002. Induction of natural competence in *Streptococcus pneumoniae* triggers lysis and DNA release from a subfraction of the cell population. Proc Natl Acad Sci U S A, 99:11:7681-6.

Steinmoen H, Teigen A, Haverstein LS. 2003. Competence-induced cells of *Streptococcus pneumoniae* lyse competence-deficient cells of the same strain during cocultivation. J Bacteriol, v. 185:24:7176-83.

Takamatsu D, Bensing BA, Prakobphol A, Fisher SJ, Sullam PM. 2006. Binding of the streptococcal surface glycoproteins GspB and Hsa to human salivary proteins. Infect Immun, 74:3:1933-40.

Struzycka, I. 2014. The oral microbiome in dental caries. Pol J Microbiol, 63: 127-35.

Tang L, Schramm A, Neu TR, Revsbech NP, Meyer RL. 2013. Extracellular DNA in adhesion and biofilm formation of four environmental isolates: a quantitative study. FEMS Microbiol Ecol, 86:3:394-403.

Tanzer JM, Thompson A, Sharma K, Vickerman MM, Haase EM, Scannapieco FA. 2012. *Streptococcus mutans* Out-competes *Streptococcus gordonii* in vivo. J Dent Res. Sage 91:513-9.

Telford JL, Barocchi MA, Margarit I, Rappuoli R, Grandi G. 2006. Pili in gram-positive pathogens. Nat Rev Microbiol, 4:7:509-19.

Terezhalmy GT, Biesbrock AR, Walters PA, Grender JM & Bartizek RD. 2008. Clinical evaluation of brushing time and plaque removal potential of two manual toothbrushes. Int J Dent Hyg, 6: 321-7.

Tetz GV, Artemenko NK, Tetz VV. 2009. Effect of DNase and antibiotics on biofilm characteristics. Antimicrob Agents Chemother, 53:3:1204-9.

Thomas VC, Hiromasa Y, Harms N, Thurlow L, Tomich J, Hancock LE. 2009. A fratricidal mechanism is responsible for eDNA release and contributes to biofilm development of *Enterococcus faecalis*. Mol Microbiol, 72:4:1022-36.

Thomann A, Brengel C, Borger C. 2016. Structure-Activity Relationships of 2-Sufonylpyrimidines as Quorum-Sensing Inhibitors to Tackle Biofilm Formation and eDNA Release of *Pseudomonas aeruginosa*. ChemMedChem. 11(22):2522-2533.

Thornby KA, Johnson A, Axtell S. 2014. Dornase Alfa for Non-Cystic Fibrosis Pediatric Pulmonary Atelectasis. Ann Pharmacother. 48:1040-1049.

Thurnheer T, Belibasakis GN. 2018. *Streptococcus oralis* maintains homeostasis in oral biofilms by antagonizing the cariogenic pathogen *Streptococcus mutans*. Mol Oral Microbiol, 33:3:234-239.

Tiwari N. 2011. Science behind human saliva. J Nat Sci Biol Med, 2:1:53-8.

Tjokro NO, Rocco CJ, Priyadarshini R, Davey ME, Goodman SD. 2014. A biochemical analysis of the interaction of *Porphyromonas gingivalis* HU PG0121 protein with DNA. PLoS One, 9:3:e93266.

To WS, Midwood KS. 2011. Plasma and cellular fibronectin: distinct and independent functions during tissue repair. Fibrogenesis Tissue Repair. 4:21.

Toyofuku M, Inaba T, Kiyokawa T, Obana N, Yawata Y, Nomura N. 2016. Environmental factors that shape biofilm formation. Biosci Biotechnol Biochem, 80:1:7-12.

Toyofuku M, Roschitzki B, Riedel K, Eberl L. 2012. Identification of proteins associated with the *Pseudomonas aeruginosa* biofilm extracellular matrix. J Proteome Res, :11:10:4906-15.

Tsukazaki T, Mori H, Echizen Y, Ishitani R, Fukai S, Tanaka T, Perederina A, Vassylyev DG, Kohno T, Maturana AD, Ito K, Nureki O. 2011. Structure and function of a membrane component SecDF that enhances protein export. Nature, 474:7350:235-8.

Turnbull L, Toyofuku M, Hynen AL, Kurosawa M, Pessi G, Petty NK, Osvath SR, Cárcamo-Oyarce G, Gloag ES, Shimoni R, Omasits U, Ito S, Yap X, Monahan LG, Cavaliere R, Ahrens CH, Charles IG, Nomura N, Eberl L, Whitchurch CB. 2016. Explosive cell lysis as a mechanism for the biogenesis of bacterial membrane vesicles and biofilms. Nat Commun, 7:11220.

Van Oss CJ. 1995. Hydrophobic, hydrophilic and other interactions in epitope-paratope binding. Mol Immunol, v. 32:3:199-211.

Veenendaal AK, Van der Does C, Dreissen AJ. 2004. The protein-conducting channel SecYEG. Biochim Biophys Acta, 1694:1-3:81-95.

Vickerman MM, Iobs I, Jesionowski AM, and S. R. Gill. 2007. Genome-wide transcriptional changes in *Streptococcus gordonii* in response to competence signaling peptide. J Bacteriol, 189:21:7799-807.

Vogkou CT, Vlachogiannis NI, Palaiodimos L & Kousoulis AA. 2016. The causative agents in infective endocarditis: a systematic review comprising 33,214 cases. Eur J Clin Microbiol Infect Dis, 35: 1227-45. Yadav

Vorkapic D, Pressler K, Schild S. 2016. Multifaceted roles of extracellular DNA in bacterial physiology. Curr Genet, 62:1:71-9.

Vrontou E, Economou A. 2004. Structure and function of SecA, the preprotein translocase nanomotor. Biochim Biophys Acta, 1694:1-3:67-80.

Wallace SM, Walton BI, Kharbanda RK, Hardy R, Wilson AP, Swanton RH. 2002 Mortality from infective endocarditis: clinical predictors of outcome. Heart, 88:1:53-60.

Wang BY, Deutch A, Hong J, Kuramitsu HK. 2011. Proteases of an early colonizer can hinder *Streptococcus mutans* colonization in vitro. J Dent Res, 90:4:501-5.

Wang BY, Kuramitsu HK. 2005. Interactions between oral bacteria: inhibition of *Streptococcus mutan*s bacteriocin production by *Streptococcus gordonii*. Appl Environ Microbiol, 71:1:354-62.

Wang J, Zhou Z, He F, Ruan Z, Jiang Y, Hua X, Yu Y. 2018. The role of the type VI secretion system vgrG gene in the virulence and antimicrobial resistance of *Acinetobacter baumannii* ATCC 19606. PLoS One, 13:2:e0192288.

Wang S, Liu X, Liu H, Zhang L, Guo Y, Yu S, Wozniak DJ, Ma LZ. 2015. The exopolysaccharide Psl-eDNA interaction enables the formation of a biofilm skeleton in *Pseudomonas aeruginosa*. Environ Microbiol Rep, 7:2:330-40..

Whitchurch CB, Tolker-Nielsen T, Ragas PC, Mattick JS. 2002. Extracellular DNA required for bacterial biofilm formation. Science, 295:5559:1487.

Wilking JN, Zaburdaev V, De Volder M, Losick R, Brenner MP, Weitz DA. 2013. Liquid transport facilitated by channels in *Bacillus subtilis* biofilms. Proc Natl Acad Sci U S A, 110:3:848-52.

Wilkins MH, Stokes AR, Wilson HR. 1952. Molecular structure of deoxypentose nucleic acids. Nature, 171:4356:738-40.

Willems RJ, Hanage WP, Bessen DE, Feil EJ. 2011. Population biology of Gram-positive pathogens: high-risk clones for dissemination of antibiotic resistance. FEMS Microbiol Rev. 35(5):872-900.

Williamson KS, Richards LA, Perez-Osorio AC, Pitts B, McInnerney K, Stewart PS, Franklin MJ. 2012. Heterogeneity in *Pseudomonas aeruginosa* biofilms includes expression of ribosome hibernation factors in the antibiotic-tolerant subpopulation and hypoxia-induced stress response in the metabolically active population. J Bacteriol, 194:8:2062-73.

Wilton M, Charron-Mazenod L, Moore R, Lewenza S. 2016. Extracellular DNA Acidifies Biofilms and Induces Aminoglycoside Resistance in *Pseudomonas aeruginosa*. Antimicrob Agents Chemother, 60:1:544-53.

Winkler MT, Osorio FA, Barahona HJ, Taffarel M. 1995. Study of neutralizing monoclonal antibodies to bovine herpes virus type-1 (Cooper strain) by immunoperoxidase and immunoelectron microscopy. FEMS Immunol Med Microbiol. 11(1):1-4.
Woodford N, Livermore DM. 2009. Infections caused by Gram-positive bacteria: a review of the global challenge. J Infect. 59 Suppl 1:S4-16.

Wu S, Liu G, Jin W, Xiu P, Sun C. 2016. Antibiofilm and Anti-Infection of a Marine Bacterial Exopolysaccharide Against *Pseudomonas aeruginosa*. Front Microbiol, 7:102.

Xiao J, Klein MI, Falsetta ML, Lu B, Delahunty CM, Yates JR 3rd, Heydorn A, Koo H. 2012. The exopolysaccharide matrix modulates the interaction between 3D architecture and virulence of a mixed-species oral biofilm. PLoS Pathog, 8:4:e1002623.

Xu Y, Kreth J. 2013. Role of LytF and AtlS in eDNA release by *Streptococcus gordonii*. PLoS One, 8:4:e62339.

Yadav MK, Chae SW & Song JJ. 2012. *In Vitro Streptococcus pneumoniae* Biofilm Formation and In Vivo Middle Ear Mucosal Biofilm in a Rat Model of Acute Otitis Induced by *S. pneumoniae*. Clin Exp Otorhinolaryngol. 5(3): 139–144.

Yang Y, Tsifansky MD, Wu CJ, Yang HI, Schmidt G, Yeo Y. 2010. Inhalable antibiotic delivery using a dry powder co-delivering recombinant deoxyribonuclease and ciprofloxacin for treatment of cystic fibrosis. Pharm Res. 27(1):151-160.

Yu C & Abbott PV. 2007. An overview of the dental pulp: its functions and responses to injury. Aust Dent J, 52: S4-16.

Zeller T, Klug G. 2006. Thioredoxins in bacteria: functions in oxidative stress response and regulation of thioredoxin genes. Naturwissenschaften, 93:6:259-66.

Zhang ZJ, Chen SH, Wang SM, Luo HY. 2011. Characterization of extracellular polymeric substances from biofilm in the process of starting-up a partial nitrification process under salt stress. Appl Microbiol Biotechnol, 89:5:1563-71.

Zhu L, Kuang Z, Wilson BA, Lau GW. 2013. Competence-independent activity of pneumococcal EndA mediates degradation of extracellular DNA and nets and is important for virulence. PLoS One, 8:7:e70363.